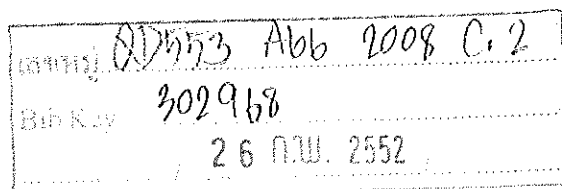


Potentiometric and Capacitive Affinity Biosensors

Apon Numnuam

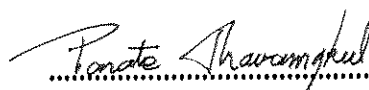


**A Thesis Submitted in Fulfillment of the Requirements
for the Degree of Doctor of Philosophy in Chemistry
Prince of Songkla University
2008**

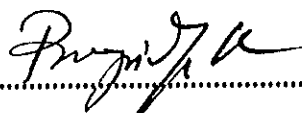
Copyright of Prince of Songkla University

Thesis Title Potentiometric and Capacitive Affinity Biosensors
Author Mr. Apon Numnuam
Major Program Chemistry

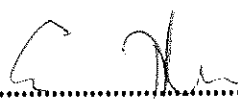
Major Advisor

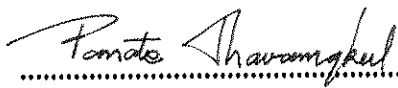

.....
(Assoc. Prof. Dr. Panote Thavarungkul)

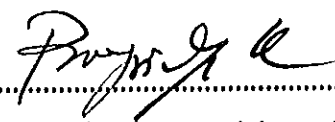
Co-advisor

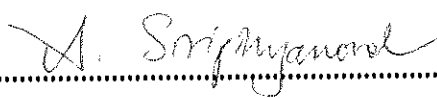

.....
(Assoc. Prof. Dr. Proespichaya Kanatharana)

Examining Committee



.....Chairperson
(Prof. Dr. Eric Bakker)


.....
(Assoc. Prof. Dr. Panote Thavarungkul)


.....
(Assoc. Prof. Dr. Proespichaya Kanatharana)


.....
(Asst. Prof. Dr. Atitaya Siripinyanond)

The Graduate School, Prince of Songkla University, has approved this thesis
as fulfillment of the requirements for the Doctor of Philosophy Degree in Chemistry


.....
(Assoc. Prof. Dr. Krerkchai Thongnoo)
Dean of Graduate School

ชื่อวิทยานิพนธ์ โฟโตนิกโอมเมทริกและคาปาซิทีฟแอฟฟินิตีไบโอเซนเซอร์

ผู้เขียน นายอากรณ์ นุ่มน่วม

สาขาวิชา เคมี

ปีการศึกษา 2551

บทคัดย่อ

วิทยานิพนธ์นี้พัฒนาและทดสอบประสิทธิภาพของอุปกรณ์ทางเคมีไฟฟ้าสำหรับตรวจวัดการจับแบบแอฟฟินิตีไบโอเซนเซอร์ทั้งโดยตรง และโดยอ้อม (direct and indirect affinity biosensor detection) การจับแบบแอฟฟินิตีตรวจวัดโดยอ้อมอาศัยหลักการโฟโตนิกโอมเมทริกโดยใช้ไอออนซีเล็กทีฟอิเล็กโทรด (potentiometric ion-selective electrode) ในการวิเคราะห์แบบแซนด์วิช (sandwich assay) โดยสารที่ต้องการวิเคราะห์ (target analyte) จะถูกจับโดยวัสดุชีวภาพ (bioaffinity molecules) ที่ตรึงบนผิวทอง หลังจากนั้นเติมวัสดุชีวภาพตัวที่สองซึ่งติดฉลากด้วยควอนตัมดอทแคดเมียมซัลไฟด์ (CdS quantum dot) จากนั้นเติมไฮโดรเจนเปอร์ออกไซด์ แคดเมียมซัลไฟด์จะถูกออกซิไดซ์เป็นแคดเมียมไอออน (Cd^{2+}) และตรวจวัดด้วยแคดเมียมไอออนซีเล็กทีฟอิเล็กโทรด (Cd^{2+} ion-selective electrode) ได้ศึกษาและทดสอบระบบโดยใช้คู่แอฟฟินิตีสองคู่ คือ ทรอมบินแอฟแทมเมอร์ (thrombin aptamer) กับ ทรอมบิน (thrombin) และดีเอ็นเอกับดีเอ็นเอ (DNA-DNA) หรือ ดีเอ็นเอไฮบริไดเซชัน (DNA hybridization) โดยการจับกันคู่แอฟฟินิตีทั้งสองคู่ที่ศึกษาในงานวิจัยนี้เป็นครั้งแรกที่ศึกษาโดยใช้ไอออนซีเล็กทีฟโฟโตนิกโอมเมทริกอิเล็กโทรด

สำหรับคู่แอฟฟินิตีของทรอมบินแอฟแทมเมอร์ (thrombin aptamer) กับ ทรอมบิน (thrombin) พบว่าไอออนซีเล็กทีฟอิเล็กโทรดสามารถตรวจวัดทรอมบิน ในช่วงความเป็นเส้นตรงระหว่าง 10 ถึง 250 ไมโครกรัมต่อลิตร และขีดจำกัดของการตรวจวัดคือ 5 ไมโครกรัมต่อลิตร หรือ 28 เฟมโตโมล (28 fmol) ในปริมาตรการวัด 200 ไมโครลิตร ซึ่งมีค่าเท่ากับ 0.14 นาโนโมลาร์ (0.14 nM) ในกรณีของดีเอ็นเอเทคนิคนี้มีความจำเพาะเจาะจงสูงโดยสัญญาณมีการเปลี่ยนแปลงเล็กน้อยเมื่อเกิดการจับของสายดีเอ็นเอที่มี 2 เบสไม่เข้าคู่กัน และให้ช่วงความเป็นเส้นตรงระหว่าง 0.01 นาโนโมลาร์ ถึง 500 นาโนโมลาร์ (0.01-500 nM) ที่ขีดจำกัดของการตรวจวัด 10 พิโคโมลาร์ (10 pM) หรือ 2 เฟมโตโมล (2 fmol) ของปริมาตรการวัด 200 ไมโครลิตร

สำหรับการตรวจวัดการจับแบบแอฟฟินิตีโดยตรงอาศัยการวัดค่าความจุไฟฟ้า (capacitance) โดยวัสดุชีวภาพ (bioaffinity molecules) จะถูกตรึงบน เซลฟ-แอสเซมเบิลโมโนเลเยอร์ (self-assembled monolayer, SAM) บนขั้วอิเล็กโทรดทองซึ่งเป็นอิเล็กโทรดทำงาน (working electrode) การจับกันอย่างจำเพาะเจาะจงของสารที่ต้องการวิเคราะห์ (target analyte) กับวัสดุ

ชีวภาพบนอิเล็กทรอนิกส์ทำงานทำให้ค่าความจุไฟฟ้า (capacitance) ลดลง ศึกษาและทดสอบประสิทธิภาพของระบบ โดยใช้คู่แอฟฟิไนต์ 3 คู่ คือ โปรตีนฮิสโตน (histone) กับ ดีเอ็นเอ (DNA) แลครีเพรสเซอร์ (*lac repressor*) กับ พลาสมิดดีเอ็นเอ (plasmid DNA) และ ดีเอ็นเอ (DNA) กับเตตราไซคลิน (tetracycline)

ในการตรวจวัดดีเอ็นเอทำโดยตรึงฮิสโตนจากไทมัสของลูกวัว (calf thymus histone) และ ของกุ้ง (shrimp histone) บนอิเล็กทรอนิกส์ทอง และใช้ตรวจวัดดีเอ็นเอจากไทมัสของลูกวัว กุ้ง และจาก แบคทีเรียอีโคไล (*E.coli*) จากการทดลองพบว่าฮิสโตนสามารถจับกับดีเอ็นเอที่มาจากแหล่งเดียวกันได้ดีกว่าต่างแหล่ง ภายใต้สภาวะที่เหมาะสมทั้งฮิสโตนจากไทมัสของลูกวัว และกุ้ง ให้ขีดจำกัดต่ำสุดของการวัดดีเอ็นเอจากทั้งสามแหล่งอยู่ที่ 1.0×10^{-5} นาโนกรัมต่อลิตร จากการศึกษาการจับกันของฮิสโตนและดีเอ็นเอจากไทมัสของลูกวัว พบว่าให้ช่วงความเป็นเส้นตรงสองช่วง คือ 1.0×10^{-5} ถึง 1.0×10^{-2} นาโนกรัมต่อลิตร และ 1.0×10^{-1} ถึง 1.0×10^2 นาโนกรัมต่อลิตร นอกจากนี้อิเล็กทรอนิกส์สามารถนำกลับมาใช้ใหม่ได้ถึง 43 ครั้ง โดยให้ค่ามีค่าเบี่ยงเบนมาตรฐานสัมพัทธ์ (relative standard deviation) 3.1 เปอร์เซ็นต์ เมื่อนำไปวิเคราะห์หาดีเอ็นเอในโปรตีนที่สกัดจากกุ้ง พบว่าจะให้เปอร์เซ็นต์การได้กลับคืน 80-116 เปอร์เซ็นต์

ในการประยุกต์ใช้ระบบคาปาซิทิฟในการตรวจวัดหาพลาสมิดดีเอ็นเอ ได้ตรึงแลครีเพรสเซอร์โปรตีนบนอิเล็กทรอนิกส์ทอง ภายใต้สภาวะที่เหมาะสมศึกษาผลของพลาสมิดที่มีลักษณะเกลียว (supercoiled plasmid DNA) และคลายเกลียว (open circular plasmid DNA) ต่อสัญญาณการตอบสนอง พบว่าทั้งพลาสมิดที่เป็นเกลียว (supercoiled plasmid DNA) และคลายเกลียว (open circular plasmid DNA) จะให้ช่วงความเป็นเส้นตรงเดียวกันสองช่วง คือ 0.0001 ถึง 0.1 นาโนกรัมต่อมิลลิลิตร และ 1 ถึง 1,000 นาโนกรัมต่อมิลลิลิตร และ ขีดจำกัดต่ำสุดของวัด 0.002 พิโคกรัมต่อลิตรและ 0.03 พิโคกรัมต่อลิตร สำหรับพลาสมิดคลายเกลียว และเป็นเกลียวตามลำดับ นอกจากนี้อิเล็กทรอนิกส์สามารถนำมาใช้ใหม่ได้มากกว่า 40 ครั้ง โดยมีค่าเบี่ยงเบนมาตรฐานสัมพัทธ์น้อยกว่า 4.0 เปอร์เซ็นต์

นอกจากนี้ระบบคาปาซิทิฟสามารถนำไปประยุกต์ใช้สำหรับตรวจวัดเตตราไซคลิน (Tetracyclines) โดยการตรึงดีเอ็นเอสายคู่ (double stranded DNA) ภายใต้สภาวะที่เหมาะสม ศึกษาผลของเตตราไซคลิน (Tetracycline) และอนุพันธ์ของเตตราไซคลิน ได้แก่ คลอเตตราไซคลิน (chlortetracycline) และ ออกซีเตตราไซคลิน (oxytetracycline) ต่อสัญญาณการตอบสนอง พบว่าจะให้ช่วงความเป็นเส้นตรง 1.0×10^{-4} ถึง 1.0×10^2 ไมโครกรัมต่อลิตร สำหรับเตตราไซคลินและคลอเตตราไซคลิน และ 1.0×10^{-3} ถึง 1.0×10^3 สำหรับออกซีเตตราไซคลิน โดยให้ขีดจำกัดต่ำสุดของการวัด 1.0×10^{-5} ไมโครกรัมต่อลิตร สำหรับเตตราไซคลินและคลอเตตราไซคลิน และ 0.5×10^{-4}

ไมโครกรัมต่อลิตร สำหรับออกซีเตตราไซคลิน นอกจากนี้อิเล็กโทรดสามารถนำกลับมาใช้ใหม่ได้ ถึง 54 ครั้ง โดยมีค่าเบี่ยงเบนมาตรฐานสัมพัทธ์ น้อยกว่า 4.0 เปอร์เซ็นต์ เมื่อนำไปวิเคราะห์เตตราไซคลินที่ตกค้างในน้ำเสียของโรงพยาบาล พบว่าจะให้เปอร์เซ็นต์การได้กลับคืน 71-102 เปอร์เซ็นต์ และทดสอบความใช้ได้ของวิธีที่พัฒนาขึ้นด้วยเทคนิคลิควิดโครมาโทกราฟีสมรรถนะสูง (High Performance Liquid Chromatography, HPLC) ซึ่งการมีอยู่ของเตตราไซคลินในตัวอย่างน้ำเสียสามารถตรวจวัดได้ทั้งเทคนิคฟลูออโรเมตริกและลิควิดโครมาโทกราฟีสมรรถนะสูง

Thesis title	Potentiometric and Capacitive Affinity Biosensors
Author	Mr. Apon Numnuam
Major Program	Chemistry
Academic Year	2008

Abstract

This thesis focuses on the development and evaluation of the performance of electrochemical transducer for direct and indirect detection of affinity biosensors. Indirect detection of affinity reactions were investigated with potentiometric ion-selective electrode. The detection rely on sandwich assay where target analyte was bound to immobilized bioaffinity molecules on the gold substrate and secondary bioaffinity molecule conjugated with CdS quantum dot label was further added. Then, CdS was dissolved with H₂O₂ yielding a diluted electrolyte background suitable for potentiometric detection of released Cd²⁺ with polymeric membrane Cd²⁺-selective microelectrode. Two affinity binding pairs were studied, thrombin aptamer-thrombin and DNA-DNA (DNA hybridization). This is the first time for both of these affinity pairs that they are demonstrated with ion-selective microelectrode.

For thrombin aptamer-thrombin binding, ion selective microelectrode gave the linearity range of 10-250 ppb with a limit of detection at 5 ppb, corresponding to 28 fmol in 200 μ l or 0.14 nM. In case of DNA hybridization, it can detect the target DNA with high selectivity, including effective discrimination against 2-base mismatched DNA and show a wide linear dynamic range of 0.01-500 nM with the limit of detection at 10 pM or 37 pg or 2 fmol in 200 μ l.

Direct detection of affinity biosensor was performed by potentiostatic capacitance measurments. Bioaffinity molecules were immobilized on self-assembled monolayer (SAM) of thioctic acid on working gold electrode (WE). The binding between target analyte and immobilized bioaffinity molecule on gold electrode cause the capacitance to decrease. The capacitance due to the direct affinity reaction could then be determined from the cureent response when a potential step was applied.

Three affinity binding pairs, histone-DNA, *lac* repressor protein-plasmid DNA and DNA-tetracyclines (TCs) were investigated in a flow injection system.

The DNA detection was investigated by immobilized histone on the electrode surface. Histones from calf thymus and shrimp were immobilized on gold electrodes covered with self-assembled monolayer (SAM) of thiocetic acid. Each of these histones were used to detect DNA from calf thymus, shrimp and *E. coli*. The studies indicated that histones can bind better with DNA from the same source and give higher sensitivity than the binding with DNA from different sources. Under optimum conditions, both histones from calf thymus and shrimp provided the same lower detection limit of $10^{-5} \text{ ng l}^{-1}$ for DNA from different sources i.e., calf thymus, shrimp and *E.coli*. For the affinity reaction between calf thymus histone and DNA two linear ranges, 10^{-5} to $10^{-2} \text{ ng l}^{-1}$ and 10^{-1} to 10^2 ng l^{-1} , were obtained. The immobilized histones were stable and after regeneration good reproducibility of the signal could be obtained up to 43 times with a %RSD of 3.1. When applied to analyze residual DNA in crude protein extracted from white shrimp good recoveries were obtained between 80-116 %.

Further application of capacitive transducer is plasmid DNA detection with immobilized *lac* repressor protein. Under optimum conditions, a study of the influence of different isoforms of plasmid DNA were detected by injecting supercoiled plasmid DNA (sc pDNA) and open circular (relaxed form) plasmid DNA (oc pDNA) into the capacitive biosensor system. The observed capacitance signal from open circular or relaxed form was similar to that of supercoiled plasmid DNA. The linear ranges were the same for both isoforms, from 0.0001 to 0.1 ng ml^{-1} and 1 to $1,000 \text{ ng ml}^{-1}$, with lower detection limits of 0.002 pg ml^{-1} and 0.03 pg ml^{-1} for open circular and supercoiled plasmid DNA, respectively (Table 10.3). The immobilized *lac* repressor protein on self-assembled monolayer (SAM) gold electrode was stable and could be reused up to more than 40 times with RSD lower than 4.0 %.

In addition, this technique was also applied for screening detection of tetracycline by immobilized double-stranded DNA on gold electrode surface. Under optimum conditions, influence of three different compounds of tetracycline(s), i.e., tetracycline (TC), chlortetracycline (CTC) and oxytetracycline (OTC), to immobilized dsDNA was studied. It showed a linear dynamic range of 10^{-4} - $10^2 \text{ } \mu\text{g l}^{-1}$ for

tetracycline and chlortetracycline, and 10^{-3} - $10^3 \mu\text{g l}^{-1}$ for oxytetracycline. The detection limit was $10^{-5} \mu\text{g l}^{-1}$ for tetracycline and chlortetracycline, and 0.5×10^{-4} for oxytetracycline (Table 10.3). The immobilized DNA was stable and after regeneration good reproducibility of signal could be obtained up to 54 times with % RSD < 4. When applied to analyze residual tetracycline in wastewater from hospital recoveries were obtained between 71-102%. The presence of tetracyclines (TCs) in wastewater sample could be detected by both biosensor and HPLC.

Acknowledgements

The completion of this thesis would be impossible without the help of many people, whom I would like to thank.

I express my special gratitude and sincere appreciation to my advisors, Associate Professor Dr. Panote Thavarungkul and Associate Professor Dr. Proespichaya Kanatharana for the opportunity to work on very interesting and challenging projects, for all the help, valuable guidance, comments, encouragement throughout my study, particularly their excellent teaching and supervision.

I would like to thank Prof. Eric Bakker and Dr. Karin Y. Chumbimuni Torres for their kindness, valuable advice and support conducted on part of my research at Department of Chemistry, Purdue University, West Lafayette, Indiana USA. The kindness of Professor Dr. Joseph Wang for giving me the scientific opportunity and financial support to do the research at The Biodesign Institute and Fulton School of Engineering, Arizona State University, Tempe, Arizona, USA.

My sincere thanks are extended to Professor Dr. Bo Mattiasson, Dr. Martin Hedström and Dr. Amro Hanora for their advice, help and support during my research at Department of Biotechnology, Center for Chemistry and Chemical Engineering, Lund University, Lund Sweden.

I would also like to thank Assistant Professor Punnee Asawatreratanakul for her help and suggestion about the biochemistry knowledge.

I also thank Associate Professor Dr. Amornrat Pongdara, Dr. Warapond Wanna and Ms. Alisa Nakkaew from Center for Genomic and Bioinformatic Research, Faculty of Science, Prince of Songkla University for their help and discussion on DNA purification. I also thank Assoc. Prof. Dr. Prapaporn Utarabhand from Department of Biochemistry, Faculty of Science, Prince of Songkla University for her discussion on extraction and purification of shrimp histone.

Thanks are also expressed to examination committee members of this thesis for their valuable time. All the help in some technical aspects rendered by staffs of Department of Chemistry, Faculty of Science, Prince of Songkla University, staffs of the Department of Biotechnology, Center for Chemistry and Chemical

Engineering, Lund University, Lund Sweden, staffs of Department of Chemistry, Purdue University, West Lafayette, Indiana USA and staffs of The Biodesign Institute and Fulton School of Engineering, Arizona State University, Tempe, Arizona, USA.

I am deeply indebted to the Royal Golden Jubilee Ph.D. Program (RGJ) of the Thailand Research Fund (TRF) for the scholarship; Center of Excellence for Innovation in Chemistry (PERCH-CIC), Commission on Higher Education, Thailand; The Swedish Research Council (VR) and The Swedish International Development Cooperation Agency research links (SIDA) and Graduate School, Prince of Songkla University for the partial support of the research fund; the National Institutes of Health, USA (RO1 ER002189 and RO1 1056047) for a grant during my visit in Purdue and Arizona, USA.

Friendship of members in Trace Analysis and Biosensor Research Center are also acknowledged for their help in many ways. Special thanks to my best friend, Kaewta Kaewtathip for her continuous support and encouragement.

Finally, I would like to express my deepest gratitude and dedication to my beloved my father, mother, brother and sisters for their love and attentions throughout my life.

Apon Numnuam

The Relevance of the Research Work to Thailand

The purpose of this Doctor of Philosophy Thesis in Chemistry (Analytical Chemistry) is to develop and evaluate the performance of electrochemical transducer for direct and indirect detection of affinity binding. Potentiometry with ion-selective microelectrode was developed for indirect detection of target DNA and thrombin protein. For direct detection, capacitive transducer was investigated for the detection of genomic DNA, plasmid DNA and tetracycline. Both indirect detection with potentiometric ion-selective microelectrode and direct detection with capacitive transducer provide good performance *i.e.*, high sensitivity, selectivity, accuracy and precision and short time analysis. They can be applied for the quantitative analysis of trace amount of target analyte by, for examples, several governmental organization in Thailand which are

- Ministry of Public Health
- Ministry of Industry
- Ministry of Environmental
- Ministry of Education

Contents

	Page
List of Tables	xix
List of Figures	xxi
Chapter 1: Introduction	1
1.1 Background and Rationale	1
1.2 Objectives of the research	4
1.3 Benefits	4
Chapter 2: Affinity Biosensors	5
2.1 Biosensor	5
2.2 Assays format for affinity biosensor	7
2.2.1 Direct assay	8
2.2.2 Indirect assay	8
2.3 Types of affinity biosensor	11
2.3.1 Immunosensor	11
2.3.2 Receptor biosensor	13
2.3.3 DNA biosensor	15
2.3.3.1 DNA hybridization biosensor	15
2.3.3.2 DNA-small molecule biosensor	16
2.3.4 Nucleotide receptor (Aptamer)-ligand biosensor	18
2.3.5 Protein binding DNA biosensor	20
2.4 Detection principle of affinity biosensor	21
2.4.1 Optical transducer	21
2.4.2 Piezoelectric transducer	24
2.4.3 Electrochemical transducer	26
Chapter 3: Electrochemical Detection of Affinity Biosensors	27
3.1 Direct electrochemical detection	27
3.1.1 Impedimetric affinity biosensors	28

Contents (Continued)

	Page
3.1.2 Capacitive affinity biosensors	34
3.1.2.1 Impedimetric	38
3.1.2.2 Potential step	40
3.2 Indirect electrochemical detection	43
3.2.1 Amperometric affinity biosensors	43
3.2.2 Voltammetric stripping affinity biosensors	45
3.2.3 Conductimetric affinity biosensors	48
3.2.4 Potentiometric affinity biosensors	50
 Chapter 4: Performance Criteria	 54
4.1 Linear range, sensitivity and limit of detection	54
4.2 Selectivity	57
4.3 Regeneration, stability and reproducibility	57
 Chapter 5: Aptamer-Based Potentiometric Measurements of Proteins Using Ion-Selective Microelectrodes	 59
5.1 Introduction	59
5.2 Materials	61
5.3 Methods	62
5.3.1 Preparation of cadmium ion selective microelectrode (Cd-ISE)	62
5.3.1.1 Cd-ISE Membrane	62
5.3.1.2 Microelectrode	63
5.3.2 Preparation of CdS quantum dot nanocrystals	64
5.3.3 Thrombin aptamer immobilization and binding assay using sandwich format	64
5.3.3.1 Preparation of oligonucleotide aptamer on gold surface	65
5.3.3.2 Preparation of CdS quantum dot– oligonucleotide aptamer conjugates	65

Contents (Continued)

	Page
5.3.3.3 Sandwich aptamer-protein assay	66
5.3.3.4 Dissolution and detection	66
5.3.4 Potentiometric Measurements	66
5.4 Results and discussion	67
5.4.1 Characterization of Cd ²⁺ ion selective microelectrode	67
5.4.2 Thrombin determination using Cd ²⁺ selective microelectrode	70
5.4.2.1 Concentration of hydrogen peroxide (H ₂ O ₂) and reaction time for dissolution of Cd ²⁺	70
5.4.2.2 Influence of incubation time	71
5.4.2.3 Influence of the concentration of secondary aptamer	72
5.4.2.4 Selectivity of thrombin aptamer	73
5.4.2.5 Calibration curve	74
5.5 Conclusions	75
 Chapter 6: Potentiometric Detection of DNA Hybridization	 76
6.1 Introduction	76
6.2 Materials	77
6.3 Methods	78
6.3.1 DNA immobilization and detection	78
6.3.1.1 Preparation of the oligonucleotide probe on the gold surface	79
6.3.1.2 Preparation of CdS quantum dot – oligonucleotide conjugate	79
6.3.1.3 Sandwich DNA hybridization assay	80
6.3.1.4 Dissolution and Detection	80
6.4 Results and Discussion	80
6.4.1 Concentration of primary DNA probe (Probe1)	81

Contents (Continued)

	Page
6.4.2 Incubation time between primary DNA probe and target DNA	81
6.4.3 Concentration of secondary probe (Probe 2)	82
6.4.4 Incubation time between secondary DNA probe and target DNA	83
6.4.5 Selectivity	84
6.4.6 Calibration curve	85
6.5 Conclusions	86
Chapter 7: Capacitive Biosensor for Quantification of Trace DNA	87
7.1 Introduction	87
7.2 Materials	89
7.3 Methods	90
7.3.1 Immobilization of histones	90
7.3.2 Capacitance measurements	91
7.3.3 Optimization of the capacitive biosensor	93
7.3.4 Determination of trace amount DNA in real sample	93
7.4 Results and discussion	93
7.4.1 Insulating property of working electrode	93
7.4.2 Capacitance measurement of the binding between immobilized histone and DNA	94
7.4.3 Optimization of the flow injection capacitive biosensor	96
7.4.3.1 Regeneration solution	96
7.4.3.2 Buffer solution	98
7.4.3.2.1 Type	98
7.4.3.2.2 Concentration	99
7.4.3.2.3 pH	100
7.4.3.3 Flow rate	101
7.4.3.4 Sample volume	102

Contents (Continued)

	Page
7.4.4 Reproducibility	105
7.4.5 Linear dynamic range and detection limit	107
7.4.6 Selectivity	108
7.4.7 Determination of residual shrimp DNA	111
7.4.7.1 Matrix matched calibration	112
7.4.7.2 Dilution	114
7.5 Conclusions	116
 Chapter 8: Capacitive Biosensor for Plasmid DNA Detection	 117
8.1 Introduction	117
8.2 Materials	118
8.3 Methods	119
8.3.1 Preparation of plasmid DNA from <i>E. coli</i> .	119
8.3.1.1 Bacterial culture and isolation of plasmid DNA	119
8.3.1.2 Plasmid DNA purification	120
8.3.2 Preparation of lac repressor modified electrodes	120
8.3.3 Capacitive measurement	121
8.3.4 Cyclic voltammetry measurements	122
8.3.5 Optimization of the capacitive biosensor	123
8.4 Results and Discussion	123
8.4.1 Plasmid DNA quality	123
8.4.2 Insulating property of working electrode	124
8.4.3 Capacitance measurement	125
8.4.4 Optimization of the capacitive biosensor system	126
8.4.4.1 Regeneration solution	126
8.4.4.2 Buffer solution	128
8.4.4.2.1 Type	128
8.4.4.2.2 pH	129
8.4.4.2.3 Concentration	130

Contents (Continued)

	Page
8.4.4.3 Flow rate	131
8.4.5 Reproducibility of the <i>lac</i> repressor electrode	134
8.5 Response for plasmid DNA with different molecular forms	134
8.6 Conclusions	136
 Chapter 9: Capacitive DNA Biosensor for Tetracyclines Detection	 137
9.1 Introduction	137
9.2 Materials	140
9.3 Methods	141
9.3.1 Immobilization of double-stranded DNA ((dsDNA)	141
9.3.2 Capacitance measurements	142
9.3.3 Optimization of the flow injection capacitive biosensor	144
9.3.4 Determination of the amount of tetracyclines in real sample	145
9.4 Results and Discussion	145
9.4.1 Electrochemical performance of the immobilization process	145
9.4.2 Optimization of flow injection capacitive biosensor	146
9.4.2.1 Regeneration solution	146
9.4.2.2 Buffer solution	148
9.4.2.2.1 Type	148
9.4.2.2.2 pH	149
9.4.2.2.3 Concentration	149
9.4.2.3 Flow rate	150
9.4.2.4 Sample volume	151
9.4.3 Reproducibility	154
9.4.4 Response for dsDNA with Tetracycline(TCs)	155
9.4.5 Mixture of different tetracyclines	157
9.4.6 Determination of tetracyclines in wastewater	158

Contents (Continued)

	Page
9.4.7 Comparison between capacitive and HPLC	161
9.5 Conclusions	164
Chapter 10: Conclusions	165
References	174
Appendices	223
Appendix A	224
Appendix B	231
Vitae	234

List of Tables

Table	Page
5.1 The EMF values of the Cd-ISE in 200 μ l sample volume for the concentration of CdCl ₂ in rang of 10 ⁻¹⁰ -10 ⁻⁵ M.	68
5.2 Selectivity coefficient ($\log K_{Cd,J}^{pot}$) determine by the separation solution method.	69
7.1 Assayed and optimized conditions of the type, pH and concentration of regeneration solution. The efficiency of DNA removal from the histone immobilized on the electrode was studied by injecting 1 ng l ⁻¹ of standard DNA solution.	98
7.2 Assayed parameters and optimized values of the capacitive system. Capacitive change is from the injection of 1 ng l ⁻¹ of calf thymus DNA.	104
7.3 Recovery of shrimp DNA from spiked crude shrimp protein (n=3); using Matrix matched calibration (Section 7.3.1) and Dilution methods (section 3.7.2)	114
8.1 Assayed and optimized values of the type, pH and concentration of regeneration solution with sample volume of 250 μ l and 100 μ l min ⁻¹ of flow rate. The efficiency of plasmid DNA removal from the <i>lac</i> repressor immobilized on the electrode was studied by injecting ng ml ⁻¹ of plasmid DNA standard.	128
8.2 Assayed and optimized values of parameters for plasmid DNA analysis by a capacitive biosensor system.	133
9.1. Assayed and optimized conditions of the type, and concentration of regeneration solution. The efficiency of tetracycline removal from the dsDNA immobilized on the electrode was studied by injecting 100 ng l ⁻¹ of standard tetracycline solution.	147
9.2. Assayed parameters and optimized values of the capacitive system. Capacitive change is from the injection of 100 ng l ⁻¹ of tetracycline.	153
9.3 Recovery tetracycline from spiked wastewater (n=3)	161

List of Tables (Continued)

Table	Page
9.4 Concentration Tetracycline obtained by capacitive biosensor.	161
9.5 Concentration of OTC, TC and CTC in wastewater analyzed by standard addition method.	163
10.1 Comparison of Analytical features of aptamer-thrombin biosensors.	167
10.2 Comparison of Analytical features of DNA hybridization biosensors.	168
10.3 Performance of flow injection capacitive biosensor systems for different analytes studied in this work.	172

List of Figures

Figure	Page
2.1 Schematic illustration of the components of a biosensor.	5
2.2 Biosensor types a) catalytic biosensor, b) affinity biosensor.	7
2.3 Direct assay format for affinity biosensor.	8
2.4 Two main types of labeled affinity sensor. a) competitive, b) sandwich assay.	10
2.5 Structure of antibody.	12
2.6 Steps involved in DNA biosensor.	16
2.7 Binding way of the small molecule to double helix DNA.	17
2.8 Typical set-up for a surface plasmon resonance biosensor. The SPR angle shift (from 1 to 2 in diagram) when biomolecules bind to the surface and change the surface layer. This change in resonance angle can be monitored in real time as plot of resonance signal versus time (Adapted from Shankaran <i>et al.</i> , 2007).	22
2.9 Illustration of two types of labeled affinity biosensor based on optical detection; a) sandwich and b) competitive assay.	23
2.10 Schematic of piezoelectric biosensors. The frequency of oscillation of a piezoelectric material is dependent on its mass. (a) On a bulk acoustic wave (BAW). (b) On surface acoustic wave (SAW).	25
3.1 Schematic represent of a simple electrified interface at electrode/ electrolyte solution interface; (a) double layer region which consist of Helmholtz planes (i.e., Inner Helmholtz plane (IHP) and outer Helmholtz plane (OHP)) and diffusion layer, C_H is the capacitance due to Helmholtz layer and C_{DL} is capacitance due to the diffusion layer; (b) Randle equivalent circuit representing each component at interface and in solution during electrochemical reaction is shown for comparison with physical components. C_{dl} , double layer capacitor; R_{et} , charge transfer resistor; W , Warburg resistor; R_s , solution resistor) (Modified from Bard and Fulkner, 2001; Park and Yoo, 2003; Wang, 2001).	29

List of Figures (Continued)

Figure	Page
3.2 Faradaic impedance spectra presented in the form of a Nyquist plot for modified electrode is controlled by; a) diffusion of the redox probe (low frequencies) and the interfacial electron transfer (high frequencies). b) diffusion of the redox probe. c) the interfacial electron transfer (Modified from Katz and Willner, 2003).	32
3.3 Typical Nyquist plot of immobilized bioaffinity molecule on the electrode surface (a) and complex of specific analyte-bioaffinity molecule (b) (Modified from Kharotonov <i>et al.</i> , 2000; Tang <i>et al.</i> , 2004).	33
3.4 Schematic diagram of capacitive affinity biosensor based on two metal plates (a) capacitance change due to the change in distance and/ or dielectric constant between two plates and (b) due to the dielectric constant using interdigitate electrode (Modified from Gebbert <i>et al.</i> , 1992; Berggren <i>et al.</i> , 2001).	36
3.5 Schematic representation of affinity biosensor based capacitive biosensor and electrical double layer organized on the electrode solution interface.	37
3.6 Bode plotsof of phase angles <i>versus</i> the log of frequency.	39
3.7 (a) $R_s(R_fC_{dl})$ equivalent circuit, where R_f is the Ohmic resistance of insulating layer that is much higher than R_s making its act like an open circuit. (b) Simple R_sC_{dl} equivalent circuit, R_s is the resistance of the solution and C_{dl} the double layer capacitance.	40
3.8 Potentiostatic step method to evaluate capacitance (a) applied potential pulse and (b) resulting current decay.	41
3.9 Logarithm of current <i>vs</i> time.	42
3.10 Schematic of the amperometric detection for affinity biosensor based (a) sandwich and (b) competitive assay by enzyme –labeled.	44

List of Figures (Continued)

Figure	Page
3.11 Anodic stripping voltametry: (a) the potential -time wave form , (b) along with voltammogram (Modifoed from Wang, 2000; Esteban and Cassassas, 1994).	46
3.12 Direct anodic stripping voltametric detection of affinity binding based on nanoparticle label (Modified from Ozsoz <i>et al.</i> , 2003; Kerman <i>et al.</i> , 2007).	47
3.13 Indirect anodic stripping voltametric detection of affinity binding based on nanoparticl label.	48
3.14 Schematic diagram of a conductivity assay in which nanoparticled labeled filled between electrode.	49
3.15 Conductivity assay based conducting polymer labeled which form the molecular wire for generating signal.	50
3.16 Schematic diagram of an electrochemical cell for potentiometric measurement.	51
3.17 Potentiometric detection of sandwich immunoassay based on capture gold nanoparticles and the deposition and subsequence dissolution of silver, which was detected with Ag-ISE.	53
4.1 Calibration curve showing relationships for determining linear range, sensitivity and limit of detection (Buck and and Lindner, 1994; Eggin, 1996; Wang, 2000).	55
4.2 Calibration graph for the detectability characteristic (Adapted from Currell, 2000).	56
5.1 Solid contact Cd-ISE microelectrode.	63
5.2 Representation of the analytical protocol: A) Formation of a mixed monolayer of thiolated aptamer on gold substrate; B) thrombin addition and binding with aptamer; C) secondary binding with CdS-labeled aptamer, D) dissolution of CdS label followed by detection using a solid-contact Cd ²⁺ - selective microelectrode.	64

List of Figures (Continued)

Figure	Page
5.3 Schematic view of potentiometric measurement in 200 μ l of ELISA microwells.	67
5.4 Calibration curves of solid-contact Cd^{2+} -selective electrode: A) in 100 ml and B) in 200- μ l samples with 10^{-4} CaCl_2 as background using ELISA microplates.	68
5.5 Time response for the Cd^{2+} -ISE in a 200 μ l sample well, containing the indicated H_2O_2 concentrations.	71
5.6 Responses at different incubation times between immobilized 1000 nM primary aptamer and 100 ppb of thrombin in 15, 30, 45, and 60 min (error bars: SD, $N = 3$). Potentiometric measurements were performed in 200 μ l samples with 10^{-4} M CaCl_2 as background electrolyte and a Ca-ISE as reference electrode.	72
5.7 Response to various concentration of secondary aptamer with 100 ppb of target thrombin previously bound to 1000 nM primary aptamer (error bars: SD, $N = 3$).	73
5.8 Potentiometric responses of the Cd^{2+} -selective electrode for the control (zero target), 500 ppb lysozyme, 500 ppb IgG (as noncomplementary targets), 50 ppb thrombin, , and 100 ppb thrombin (as complementary target) after aptamer-thrombin interaction.	74
5.9 Potentiometric monitoring of thrombin concentration <i>via</i> CdS quantum dot label in 200 μ l microwells with the aptamer-thrombin sandwich assay (error bars: SD, $N = 3$).	75
6.1 Representation of analytical protocol : (A) Formation of mixed monolayer of DNA probe on gold substrate: (B) hybridization with target DNA: (C) second hybridization with CdS-labeled probe and (D) dissolution of CdS tag followed by detection using ion selective electrode.	78

List of Figures (Continued)

Figure	Page
6.2 Effect of concentration of immobilized primary DNA probe to 100 nM of target DNA using 1000 nM of secondary DNA.	81
6.3 Responses of different incubation times between 1000 nM of immobilized primary probe, 100 nM of target DNA and 1000 nM secondary probe.	82
6.4 Responses of different concentrations of secondary DNA probe with 100 nM target bound to 1000 nM primary probe.	83
6.5 Responses of different incubation times between 1000 nM of secondary probe and 100 nM target DNA.	84
6.6 Potentiometric responses of the cadmium-selective electrode for the control (zero target), 500 nM noncomplementary, 500 nM 2-base mismatch, 10nM of target and 100 nM of target DNA (as complementary targets) after DNA hybridization.	85
6.7 Potentiometric monitoring of DNA concentration via CdS quantum Dot label in 200 μ L microwells with the DNA hybridization sandwich assay.	86
7.1 Wrapping of DNA around nucleosome core, Nucleosome composed of the pair of histone, H2A, H2B, H3 and H4 to form an octamer core structure and H1 acts as the linker between nucleosome particle (Adapted from Reece, 2004).	89
7.2 Schematic diagram of the flow injection capacitive biosensor system. The total capacitance measured at the working electrode/solution Interface (C_{tot}) comes from C_{SAM} ; the capacitance of self-assembled thioctic acid monolayer, $C_{Histone}$; the capacitance of histone layer and C_{DNA} ; the capacitance DNA analyte interaction.	92

List of Figures (Continued)

Figure	Page
7.3 Cyclic voltammograms of a gold electrode obtained in 5 mM $K_3[Fe(CN)_6]$ containing 0.1 M KCl solution at scan rate of 0.1 V s^{-1} . All potentials are given vs Ag/AgCl. (A) clean gold, (B) thiocetic acid covered gold, (C) histone modified thiocetic acid couple gold, and (D) as in (C) but after 1-dodecanethiol treatment.	94
7.4 An example of the capacitance (C_{tot}) plots as a function of time. The binding between histone and DNA cause the capacitance to decrease (ΔC_1) with subsequent signal increase due to dissociation under regeneration conditions. After regeneration of the system can be reused to detect a new injection of DNA (ΔC_2).	96
7.5 Response of the flow injection capacitive biosensor system to DNA using difference buffer solutions.	99
7.6 Response of the capacitive biosensor system to 1 ng l^{-1} at different concentrations of Tris- HCl buffer at pH 7.2.	100
7.7 Effect of the pH of Tris-HCl buffer solution on response to 1 ng l^{-1} DNA.	101
7.8 Response of the flow injection capacitive biosensor system at different flow rate.	102
7.9 Response of capacitive biosensor to 1 ng l^{-1} DNA at different sample volume.	103
7.10 Reproducibility of the response from histone modified electrode to injection of 250 μ l standard calf thymus DNA (1 ng l^{-1}) with regeneration steps between each individual assay.	106
7.11 Cyclic voltammogram of modified gold electrode obtained in 0.05 M ($K_3[Fe(CN)_6]$) solution, (a) is the response when on the electrode surface was blocked by 1-dodecane thiol before used and (b) after used for 50 times.	106

List of Figures (Continued)

Figure	Page
7.12 Capacitance change vs. the logarithm of calf thymus DNA concentration detected by immobilized calf thymus histone modified electrode under optimum conditions (100 $\mu\text{l min}^{-1}$ flow rate, 250 μl sample volume, 10 mM Tris-HCl buffer, pH 7.00).	108
7.13 Calibration curve for DNA from calf thymus, white shrimp and E.coli with (a) immobilized calf thymus histone and (b) white shrimp histone.	109
7.14 Effect of DNA from calf thymus, shrimp, E.coli and their mixture on the binding with calf thymus histone.	110
7.15 Response of histone to DNA and bovine serum albumin (BSA).	111
7.16 Standard and matrix matched calibration curve of crude shrimp protein sample.	113
7.17 The standard curve and spiked curve for the study of matrix interference of shrimp sample; (a) for immobilized calf thymus histone and (b) immobilized shrimp histone.	115
8.1 Schematic diagram showing the flow injection capacitive biosensor system. The electrode modified with <i>lac</i> repressor was inserted as the working electrode in a three electrode flow cell with a volume of 10 μl . As reference and auxiliary electrodes, a platinum wire and a platinum foil were used, respectively. An extra Ag/AgCl reference was placed in the outlet flow.	122

List of Figures (Continued)

Figure	Page
<p>8.2 (a) Agarose gel electrophoresis of plasmid DNA from clarified lysate. Lane 1 and 6, supercoiled DNA ladder; lane 2, clarified lysate ; lane 3, after size-exclusion chromatography; lane 4 and 5, after preconcentration with isopropanol. (b) Agarose gel electrophoresis when the interchange between supercoiled plasmid DNA (sc pDNA) to open circular plasmid DNA (oc pDNA) was performed using a thermal transition. Lane 1, purified supercoiled plasmid DNA (before heating); lane 2, empty; lane 3-6, fter heat at 95 °C for 15 min and (c) show the band of open circular form (lane 2 and 4) after purification by using siz-exclusion chromatography.</p>	124
<p>8.3 Cyclic voltammograms of a gold electrode obtained in 5 mM $K_3[Fe(CN)_6]$ containing 10 mM KCl solution at a scan rate of 10 mV s^{-1}. All potentials are given vs SCE. (A) clean gold, (B) thioctic acid covered gold, (C) <i>lac</i> repressor modified thioctic acid couple gold, and (D) as in (C) but after 1-dodecanethiol treatment.</p>	125
<p>8.4 Schematic view of the capacitance (C) as a function of time resulting from the binding between <i>lac</i> repressor and pDNA with subsequent signal increase due to dissociation under regeneration conditions where C_{SAM} is the capacitance of the self-assembled thiol monolayer, $C_{lac R}$; the capacitanceof <i>lac</i> repressor protein layer, C_{pDNA} ; the capacitance of plasmid DNA analyte interaction and C_{total}; the total capacitance change measured at the working electrode/solution interface.</p>	126
<p>8.5 Response of the flow injection capacitive biosensor system from different buffer solution.</p>	129
<p>8.6 Effect of the pH of Tris-HCl buffer solution.</p>	130
<p>8.7 Response of the capacitive biosensor system to different concentration of Tris- HCl buffer at pH 7.4.</p>	131

List of Figures (Continued)

Figure	Page
8.8 Response of the flow injection capacitive biosensor system at Different flow rates.	132
8.9 Reproducibility of the response from <i>lac</i> repressor modified electrode to injection of 250 μ l standard plamid DNA (10 ng ml ⁻¹) with regeneration steps between each individual assay.	134
8.10 Calibration curve of supercoiled and open circular plasmid DNA at optimum conditions, showing two linear ranges with difference sensitivity from 0.0001 to 0.1 ng ml ⁻¹ and 1 to 1000 ng ml ⁻¹ .	135
9.1 Structure of tetracycline and its derivatives (Modified from Santiago Valverde <i>et al.</i> , 2007).	138
9.2 Schematic reaction mechanism for dsDNA immobilized on a self-assembled thioctic monolayer (Modified from Huang <i>et al.</i> , 2000; Limbut <i>et al.</i> , 2006).	142
9.3 Schematic representation of the different layer on the electrode surface. The total capacitance measured at the working electrode/ solution interface (C_{tot}) comes from C_{SAM} ; the capacitance of self-assembled thioctic acid monolayer, C_{DNA} ; the capacitance of DNA layer and C_{TC} ; the capacitance tetracyclines analyte interaction.	143
9.4 An example of the capacitance (C_{Tot}) plots as a function of time. The binding between tetracycline and DNA cause the capacitance to decrease (ΔC_1) with subsequent signal increase due to dissociation under regeneration conditions. After regeneration of the system can be reused to detect a new injection of tetracycline (ΔC_2).	144
9.5 Cyclic voltammograms of a gold electrode obtained in 5 mM $K_3[Fe(CN)_6]$ containing 0.1 M KCl solution at scan rate of 0.1 V s ⁻¹ . All potentials are given vs Ag/AgCl. (A) clean gold, (B) thioctic acid covered gold, (C) dsDNA modified thioctic acid couple gold, and (D) as in (C) but after 1-dodecanethiol treatment.	146

List of Figures (Continued)

Figure	Page
9.6 Response of the flow injection capacitive biosensor system from different buffer solution.	148
9.7 Effect of the pH of Tris-HCl buffer solution on response to 100 ng l ⁻¹ tetracycline.	149
9.8 Response of the capacitive biosensor system to 100 ng l ⁻¹ at different concentration of Tris-HCl buffer pH 7.2.	150
9.9 Response of the flow injection capacitive biosensor at different flow rate.	151
9.10 Response of the flow injection capacitive biosensor at different sample volume.	152
9.11 Reproducibility of the response from dsDNA modified electrode to injection of 250 µl standard tetracycline (100 ng l ⁻¹) with regeneration steps between each individual assay.	154
9.12 Cyclic voltammogram of modified gold electrode obtained in 0.05 M (K ₃ [Fe(CN) ₆] solution, (a) is the response when on the electrode surface was blocked by 1-dodecane thiol before used and (b) after used for 63 times.	155
9.13 Structure of Tetracycline, Chlortetracycline and Oxytetracycline.	156
9.14 Calibration curves of tetracycline, chlortetracycline and oxytetracycline at optimum conditions.	157
9.15 Effect of tetracycline (TC), chlortetracycline (CTC) , oxytetracycline (OTC) and their mixture on binding with dsDNA.	158
9.16 Standard calibration curve and spiked curve of untreated and treated wastewater.	159
9.17 Standard calibration curve and spiked curve of untreated and treated wastewater after 1,000 times dilution.	160
9.18 Chromatogram of OTC, TC and CTC.	162

List of Figures (Continued)

Figure	Page
9.19 Standard addition calibration of tetracycline in untreated wastewater sample.	163

Chapter1

Introduction

1.1 Background and Rationale

Currently there is a need for the determination of trace amounts of target analytes present in food, biological products, environmental or medical samples, especially when the samples contain a very low concentration of target analyte and are in the presence of interfering substances. An ideal analytical device would be one that is specific and sensitive to the target analyte with no sample pretreatment and at the same time is simple to use, not expensive and provide fast analysis. One possible approach is an affinity biosensor. In recent years affinity biosensors have been developed to detect the binding of target analytes to their specific bioaffinity molecules immobilized on the surface of transducers (Gizeli and Lowe, 1996; Luppá *et al.*, 2001; Wang, 2000). Bioaffinity molecules that have been used include antibodies, receptor proteins, nucleic acids and aptamers (Carmon *et al.*, 2005; Drummond *et al.*, 2003; Hock, 1997; Tombelli *et al.*, 2005a; 2005b; 2005c). A variety of signal transducers have been interfaced to affinity biosensor such as, electrochemical, piezoelectric and optical (Zhai *et al.*, 1997; Luzi *et al.*, 2003; Rogers, 2000).

In general, two different assay formats, indirect (labeled) and direct (label-free), are used in an affinity biosensor (Ghindilis *et al.*, 1998; Luppá *et al.*, 2001). In the case of indirect assays, the detection of the analyte and bioaffinity recognition molecule relies on the determination of a label molecule which can be detected through either sandwich or competitive assay format. Either bioaffinity molecule or analyte has to be labeled with a signal-generating component. A labeled component is therefore used to generate a signal which enables quantification of the analyte. This label can be optical, electrochemical or mass related and thus permits the use of these transduction principles (Baeumner, 2003). Although this type of analysis is rather inconvenient because of the need of label molecules, which may be complicated and time-consuming (Cui *et al.*, 2003). However, it can help improve the sensitivity of the detection (Wang *et al.*, 2003; Wu *et al.*, 2007)

In contrast, in the direct format, an affinity reagent is immobilized on the surface and binding of corresponding analyte is detected directly. This type of assay is only applicable in combination with particular principles, which allows the determination of change of the physical properties of the surface during the affinity complex formation. These can be the change in mass, refractive index, impedance or capacitance (Berggren and Johansson, 1997; Berggren *et al.*, 1998; 2001; Botidean *et al.*, 1998; Cui *et al.*, 2003; Hedström *et al.* 2005; Limbut *et al.*, 2006a; 2006b; 2007; Sung *et al.* ., 2006; Thavarungkul; 2007; Wu *et al.*, 2005; Nguyen *et al.*, 2007; Vaisocherova *et al.*, 2007; Wang *et al.*, 2004; Zhou *et al.*, 2002). The main disadvantages of these binding event are limited to the event itself and mainly applied to single analyte (Bacumner, 2003; Bilitewski, 2006). However, the advantages of direct affinity are simplicity (does not require label molecules), fast, uncomplicated and possibility for real-time measurement.

Among the various types of transducers that have been applied for affinity biosensors electrochemical transducer is in general more superior because of the rapid response, simple handling and low cost (Palecek and Fojta, 1994; Wang, 1999). Electrochemical transducer employed for indirect (labeled) affinity biosensor are based on amperometric (Grindilis *et al.*, 1998; Kaku *et al.*, 1993; Kaneki *et al.*, 1994), conductimetric (Segeyeva *et al.*, 1998) or potentiometric principle (Benilova *et al.*, 2006; Boitieux *et al.*, 1981; Chumbimuni-Torres *et al.*, 2006; Fonong and Rechnitz 1984; Gebauer and Rechnitz, 1982; Koncki *et al.*, 1998; Thürer *et al.* 2007). The labels are mostly enzymes (Grindilis *et al.*, 1998; Kaneki *et al.*, 1994) and nanoparticles (Chumbimuni-Torres *et al.*, 2006; Thürer *et al.* 2007; Wang *et al.*, 2002; Wang *et al.*, 2003), the latter has recently received considerable attention. Nanoparticle-based electrochemical detection includes, for examples, the use of gold (Dequaire *et al.*, 2000; Das *et al.*, 2006), silver (Chumbimuni-Torres *et al.*, 2006; Wang *et al.*, 2003) and semiconductor nanocrystal tracer (Choi *et al.*, 2006; Liu *et al.*, 2004). These nanoparticle-based electrochemical method commonly rely on anodic stripping voltametry (ASV) due to its intrinsic preconcentration step that allows one to achieve ultratrace level detection limit (Wang, 1985).

Potentiometric detection using ion-selective electrodes (ISEs) is also an attractive principle for trace level analysis in confined samples. In potentiometry

the direct relationship between analyte activity and observed potential suggests that no scaling laws exist, because of this, there is no expected deterioration of the signal or detection limit as the sample volume is reduced. This rather unique result has made potentiometry as a preferred method when dealing with ultra-miniaturized systems (Rubinova *et al.*, 2007). Recent improvements in the detection limits of ion-selective electrodes based on polymeric membranes containing selective receptors (ionophores) making it possible to use miniaturized ISEs to detect femtomole amounts of ions in microvolume samples (Malon *et al.*, 2006; Rubinova *et al.*, 2007). Application of ISEs for ultrasensitive immunoassays in connection with nanoparticle amplification labels has also been reported (Chumbimuni-Torres *et al.*, 2006; Thüerer *et al.*, 2007). Therefore, we would like to investigate this further and a part of the work present in this thesis describes the investigation of indirect electrochemical detection of bioaffinity reaction based on potentiometric ion selective electrodes to detect aptamer-protein binding and DNA hybridization in sandwich assay employing CdS quantum dot labels. To our knowledge no one has applied this transducer to detect these types of affinity binding.

In the case of label-free electrochemical affinity biosensor, several transducer principles have been employed *i.e.*, potentiometric (Tang *et al.*, 2005; 1987; Yuan *et al.*, 2004), amperometric (Ramanaviciene and Ramanavicius, 2004), conductimetric (Kanungo *et al.*, 2002; Yagiuda *et al.*, 1996) and impedimetric (Berdar *et al.*, 2006; Bonanni *et al.*, 2006; Cooreman *et al.*, 2005; Eugeni, 2003; Radi *et al.*, 2005; Thavarungkul., 2007; Zou *et al.*, 2007). In addition capacitive detection system has also been considered as a highly sensitive approach (Berggren and Johansson, 1997; Berggren *et al.*, 1998; Bontidean *et al.*, 1998; 2000; Hedström *et al.*, 2005; Hu *et al.*, 2002; 2005; Jiang *et al.*, 2003; Limbut *et al.*, 2006a; 2006b; 2007). These transducer have advantages such as sensitive, can detect the analyte directly without the need for label within short analysis time (Berggren, 2001; Ghindilis *et al.*, 1998; Lippa *et al.*, 2001). For these reasons, another part of this thesis investigated the detection of bioaffinity interaction with analyte by a label-free capacitive transducer. These were done through the study of three affinity binding pairs.

1.2 Objectives of the research

The aims of these studies are to develop and evaluate the performance of potentiometric ion selective electrodes and capacitive transducers to analyze bioaffinity binding. To achieve these objectives, five subprojects were conducted using these two electrochemical detection principles. Two projects were performed by indirect-potentiometric ion selective electrode which are applied for the first time to study the bioaffinity interaction of;

1. aptamer-protein
2. DNA hybridization

The other three projects investigated by direct capacitive affinity biosensors were;

1. direct detection of affinity binding between histone protein and DNA.
2. monitoring of plasmid DNA by affinity binding to *lac* repressor protein
3. study the affinity binding of nucleic acid to tetracycline.

1.3 Benefits

It is expected that both potentiometric ion selective electrodes and capacitive transducers, with all their advantages, i.e., high sensitivity, selectivity, accuracy and precision, and short time analysis, will become an alternative approach to detect trace amount of affinity binding analyte which can be applied for many areas including diagnosis, food processing and environmental monitoring.

Chapter 2

Affinity Biosensors

2.1 Biosensor

A biosensor is an analytical device incorporating biological sensing element and transducer. The biological sensing element is responsible for the selective recognition of analyte and generating the physicochemical signal monitored on the transducer, which converts an observed change into a measurable signal, usually an electrical signal whose magnitude is proportional to the concentration of specific chemical or set of chemicals (Eggins, 1996; Turner, 1987) (Figure 2.1). Many types of biological sensing elements have been used in biosensor, these are enzyme, whole cell, tissue, nucleic acid, antigen, antibody and receptor. The transducer can be electrochemical, optical, piezoelectric and calorimetric (Eggins, 1996; Thévenot *et al*, 1999).

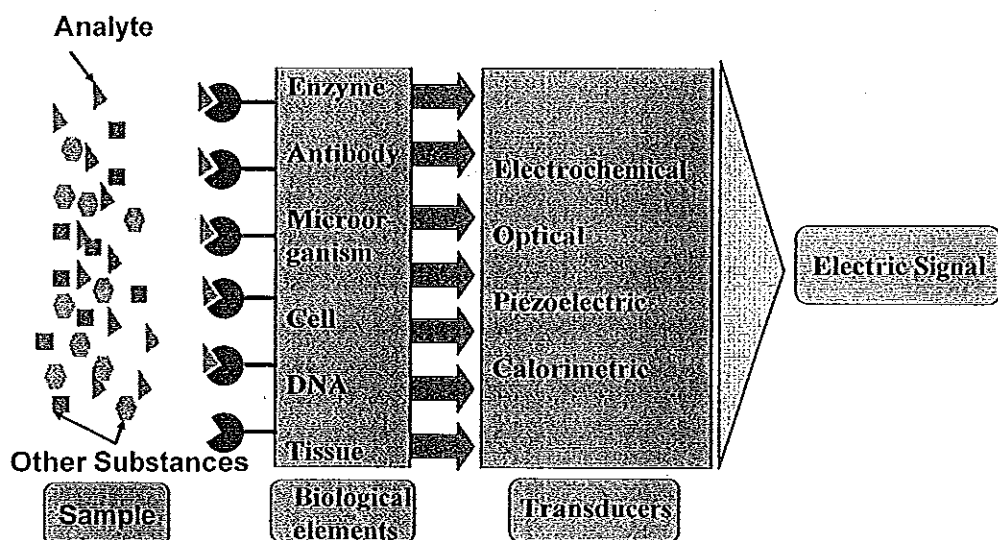


Figure 2.1 Schematic illustration of the components of a biosensor

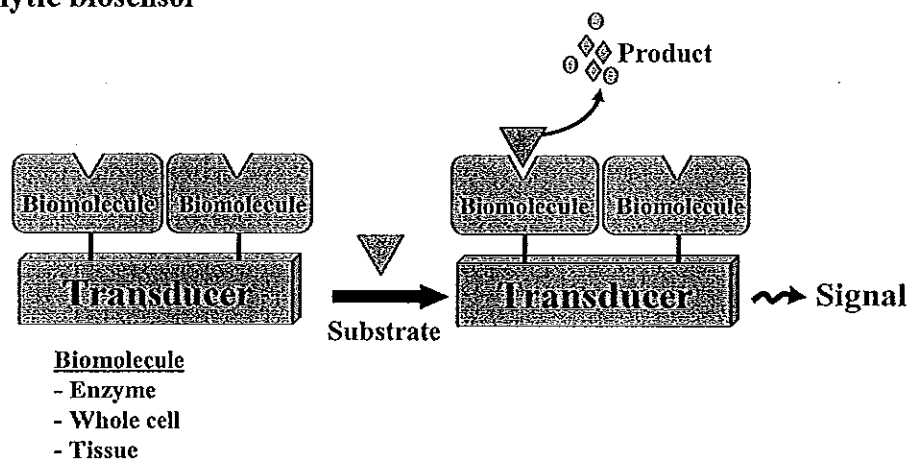
Since biosensors offers advantages over classical techniques in term of selectivity and reduces cost of analysis (Collings and Caruso, 1997), potential for miniaturization, facility of automation, simple and portable equipment various

construction for fast analysis and monitoring, it was applied in fields, such as industrial process control, health care and environmental monitoring (Castillo *et al*, 2004; Turner, 1987). In general, depending on the recognition properties of most biological components, two biosensor categories are recognized which are catalytic and affinity biosensors (Figure 2.2) (Thévenot *et al*, 1999; 2001)

Catalytic biosensors are based on the detection of the change of the solution property, consumption of the substrate or the product of the conversion reaction of substrate by the biological sensing element. Biological sensing elements commonly used in catalytic biosensors are enzymes (mono or multienzyme), whole cells (microorganism, such as bacteria, fungi, eukaryotic cell, yeast) cell organelles and plant or animal tissue slices (Davis *et al*, 1995). Transducer frequently used for biocatalytic reaction are electrochemical, piezoelectric, optical and calorimetric (Lei *et al*, 2006; Mello *et al*, 2002; Thévenot *et al*, 1999; 2001) (Figure 2.2a)

For affinity biosensor, the operation is based on the interaction of analyte with macromolecules. Thus, equilibrium is usually reached and there is no further consumption of analyte by immobilized bioaffinity recognition element (Figure 2.2b) (Thévenot *et al*, 1999). Several types of bioaffinity molecules have been used in biosensors, including antibodies, receptor protein, nucleic acid and aptamer and these have been reviewed by many authors (Carmon *et al*, 2005; Drummond *et al*, 2003; Hock, 1997; Tombelli *et al*, 2005a; 2005b; 2005c). A variety of signal transducers have been interfaced to affinity biosensor such as, electrochemical, piezoelectric and optical which may also be found in several reviews (Junhui *et al*, 1997; Luzi *et al*, 2003; Rogers, 2000). Interest in affinity biosensors is based on the fact that there is a wide range of affinities available and these will help to expand the number of analytes that can be selectively detected. Potential application areas for affinity based biosensor include diagnosis, food processing and environmental monitoring (Kurosawa *et al*, 2006; Rogers *et al*, 2000; Tombelli *et al*, 2005a; 2005b; Wu *et al* 2007)

a.) Catalytic biosensor



b.) Affinity biosensor

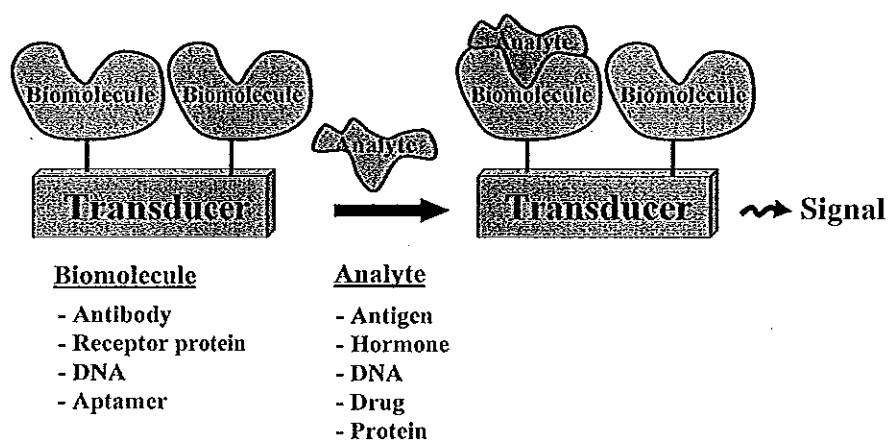


Figure 2.2 Biosensor types a) catalytic biosensor, b) affinity biosensor

2.2 Assays format for affinity biosensor

There are two different assay formats in affinity biosensors, direct (label-free) and indirect (labeled) (Ghindilis *et al.*, 1998; Luppá *et al.*, 2001)

2.2.1 Direct assay

In this type of assay analyte is bound by its bioaffinity elements and is detected directly (Figure 2.3). This direct assay format is only applicable in combination with particular principle, which allows the determination of change of the physical properties of the surface during the affinity complex formation such as electrochemical transducer to detect the potential, current, resistance or capacitance change at the surface of the transducer (Bart *et al.*, 2005; Berggren and Johansson, 1997; Berggren *et al.*, 1998; 2001; Botidean *et al.*, 1998; Hedström *et al.* 2005; Limbut *et al.*, 2006; 2007; Thavarungkul; 2007; Wu *et al.*, 2005), optical transducer to detect the change in optical properties (Cui *et al.*, 2003; Nguyen *et al.*, 2007; Vaisocherova *et al.*, 2007; Wang *et al.*, 2004) and piezoelectric transducer to detect the change in mass (Shen *et al.*, 2005; Skládal *et al.*, 2004; Sung *et al.*., 2006; Zhou *et al.*, 2002).

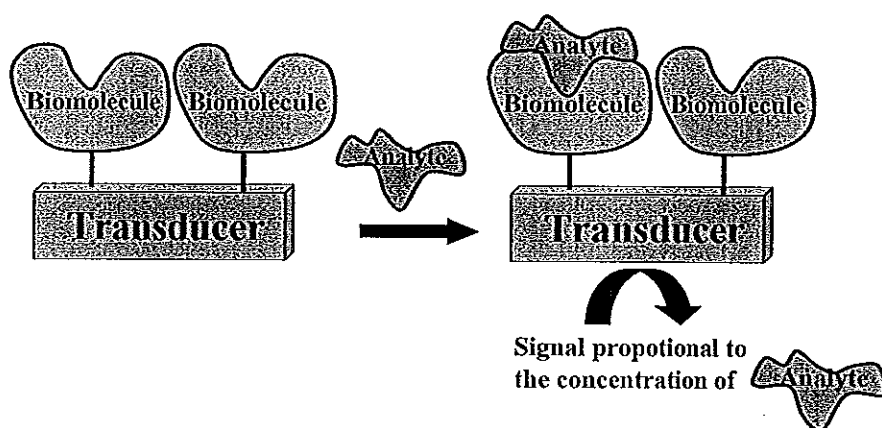


Figure 2.3 Direct assay format for affinity biosensor

2.2.2 Indirect assay

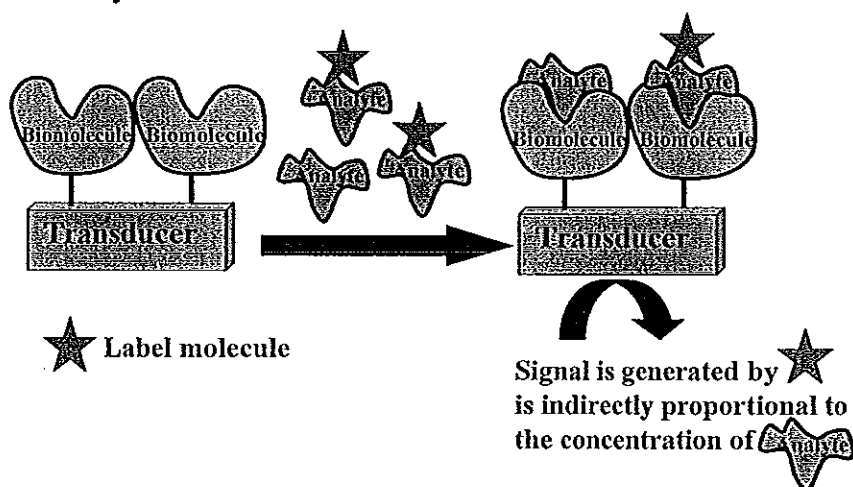
For this assay, the detection of the binding between analyte and its bioaffinity recognition molecule relies on the determination of a label molecule. A great variety of labels have been applied in indirect assay. They can be enzymes such as horseradish peroxidase, alkaline phosphatase, glucose oxidase, catalase, laccase (Ghindilis *et al.*, 1992; Kaku *et al.*, 1993; Kaneki *et al.*, 1994); electroactive compound such as ferrocene (Mir and Katakis, 2008; Radi *et al.*, 2006a; 2006b; Wu *et al.*, 2007); fluorescence such as rhodamine, fluorescene, ruthedium diimine complex

(Karlström and Nygren, 2001; Oillic *et al.*, 2007; Ramanavicius *et al.*, 2007; Watterson *et al.*, 2002) and nanoparticles such as gold, silver and quantum dots (Wang *et al.*, 2002; Wang *et al.*, 2003).

The two widely used principles for labeled affinity sensor are competitive and sandwich assays. In a competitive assay format the analyte (target) competes with the labeled target analyte, which is added in defined constant amount, to the binding sites presented by the immobilized binding bioaffinity recognition molecules (Figure 2.4a). In this format the degree of binding of the label molecule decreases with increasing analyte concentration.

In the other category, sandwich assay, the analyte is captured between two binding partners (Figure 2.4b), of which one is immobilized and the other labeled and added either together with the sample or in the second step after incubation of the sample and removal of unbound constituents. In this assay yields the signal is directly proportional to the analyte concentration (Baeumner, 2003; Bilitewski, 2006).

a). Competitive assay format



b). Sandwich assay format

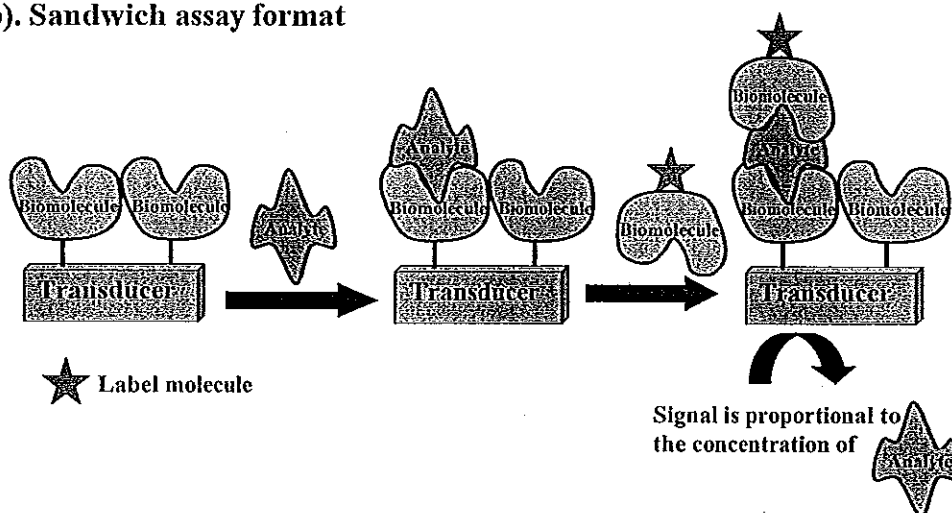


Figure 2.4 Two main types of labeled affinity sensor. a) competitive, b) sandwich assay

2.3 Types of affinity biosensor

Affinity sensors utilize selective binding of certain biomolecules toward specific target species. The bioaffinity recognition process is governed by the shape and size of receptor pocket and the interested ligands (analytes). The high specificity and affinity of these biochemical binding reaction leads to highly sensitive sensing devices (Wang, 2000). Affinity biosensor can be named, based on the bioaffinity sensing molecules, as immunosensors (Ghrindilis *et al.*, 1992; 1998; Hock, 1997; Killard *et al.*, 1995; Rorers, 2000), receptor biosensors (Rogers, 2000; Subrahmanyam *et al.*, 2002), DNA biosensor (Rauf *et al.*, 2007; Tombelli *et al.*, 2005c; Wang *et al.*, 1997; 2001; Zhou *et al.*, 2002), nucleic receptor (aptamer) biosensors (Bang *et al.*, 2005; Hansen *et al.*, 2005; Hianik *et al.*, 2005; Ikebukuro *et al.*, 2005; Rodriguez, *et al* 2005) and DNA-protein biosensors (Abrahamsson, *et al.*, 2004; Bontidean *et al*, 2001; Miao *et al.*, 2008).

2.3.1 Immunosensor

Most reported affinity biosensors are based on an immunological reaction involving the shape recognition of antigen (Ag) by the antibody (Ab) binding site to form the antibody/antigen (Ab/Ag) complex (Rogers, 2000; Wang, 2000). Antibodies are immune system-reacted proteins called immunoglobulins, generated in response to the challenge of an immunogen (*i.e.*, antigen) in the host cell (Killard *et al.*, 1995; Rogers, 2000). Antibody are structurally similar and divided into five major classes *i.e.*, IgA, IgD, IgE, IgG and IgM (Gizeli and Lowe, 2002; Hermanson *et al.*, 1992). They are differed in size, charge, amino acid composition and carbohydrate content. There are two types of antibodies *i.e.*, polyclonal antibody and monoclonal antibody. Polyclonal antibodies (pAb) have an affinity for the target, and are directed to different bonding site with different binding affinity. Monoclonal antibodies (mAb), because they are produced from one type of immune cell, have higher sensitivity and selectivity than polyclonal antibody and are, therefore, preferred (Vestergard *et al.*, 2007).

Antibody molecules consist of two identical heavy chains (H) and two identical light chains (L) (Figure 2.5). The two heavy chains are held together by disulfide (-s-s-) linkages. Light chains are also attached to the heavy chain by disulfide bonds so that one light chain associates with one heavy chain. Antibodies are typically represented schematically as “Y shaped” structure. Antibody binding sites are located at the end of the two arms (Fab units) of this “Y shaped”. The tail end of the “Y” referred to as Fc unit, is less variant and contain species-specific structure, commonly used as antigen for production of species-specific antibodies (Rogers, 2000).

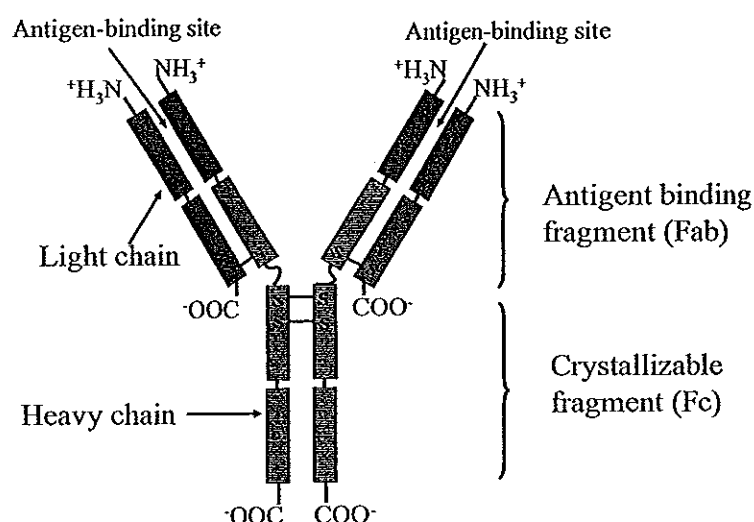


Figure 2.5 Structure of antibody

The interaction between antigen and antibody is dependent on the complementary of the fit of antigenic determinate to the binding site of antibody. The binding force present in the antibody-antigen complex are non-covalent forces such as electrostatic interaction, hydrogen bonding, hydrophobic interaction and Van der Waals interaction (Gizeli and Lowe, 2002). Because the interaction of antigen-antibody has high affinity and specificity, it has been widely employed in biosensing systems as has been shown in a number of reviews (Ghrindilis et al., 1992; 1998; Hock, 1997; Killard *et al.*, 1995; Rogers, 2000).

In immunosensors either an antigen or antibody is immobilized on solid-state surface and participated in bioaffinity interaction with the other

component, allowing detection and quantification of an analyte of interest. Several reviews have reported the use of many type of transducers which are electrochemical (Berggren, 2001; Guan *et al.*, 2004, Jonathan and Daniel, 2007) optical (Homola, 2003; 2008; Mu, 2001; Patel, 2002; Yang and NgO, 2000) and transducer sensitive to change in mass (Chu *et al.*, 1995; Kurosawa *et al.*, 2006; Lu *et al.*, 2000). The sensor may operate either by a direct assay *i.e.*, the change in the property produced directly by antigen-antibody binding reaction and detected in real time, or an by indirect assays requiring a label on one of the biomolecule to produce a change in the label molecule property to be measure. Potentials application that have been presented in several reviews are clinical analysis (Lin and Ju, 2005; Lippa *et al.*, 2001), environmental monitoring (Baceumner, 2003; Jiang *et al.*, 2008; Marco and Baceló, 1996) and food processing (Baceumner, 2003; Jiang *et al.*, 2008; Ligler *et al.*, 2003; Ricci *et al.*, 2007).

2.3.2 Receptor biosensor

Molecular receptors are cellular, typically membrane, proteins that bind specific chemicals (ligands) in a manner that results in the conformation change triggering a cellular response (Rogers, 2000; Subrahmanyam *et al.*, 2002). Unlike most antibody binding (aimed at specific substance), receptors tend to bind classes of substance possessing common chemical properties that dictate the binding affinity (Wang, 2000). Membrane receptors are diverse due to there different structure and functionality in the cell. Three difference classes can be categorized, which are channel receptors, G-protein linked receptors, receptor with single transmembrane segments (Haga, 1995)

- Ion channel receptor

Ion channel receptors are mainly oligomers composed of heterogeneous subunits, incorporating function into oligomeric structure. Their function is rapid communication in the nervous system. Ligands specific for this class of receptor include neurotransmitter, such as acetylcholine, glutamate and serotonin (Subrahmanyam *et al.*, 2002. Haga *et al.*, 1995; Uto *et al.*, 1990).

- G-protein linked receptor

G-protein linked receptors mediate the cellular response to an enormous diversity of signaling molecules. The species of this receptor are diverse and include amine, amino acid, nucleotide, lipid, peptide and protein. The ligands belonging to this class are important target analyte for sensor technology include all neurotransmitters, most hormone and autocoids (Haga *et al.*, 1995; Ryan Preston and McFadden, 2001; Subrahmanyam *et al.*, 2002).

- Receptors with single transmembrane segments

A group of receptors with single transmembrane segments include growth factors, such as epidermal growth factors, fibroblast growth factors and nerve growth factors. Typical ligands for this type of receptor are protein such as phosphorylase C, GTPase-activating protein (Klammt *et al.*, 2007; Lundström and Svensson, 1998; Subrahmanyam *et al.*, 2002).

Receptor-based biosensors have been developed to detect several target analyte such as, viruses and bacteria (Biorn *et al.*, 2004; Hoffman *et al.*, 2000; Ma *et al.*, 1998), hormones (Granek and Rishpon, 2002; Seifert *et al.*, 1999), nitrogen monoxide (Barker *et al.*, 1998; 1999), toxin (Ngundi, 2006; Song and Swanson, 199;), drugs (Bertucci *et al.*, 2003) and metal ion (Ito, 2001).

There are many types of transducers used to detect the binding of analyte (ligand) to an immobilized ligands, *i.e.*, electrochemical (Granek and Rishpon, 2002; Tien *et al.*, 1997), optical (Bertucci *et al.*, 1998; Kamel *et al.*, 2005) and piezoelectric (Michazik *et al.*, 2005; Sung *et al.*, 2005). The operation is measured either indirectly by labeling one of the components, such as sandwich type assay by enzyme labels (Wendler *et al.*, 2005) or fluorescent labels (Rogers *et al.*, 1992) or directly due to the change in the property produced by receptor-ligand binding reaction (Granek and Rishpon, 2002; Kamel *et al.*, 2005; Michazik *et al.*, 2005)

Although this technique is promising for specialized analyses, reports on receptor based biosensor are relatively few compared to immunosensors. This is mostly likely because these devices are difficult to design and the biological receptor proteins or tissues containing them are difficult to isolate and are rather unstable (Rogers, 2000; Subrahmanyam, *et al.*, 2002)

2.3.3 DNA biosensor

Deoxyribonucleic acid, DNA, is the molecule that encodes genetic information. It is coiled to form double helix or double strand DNA held together with hydrogen bonds between base pairs of nucleotide. The four nucleotides in DNA contain the bases adenine (A), guanine (G), cytosine (C) and thymine (T). In nature, base pairs form only between A and T and between G and C (Junhui *et al.*, 1997).

The use of DNA based biosensors are mostly based on the highly specific hybridization of complementary strands of DNA molecules which are important for detecting the specific base sequence in human, viral and bacterial nucleic acids, with applications ranging from the detection of disease-causing (Chee *et al.*, 1996 Li, *et al.*, 2007; Meric *et al.*, 2002), food contaminating organisms to the forensic and environmental research (Lazerges *et al.*, 2006; LaGier *et al.*, 2005; Zezza *et al.*, 2006). In addition the interaction of DNA with small molecular weight molecules have been developed for rapid screening of some target pollutants or drugs (Chiti *et al.*, 2001; Erdem and Ozoz, 2002).

2.3.3.1 DNA hybridization biosensor

DNA hybridization biosensors commonly rely on the immobilization of a single strand (ss) oligonucleotide probe onto a transducer surface to be recognized by hybridization with its complementary sequence. The binding of the surface-confined and its complementary target strands is translated into an electrical signal (Figure 2.6). Potential application for detection of specific DNA sequence based on DNA hybridization is significant in many area including clinical for diagnosis of genetic diseases (Li, *et al.*, 2007; Meric *et al.*, 2002), in environmental and food areas for the detection of genetically modified organism (GMO) or pathogens (Capini *et al.*, 2004; Chiti *et al.*, 2001; Erdem and Ozoz, 2002). Many types of signal transducers reported for DNA hybridization biosensor may be found in several reviews and are based on electrochemical (Li *et al.*, 2007; Lin *et al.*, 2007; Mandong *et al.*, 2007; Rauf *et al.*, 2007; Wang *et al.*, 1997; 2001), piezoelectric (Hur *et al.*, 2005; Sklădal *et al.*, 2004; Tombelli *et al.*, 2005c; Wu *et al.*, 2007; Zhou *et al.* 2002) and optical detection principles (Kim *et al.*, 2007; Lenigk *et al.*, 2007; Niu *et*

al., 2007; Schmidt *et al.*, 2002; Wu; *et al.*, 2007; Zezza *et al.*, 2006). Similar to other affinity biosensors, DNA biosensors can be operated either in direct assays i.e., the change in the property is produced directly by hybridization (Li *et al.*, 2007; Tombelli *et al.*, 2000; Zezza *et al.*, 2006; Zhou *et al.*, 2002) or as indirect assay format. Labels include electroactive molecules e.g. methylene blue, ferrocene, used in electrochemical (Erdem *et al.*, 2000; Marraza *et al.*, 1999; Meric *et al.*, 2002; Wang *et al.*, 1998), nanoparticle (Hanaee *et al.*, 2007; Kalogianni *et al.*, 2006; Storhoff *et al.*, 2004; Wang *et al.* 2001), enzyme (Alfonta *et al.*, 2001; Kim *et al.*, 2003;) or fluorescence labels (Buke *et al.*, 2003; Mao *et al.*, 2004; Talavera *et al.*, 2000).

Because the base-pairing interaction between complementary sequence are both specific and robust, the DNA hybridization biosensor is especially well suitable for clinical, environmental and food applications (Drummond *et al.*, 2003). However, some of the immobilized oligonucleotide probes can lie flat on the surface of the transducer, making it become inaccessible to hybridization which lead to a decrease in sensitivity and specificity (Pang *et al.*, 1996).

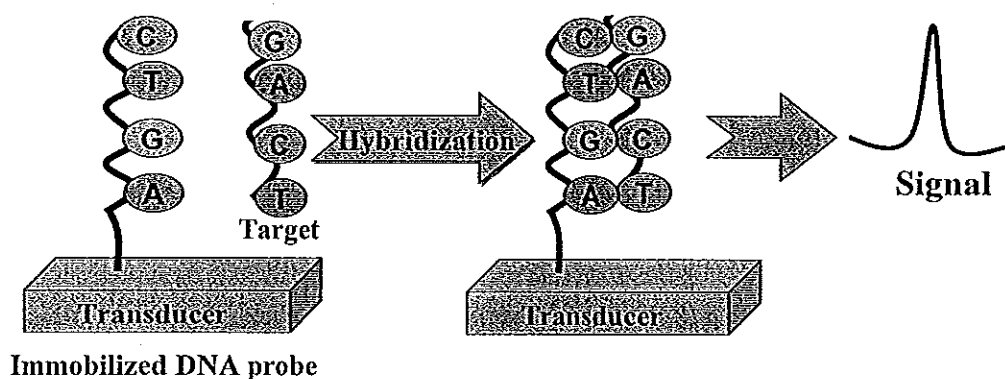


Figure 2.6 Steps involved in DNA biosensor

2.3.3.2 DNA-small molecule biosensor

There is also an increased use of nucleic acid as a tool in recognition and monitoring of a number of compounds of analytical interest. This technique is based on the molecular interaction between the DNA and the target toxic pollutants such as polychlorinated biphenyls (PCBs), polycyclic aromatic hydrocarbons,

aflatoxin, and aromatic amines, herbicides (Chiti *et al.*, 2001; Marazza *et al.*, 1999; Oliveira-Brett *et al.*, 2002) or drug, i.e. antibiotic (Nawaz *et al.*, 2006; Oliveira-Brett *et al.*, 2002; Erdem and Ozsoz, 2002; Piedade *et al.*, 2002;) in order to develop devices for rapid screening of these compounds.

The binding of molecules which are small aromatic ligand molecules to DNA double helical structure involves electrostatic interactions with the negatively charged nucleic sugar-phosphate structure (which is generally nonspecific), in a way of an intercalative penetrating into the DNA double-helix between adjacent base pairs and minor and major DNA grooves binding of the side groups of the molecules via hydrogen bonds, electrostatic interactions, or van der Waals contacts, with edges of base pairs or sugar-phosphate backbone (Gherghi, *et al.*, 2004; Rauf *et al.*, 2005; Erdem and Ozsoz, 2002) (Figure 2.7).

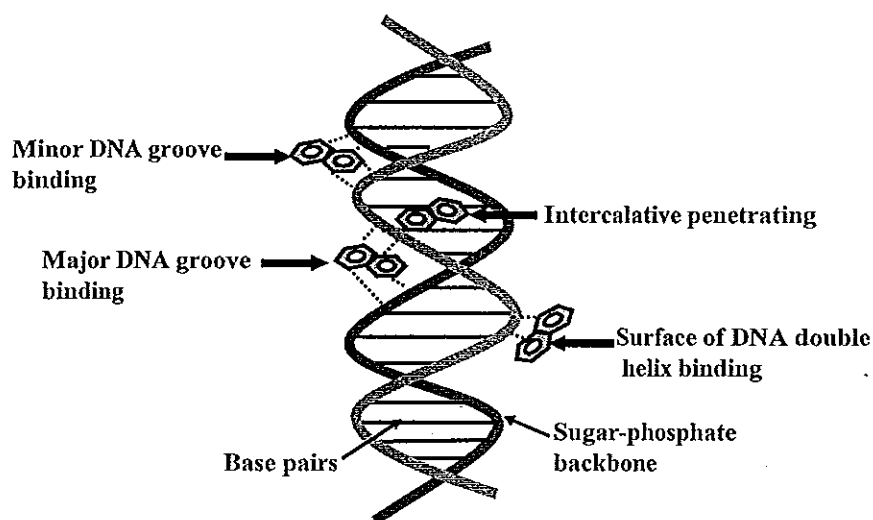


Figure 2.7 Binding way of the small molecule to double helix DNA

The double strands of DNA (ds DNA) is immobilized on the transducer, the binding of small molecules to DNA results in a significant change in the DNA conformation affecting the transduction signal. Some interaction studies based on the ability of compounds to interact directly with DNA and employing the biosensor technology have already been reported by some authors using different transducers, mainly electrochemical and optical. In particular, electrochemical transducers by detecting the change in the DNA redox properties (i.e. in the oxidation of the in guanine base) (Marazza *et al.*, 1999; Wang *et al.*, 1996; Wang *et al.*, 1997)

or detect the amount of electroactive analyte trapped on DNA layer (Chiti *et al.*, 2001; Wang *et al.*, 1996), surface plasmon resonance (SPR) was also used for detecting this binding (McKnight *et al.*, 2004; Tombelli *et al.*, 2002; Wang *et al.*, 2002).

Although this device has been increasing the used for screening of many compounds of interest with high level of sensitivity together with a rapid analysis time (Chitti *et al.*, 2001). However, it is not selective to only one compound and hence further confirmation with standard method is required (Rauf *et al.*, 2005).

2.3.4 Nucleotide receptor (Aptamer)-ligand biosensors

Aptamers are oligonucleotide (DNA or RNA) that are commonly evolved via a combinatorial chemistry technique known as a systematic evolution of ligands by exponential enrichment (SELEX) which is a technique for screening large libraries of oligonucleotide by iterative process of *in vitro* selection and purification (Ellington and Szostak, 1990; Tuerk and Gold, 1990). The SELEX method has permitted the identification of RNA/DNA molecules, from very large populations of random sequence oligomers (DNA or RNA libraries), which bind to the target molecules with very high affinity and specificity. Selections are frequently carried out with DNA/RNA pools due to known ability of DNAs/RNAs to fold into the complex structures which can be a source of diversity of their function. They can be selected using a variety of targets from small molecules to whole cell organism (Pestourie *et al.*, 2005).

High affinity aptamers have been selected to bind many different targets such as organic dyes (Ellington and Szostak, 1990), amino acids (Famulok and Szostak, 1992), antibiotics (Schurer *et al.*, 2001; Tereshko *et al.*, 2003), peptides (Baskerville *et al.*, 1999), proteins (Wen *et al.*, 2001) and vitamins (Wilson *et al.*, 1998). Aptamers show a very high affinity for their targets, with dissociation constant typically from micromolar to low picomolar, comparable to those of some monoclonal antibodies, sometime even better (Jenison *et al.*, 1994). The high affinity of aptamers for their targets is given by their capability of folding upon binding their target molecules, they can incorporate small molecules into their nucleic structure or integrate into the structure molecules such as proteins (Herman and Patel, 2000).

In comparison to antibodies, several reviews have reported that aptamer receptors have a number of advantages that make them very promising in analytical and diagnosis applications. The main advantage is the overcoming of the use of animals for their production. Most antibody production starts in biological systems by inducing an immune response to the target analyte, but the immune response can fail when the target molecules has a structure similar to endogenous protein. In addition, generation of antibodies *in vivo* means that it is the animal immune system that selects the sites on the target protein to which the antibody bind. The *in vivo* parameters restrict the identification of antibodies that can recognize targets only under physiological conditions. Moreover, the aptamer selection process can be manipulated to obtain aptamers that bind a specific region of the target and which specific binding properties in different binding conditions. After selection, aptamers are produced by chemical synthesis, modifications in aptamer can be introduced enhancing the stability, affinity and specificity of molecules. Finally, because of their simple structure, sensor layers based on aptamer can be regenerated more easily than antibody-based layer, are more resistant to denaturation and have a longer shelf life (Cai *et al.*, 2006; Ósullivan, 2002; Tombelli *et al.*, 2005a; 2005b; 2005c)

Because of a multitude of advantages of aptamers over antibody, there has been strong a interest for the application of aptamers as biocomponent in biosensors. A number of reviews reported that proteins are the most commonly studied binding pair of aptamer based biosensors such as thrombin (Bang *et al.*, 2005; Hansen *et al.*, 2005; Hianik *et al.*, 2005; Ikebukuro *et al.*, 2005; Xiao, *et al.*, 2005), lysozyme (Hansen *et al.*, 2005; Rodriguez., *et al* 2005), human IgE (Xu *et al.*, 2005), HIV-1 Tat protein (Minunni *et al.*, 2004) and a platelet derived growth factor (PDGF-BB) (Fang *et al.*, 2001; Huang *et al.*, 2005). The use of aptamers as sensors for small molecules has not been studied nearly as extensively as protein targets. Small molecules are more difficult to develop than protein sensors since there are far fewer moieties for aptamer binding (Wen *et al.*, 2001). There are only a few reports for aptamer based sensor for small molecule, such as cocaine (Baker *et al.*, 2006).

The binding of analyte to an immobilized aptamer can be measured indirectly by enzyme labels (Ikebukuro *et al.*, 2005; Mir *et al.*, 2006; Baldrich *et al.*,

2005) or nanoparticle labels (i.e. gold, silver or quantum dot) (Hansen *et al.*, 2005; Huang *et al.*, 2005; Mathew Levy, 2005; Palov *et al.*, 2004). Many types of transducers have been developed with aptamers immobilized on the sensing surface which are electrochemical (Baldrich *et al.*, 2005; Ikebukuro *et al.*, 2005), or fluorescence (Fang *et al.*, 2001; Heyduk and Heyduk, 2005; Jhaveri, *et al.*, 2000). The binding has also been measured directly by optical (Tombelli *et al.*, 2005), piezoelectric (Hianik *et al.*, 2005; Minumni *et al.*, 2004; Tombelli *et al.*, 2005a; 2005b) and electrochemical transducers (Cai *et al.*, 2006; Cheng *et al.*, 2007; Rodriguez *et al.*, 2005; Xiao, *et al.*, 2005; Xu *et al.*, 2006).

2.3.5 Protein binding DNA biosensor

The complex of protein-DNA binding in chromosomes (histone-DNA) (Cui *et al.*, 2005) or in cellular processes occur in transcription, recombination, restriction or replication (Miao *et al.*, 2008; Pandolfi, 2001; Wang *et al.*, 2006) has attracted attention to apply these bindings for a new type of affinity biosensor for medical diagnosis and target for drug development (Pandolfi, 2001). For example, immobilized DNA to detecting the transcription factor that regulated a wide variety of biological process such as inflammation, apoptosis and cancer (Miao *et al.*, 2008). In contrast, proteins can be applied as immobilized recognition element to detect DNA. For example, immobilized histone protein for detecting DNA in a lysed cell culture which is important in biotechnology production process (Abrahamsson, *et al.*, 2004). The binding of analyte to an immobilized bioaffinity molecule can be measured by electrochemical or optical transducers (i.e., surface plasmon resonance) which may be found in several reports (Abrahamsson, *et al.*, 2004; Bontidean *et al.*, 2001; Miao *et al.*, 2008; Wang *et al.*, 2006).

2.4 Detection principle of affinity biosensor

Many types of transducers have been used to detect binding in affinity biosensors. Most of these transducer are based on optical, piezoelectric and electrochemical principles (Junhui *et al.*, 1997; Luzzi *et al.*, 2003; Rogers, 2000).

2.4.1 Optical transducer

Optical transducer can employ a number of techniques to detect the presence of a target analyte. They are based on a method to detect the change in absorbance (Deinum *et al.*, 2002), luminescence (Burke *et al.*, 2003; Cummins *et al.*, 2006) or refractive index (Homola *et al.*, 1999; 2003).

For label-free optical detection, surface plasmon resonance (SPR) is now being a widely used technique. In principle, the SPR measure the refractive index change caused by the binding of an analyte to bioaffinity recognition molecules immobilized on the sensor surface (Patel, 2002). The interaction is monitored in real time and the amount of bound ligand and rates of association and dissociation can be measured with high precision (McDonnell, 2001; Pattnaik, 2005).

The SPR phenomenon occurs when plane polarized light is reflected from a gold film deposited on a glass support (Liedberg, 1983). Photons interact with the free electron cloud (plasmon) in the metal film at a specific angle, the SPR-angle, and cause a drop in the reflected light. Refractive index changes near the surface give rise to a shift of the resonance angle. The shift is directly proportional to the mass increase and mass concentration can thus be measured (Homola *et al.*, 1999; 2003; McDonnell, 2001; Pattnaik, 2005). The analysis principle is summarized in Figure 2.8.

Application of SPR to biosensors has shown promise in determination of concentrations, kinetic constants and binding specificity of individual biomolecular interaction steps. Antibody–antigen interactions, peptide–protein, DNA hybridization, biomolecule–cell receptor interactions, and DNA/receptor–ligand interactions can all be analyzed. However, SPR method has a major disadvantage for bioanalytical

applications. It is difficult to detect low concentrations or low molecular mass analytes (Dong and Chen, 2002; Orazio, 2003).

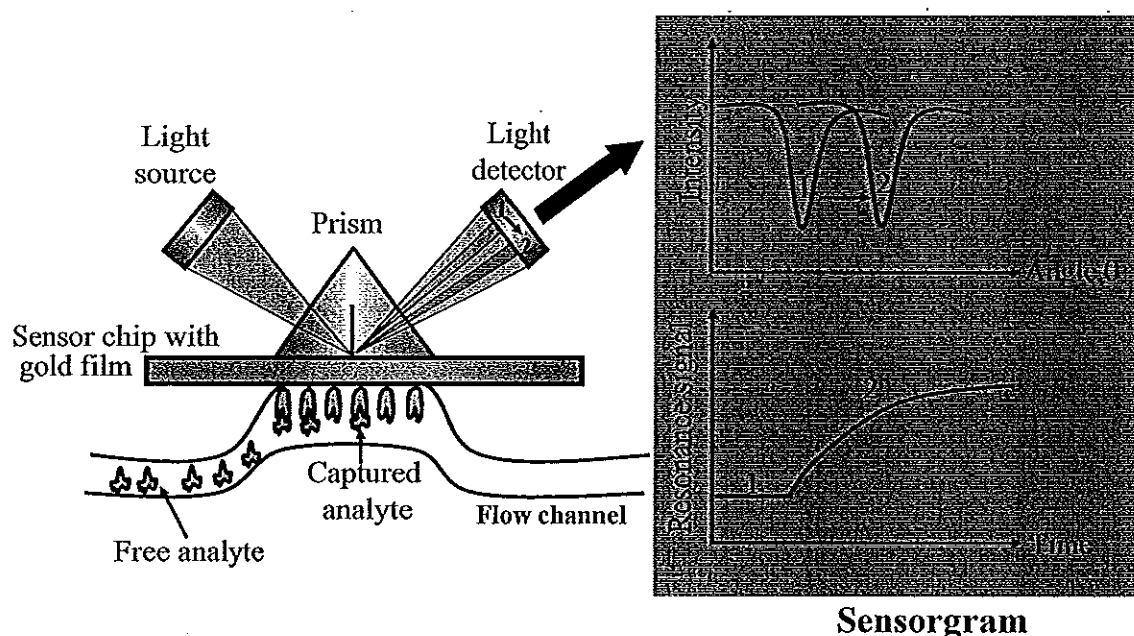


Figure 2.8 Typical set-up for a surface plasmon resonance biosensor. The SPR angle shift (from 1 to 2 in diagram) when biomolecules bind to the surface and change the surface layer. This change in resonance angle can be monitored in real time as plot of resonance signal versus time (Adapted from Shankaran *et al.*, 2007)

Optical affinity biosensors based on the detection of label molecules are more commonly used. Fluorescent labels serve as marker which are responsible for the high sensitivity of assay (Ghlidilis *et al.*, 1998; Mallat and Barceló, 2001, Medyantseva *et al.*, 2001). The two assay format of indirect affinity detection, *i.e.* competitive and sandwich assay, can be detected. Bioaffintiy molecules were immobilized on the surface of the transducer or waveguides, the complex formation of the fluorescent labeled bioaffintiy molecules on this region is detected by photodiode or photomultiplier tube when the label is excited by the incident light from light source (Figure 2.9) (Gizeli and Lowe, 2002). Fluorescent label molecules often used are organic dye fluorescence molecules such as thiozole orange, editidium bromide, cyanide dye (Cy5) (Bakaltcheva *et al.*, 1998; 1999; Hock, 1997; Jakeway and Krull, 1999; Wang and Ulrich, 2005) or quantum dot nanoparticle labels (Cui *et*

al., 2007; Deng *et al.*, 2007; Kerman *et al.*, 2007; Lee *et al.*, 2004; Liu *et al.*, 2007; Shen *et al.*, 2007; Yeh *et al.*, 2005; Zhu *et al.*, 2004).

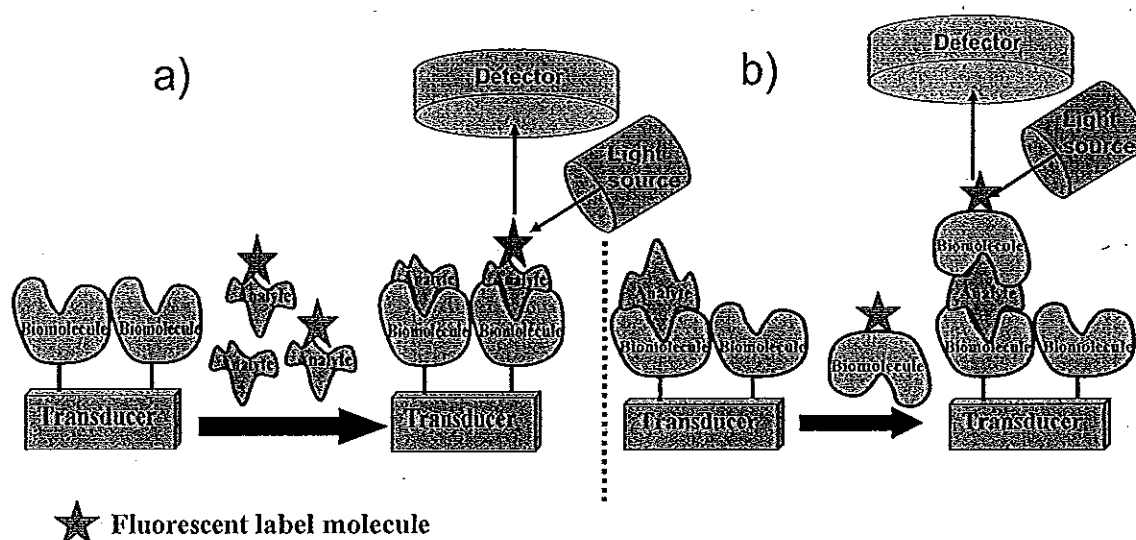


Figure 2.9 Illustration of two types of labeled affinity biosensor based on optical detection; a) sandwich and b) competitive assay

Optical detection of enzyme labels has also been used in the development of affinity sensor. In principle, enzymes are able to catalyze reaction of substrate transformation accompanied with formation of fluorophore product that is used for quantification of the analyte. However, enzyme labeled based optical detection have only been successful and described by a few reports (Ermenko *et al.*, 1998; Ramanavicius *et al.*, 2007)

Label based optical detection have been applied for different affinity interactions such as immunosensors (Bakaltcheva *et al.*, 1998; 1999; Hock, 1997; Liu *et al.*, 2007; Deng *et al.*, 2007; Ermenko *et al.*, 1998; Ramanavicius *et al.*, 2007), DNA hybridizations (Almadidy *et al.*, 2002; Aslan *et al.*, 2006; Bourdon *et al.*, 2001; Celep *et al.*, 2003; Jakeway and Krull, 1999; Kim *et al.*, 2006; Wang and Ulrich, 2005) and receptor-ligand (Gokulrangan *et al.*, 2005; Liu *et al.*, 2007; McCauley *et al.*, 2003).

The high sensitivity of fluorescence detection from labeled molecules is the main advantage of this assay. However, the limitations of this technique are the background signals and spectral overlap (Ghindilis *et al.*, 1998).

2.4.2 Piezoelectric transducer

Piezoelectrics are materials, such as quartz (SiO_2), lithium niobate (LiNbO_3), zinc oxide (ZnO), gallium arsenide (GaAs) and lithium tantalite (LiTaO_3) (Clair *et al.*, 1996), that may be brought into resonance by the application of an external alternating electric field. The frequency of the resulting oscillation is determined by the mass of the crystal. In principle, the crystal of the piezoelectric biosensor is coated with the appropriate biomolecule that selectively interacts with the analytes, subsequent binding increases the mass of the coated crystal and this alters its basic frequency of oscillation. Piezoelectric for affinity biosensor may classify in two modes which are bulk acoustic wave (BAW) and surface acoustic wave (Bunde *et al.*, 1998; Marco and Barcel, 1996) (see Figure 2.10)

(i) Bulk acoustic wave (BAW)

This device is quartz crystal microbalance (QCM) which consists of thin quartz disk with electrode plated on its two sides (Figure 2.10a). The binding of the analytes occurs on the coated surface of a piezoelectric crystal connected to an oscillator circuit. Resonance occurs in the entire mass of the crystal. If bioaffinity receptor-coated crystal is placed in an atmosphere containing the selected analyte the affinity reaction will produce an increase in the mass of the crystal. The resonant frequency will therefore decrease according to the Sauerbrey equation:

$$\Delta f = -\frac{C_Q f^2 \Delta m}{A} \quad (2.1)$$

Where Δf is the change in fundamental frequency, C_Q is the sensitivity (which for quartz = $2.26 \times 10^{-6} \text{ cm}^2 \text{ g}^{-1}$), f is the resonant frequency of the crystal, A is the area of the crystal, and Δm is the mass change deposited (Collings and Caruso, 1997).

(ii) Surface acoustic wave (SAW)

In SAW device, electrodes are on the same side of crystal known as an interdigital transducer (Figure 2.10b). In this method, the oscillation of piezoelectric crystal is at a higher frequency and an acoustic wave is generated by application of an

alternative voltage across a pattern of metal electrode. The adsorption of sample to crystals slow the acoustic wave, the velocity change is proportional to the analyte concentration and causes a shift of frequency (Marco and Barcelo, 1996, Morgan, *et al.*, 1996). The frequency shift of piezoelectric crystal is proportional to the mass change according to the Sauerbrey equation.

Piezoelectric transducer were successfully used for many different of the binding between bioaffinity-analyte detection, such as, immunosensor (Chu *et al.*, 1995; Konig and Gratzel 1994; 1995; Lu *et al.*, 2000; Shen *et al.*, 2005; Su *et al.*, 1999; Suri *et al.*, 1995; Tajima *et al.*, 1998; Yang and Chen, 2002), DNA hybridization (He and Liu, 2004; Hur *et al.*, 2005; Skládal *et al.*, 2004; Tombelli *et al.*, 2005 a; 2005b; Zhou *et al.*, 2002) and DNA/receptor–ligand interactions (Minuni *et al.*, 2004; Tombelli *et al.*, 2005).

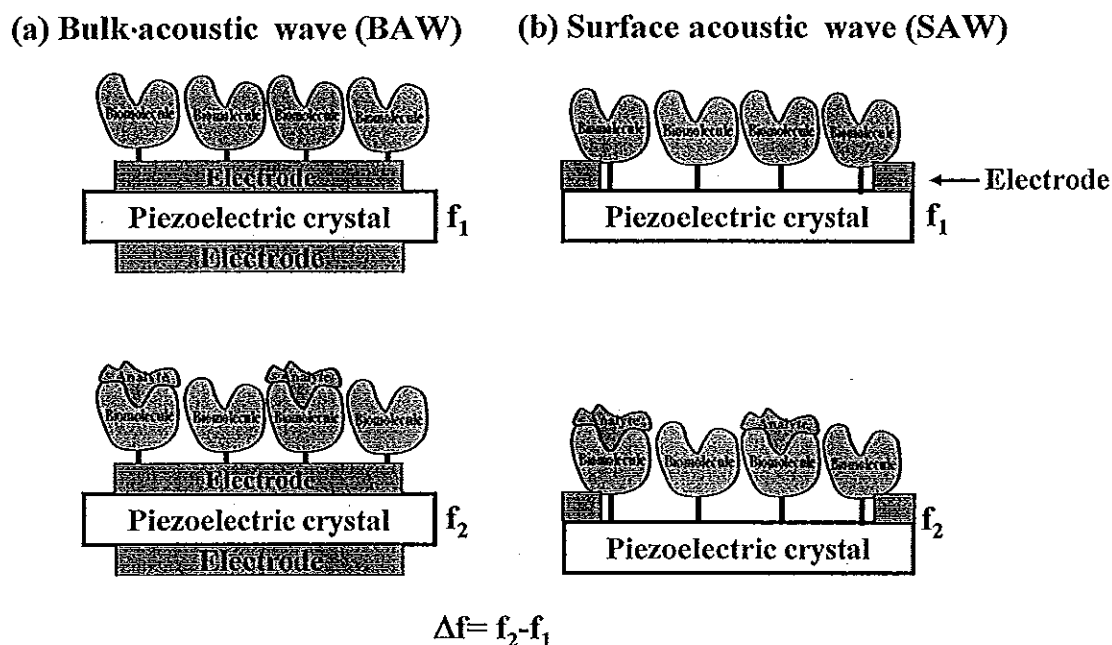


Figure 2.10 Schematic of piezoelectric biosensors. The frequency of oscillation of a piezoelectric material is dependent on its mass. (a) On a bulk acoustic wave (BAW). (b) On surface acoustic wave (SAW)

The advantage of piezoelectric transducer for affinity biosensor lies in the direct measurement of affinity interaction. In this case, no label is necessary and

no additional chemicals are used. Limitations of this technology is the interferences produced when used on liquid media (Geddes et al., 1994; Kosslinger et al., 1992)

2.4.3 Electrochemical transducer

Electrochemical transducers offer good possibilities for sensitive detection of target analyte (*i.e.*, antigen, protein, DNA). Electrochemical detection of affinity interaction are used for both direct assays (Bart *et al.*, 2005., Berggren and Johansson, 1997; Berggren *et al.*, 1998; 2001; Botidean *et al.*, 1998; Hedström et al., 2005; Limbut *et al.*, 2006; 2007; Thavarungkul; 2007; Wu *et al.*, 2005) and indirect assays.

Electrochemical transducers are, in general, superior to other transducers because of their rapid response, simple handling and low cost (Palecek and Fojta, 1994; Wang, 1999). Therefore, electrochemical transducer for affinity binding are preferred and this is the subject of a review in the next chapter.

Chapter 3

Electrochemical Detection of Affinity Biosensors

Electrochemical detection is the measurement of electrical properties such as current, potential, or charge, and their relation to chemical or biological compounds which provides a sensitive method for trace analysis of these materials. For affinity biosensor, electrochemical detection employs several transduction principles, *i.e.*, amperometric (Grindilis *et al.*, 1998; Kaku *et al.*, 1993; Kaneki *et al.*, 1994), voltammetric stripping (Gonzalez Garcia and Casta Garcia, 1995; Liu and Lin, 2005; Wang *et al.*, 2002), conductimetric (Kanungo *et al.*, 2002; Segeyeva *et al.*, 1998; Yaguida *et al.*, 1996), impedimetric (Berdar *et al.*, 2006; Bonanni *et al.*, 2006; Cooreman *et al.*, 2005; Eugenii, 2003; Radi *et al.*, 2005; Thavarungkul., 2007; Zou *et al.*, 2007), potentiometric (Benilova *et al.*, 2006; Boitieux *et al.*, 1981; Chumbimuni-Torres *et al.*, 2006; Fonong and Rechnitz 1984; Gebauer and Rechnitz, 1982; Koncki *et al.*, 1998; Thüerer *et al.* 2007). and capacitive (Berggren *et al.*, 1998; 2001; Bontidean *et al.* 1998; 2003; Hedström *et al.*, 2004; Hu, *et al.*, 2002; 2005; Jiang *et al.*, 2003; Limbut *et al.*, 2006a; 2006b; 2007).

As described in chapter 2 (section 2.2), there are two assay formats in affinity biosensors, *i.e.*, direct and indirect, and electrochemical detection can be applied for both types of assay. In this chapter direct and indirect electrochemical detection for affinity biosensors are reviewed.

3.1 Direct electrochemical detection

This technique is based on the detection of the change in physical properties as a result of the bioaffinity complex formation. The surface of the electrochemical transducer (electrode) modified by bioaffinity agent is the basis for detection (Ghindilis *et al.*, 1998). The complex formation leads to a modification of surface property and results in a change in the transducer signal. Resistance or capacitance change detection based on the impedimetric and capacitive transducer, were usually reported as the detection principle for direct affinity biosensors (Bart *et al.*, 2005; Berggren *et al.*, 1998; Bontidean *et al.*, 1998; Grant *et al.*, 2006; Hedström

et al., 2005; Hleli *et al.*, 2006a; 2006b; Hu *et al.*, 2002; 2005; Jiang *et al.*, 2003; Jie *et al.*, 1999; 2000; Kim *et al.*, 2003; Limbut *et al.*, 2006a; 2006b; 2007; Rahman *et al.*, 2007; Thavarungkul *et al.*, 2007)

3.1.1 Impedimetric affinity biosensors

Electrochemical impedance spectroscopy (EIS) is a powerful tool for the analysis of interfacial properties change of modified electrodes upon biorecognition events occurring at the modified surface. Impedance measurement provides detail information on capacitance/ resistance change occurring at conductive or semiconductive surfaces (Guan *et al.*, 2004; Katz and Willner, 2003). Electrochemical transformations occurring at the electrode/electrolyte interface can be explained based on the theory of the electrical double layer (Figure 3.1a). When a potential is applied to an electrode, a double layer of charges takes place at the electrode/solution interface due to its conducting propriety. Excess charge on the metallic phase gets organized at the solution interface, causing a charge separation. As a result, two layers of charges with opposite polarity get organized at the electrode/solution interface, forming the double layer of charges as represented in Figure 3.1a. (Bard and Faulkner, 2001). In solution, three different theoretical layers can be distinguished: the inner Helmholtz plane (IHP), the outer Helmholtz plane (OHP) and the Gouy-Chapman diffuse layer (GCDL). The IHP is the closest to the electrode, and is made of solvent molecules, e.g. water, which are polarized, thus oriented. The following layer is the OHP, where solvated ions can approach the surface. The interaction between charged metal and solvated ions is governed by long-range electrostatic forces. The solvated ions are non-specifically adsorbed, as the interaction is independent from chemical properties. The next layer is the GCDL, which extends from the OHP to the bulk solution (Bard and Flulkner, 2001; Packirisamy and Kolb, 1996; Schmickler, 1996; Wang, 2001).

The layers have different electrostatic potential (Figure 3.1a): the potential energy decreases linearly from IHP to OHP, and exponentially through GCDL. The two regions with linear and exponential decay are the electrical double layer (EDL). The occurring of electrochemical transformer at electrode/electrolyte interface can usually be modeled by an electronic equivalent circuit, also called a

Randles circuit (Figure 3.1b). The component consist of a double layer-capacitor (C_{dl}) in parallel with a polarization resistor (also known as a charge-transfer resistor) (R_{et}) and a Warburg impedance (Z_w), connected in series with resistor that measures the resistance of the electrolyte solution (R_s). Some of these components can be extracted from the corresponding experimental impedance spectrum.

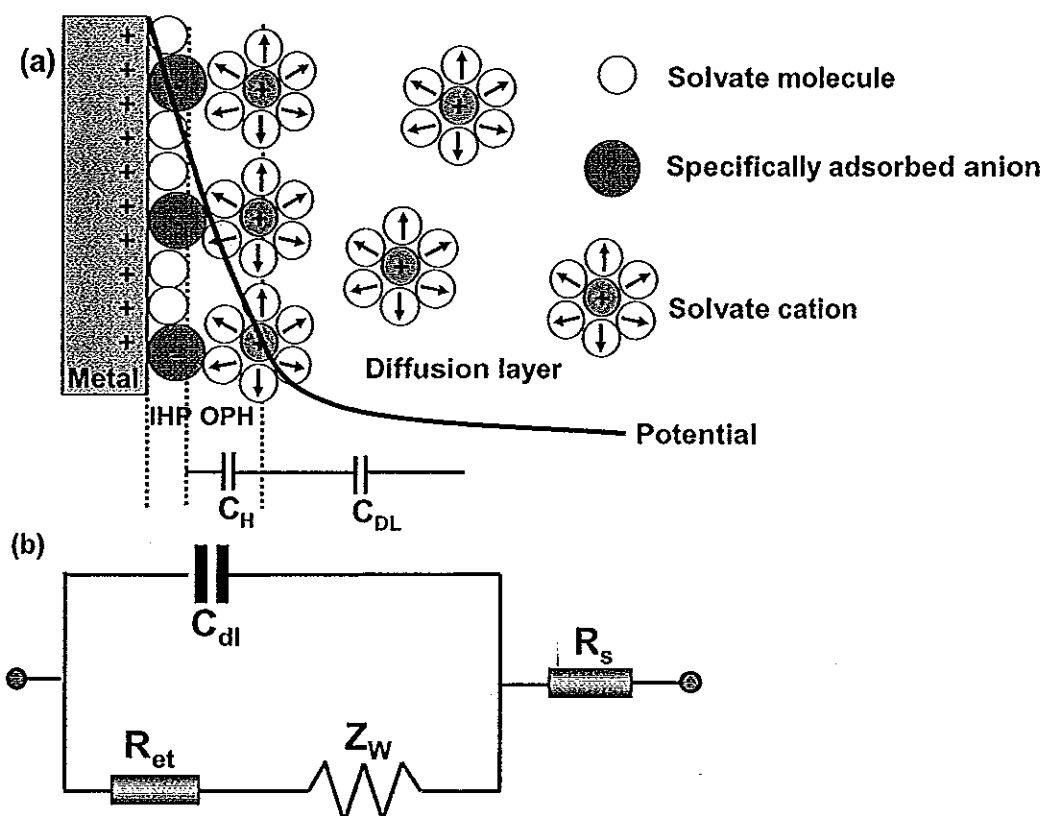


Figure 3.1 Schematic represent of a simple electrified interface at electrode/electrolyte solution interface; (a) double layer region which consist of Helmholtz planes (i.e.,Inner Helmholtz plane (IHP) and outer Helmholtz plane (OHP)) and diffusion layer, C_H is the capacitance due to Helmholtz la yer and C_{DL} is capacitance due to the diffusion layer; (b) Randle equivalent circuit representing each component at interface and in solution during electrochemical reaction is shown for comparison with physical components. C_{dl} , double layer capacitor; R_{et} , charge transfer resistor; W , Warburg resistor; R_s , solution resistor) (Modified from Bard and Flulkner, 2001; Park and Yoo, 2003; Wang, 2001).

The two components of the electronic scheme, R_s and Z_w , represent the bulk properties of the electrolyte solution and diffusion features of the redox probe in the solution. Therefore, these parameters are not affected by chemical transformation occurring at the electrode surface. The other two components in the scheme, C_{dl} and R_{et} depend on the dielectric and insulating features at the electrode/electrolyte interface and are controlled by the surface modification of the electrode. In fact, the electron transfer resistance, R_{et} , controls the interfacial support (Alfonta *et al.*, 2001; Katz *et al.*, 2001).

The impedance is calculated as the ratio between the system voltage phasor, $U(\omega)$, and the current phasor, $I(\omega)$, which are generated by a frequency response analyzer during experiment, similarly to the Ohm's law

$$Z(\omega) = \frac{U(\omega)}{I(\omega)} \quad \omega = 2\pi f \quad (3.1)$$

where ω and f (excitation frequency) have units of rad.s^{-1} and Hz, respectively. To make the derivation of the equation and its interpretation straightforward, the contribution of the Warburg component, resulting from the diffusion of the ion from bulk solution to the electrode interface, is neglected since it is small due to the limited of distance that ions must diffuse (Mansfeld *et al.*, 1998; Park and Yoo, 2003). A straightforward impedance expression of equivalent circuit can be derived by applying Ohm's law to two components connected in parallel. One of these is R_{et} , and the other is $1/(j\omega C_{dl})$, in which C_{dl} is the double layer capacitance.

$$\begin{aligned} Z(\omega) &= R_s + \frac{R_{et}}{1 + j\omega R_{et} C_{dl}} \\ &= R_s + \frac{R_{et}}{1 + \omega^2 R_{et}^2 C_{dl}^2} - \frac{j\omega \omega_{et}^2 C_{dl}}{1 + \omega^2 R_{et}^2 C_{dl}^2} \end{aligned} \quad (3.2)$$

Where $j = \sqrt{-1}$

The complex impedance of equation 3.2 can be presented as the sum of real, $Z_{re}(\omega)$, and imaginary, $Z_{im}(\omega)$, components (Equation 3.3) that originate mainly from resistance and capacitance of the cell, respectively (Bard and Faulkner, 2001; Katz and Willner, 2003; Park and Yoo, 2003).

$$Z(\omega) = Z_{im}(\omega) + jZ_{re}(\omega) \quad (3.3)$$

A Nyquist plot, a plot between imaginary part (Z_{im}) and real part (Z_{re}) is usually performed. Figure 3.2 shows an example of Nyquist plot where a typical shape of a Faradaic impedance spectrum is presented in the form of an impedance complex plane diagram. This includes a semicircle region lying on the axis followed by straight line. The semicircle portion, observed at high frequencies, corresponds to the electron transfer-limited process, whereas the linear part is characteristic of the lower frequency range and represents the diffusionally limited electrochemical process (Figure 3.2 a). In the case of very fast electron transfer process, the impedance spectrum could include only the linear part (Figure 3.2b), whereas a very low electron transfer step resulted in a large semicircle region (Figure 3.2c).

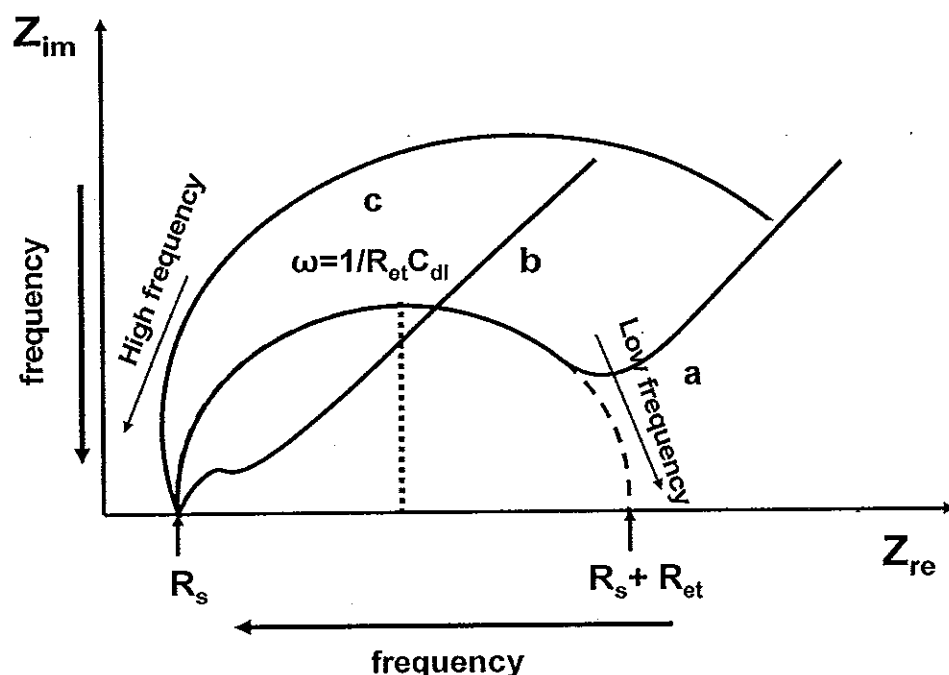


Figure 3.2 Faradaic impedance spectra presented in the form of a Nyquist plot for modified electrode is controlled by; a) diffusion of the redox probe (low frequencies) and the interfacial electron transfer (high frequencies). b) diffusion of the redox probe. c) the interfacial electron transfer (Modified from Katz and Willner, 2003).

At high frequencies the frequency-dependent term of Equation 3.2 vanished, resulting in $Z(\omega) = Z_{re}(\omega) = R_s$, which is an intercept on $Z_{re}(\omega)$ axis on high frequency side. For low frequency, Equation 3.2 becomes $Z(\omega) = R_s + R_{et}$ which is an intercept on $Z_{re}(\omega)$ axis on the low frequency side. At the frequency where the maximum $Z_{im}(\omega)$ is observed, the straightforward relationship $R_{et}.C_{dl} = 1/\omega_{max} = 1/(2Jf_{max})$ can be obtained and this indicates how the reaction take place. If $R_{et}.C_{dl}$ is known, C_{dl} can be obtained because R_{et} is already known from the low frequency intercept on the $Z_{re}(\omega)$ axis. Thus, the Nyquist plot gives all the necessary information about the electrode/electrolyte interface and the reaction (Katz and Wilnelner, 2003; Park and Yoo, 2003; Tang *et al.*, 2004).

For affinity binding, impedance measurement is an effective technique to probe the interfacial properties of bioaffinity molecule-analyte reaction at modified electrode surface (Kharotonov *et al.*, 2000; Tang *et al.*, 2004). When the specific

analyte bind to the surface immobilized bioaffinity molecules the electron transfer resistance (R_{et}) will increase, which relates to a large semicircle in the Nyquist plot (Figure 3.3).

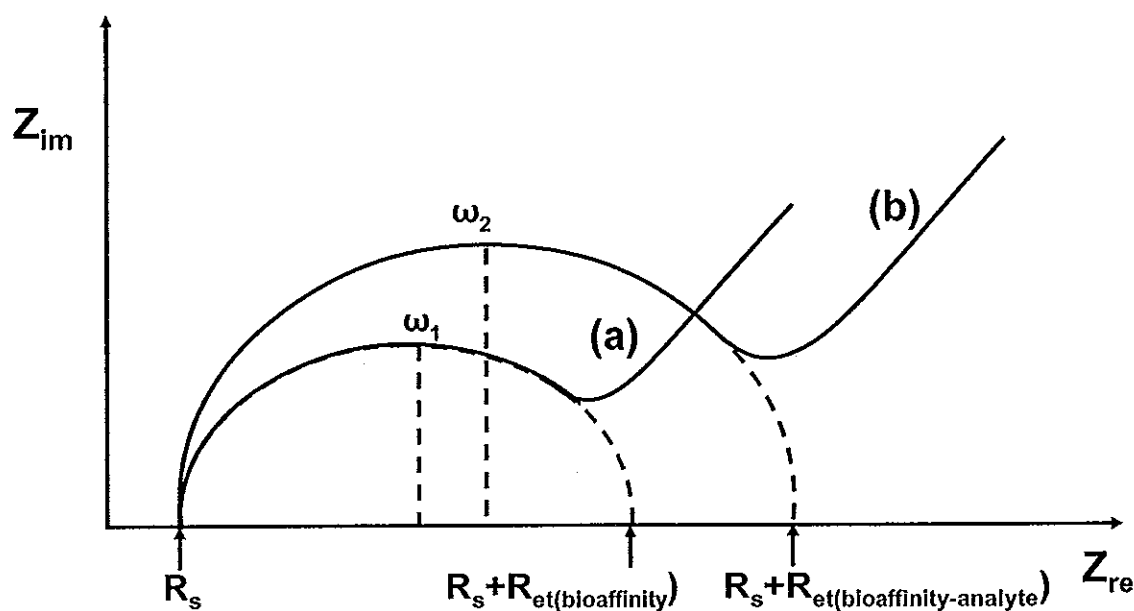


Figure 3.3 Typical Nyquist plot of immobilized bioaffinity molecule on the electrode surface (a) and complex of specific analyte-bioaffinity molecule (b) (Modified from Kharitonov *et al.*, 2000; Tang *et al.*, 2004)

The change of the electron transfer resistance (ΔR_{et}) is the difference between the value of electron transfer resistance after specific analyte binding to bioaffinity molecules ($R_{bioaffinity-analyte}$) and the electron-transfer resistance of the immobilized bioaffinity molecules ($R_{bioaffinity}$) (Katz and Wilnelner, 2003; Knaritonov *et al.*, 2000; Tang *et al.*, 2004).

$$\Delta R_{et} = R_{et(bioaffinity-analyte)} - R_{et(bioaffinity)} \quad (3.4)$$

Impedimetric affinity biosensors based the change of electron transfer resistance (ΔR_{et}) detection from Nyquist plot has been developed for many analyte-bioaffinity molecule interaction, particular directly detection (label-free) such as antibody-antigen (immunosensor) (Grant *et al.*, 2005;; Hleli *et al.*, 2006a; 2006b; Jie *et al.*, 1999; Navrátilová and Skládal, 2004; Rahman *et al.*, 2007; Tang *et al.*, 2004), DNA hybridization (Berdat *et al.*, 2007; Cai *et al.*, 2004; Gautier *et al.*, 2007; Li *et al.*, 2007; Ma *et al.*, 2006; Peng *et al.*, 2007; Vagin *et al.*, 2002; Yang *et al.*, 2007) and aptamer-protein reaction (Cai *et al.*, 2006; Radi and ÓSalivan, 2006a; 2006b; Rodriguez *et al.*, 2005, Zayats *et al.*, 2006).

Although the evaluation of electron transfer resistance through impedance was an effective method to prove the electron transfer resistance features of the surface of the modified electrode. However, the data of this principle detection is difficult to interpret and it is not suitable for real-time measurements (Bordi *et al.*, 2002; Guiducci *et al.*, 2004).

In addition, in Nyquist plot the capacitance (C_{dl}) can also be obtained at the frequency (ω_1 and ω_2 in Figure 3.3) where the maximum $Z_{im}(\omega)$ is observed and the change of capacitance (ΔC_{dl}) was also used as indication of affinity binding. It will be described in further section.

3.1.2 Capacitive affinity biosensors

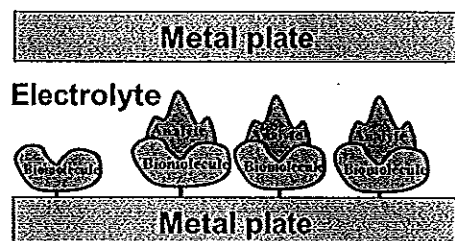
The measurement of capacitance is based on the change in dielectric properties or charge distribution when bioaffinity-analyte complex form on the electrode surface (Berggren *et al.*, 2001; Gebbert *et al.*, 1992). Capacitive affinity biosensor can be designed in two different ways, either by measuring the capacitance between parallel metal plates (Gebbert *et al.*, 1992) or by measuring the capacitance at the electrode/solution interface (Berggren and Johansson, 1997; Berggren *et al.*, 1998; Bontidean *et al.*, 1998; 2000; Hedström *et al.*, 2005; Hu *et al.*, 2002; 2005; Limbut 2006a; 2006b; 2007).

In the first approach, the capacitance between parallel metal plate separated by a certain distance and with a dielectric in between, The capacitance can be described by

$$C = \frac{\epsilon\epsilon_0 A}{d} \quad (3.5)$$

Where, ϵ is dielectric constant of material between the plates, ϵ_0 is the electric constant for vacuum, A is the area of the plate and d is the distance between the plates. When the bioaffinity molecule is immobilized on one plates the capacitance can be detected as a change of the thickness of a layer immobilized and/or as a change in the dielectric constant causes by the binding or releasing of analyte (Figure 3.4a). In the case of interdigitated electrodes with bioaffinity molecule immobilized in between, the forming of the complex will change the dielectric properties between the electrode causing the change in capacitance (Figure 3.4b).

(a) Parallel metal plates



(b) Interdigitated electrode

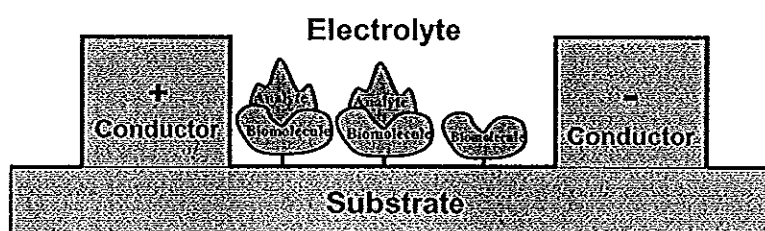


Figure 3.4 Schematic diagram of capacitive affinity biosensor based on two metal plates (a) capacitance change due to the change in distance and/ or dielectric constant between two plates and (b) due to the dielectric constant using interdigitate electrode (Modified from Gebbert *et al.*, 1992; Berggren *et al.*, 2001)

The disadvantages associated with this approach are difficulties in producing a short and reproducible distance between two plates, and its sensitivity to changes in the bulk solution (Berggren *et al.*, 2001).

The second approach, the capacitance is measured at metal/solution interface. In this case the capacitance measurement principle is based on the theory of electrochemical double layer (EDL) as described previously in section 3.3.1. The structure is equivalent to a parallel-plane capacitor. For two capacitors connected in series (Figure 3.1a), the double layer capacitance (C_{dl}) is the final total capacitance (C_{tot}) which can be calculated as;

$$\frac{1}{C_{dl}} = \frac{1}{C_{tot}} = \frac{1}{C_H} + \frac{1}{C_{DL}} \quad (3.6)$$

Where C_H is the capacitance due to the Helmholtz layer and C_{DL} is the capacitance due to the Gouy-Chapman diffusion layer (GCDL).

In biosensor, the electrode surface has been modified by the sensing layer. Therefore, the electrical double (ECL) is obligated away from the electrode surface. Figure 3.5 shows an example of a bioaffinity element-based capacitive biosensor electrode modification, where self assembled monolayer (SAMs) is used as the immobilization method, bioaffinity molecules is attached to the electrode surface.

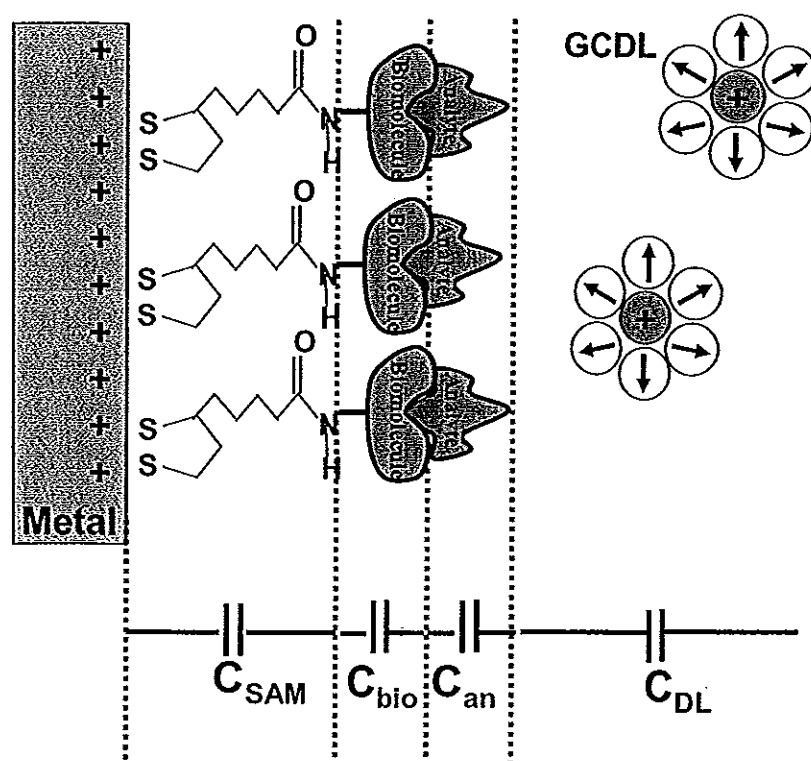


Figure 3.5 Schematic representation of affinity biosensor based capacitive biosensor and electrical double layer organized on the electrode solution interface

The capacitance at such a surface can be described to be built up of several capacitance in series (Figure 3.5). The two capacitors constitute the insulating layer on the electrode surface. These capacitors include the anchoring thiol of SAM (C_{SAM}) and the immobilized of bioaffinity molecule layer (C_{bio}), respectively. Binding of analyte to the bioaffinity recognition layer is described by C_{an} . The last

capacitor is described by the concentration dependent diffusion layer (C_{DL}) extending out into the bulk of solution. The total capacitance (C_{tot}) can then be described by

$$\frac{1}{C_{tot}} = \frac{1}{C_{SAM}} + \frac{1}{C_{bio}} + \frac{1}{C_{an}} + \frac{1}{C_{DL}} \quad (3.7)$$

There are several ways to determine electrical double layer (EDL) as capacitance such as, cyclic voltammetry (Ding *et al.*, 2005; Lang *et al.*, 1994), current step (Bard and Faulkner, 2001), impedimetric (Betty *et al.*, 2007; Li *et al.*, 2005; Wu *et al.*, 2005; Yang *et al.*, 2005) and potential step (Berggren and Johansson, 1997; Berggren *et al.*, 1998; Bontidean *et al.*, 1998; 2000; Hedström *et al.*, 2005; Hu *et al.*, 2002; 2005; Jiang *et al.*, 2003; Limbut *et al.*, 2006a; 2006b; 2007). However, in affinity biosensor, impedimetric and potential step are the most commonly used for determining the capacitance.

3.1.2.1 Impedimetric

As described in section 3.1.1 impedance measurement provides detail information on capacitance/resistance change occurring at electrode/electrolyte interface. From the Nyquist plot (Figure 3.3.) the capacitance can be obtained at the frequency (ω_1 and ω_2) which observed at the maximum value of $Z_{im}(\omega)$. The capacitance can be given by the relationship $R_{et} \cdot C_{dl} = 1/\omega_{max} = 1/(2\pi f_{max})$ and C_{dl} can be obtained, because R_{et} is known from the intercept on the $Z_{re}(\omega)$. Therefore, the value of the capacitance of the immobilized bioaffinity molecule ($C_{bioaffinity}$) and after specific analyte binding to bioaffinity molecule ($C_{bioaffinity-analyte}$) were obtained at the maximum frequency ω_1 and ω_2 , respectively. The change of the capacitance (ΔC_{dl}) is calculated by

$$(\Delta C_{dl}) = C_{dl(bioaffinity-analyte)} - C_{dl(bioaffinity)} \quad (3.8)$$

Although the detection of the capacitance change (ΔC_{dl}) from Nyquist plot has been developed for a number of affinity binding pairs such as antibody-antigen (immunosensor) (Grant *et al.*, 2005; Jie *et al.*, 1999), aptamer-protein

reaction (Liao and Ciu, 2007). However, the data of this principle detection is difficult to interpret and it is not suitable for real time measurement.

To detect the change in real time, impedance due to the capacitance can be monitored at a certain frequency. This can be done by the Bode plot *i.e.*, the plot of the phase shift *versus* of log frequency (Figure 3.6). The phase shift is zero when the impedance is mainly resistive and becomes more capacitive as the phase shift gets closer to 90° (Park and Yoo, 2003; Wu *et al.*, 2005). Therefore, the optimal frequency to detect the capacitance change could be found at phase angle closest to 90° in the Bode plot (Figure 3.6). At this frequency the capacitance change can be derived from the imaginary part, Z_{im} , of the complex impedance spectra.

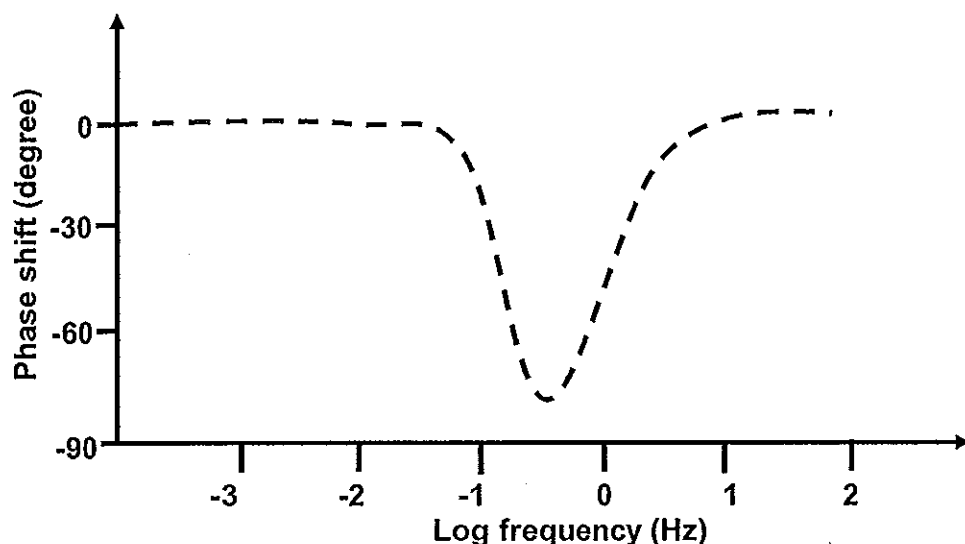


Figure 3.6 Bode plot of phase angles *versus* the log of frequency.

The detection of capacitive in real time from impedimetric has been developed for many analytes in immunosensor detection such as interferon- γ (Bart *et al.*, 2005) and penicillin G (Thavarungkul; 2007). Although the capacitance can be monitored in real time from impedimetric, however the instrumentation is expensive (Berggren *et al.*, 1997; 1999)

3.1.2.2 Potential step

In this technique the capacitance is obtained from the current response measured at the electrode/solution interface in a potentiostatically controlled experimental by applying an electrical perturbation signal to the electrode (Berggren *et al.*, 1998, 2001). For the capacitive affinity biosensor where the electrode is coated by an insulating layer, an accurate equivalent circuit should be $R_s(R_fC_{dl})$ as shown in Figure 3.7a. Because the electrode is insulated, R_f (Ohmic resistance of insulating layer) is much more than R_s . This made R_f acting like an open circuit and the system could thus be simplified as an R_sC_{dl} equivalent circuit. The simple model of resistor and capacitor in series (R_sC_{dl} model) (Figure 3.7b) has been used successfully for evaluation of capacitance for the electrode/solution interface system (Berggren *et al.*, 1998; Bontidean *et al.*, 1998; 2000; Hedström *et al.*, 2005; Hu *et al.*, 2002; 2005; Jiang *et al.*, 2003; Limbut *et al.*, 2006a; 2006b; 2007).

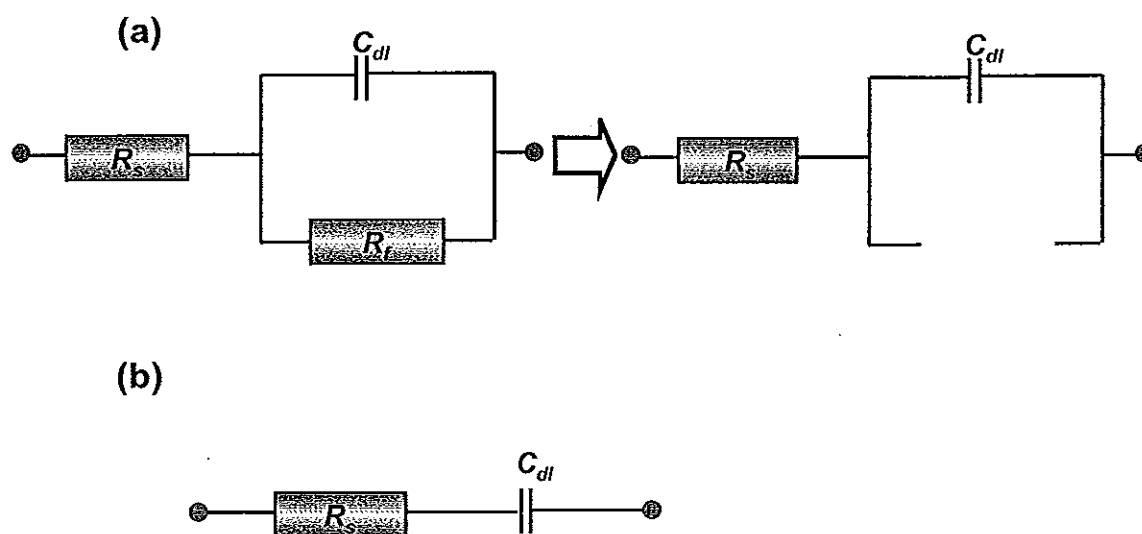


Figure 3.7 (a) $R_s(R_fC_{dl})$ equivalent circuit, where R_f is the Ohmic resistance of insulating layer that is much higher than R_s making its act like an open circuit. (b) Simple R_sC_{dl} equivalent circuit, R_s is the resistance of the solution and C_{dl} the double layer capacitance.

When a defined potential perturbation, also called potential pulse, is applied to a working electrode for a defined period (Figure 3.8a). The resulting

discharging current decays exponentially (Figure 3.8b). $R_s C_{dl}$ circuits, where a resistance and capacitance are connected in series, show a behavior well described by the theoretical exponential decay, expressed in Equation 3.9.

$$i(t) = \frac{u}{R_s} \exp\left(-\frac{t}{R_s C_{tot}}\right) \quad (3.9)$$

where $i(t)$ is the current response as a function of time, u is the applied pulse potential, R_s is the resistance of the solution and C_{tot} is the total capacitance at the electrode/solution interface.

As a linear relationship exists between $\ln i(t)$ and t , C_{tot} and R_s can be calculated from the linear least-square fitting (Figure 3.9) of the natural logarithm of Equation 3.9.

$$\ln i(t) = \ln \frac{u}{R_s} - \frac{t}{R_s C_{tot}} \quad (3.10)$$

Then, C_{tot} and R_s can be obtained from the slope and intercept of the linear least square of $\ln i(t)$ versus t (Berggren and Johansson 1997; Berggren *et al.*, 1998; 2001; Biotdean *et al.*, 1998; 2001).

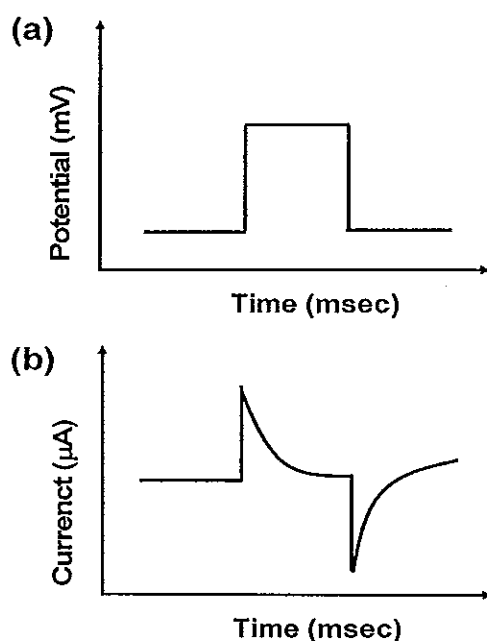


Figure 3.8 Potentiostatic step method to evaluate capacitance (a) applied potential pulse and (b) resulting current decay.

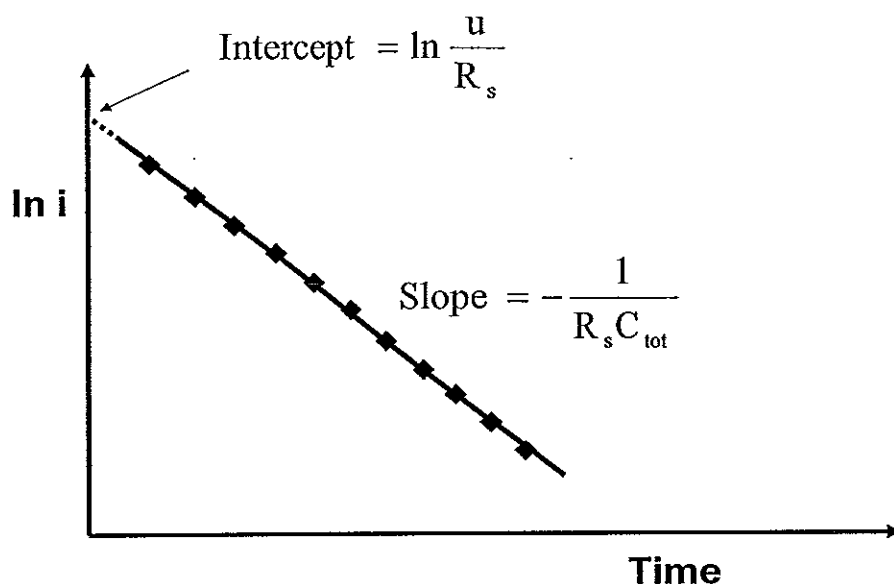


Figure 3.9 Logarithm of current vs time

This technique of capacitance measurement can provide label-free detection of affinity reaction with high sensitivity and specificity. More importantly it has been shown to be able to detect compound at very low concentration. (Berggren and Johansson, 1997; Berggren *et al.*, 1998; Bontidean *et al.*, 1998; 2000; Hedström *et al.*, 2005; Hu *et al.*, 2002; 2005; Jiang *et al.*, 2003; Limbut *et al.*, 2006a; 2006b; 2007). For these reasons, a part of this thesis investigated the detection of bioaffinity interaction with analyte by label-free capacitive measurement obtained from potential step.

For capacitive detection, a special immobilization technique is required, since the detection relies on the detection of interfacial changes originating from biorecognition events at the electrode surface (Katz and Willner, 2003), therefore, the electrode surface has to be electrically insulated. Self assembled monolayer (SAM) is one possible method that can fulfill this requirement (Wrobel, 2001) and is particularly suitable immobilization technique for capacitive biosensors (Riepl *et al.*, 1999). SAM can be formed by spontaneous adsorption of alkanethiol on gold surface that takes place at room temperature (Nuzzo and Allara, 1983; Porter *et al.*, 1987). The affinity between sulfur atom of alkanethiol and gold atom allows electrochemical insulation of the gold surface (to avoid faradic processes). It is also an

excellent immobilization technique for proteins. Moreover, proteins are shielded from direct contact with the metallic surface (Wadu-Mesthrige *et al.*, 2000). Therefore, SAM are preferred as immobilization technique in this work.

3.2 Indirect electrochemical detection

For this technique, the detection of the binding between analyte and its bioaffinity recognition molecule relies on the determination of a label molecule. A great variety of labels have been applied in indirect assay such as various enzyme (Ghindilis *et al.*, 1992; Kaku *et al.*, 1993; Kaneki *et al.*, 1994); and nanoparticle such as gold, silver and quantum dots (Wang *et al.*, 2002; Wang *et al.*, 2003).

There are several electrochemical transducers to detect the electrical signal from the binding of the analyte and its bioaffinity molecule such as, amperometric, voltammetric stripping, conductimetric and potentiometric.

3.2.1 Amperometric affinity biosensors

Amperometry is the measurement of a current flow generated by an electrochemical reaction at constant voltage (Luppa *et al.*, 2001; Ricci *et al.*, 2007). For biosensors, the technique is generally performed by using a three-electrode system consists of a working electrode with immobilized bioaffinity molecules (commonly made of inert metals such as platinum, gold, or carbon), a standard reference electrode (Ag/AgCl reference electrode or saturated calomel electrode) and an auxiliary electrode (e.g. a platinum wire). Since most (protein) analytes are not intrinsically able to act as redox partners in an electrochemical reaction, indirect detection of products of an enzymatic reaction are needed for the electrochemical reaction of the analyte at the sensing electrode. Generally the detection is performed by either sandwich or competitive assay (Djellouli *et al.*, 2007; Fu-Chun *et al.*, 2007; Gau *et al.*, 2001). In a sandwich assay the secondary bioaffinity molecule is labeled with a enzyme and the electrochemically active product from specific enzyme/substrate reaction is determined by amperometry. The generated current is directly proportional to specific analyte-bioaffinity molecule binding as shown in Figure 3.10a. For competitive assays the analyte competes with the enzyme labeled target analyte. The binding of the enzyme labeled decreases with increasing analyte

concentration, thus, the generated current is indirectly proportional to analyte concentration (Figure 3.10b).

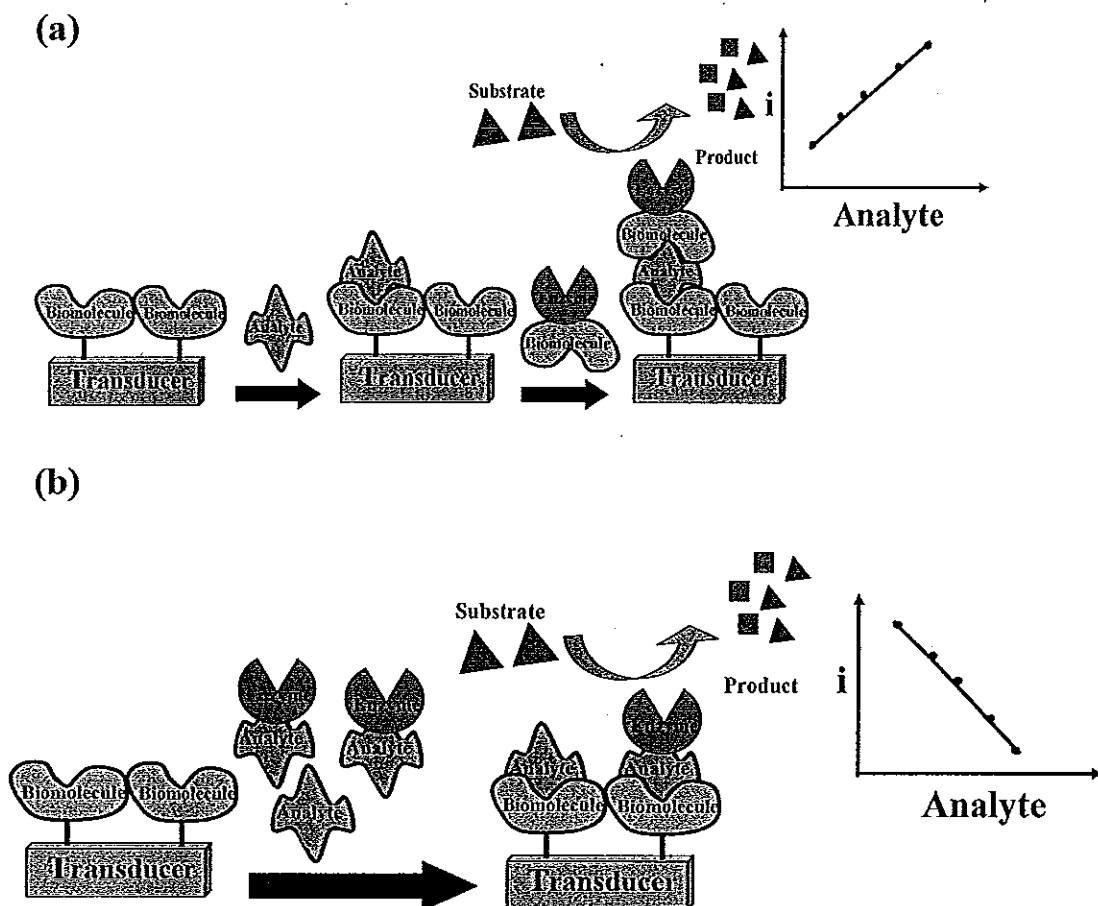


Figure 3.10 Schematic diagrams of the amperometric detection of affinity biosensor based (a) sandwich and (b) competitive assay by enzyme-labeled

Several enzymes have been successfully applied as a label for this technique which are horseradish peroxidase (HRP) (Djellouli *et al.*, 2007; Fu-Chen *et al.*, 2007), glucose oxidase (Gau *et al.*, 2001), alkaline phosphatase (Wang *et al.*, 2004), and urease (Campanella *et al.*, 1999). This technique has been applied for immunosensors (Campanella *et al.*, 1999; Fu-chen *et al.*, 2007), DNA hybridization (Djelloulli *et al.*, 2007; Gau *et al.*, 2001; Wang *et al.*, 2004) and aptamer-analyte detection (Ikebukuro *et al.*, 2004).

In addition, a few applications used nanoparticles as catalytic labels to amplify the signal in this type of assay. It has been reported that nanoparticles, such as platinum (Polsky *et al.*, 2006) and silver (Wu *et al.*, 2006) show excellent electrocatalytic activity to reduction in the presence of hydrogen peroxide and these techniques have been successfully applied for the detection of DNA hybridization (Polsky *et al.*, 2006; Wu *et al.*, 2006).

The main advantages of amperometric affinity biosensor are low cost, ease of operation and disposability. However it has some disadvantages such as, very noisy response and interference from electroactive species that could be present in the sample solution (Ghlindilis *et al.*, 1998; Gooding *et al.*, 2001).

3.2.2 Voltammetric stripping affinity biosensors

Stripping analysis is an extremely sensitive electrochemical technique for measuring trace metals. This technique comprises a variety of electrochemical approaches having a step of preconcentration onto the electrode prior to voltammetric measurement. The major advantages of stripping voltammetric to direct voltammetric measurement is that preconcentration factors of 100 to more than 1,000 can be achieved (Wang 2000). In general, affinity binding detection based on stripping analysis, indirect detection with nanoparticle as labeled molecules such as gold, silver nanoparticles and quantum dots are the most used (Cui *et al.*, 2003; 2007; Dai *et al.*, 2006; Dequair *et al.*, 2000; Hansen *et al.*, 2006; Lui *et al.*, 2004; 2007; Wu *et al.*, 2007). In the group of stripping voltammetry involving electrolytic preconcentration there are several well-known schemes such as anodic stripping, cathodic stripping or adsorptive stripping voltammetry. Among the stripping methods, anodic stripping voltammetry is currently the most used technique for affinity binding detection (Wang *et al.*, 2003).

In anodic stripping voltammetry (ASV) the metals are preconcentrated by electrodeposition onto the electrode. The deposition is done by cathodic deposition at a control time and potential. The potential is then scanned anodically, during scan deposited metal on the electrode are reoxidized, stripped out of the electrode which is a function of metal standard potential (Figure 3.11).

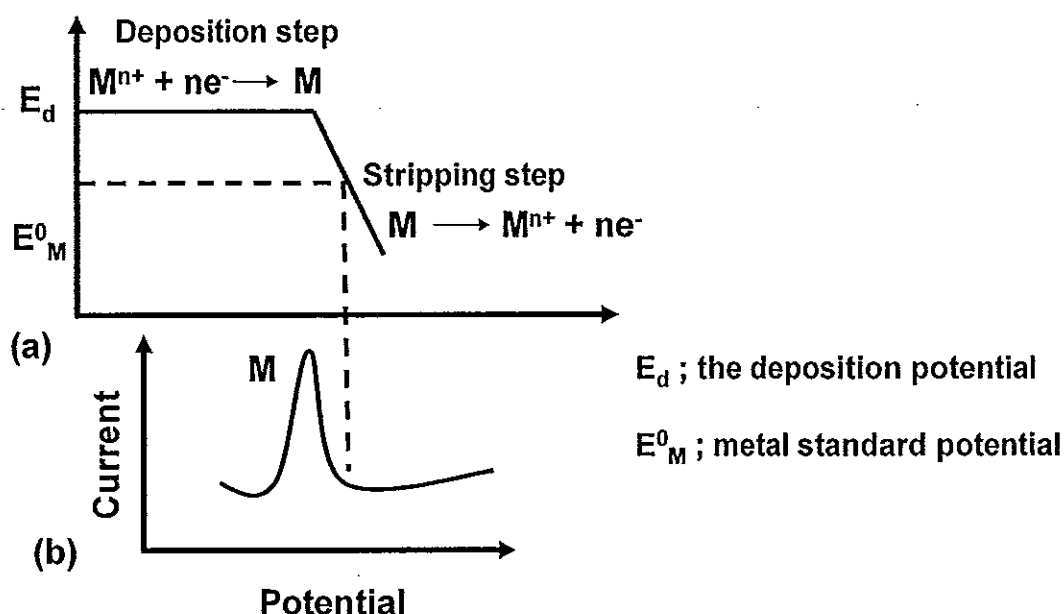


Figure 3.11 Anodic stripping voltammetry: (a) the potential -time wave form , (b) along with voltammogram (Modifoed from Wang, 2000; Esteban and Cassassas, 1994)

The application of anodic stripping voltammetric techniques for affinity binding detection with nanoparticle labels is based on either direct methods, without any previous chemical dissolution of nanoparticles (Gonzalez Garcia and Casta Garcia, 1995; Liu and Lin, 2005; Kerman *et al.*, 2004; Pumela *et al.*, 2005; Wang *et al.*, 2002) or indirect methods based on previous dissolution of nanoparticles obtained and analyzing the corresponding ions (Cui *et al.*, 2003; 2007; Dai *et al.*, 2006; Dequair *et al.*, 2000; Lui *et al.*, 2007).

Direct voltammetric detection of nanoparticles comprises solid-state analysis, where the metal forming nanoparticles are detected electrochemically without any preliminary dissolution steps to liberate the metal ions in solution. However, this type of detection needs direct contact between electrode surface and the nanoparticle labels. A general procedure of these method is that the target is first captured by an immobilized bioaffinity molecule on the solid-substrate, then the secondary bioaffinity molecules with nanoparticle labels is added. Finally the nanoparticle label is directly stripped on the electrode (Figure 3.12)

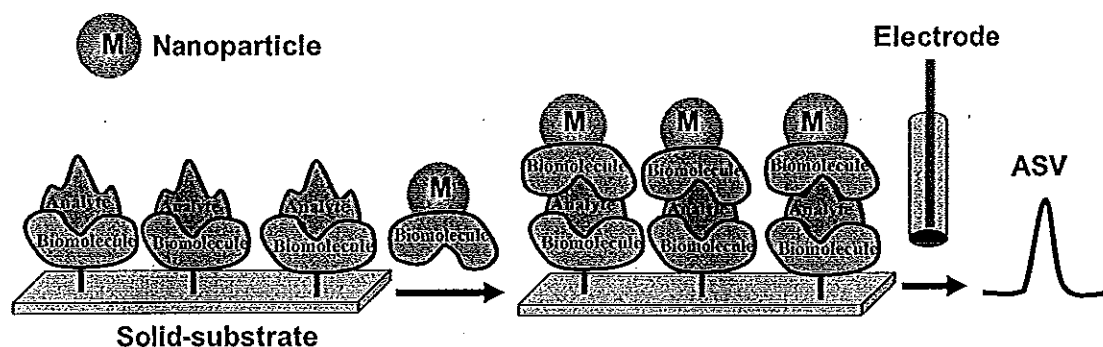


Figure 3.12 Direct anodic stripping voltammetric detection of affinity binding based on nanoparticle label (Modified from Kerman *et al.*, 2007)

This direct stripping voltammetric detection has been developed for some analyte–bioaffinity interactions such as immunosensors (Ambrosi *et al.*, 2007; Gonzalez Garcia and Costa Garcia, 1995) and DNA (Kerman *et al.*, 2007; Pumera *et al.*, 2005).

For indirect analysis, very sensitive nanoparticle label detection can be performed by oxidative dissolution of nanoparticles into the corresponding metal ion by anodic stripping. This technique was investigated by dissolution of metal nanoparticle labels after binding to target analyte by using the chemical reagents such as hydrogen bromide (HBr) (Authier *et al.*, 2001) or nitric acid (HNO₃) (Cai *et al.*, 2002; Liu *et al.*, 2004) and hydrochloric acid (HCl) (Wu *et al.*, 2007) into the metal ion and the solubilized metal ion was detected by anodic stripping (Figure 3.13).

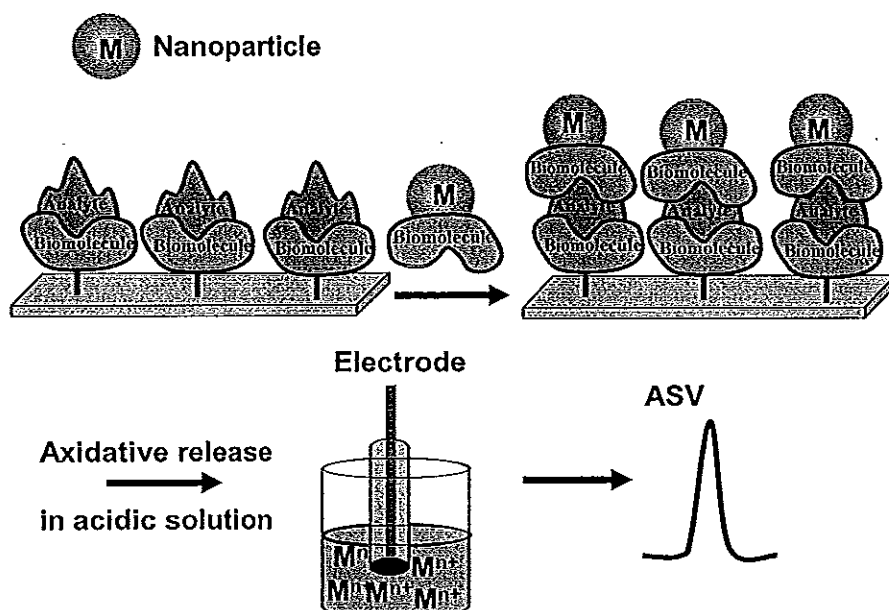


Figure 3.13 Indirect anodic stripping voltametric detection of affinity binding based on nanoparticle label.

This technique has also been applied as the detection principle for immosensors (Cui *et al.*, 2007; Dequaire *et al.*, 2000; Liu *et al.*, 2004; 2007) and DNA hybridization (Authier *et al.*, 2001; Cai *et al.*, 2002; Wu *et al.*, 2007).

The main advantage of this technique is its high sensitivity, enabling it to detect the analyte at low concentration. However, sometime the sensitivity is lost when non-tagging nanoparticle which occurs in the assay process may be adsorbed on the container surface (Ambrosi *et al.*, 2008).

3.2.3 Conductimetric affinity biosensors

This affinity biosensor transducer measures the alteration of the electrical conductivity in a solution at constant voltage caused by biochemical reaction which specifically generate or consume ions (Luppa *et al.*, 2001). There are only a few applications of these device for directly detection of affinity binding, since the change of the conductivity at the electrode during affinity complex formation is small (Yagiuda *et al.*, 1996), therefore, amplification of the conductivity signal based on indirect detection is employed.

For indirect detection of this assay, metal nanoparticles represent an excellent labeling system that can generate significant conductance or resistance changes when the binding event occurs (Ambrosi *et al.*, 2008). This approach was investigated by immobilizing bioaffinity molecules on the surface between the electrode gaps. After the interaction with the target analyte, the conductivity was detected after the secondary tagging with metal nanoparticles (i.e. gold or silver) (Figure 3.14). The assay of conductivity has been employed for both immunosensors and DNA detection (Park *et al.*, 2002).

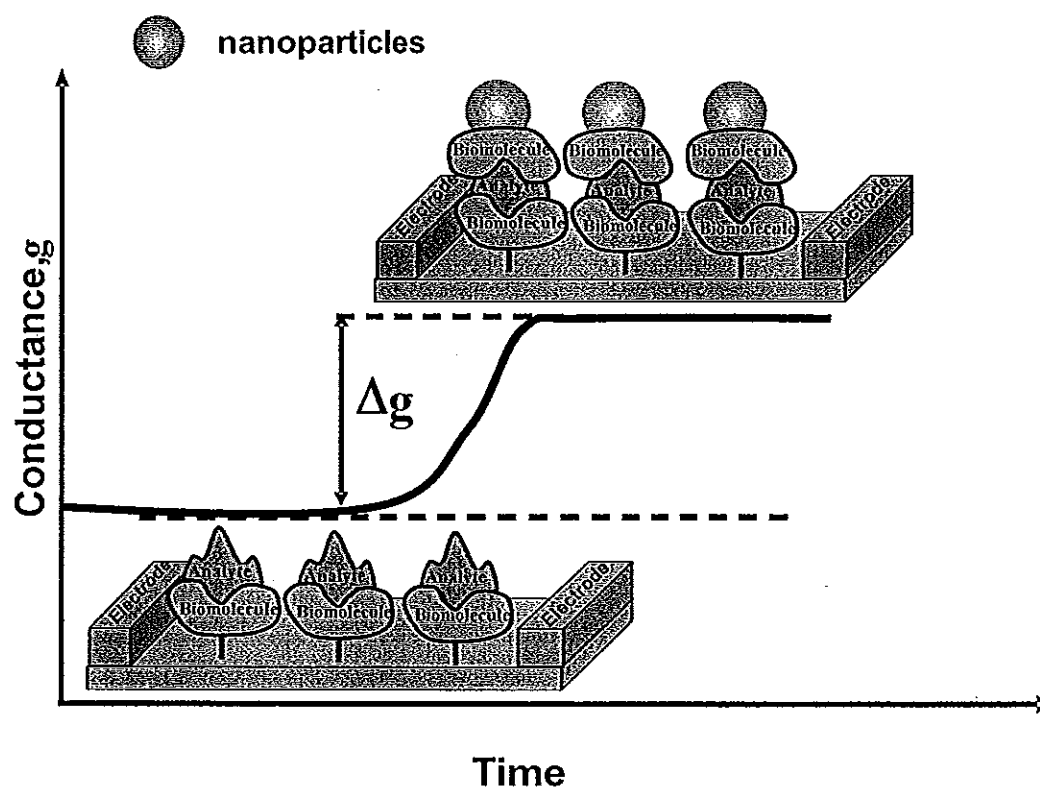


Figure 3.14 Schematic diagram of a conductivity assay in which nanoparticled labeled filled between electrodes.

In addition conducting polymer labels such as polyaniline (PANI) have also been used for this detection assay (Muhammad-Tahir and Alocilja, 2003). The technique relies on a sandwich assay when a secondary bioaffinity molecule conjugated to the immobilized bioaffinity molecules was captured between the

electrode gaps (Figure 3.15). PANI in a sandwich structure forms a molecular wire and bridges two electrodes for signal generation. This assay has been successfully used to detect food-borne pathogens by immunoassay (Muhammad-Tahir and Alcocilja, 2003).

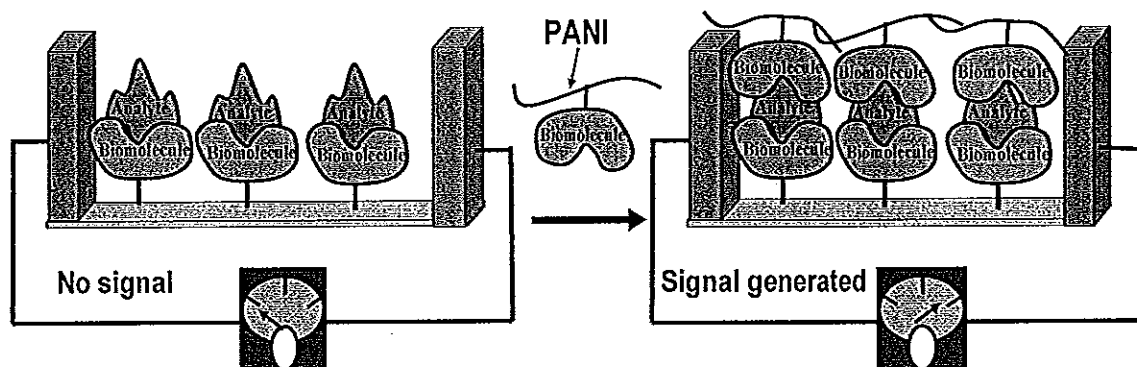


Figure 3.15 Conductivity assay based conducting polymer labeled which form the molecular wire for generating signal.

The advantages of conductimetric affinity biosensor are inexpensive, reproducible and disposable sensors. However, conductimetric sensor may also have problems with nonspecificity of measurements, because the resistance or the conductance of solution is determined by the migration of all ions present (Byfield and Abuknesha, 1994; Morgan *et al.*, 1996).

3.2.4 Potentiometric affinity biosensors

Potentiometric transducers are based on the determination of the potential difference between working and reference electrode when there is no current flowing between them. According to the Nernst equation the potential change of the working electrode is directly proportional to the logarithm of the ion activity of the specific analyte in solution (Wang, 2000). The equipment required for potentiometric measurement include working electrode (metal or membrane electrode), reference electrode (Ag/AgCl electrode, or saturated calomel electrode) and potential measuring device (Figure 3.16). Among the working electrodes, ion

selective electrodes (ISEs) based on thin films of a selective membrane as recognition element are the most commonly used.

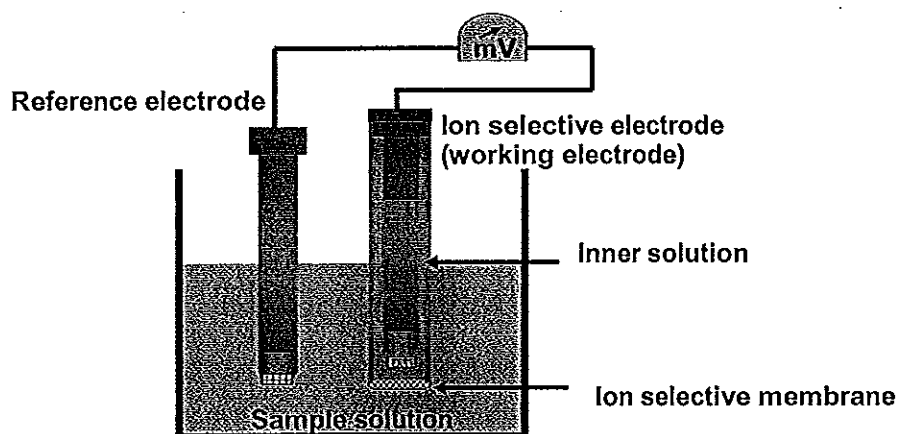


Figure3.16 Schematic diagram of an electrochemical cell for potentiometric measurement.

Ion-selective electrodes (ISEs) are mainly membrane-based devices, consisting of permselective ion-conducting material, which separate the sample from the inside of the electrode and containing the selective receptors (ionophores) which is highly specific to the ion of interest. A potential arises when the membrane separate two solution of different ion activity. The ion- recognition (binding) event generates a boundary potential at the membrane-sample interface. Another phase boundary is generated at the inner surface of the membrane (at the membrane- filling solution interface). The membrane potential corresponds to the potential difference across the membrane (Bakker and Pretsch, 2002; Wang, 2000). The resulting potential, which reflects the unequal distribution of the analyte ion across the boundary can be described as

$$E = \frac{RT}{nF} \ln \left(\frac{k_i a_{i,(aq)}}{a_{i,(m)}} \right) \quad (3.11)$$

Where E is the potential produced across the membrane of the analyte ion in the sample (outer and inner solution), k_i is a fuction of the relative free energy of salvation in both sample and membrane phase, R is the universal gas constant (8.314 J

$\text{k}^{-1} \text{mol}^{-1}$), T is the absolute temperature, n is the number of the electron, F is the faradaic constant (96,487 coulombs) and a is the activity of analyte ion.

Since the application of potentiometry with ion selective membrane electrodes for direct detection is based on a affinity reaction which provides low sensitivity and precision (Green, 1987), the labeled assay based potentiometric ion-selective electrode is an alternative way for detecting affinity reaction. Recently, potentiometric based on nanoparticle labeling (Chumbimuni-Torres *et al.*, 2006; Thürrer *et al.*, 2007) and miniaturized ion-selective electrodes (ISEs) with very low limit of detection was developed. Recent improvements in the detection limits of ion-selective electrodes based on polymeric membranes containing selective receptors (ionophores) make it possible to use miniaturized ISEs to detect femtomole amounts of ions in microvolume samples (Malon *et al.*, 2006; Rubinova *et al.*, 2007). Application of ISEs for ultrasensitive immunoassays in connection with nanoparticle amplification labels has also been reported (Chumbimuni-Torres *et al.*, 2006; Thürrer *et al.*, 2007). The first application of miniaturized ISEs for ultrasensitive nanoparticle based detection of protein interactions used a silver ion selective microelectrode for sandwich immunoassay in connection with the capture and silver enlargement of gold nanoparticle tracers (Chumbimuni-Torres *et al.*, 2006). The silver was then dissolved with hydrogen peroxide into silver ions. These were subsequently detected with a solid contact Ag^+ -selective microelectrode (Figure 3.17) This approach may form the basis for highly sensitive bioaffinity assays.

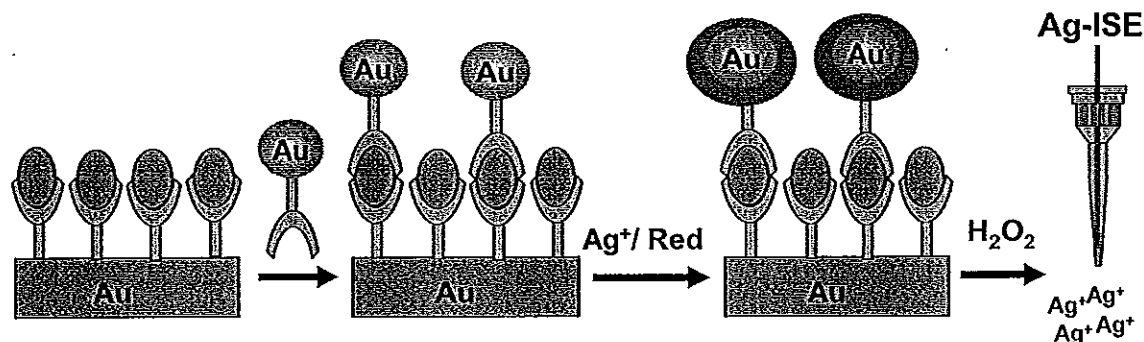


Figure 3.17 Potentiometric detection of sandwich immunoassay based on capture gold nanoparticles and the deposition and subsequent dissolution of silver, which was detected with Ag-ISE.

More recently, the use of potentiometric bioaffinity assay for protein using cadmium-selenide quantum dot (CdSe) as a label on a secondary antibody (Thuerer *et al.*, 2007) was reported, with a sandwich immunoassay format. CdSe labels were directly dissolved with hydrogen peroxide in microtiter plates without further chemical enhancement and the released cadmium ions were detected with miniaturized Cd-ISEs.

It is expected that various biomolecular interactions can be monitored with the assays based on different nanoparticle tracers and corresponding ISEs. The low detection limit from this detection method was reached without a preconcentration step, which is commonly used in other electrochemical transducer such as stripping methods. However without nanoparticle labels, it appears theoretically impossible for potentiometric sensor to detect the signal from bioaffinity binding. For these reasons, another part of the work presented in this thesis describes the investigation of indirect electrochemical detection of bioaffinity reaction based on potentiometric ion selective electrodes.

Chapter 4

Performance Criteria

For analytical methods, the characterization of its response is important. The performance criteria needed to be evaluated depend on the purpose of the method (Theverniers *et al.*, 2004). The performances of biosensors are evaluated based on the criteria listed below.

4.1 Linear range, sensitivity and limit of detection

Affinity biosensor calibration is usually performed by using standard solutions of analyte and plotting the response *versus* the analyte concentration or the response change *versus* the logarithm of analyte concentration (Thévenot *et al.*, 2001). For any quantitative method it is necessary to determine the range of analyte concentration over which the method can be applied (Wenclawiak *et al.*, 2004). Linearity range is the ability of the method to obtain test result proportional to the concentration of the analyte between the upper and lower levels to produce a linear response (Swartz and Krull, 1997) (Figure 4.1). For a good calibration curve, the linearity range should be wide in order to cover the unknown concentration. (Hibbert and Gooding, 2006)

Another important performance parameter is sensitivity. A method is called sensitive if a small change in concentration or amount of analyte causes a large change in the measured signal (Taverniers *et al.*, 2004), i.e., the higher the value of sensitivity the better. The sensitivity of the method is determined within the linear concentration of the calibration curve. In general, sensitivity refers to the slope of the linear concentration range of the biosensor calibration curve which is determined by the ratio of the response change *versus* analyte concentration ($\Delta R/\Delta C$) or the response change *versus* the logarithm of analyte concentration ($\Delta R/\log C$) (Figure 4.1) (Thévenot *et al.*, 2001)

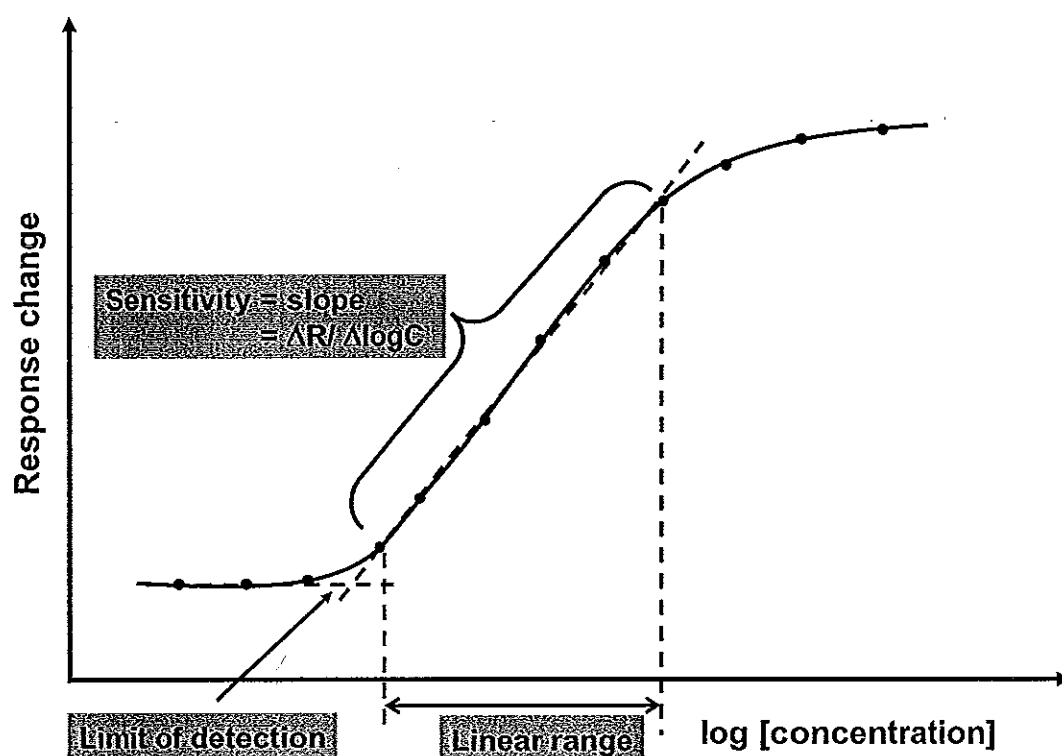


Figure 4.1 Calibration curve showing relationships for determining linear range, sensitivity and limit of detection (Buck and Lindner, 1994; Eggin, 1996; Wang, 2000)

In addition to linearity and sensitivity the analytical limit of determination of a method is also needed to be considered. The limit of detection (LOD) is defined as the lowest concentration of the analyte in a sample that can be detected, though not necessarily quantified (Swartz and Krull, 1997). There are several methods to evaluate LOD (Miller and Miller, 2000; Taverniers *et al.*, 2004). The LOD describes in this thesis follows either the IUPAC recommendation in 1994 (Buck and Lindner, 1994) or the signal-to-noise ratio method (Taverniers *et al.*, 2004). For 1994 IUPAC recommendation (Buck and Lindner, 1994), the calibration has the shape as shown in Figure 4.1, the limit of detection (LOD) is defined as the concentration of analyte at which the extrapolated linear portion of the calibration curve intersects the baseline—a horizontal line corresponding to zero change in response over several decades of concentration change.

If the calibration curve has the shape as shown in Figure 4.2 the limit of detection based on signal-to-noise was employed. This was determined by comparing measured signals from samples and establishing the minimum concentration at which the analyte can be reliably detected by exceeding the standard deviation of blank signal (σ). The LOD corresponds to that signal where the “signal - to-noise” ratio is 3:1 (Taverniers *et al.*, 2004). The minimal detectable signal (S_{\min}) or signal at the limit of detection was obtained by Equation 4.1

$$S_{\min} = 3\sigma \quad (4.1)$$

The concentration at the limit of detection (C_L) was then obtained as a function of S_{\min} as follows

$$C_L = \frac{(S_{\min} - S_{\text{blank}})}{m} \quad (4.2)$$

Where m is the analytical sensitivity, and S_{blank} is the value of the blank response.

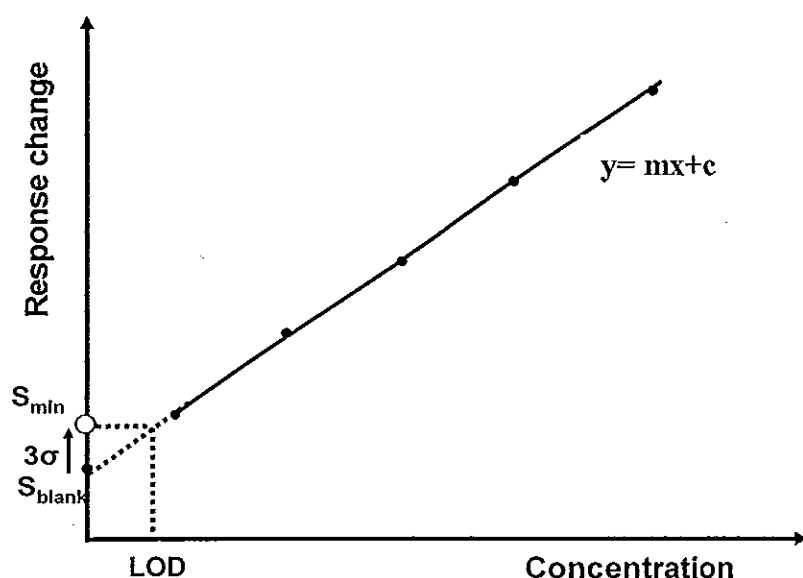


Figure 4.2 Calibration graph for the detectability characteristic (Adapted from Currell, 2000)

4.2 Selectivity

This factor is the ability to discriminate between different substrates and concerns the range of chemical species, that can interact with the system. Selectivity depends on the nature of the biological material (i.e. enzyme, antibody or nucleic acid) as well as on the operation parameters (Eggins, 1996). Method for biosensor selectivity determination can be performed by measuring the biosensor response to interference substance. A calibration curve for each interfering substance is plotted and compared to analyte calibration curve, under identical operating conditions (Thevenot *et al.*, 2001). The selectivity of the work presented was tested by introducing different substances that have physical or chemical characteristics similar to the target analyte or in the presence of other interference substances, such as those in the sample matrix.

4.3 Regeneration, stability and reproducibility

The interaction between target analyte and the immobilized biorecognition element employed in this work is via non-covalently binding, *i.e.*, electrostatic interactions, hydrogen bonding, hydrophobic interactions and Van der Waals interactions (Byfield and Abuknesha, 1994; Gizeli and Lowe, 2002; Rabbany *et al.*, 1994). Thus, the dissociation of the target analyte-biorecognition element complex is possible by using a regeneration solution. Regeneration allows surfaces to be reused many times, and this helps to reduce the cost of analysis. The regeneration of the biosensor system presented in this thesis was evaluated by considering the residual activity of the biorecognition electrode after regeneration. Although the activity of the affinity biosensor can be regenerated, all biological materials deteriorate in time, especially when they are removed from their natural environment. This means that one of the major drawbacks with biosensors is that the biological components usually have a fairly limited lifetime before it needs replacing. All developments of new biosensor include studies to show how the response of the biosensors change with time (Eggins, 1996; Thevenot *et al.*, 1999; 2001). The operational stability of the biosensor system presented in this thesis was investigated by monitoring the change of the signal of biological element modified electrodes at the same concentration of standard target analyte over a period of time.

Reproducibility is also another important factor with any analytical technique, but especially so with biosensors, where it is impossible to reproduce the quality of biological preparation as well as with ordinary chemical substances. Reproducibility is a measure of the scatter or the drift in a series of observations or results performed over a period of time (Thévenot *et al.*, 1999; 2001). In biosensor systems the expected reproducibility between replicate determinations should be less than $\pm 5-10\%$ (the relative standard deviation, % RSD) (Eggins, 1996).

Chapter 5

Aptamer-Based Potentiometric Measurements of Proteins Using Ion-Selective Microelectrodes

5.1 Introduction

Aptamers are nucleic acid ligands that have been designed through an *in vitro* selection process called SELEX (Systematic Evolution of Ligands by Exponential Enrichment) (Ellington and Szostak, 1999). Such aptamers hold great promise as affinity ligands for the biosensing of disease-related proteins and for developing protein sensing arrays (Hesselbert *et al.*, 2000; McCauley *et al.*, 2003; Osbourne *et al.*, 1997; ÓSuvillan, 2002; Stadtherr *et al.*, 20005; Xu *et al.*, 2005). Owing to their relative ease of isolation and modification, good stability, and wide applicability, they appear to be excellent alternatives to antibodies (Jayasena, 1999; Luzzi *et al.*, 2003). The attractive biosensing properties of aptamer recognition elements have been illustrated in connection with a colorimetric method, but the lower detection limit was only in the μM range (Liu and Lu, 2004; Stojanovic and Landry, 2002). Another detection scheme has been based on changes in fluorescence properties upon binding the fluorophore-labeled aptamer to the target (Fang *et al.*, 2001; Heyduk and Heyduk, 2005; Jhaveri *et al.*, 2000; Stojanovic *et al.*, 2001). However, this fluorescence response is usually weak and, owing to the difficult design of signaling aptamers, the method is not easy to generalize. Lower detection limits in the 10 nM range have been obtained with piezoelectric analyzers (Bini *et al.*, 2007).

In recent years, different electrochemical strategies have been developed for monitoring the interaction between aptamer and target analytes. The electrochemical methods are, in general, superior to the optical ones because of rapid response, simple handling, and low cost (Palecek and Fojta, 1994; Wang, 1999; 2000). Electrochemical aptamer biosensors are based, among others, on a binding-induced label-free detection (Cai *et al.*, 2006; Cheng *et al.*, 2007; Rodriguez *et al.*, 2005; Xiao *et al.*, 2005; Xu *et al.*, 2006), on enzymes (Baldrich *et al.*, 2004;

Ikebukuro *et al.*, 2005), or on nanoparticle labels (Hansen *et al.*, 2006). Excellent values in the fM range have been achieved with impedance spectroscopy and amplification by chemical means to denature the protein captured by an aptamer on the electrode surface (10 fM) (Xu *et al.*, 2006) and, very recently, by electrogenerated chemiluminescence *via* target protein-induced strand displacement (1 fM) (Wang *et al.*, 2007). Recently, the nanomaterial-based electrochemical detection of proteins has received considerable attention. The methods include the use of gold nanoparticles (Das *et al.*, 2006; Dequaire *et al.*, 2000) or semiconductor nanocrystal tracers (Choi *et al.*, 2006; Liu *et al.*, 2004). Usually, detection is made by anodic stripping voltammetry (ASV), which due to its intrinsic preconcentration step allows to achieve ultra-low detection limits (Wang, 1985).

Potentiometry with ion-selective electrodes (ISEs) represents an attractive tool for trace metal analysis in confined samples. Since with this method, the direct relationship between analyte activity and observed potential is independent of the sample volume, no deterioration of the signal or lower detection limit is expected upon reducing the volume. This is rather unique and establishes potentiometry as a preferred method when dealing with miniaturized analytical microsystems (Malon *et al.*, 2006; Robiva *et al.*, 2007). Recent improvements in the detection limits of ISEs based on polymeric membranes containing selective receptors (ionophores) have yielded sensors for the direct measurement in the subnanomolar concentration range (Ceresa *et al.*, 2002). It is now possible to use miniaturized ISEs for detecting sub-femtomole amounts of ions in microvolume samples (Malon *et al.*, 2006; Robiva *et al.*, 2007).

Recently, potentiometric microsensors have been demonstrated. They are very attractive for ultra-sensitive immunoassays in connection with nanoparticle amplification labels (Chumbimuni-Torres *et al.*, 2006). By reducing the sample volume and using quantum dot tags, the lower detection limit has been improved to $<10 \text{ ng ml}^{-1}$ (Thürer *et al.*, 2007). This project reports for the first time the use of a potentiometric microsensor for monitoring biomolecular interactions of an aptamer coupled to cadmium sulfide (CdS) tags. We use an aptamer known to bind the blood-clotting protein thrombin as a model system (Bock *et al.*, 1992). Thrombin, the last enzyme protease involved in the coagulation cascade, converts fibrinogen to insoluble

fibrin, which forms the fibrin gel either in physiological conditions or a pathological thrombus. The concentration of thrombin in blood can vary considerably. However, since a trace level of thrombin (high picomolar range) in blood has been found to be associated with coagulation abnormalities (Bichler *et al.*, 1995), it is important to assess this protein with high sensitivity.

5.2 Materials

Thrombin from human plasma, Tris-HCl, 6-mercapto-1-hexanol, tris(carboxethyl) phosphine (TCEP), potassium dihydrogenphosphate, and dipotassium hydrogenphosphate were purchased from Sigma (St. Louis, MO). The nucleic acid aptamers were obtained from Integrated DNA Technologies Inc. (Coralville, IA). The following oligonucleotide sequences were used:

Aptamer 1 (primary aptamer): 5'-HS-TTT TTT TTT TGG TTG GTG TGG TTG G-3'

Aptamer 2 (secondary aptamer): 5'-HS-TTT TTT AGT CCG TGG TAG GGC AGG TTG GGG TGA CT-3'.

Chemicals for the synthesis of CdS quantum dots, sodium bis(2-ethylhexyl) sulfosuccinate (AOT), $\text{Cd}(\text{NO}_3)_2$, Na_2S , cystamine, sodium 2-mercaptoethane sulfonate, and the solvents were obtained from Sigma. The ionophores, *N,N,N',N'*-tetradodecyl-3,6-dioxaoctanedithioamide (ETH5435), *N,N*-dicyclohexyl-*N',N'*-dioctadecyl-3-oxapentane di amide (ETH 5234), the lipophilic cation exchanger, sodium tetrakis [3,5-bis(trifluoromethyl)phenyl]borate (NaTFPB), the lipophilic salt, tetradodecylammoniumtetrakis(4-chlorophenyl)borate (ETH 500), 2-nitrophenyl octyl ether (*o*-NPOE), poly(vinyl chloride) (PVC), and tetrahydrofuran (THF) were purchased in Selectophore[®] or puriss grade from Fluka (Buchs, Switzerland). The solvent, CH_2Cl_2 and H_2O_2 , were obtained from Fisher (Pittsburgh, PA). Poly(3-octylthiophene) (POT) was synthesized as reported (Jarvinen *et al.*, 1995) In brief, polymerization of 3-octylthiophene was carried out in a chloroform solution containing 0.13 M of the monomer and 0.5 M of FeCl_3 . The monomer was slowly added to the mixture of FeCl_3 and chloroform. Polymerization time was 25 minutes and temperature 20 °C. The polymer was precipitated from a mixture by adding ethanol and hydrochloric acid. It was then dissolved in chloroform and

washed with water to separate the unreacted ferric chloride and insoluble material and 7 % ammonia solution was added to further separate the insoluble material and washed again with water. After the final wash it was dried under vacuum at room temperature. The methyl methacrylate-decyl methacrylate (MMA-DMA) copolymer matrix was synthesized using a procedure reported previously (Qin *et al.*, 2002). Methacrylic copolymers were synthesized via thermally initiated free radical solution polymerization. Each monomeric unit were added to 5 ml of dry ethyl acetate. The solution was purged with N₂ for 10 minutes before adding 3.4 mg of the initiator 2,2'-azobis(isobutyronitrile) (AIBN). The homogeneous solution was continuously stirred and the temperature was ramped to 85 °C, which was maintained for 16 h. After the reaction was completed, the solvent was evaporated and the polymer was redissolved in 10 ml of dioxane. The polymer solution was added drop wise to 800 ml of distilled water under vigorous stirring. The white precipitate was collected and dissolved in 25 ml of methylene chloride, followed by water removal with anhydrous Na₂SO₄ and filtering. The solvent was evaporated and the transparent polymer was air dried. All stock and buffer solutions were prepared using autoclave doubly deionized water (18.2 MΩ cm)

5.3 Methods

5.3.1 Preparation of cadmium ion selective microelectrode (Cd-ISE).

5.3.1.1 Cd-ISE Membrane

The Cd-ISE membrane was prepared by dissolving 60 mg of the following components in CH₂Cl₂ (0.8 ml); ETH 5435 (1.27 wt%, 15 mmol kg⁻¹), NaTFPB (0.46 wt%, 5 mmol kg⁻¹), ETH 500 (1.15 wt%, 10 mmol kg⁻¹) and copolymer MMA-DMA (97.12 wt%). The membrane solution was degassed by purging it with N₂ before use. The membrane for the Ca-ISE, used as a pseudoreference electrode, was prepared by dissolving 140 mg of the following components in THF (1 ml): ETH 5234 (0.87 wt%, 10.9 mmol kg⁻¹), NaTFPB (0.47 wt%, 5.12 mmol kg⁻¹), PVC (32.2 wt%), and *o*-NPOE (66.3 wt%). The solution was left to evaporate for 1 h, 20 µl was then filled into a 100-µl pipette tip and left to dry

for at least 24 h. Then, the membrane was conditioned in 100 ml of 10^{-3} M CaCl_2 for 1 day.

5.3.1.2 Microelectrode

The solid contact Cd^{2+} -selective microelectrode was prepared by using a 2 cm long Au wire (200 μm diameter) as solid substrate soldered to a Ag wire for electric contact. Before use, the Au wires were thoroughly cleaned with 10% sulfuric acid and rinsed with water, then dried with acetone, and left in CHCl_3 for 5 min. The solution of Poly (3-octylthiophene) (POT) (25 mM with respect to the monomer in CHCl_3) was applied along the Au wire by drop-casting at least three times or until the color of the wire became black, and then left to dry. The wires were inserted into a polypropylene tip so that they were level with the end of the micropipette tip as showed in Figure 5.1. Finally, 20 μl of the membrane cocktail, previously prepared, was dropped into the tip of the micropipette tip, on the top of the wire. The process was repeated three times at 15 min intervals and allowed to dry for 2–3 h for the total evaporation of CH_2Cl_2 . The microelectrodes were conditioned, 1 day each, first in 10^{-3} M CdCl_2 and subsequently in 10^{-9} M CdCl_2 with 10^{-4} M CaCl_2 .

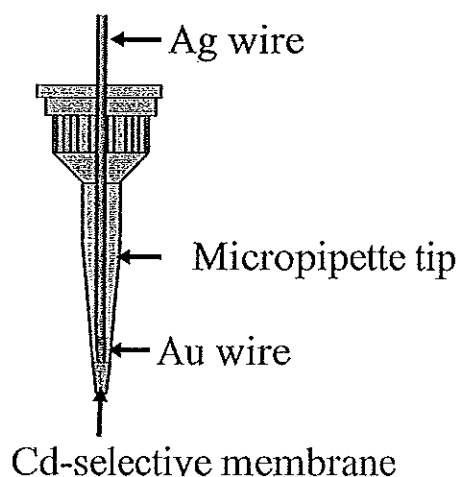


Figure 5.1 Solid contact Cd-ISE microelectrode

5.3.2 Preparation of CdS quantum dot nanocrystals

Quantum dot (QD) nanoparticles were prepared using a slightly modified procedure reported previously (Willner *et al.*, 2001). First, sodium bis(2-ethylhexyl) sulfosuccinate (AOT) (14.0 g) was dissolved in a mixture of *n*-hexane (200 ml) and water (4 ml). The resulting solution was separated into two sub-volumes of 120 ml and 80 ml. A 0.48 ml-aliquot of a 1 M $\text{Cd}(\text{NO}_3)_2$ solution was added to the 120 ml sub-volume, while 0.32 ml of a 1 M Na_2S solution was added to the 80 ml sub-volume. The two solutions were stirred for 1 h, then mixed and stirred for an additional hour under N_2 . The quantum dots were capped by adding cystamine (0.34 ml, 0.32 M) and sodium 2-mercaptoethane sulfonate (0.66 ml, 0.32 M) and mixing under N_2 for 24 h. Evaporation of hexane *in vacuo* yielded the CdS quantum dot nanocrystals, which were washed with pyridine, hexane, and methanol.

5.3.3 Thrombin aptamer immobilization and binding assay using sandwich format

Schematic represent of the immobilization of aptamer, its binding with thrombin and the detection are shown in Figure 5.2. The procedure is described as follows;

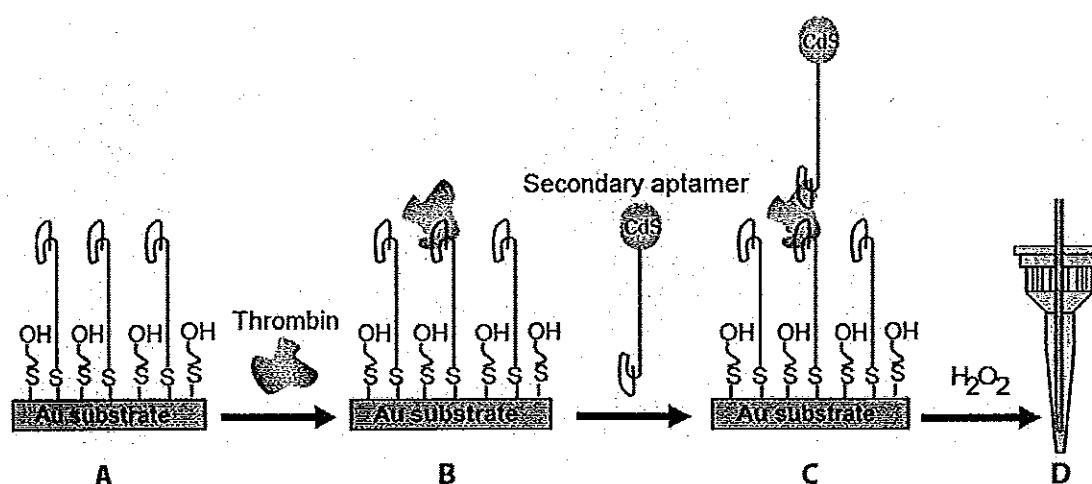


Figure 5.2 Representation of the analytical protocol: A) Formation of a mixed monolayer of thiolated aptamer on gold substrate; B) thrombin addition and binding with aptamer; C) secondary binding with CdS-labeled aptamer, D) dissolution of CdS label followed by detection using a solid-contact Cd^{2+} -selective microelectrode.

5.3.3.1 Preparation of oligonucleotide aptamer on gold surface

The immobilization of oligonucleotides was based on mixed self-assembled monolayer (Fig 5.2A), follows a previous report (Hansen *et al.*, 2006).

Cleavage of dithiol protecting group. Thiolated aptamers were received with disulfide protecting groups. The disulfide-protected nucleotides (100 μ M, 10 μ l) were diluted with autoclave water to 100 μ l and treated with 1 mg of tris(carboxethyl) phosphine (TCEP) for 30 min, followed by purification using a MicroSpinTM G-25 column obtained from Amersham Biosciences (Buckinghamshire, UK).

Gold substrates. The gold substrates were obtained from Denton Vacuum LLC (Moorestown, NJ), machine cut (Advotech Company Inc., Tempe, AZ) to identical pieces (6.0 x 3.0 x 0.2 mm³), assuming a uniform thickness.

Preparation of mixed monolayers. Gold substrates were cleaned in Piranha solution and rinsed with water prior to use. (*Safety note:* the Piranha solution should be handled with extreme caution.) The oligonucleotide monolayer was generated by treating the gold substrates with a 1 μ M thiolated oligonucleotide aptamer solution (100 μ l) in a potassium phosphate buffer (1 M, pH 8.0) overnight, followed by removal of the solution. The surface of the gold substrates was then blocked by a 10-min treatment with 6-mercapto-1-hexanol (0.1 M, 100 μ l), followed by washing with water.

5.3.3.2 Preparation of CdS quantum dot-oligonucleotide aptamer conjugates

The CdS-oligonucleotide conjugate was prepared by using a modified protocol published earlier (Hansen *et al.*, 2006; Wang *et al.*, 2002). First, CdS quantum dot suspension (0.2 mg ml⁻¹, 500 μ l) was exposed to 750 nM of thiolated oligonucleotide secondary aptamer (aptamer 2). The mixture was stirred overnight at room temperature. The quantum dot-aptamer conjugate was collected by centrifugation at 10,000 rpm for 45 min, removal of supernatant, and resuspension in binding buffer (50 mM Tris-HCl, 100 mM NaCl, 5 mM KCl, and 1 mM MgCl₂; pH 7.4)

5.3.3.3 Sandwich aptamer-protein assay

The aptamer-modified gold substrates were incubated for 1 h with the desired amount of thrombin (Figure 5.2 B) in binding buffer (100 μ l) followed by washing with washing buffer (50 mM Tris-HCl, 0.1% Tween 20; pH 7.4). Then, the gold substrates were incubated with quantum dot–oligonucleotide secondary aptamer for 60 min at room temperature as shown in Figure 5.2C. The supernatant was removed, the gold substrates were washed twice with washing buffer (each 100 μ l), and transferred to new microwells, where they were washed 4 times, again with the washing buffer (each 100 μ l) and twice with water.

5.3.3.4 Dissolution and detection

Hydrogen peroxide was used for the dissolution step since it was observed that it can efficiently oxidize the CdS quantum dots after carefully optimizing concentration and reaction time (Thürer *et al.*, 2007). In the final assay, dissolution of CdS was carried out by the addition of 0.01 M H_2O_2 in 10^{-4} M CaCl_2 (100 μ l) for 1 h to ensure complete oxidation and detect the released Cd^{2+} by potentiometric cadmium ion-selective electrode (Figure 5.2D). The detection was performed in microwells (Corning Inc., NY). Prior to the measurements, each well was pretreated with 10% HNO_3 overnight to removed any trace metal which might be on the surface of the well and then washed at least 5 times with deionized water and left to dry.

5.3.4 Potentiometric Measurements

Potentiometric measurements were performed in stirred solutions at room temperature (22 $^{\circ}\text{C}$) with a PCI MIO16XE data acquisition board (National Instruments, Austin, TX) connected to a four-channel interface (WPI, Sarasota, FL). Measurements were performed in ELISA microwells containing 180 μ l of 10^{-4} M CaCl_2 and adding 20 μ l of sample, using a Cd-ISE as working electrode and a Ca-ISE as reference and a small magnetic stirring bar as shown in Figure 5.3.

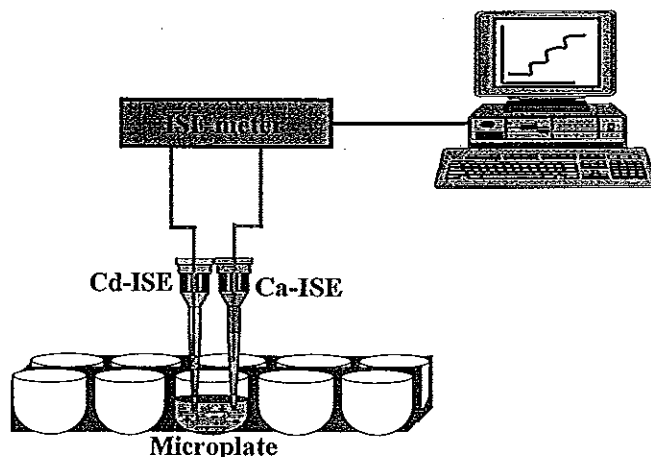


Figure 5.3 Schematic view of potentiometric measurement in 200 μl of ELISA microwells.

5.4 Results and discussion

5.4.1 Characterization of Cd^{2+} ion selective microelectrode

Solid-contact ISEs with nanomolar detection limits can now be routinely prepared for different ions (Chumbimuni-Torres *et al.*, 2006). Such electrodes are easily miniaturized to operate in samples of very small volume (Malon *et al.*, 2006; Robinova *et al.*, 2007). In this work, a novel solid-contact Cd^{2+} -selective microelectrode has been developed, which is based on the copolymer matrix MMA-DMA and the ionophore ETH 5435 (Ion *et al.*, 2006).

The novel Cd-ISE was first characterized in large samples of 100 ml. As shown in Figure 5.4A, with a background of 10^{-4} M CaCl_2 , it displays a very good lower detection limit of 100 pM. In microwell plates of 200 μl sample volume, the detection limit is higher one order of magnitude (Figure 5.4B). Yet, it is still in the nanomolar range (1 nM) with the same background. The reproducibility of the solid-contact microelectrodes in 200- μl samples was evaluated by recording three different calibration curves over the concentration range of 10^{-10} – 10^{-5} M. After each measurement, the electrode was washed for 5 min to eliminate possible memory

effects. The results in Table 5.1 show good reproducibility of the calibration equation and the relative standard deviation of the EMF for each concentration was < 1 mV.

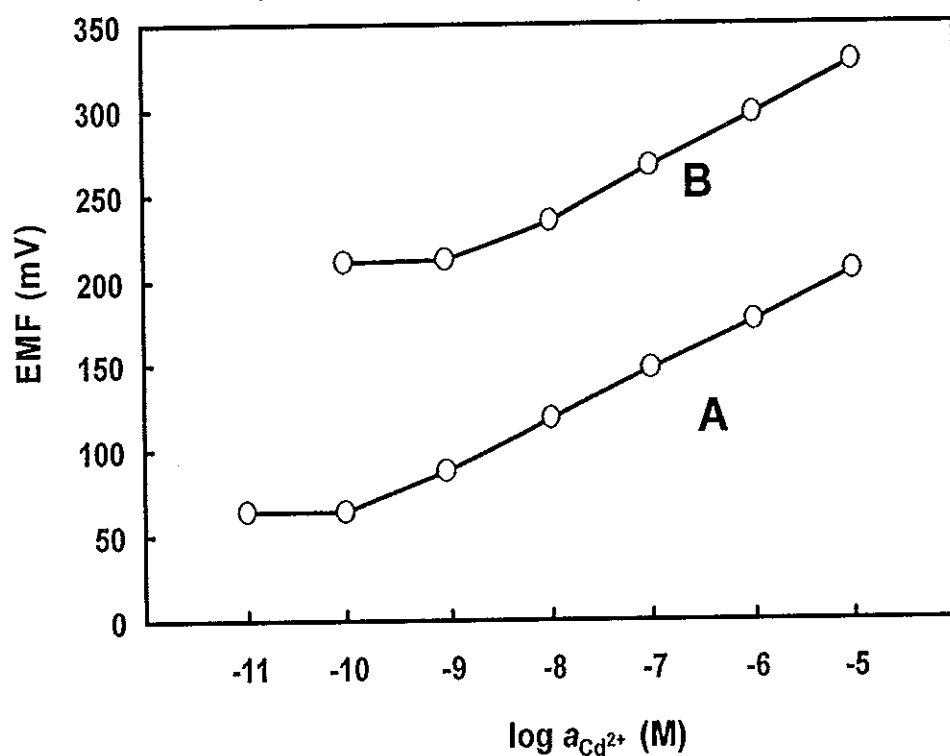


Figure 5.4 Calibration curves of solid-contact Cd^{2+} -selective electrode: A) in 100-ml and B) in 200- μl samples with 10^{-4} CaCl_2 as background using ELISA microplates.

Table 5.1 The EMF values of the Cd-ISE in 200 μl sample volume for the concentration of CdCl_2 in range of 10^{-10} - 10^{-5} M

Adding time	EMF (mV)						Linear equation	r
	log Concentration of CdCl ₂ , (log [CdCl ₂]) (M)							
	-10.0	-9.0	-8.0	-7.0	-6.0	-5.0		
1	211.34	210.63	235.69	264.05	295.63	326.71	y=29.2±0.8x + 471±6	0.999
2	211.87	209.60	236.27	263.47	294.72	327.39	y=29.4±0.8x + 472±6	0.999
3	211.76	210.54	235.39	264.48	295.42	328.09	y=29.5±0.9x + 473±6	0.999
Average	211.6 ± 0.2	212.7 ± 0.6	234.8 ± 0.5	263.3 ± 0.5	296.9 ± 0.5	327.4 ± 0.7		

For selectivity measurements, the Cd-ISE membranes were conditioned in 10^{-3} M CaCl_2 for 2 days in order to avoid primary ions leaching from the membrane (Bakker, 1997). For interfering ion such as Ca^{2+} , H^+ and Na^+ , a calibration curve was recorded and the selectivity coefficients were calculated using the separate solutions method (Bakker *et al* 2000). The calibration plot were determined in pure cadmium and interfering with a series of solutions with varying the concentration. The selectivity coefficients were then calculated according to Equation 1 from a cadmium and an interfering sample at equal concentration

$$\log K_{\text{Cd},J}^{\text{pot}} = \frac{2F\{E_J - E_{\text{Cd}}\}}{2.303RT} + \log \left(\frac{a_{\text{Cd}}}{a_J^{2/z_j}} \right) \quad (5.1)$$

where J represents the interfering ion, $K_{\text{Cd},J}^{\text{pot}}$ is the selectivity coefficient, z_j is the valency of the interfering ion tested, E_{Cd} and E_J are the potential outputs in testing solution, a is the activity of the interfering and primary ion, R is the gas constant, F is the Faraday constant and T is the absolute temperature. Table 5.2 shows that the membranes exhibit good selectivities for the relevant interfering ions, Ca^{2+} , H^+ and Na^+ with the corresponding logarithmic selectivity coefficients.

Table 5.2 Selectivity coefficient ($\log K_{\text{Cd},J}^{\text{pot}}$) determined by the separation solution method.

Ion	Selectivity coefficient
	$\log K_{\text{Cd},J}^{\text{pot}}$
Cd^{2+}	0.00
Ca^{2+}	-7.04
H^+	3.88
Na^+	-4.59

Owing to the high selectivity of Ca^{2+} , it was selected as the background electrolyte together with a Ca^{2+} -selective pseudoreference electrode. For this purpose, the selectivity of the Ca-ISE for Cd^{2+} was again, determined by separation solution method, and found to have the value $\log K_{\text{Ca,Cd}}^{\text{Pot}} = -3.15$, which is sufficiently high.

5.4.2 Thrombin determination using Cd^{2+} selective microelectrode

Our goal is to show that protein (thrombin) can be quantified by potentiometric detection of Cd^{2+} release from the CdS quantum dots used as a label, couple to aptamer via a simpler assay setup, that allows us to improve the detection limit and the time of the assay and to create a more robust methodology for bioassay, using ion selective microelectrodes with low detection limit.

In the experiment, sandwich assay was used and two different aptamers, binding to the protein at different sites, were chosen as shown in 5.2. The sandwich assay for aptamer-thrombin binding, involving the immobilization of thiolated primary aptamer on gold substrate (A), along with binding with thrombin (B), followed by adding a secondary aptamer conjugate to CdS-QD tags (C). Then, the quantum dot is dissolved with 0.01 M H_2O_2 and the released Cd^{2+} is detected with Cd^{2+} -ISE (D).

Optimization of some parameters of the aptamer-thrombin interaction when performing the measurement according to Figure 5.2 was needed to improve the detection of thrombin with the ion selective microelectrode, and these were studied as follows.

5.4.2.1 Concentration of hydrogen peroxide (H_2O_2) and reaction time for dissolution of Cd^{2+}

For aptamer-based protein detection, the CdS quantum dot labels were oxidized with H_2O_2 since HNO_3 , the standard oxidizing agent for anodic stripping voltammetry (ASV) (Hansen *et al.*, 2006), would deteriorate the lower detection limit due to proton interference. The influence of H_2O_2 on the response of the solid-contact microelectrodes was examined by using three different concentrations of hydrogen peroxide, 1 M, 0.1 M and 0.01 M for the dissolution of cadmium. Figure 5.5 shows

the potentiometric response of the Cd^{2+} -selective electrode immersed in 200- μl wells containing different concentrations of H_2O_2 . The response gradually increases and gives final potential readings after 15 min. While an increase in its concentration accelerates the dissolution (Thürer *et al.*, 2007) no influence on the potentiometric response was observed at ≤ 0.01 M H_2O_2 . A concentration of 0.01 M H_2O_2 was selected for further experiments since some signal drifts were observed with 0.1 M H_2O_2 , which was probably due to the interaction of H_2O_2 with the conducting polymer.

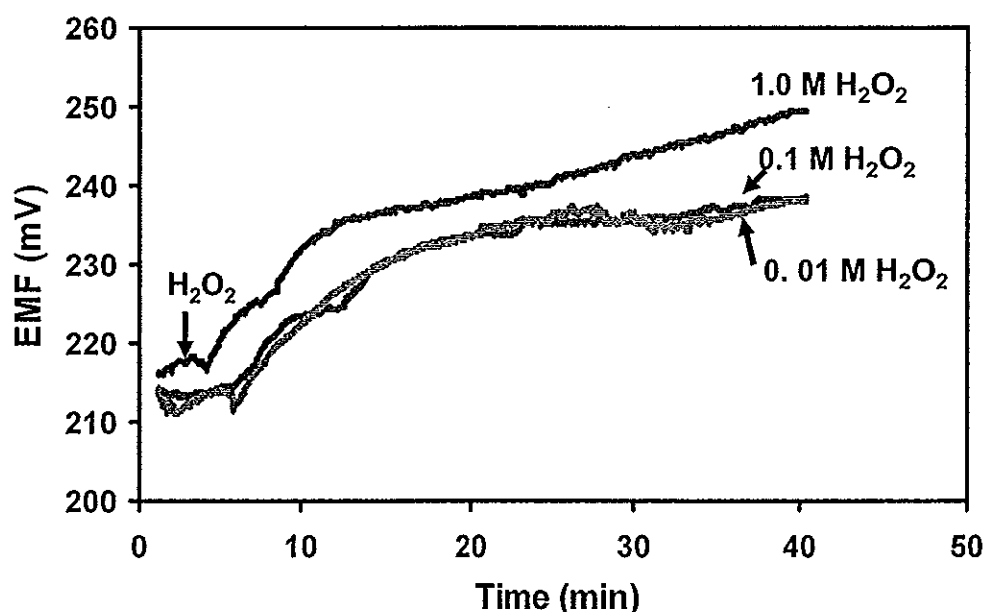


Figure 5.5 Time response for the Cd^{2+} -ISE in a 200 μl sample well, containing the indicated H_2O_2 concentrations.

5.4.2.2 Influence of incubation time

The effect of the incubation time of the aptamer-thrombin binding was examined over the range of 15–60 min (Figure 5.6). With 1000 nM immobilized primary aptamer and 100 ppb of thrombin, the EMF increased with increasing binding time, but at times longer than 45 min, the increase was no longer very significant. Based on these results, an incubation time of 60 min was chosen for all further experiments.

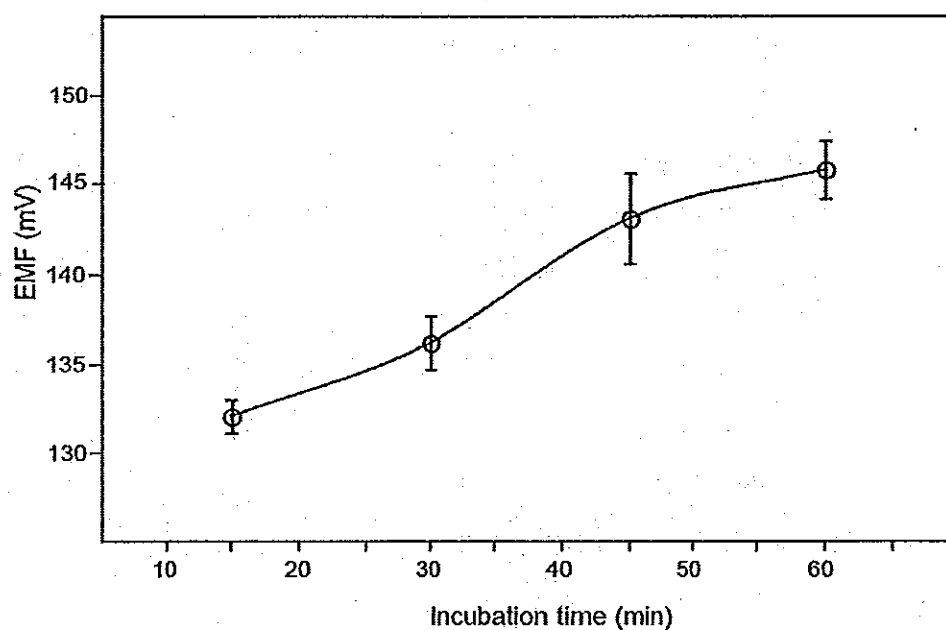


Figure 5.6 Responses at different incubation times between immobilized 1000 nM primary aptamer and 100 ppb of thrombin in 15, 30, 45, and 60 min (error bars: SD, $N = 3$). Potentiometric measurements were performed in 200- μ l samples with 10^{-4} M CaCl_2 as background electrolyte and a Ca-ISE as reference electrode.

5.4.2.3 Influence of the concentration of secondary aptamer

The concentration of the CdS-labeled secondary aptamer was varied between 250 and 1000 nM using 1000 nM primary aptamer and 100 ppb thrombin. The signal increased with increasing concentration but this trend declined at >500 nM (Figure 5.7). Since the nonspecific adsorption slightly increased at 1000 nM concentration, 750 nM was chosen for subsequent experiments.

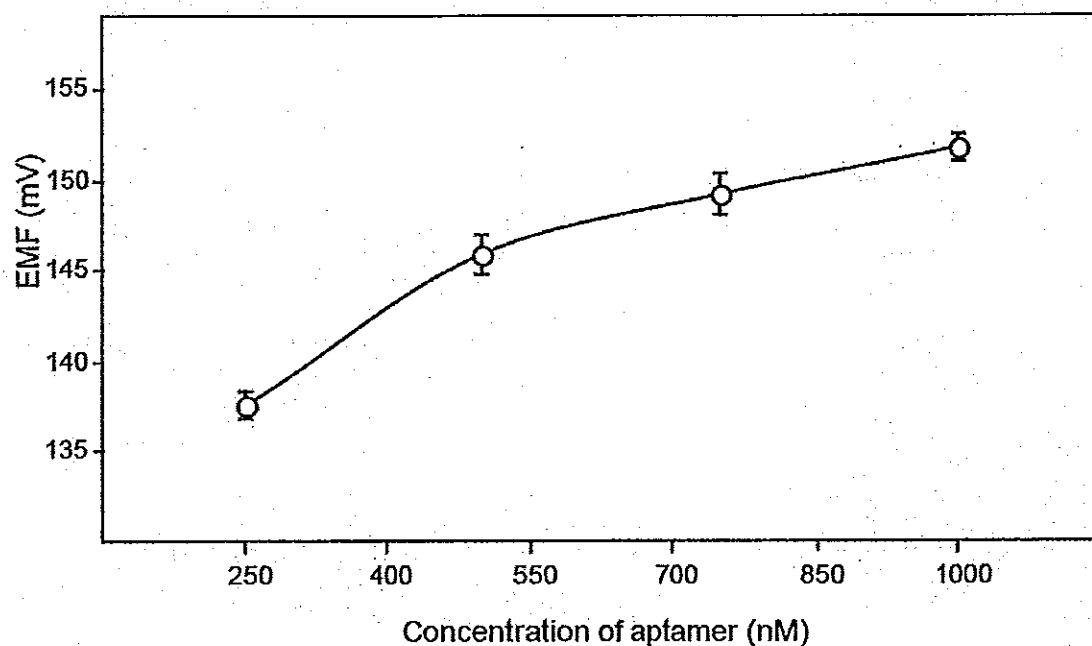


Figure 5.7 Response to various concentration of secondary aptamer with 100 ppb of target thrombin previously bound to 1000 nM primary aptamer (error bars: SD, $N = 3$).

5.4.2.4 Selectivity of thrombin aptamer

The selectivity of the thrombin aptamer was tested with the assay parameters as selected above. Two proteins i.e lysozyme and IgG, found in serum (Björhall et al., 2005; Chen et al., 2008), were used to test the selectivity of the system for thrombin. As shown in Figure 5.8, 500 ppb of lysozyme or IgG showed EMF responses that were not significantly higher than for the control and less than half of the response to a 10 times smaller concentration of thrombin.

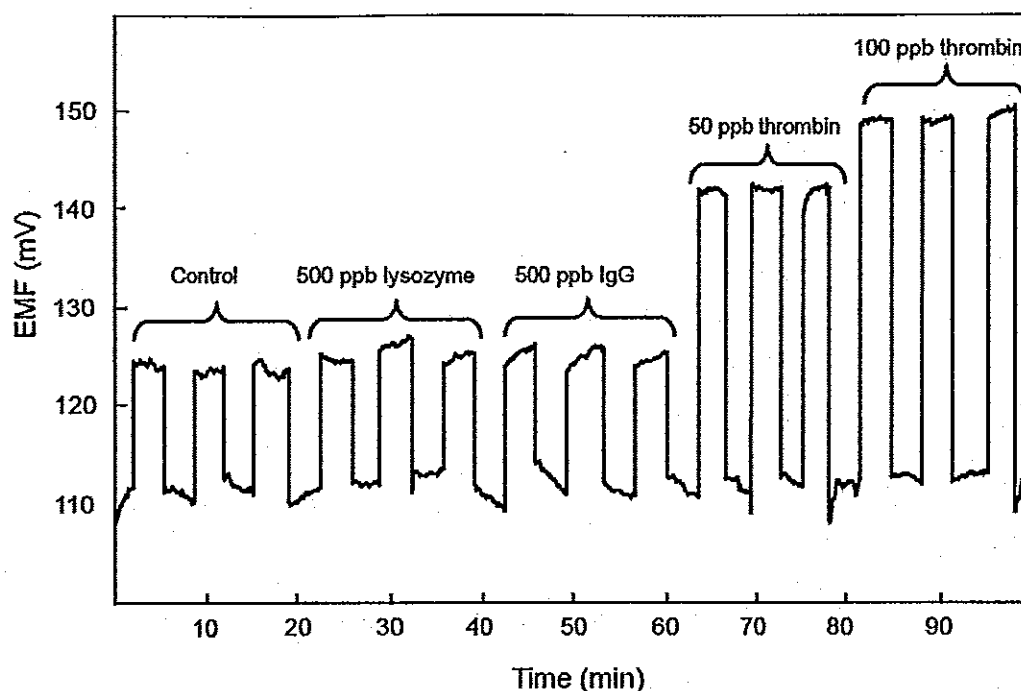


Figure 5.8 Potentiometric responses of the Cd^{2+} -selective electrode for the control (zero target), 500 ppb lysozyme, 500 ppb IgG (as noncomplementary targets), 50 ppb thrombin, , and 100 ppb thrombin (as complementary target) after aptamer-thrombin interaction.

5.4.2.5 Calibration curve

The results of a typical series of measurements with thrombin concentrations from 5 to 1000 ppb are shown in Figure 5.9. The EMF response of the Cd-ISE vs. $\log [\text{thrombin}]$ is close to linear and offers a sufficient concentration dependence suitable for thrombin measurements over a wide dynamic range of 10–250 ppb. The EMF value at the lowest concentration of 5 ppb was 1.88 mV above the control and the standard deviation of the noise of the control was 0.15 mV ($N=13$, 1 min). Thus, the lower limit of detection is ca. 5 ppb. This corresponds to 28 fmol of thrombin in 200- μl samples or 0.14 nM and compares well to results obtained with other reported sensors such as piezoelectric transducers (Bini *et al.*, 2007; Hianik *et al.*, 2005) or electrochemical sensors (of the order of 10 nM) (Hianik *et al.*, 2005; Mir *et al.*, 2006; Xiao *et al.*, 2005).[1-3] Significantly lower detection limits were obtained

with impedance spectroscopy and amplification by chemical means to denature the protein captured by an aptamer on the electrode surface (10 fM) (Xu *et al.*, 2006) and, very recently, by electrogenerated chemiluminescence *via* target protein-induced strand displacement (1 fM) (Wang *et al.*, 2007).

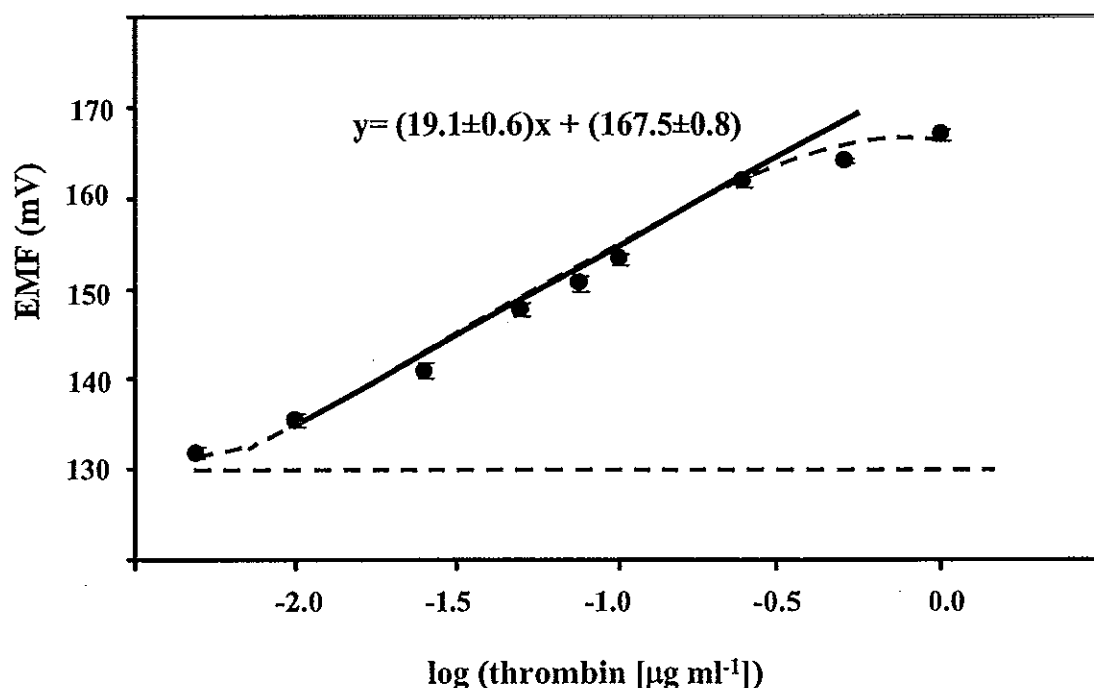


Figure 5.9 Potentiometric monitoring of thrombin concentration *via* CdS quantum dot label in 200- μl microwells with the aptamer-thrombin sandwich assay (error bars: SD, $N = 3$).

5.5 Conclusions

For the first time, we demonstrate that ion-selective microelectrodes can be used for monitoring protein-aptamer interactions with semiconductor nanocrystal labels in an ELISA microplate format. It is important to emphasize that a low detection limit of 5 ppb or 28 fmol of thrombin was reached without a preconcentration step typically used in other electrochemical techniques. This was possible in conjunction with a reduction of the sample volume and the excellent lower detection limit of the Cd-ISE used. It is expected that various biomolecular interactions can be monitored with similar assays based on different nanoparticle tracers and corresponding ISEs.

Chapter 6

Potentiometric Detection of DNA Hybridization

6.1 Introduction

The detection of sequence-specific DNA is of central importance to the diagnosis and treatment of genetic disease, for the detection of infectious agents, drug screening and reliable of forensic science (Millan *et al.*, 1993; Ohmichi *et al.*, 2005; Pina *et al.*, 2004). Various methods have been successfully used to detect sequence selective DNA hybridization, including optical (Cao *et al.*, 2002; Piunno *et al.*, 1995; Taton *et al.*, 2000), electrochemical (Cai *et al.*, 2003; Wang *et al.*, 2001; 2003; Zhu *et al.*, 2004) and piezoelectric (Tombelli *et al.*, 2006; Wu *et al.*, 2007). Among them, electrochemical methods have received considerable attention in connection to the detection of DNA hybridization because of their high sensitivity, compatibility, portability, low cost, minimal power requirement and independence of sample turbidity or optical pathway (Wang, 2002).

Various strategies have been developed for such electrical transduction of DNA hybridization. These include monitoring the increased electrochemical response of a redox active indicator (that recognizes the DNA duplex) (Marrazza *et al.*, 1999; 2000; Millan and Mikkelsen, 1993) and probing hybridization-induced changes in the intrinsic signal of nucleic acids (Johnston *et al.*, 1995; Wang *et al.*, 1998) or of other interfacial properties (Berggren *et al.*, 1999). The overall sensitivity of such electrochemical assays can be improved by using a label that can be detected with high sensitivity. Oligonucleotide bearing enzyme labels (Alfonta *et al.*, 2001; Kim *et al.*, 2003), electroactive (Ihara *et al.*, 1997) or nanoparticle label (Cai *et al.*, 2003; Wang *et al.*, 2001; 2002; 2003; Zhu *et al.*, 2004) have been used to generate highly sensitive electrical signals.

The use of nanoparticle-based electrochemical detection of DNA has recently received considerable attention. These include the use of gold nanoparticles (Wang *et al.*, 2002; 2003), silver (Wang *et al.*, 2001; 2003) semiconductor nanocrystal tracer (Wang *et al.* 2002; 2003; Zhu *et al.*, 2004), as well as carbon

nanotube (Wang *et al.*, 2003). These nanoparticle-based electrochemical method commonly rely on anodic stripping voltametry (ASV) due to its intrinsic preconcentration step that allows one to achieve ultratrace level detection limit (Wang, 1985).

As described in chapter 5, potentiometry with ion-selective electrodes (ISEs) is attractive for trace level analysis. Miniaturized electrode have been designed with excellent lower of detection limit in small sample volume (Ceresa *et al.*, 2002; Malon *et al.*, 2006; Robinova *et al.*, 2007) and are applied based on nanoparticles, including quantum dots as labels for the detection of proteins (Chumbimuni-Torres *et al.*, 2006; Thüerer *et al.*, 2007). Therefore, this project reports for the first time the use of a potentiometric microsensor for monitoring DNA hybridization based on sandwich assay by conjugated cadmium sulfide quantum dot (CdS) as a label with secondary DNA probe and detect the cadmium release ion with cadmium ion-selective electrode.

6.2 Materials

Tris-HCl, 6-mercapto 1-hexanol, potassium dihydrogenphosphate and dipotassium hydrogenphosphate were purchased from Sigma (St. Louis, MO). Nucleic acids were obtained from Integrated DNA Technologies Inc (Coralville, IA). The following oligonucleotide sequences were used:

Probe 1: 5'-SH-GAC CTA GTC CTT CCA ACA GC-3'

Probe 2: 5'- GGG TTT ATG AAA AAC ACT TTT TTT TT-SH-3'

Target: 5'-AAA GTG TTT TTC ATA AAC CCA TTA TCC AGG ACT GTT TAT AGC TGT TGG AAG GAC TAG GTC-3'

Non complementary; 5'-TTC CTT AGC CCC CCC AGT GTG CAA GGG CAG TGA AGA CTT GAT TGT ACA AAA TAC GTT TTG-3'

2-base mismatch: 5'-AAA GTG TTT TTC ATA AAC CCA TTA TCC AGG ACT GTT TAT AGC TGT TTG AAG GGC TAG GTC-3'

Chemicals for the synthesis of CdS quantum dots, preparation of the cadmium ion- selective membrane and calcium ion-selective membrane are as

described in section 5.2, all stock and buffer solutions were prepared using autoclaved double deionized water (18.2 M Ω cm).

6.3 Methods

Cadmium ion selective microelectrode (Cd-ISE) and calcium ion-selective electrode were prepared as described in section 5.3.1. Cadmium sulfide quantum dot was synthesized as described previously in section 5.3.2

6.3.1 DNA immobilization and detection

In the experiment, sandwich assay was used for DNA hybridization detection where the target DNA is captured by the primary DNA probe modified previously on the gold substrate, followed by adding the secondary DNA probe conjugated previously to the cadmium sulfide quantum dots (CdS), used as label. The CdS is then dissolved with hydrogen peroxide to yield diluted electrolyte backgrounds solution suitable for the potentiometric detection of the released cadmium ions with a polymer membrane cadmium ion-selective microelectrode as shown Figure 6.1 .

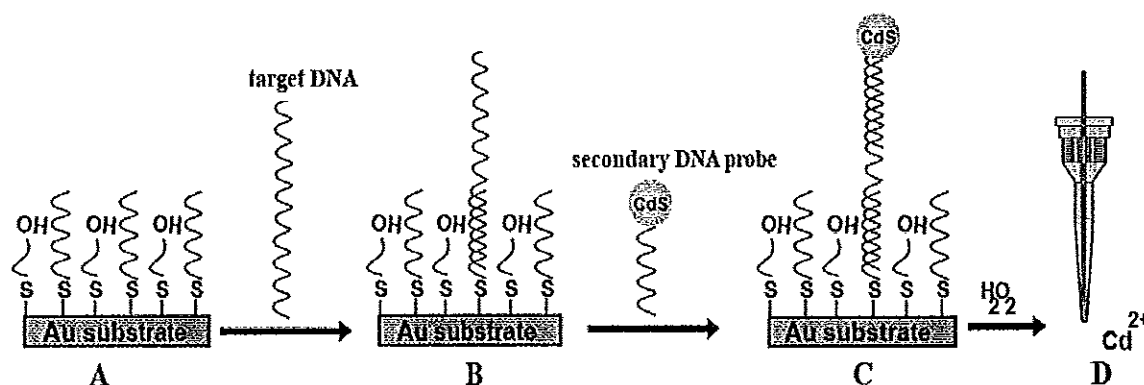


Figure 6.1 Representation of analytical protocol : (A) Formation of mixed monolayer of DNA probe on gold substrate: (B) hybridization with target DNA: (C) second hybridization with CdS-labeled probe and (D) dissolution of CdS tag followed by detection using ion selective electrode.

The immobilization of oligonucleotide, binding assay and detection were investigated, modified slightly as from the one reported previously in section 5.3.3. The steps are described as follows;

6.3.1.1 Preparation of the oligonucleotide probe on the gold surface

Cleaving the dithiol protecting group. The disulfide-protected nucleotides (100 μM , 10 μl) were diluted in autoclave water to 100 μl and treated with Tris(carboxethyl) phosphine (TCEP) (1 mg) for 30 min, followed by purification using a MicroSpinTM G-25 column obtained from Amersham Biosciences (Buckinghamshire, UK).

Preparation of the gold substrates. The gold substrates were obtained from Denton Vacuum LLC (Moorestown, NJ), machine cut (Advotech Company Inc., Tempe, AZ) to identical pieces (of 6 x 3 x 0.2 mm size), assuming a uniform thickness.

Preparation of the mixed monolayer. The gold substrates were cleaned first in Piranha solution and rinsed with water prior to use. (*Safety note:* the Piranha solution should be handled with extreme caution.) The oligonucleotide monolayer was generated by treating the gold substrates with 100 μl of a thiolated-oligonucleotide solution in phosphate buffer (0.05 M, pH = 7.0) for overnight, followed by removal of the solution. The surface of the gold substrates was then blocked by a 10 min treatment with 6-mercapto-1-hexanol (0.1M, 100 μl), followed by washing with water.

6.3.1.2 Preparation of CdS quantum dot – oligonucleotide conjugate

500 μl of CdS quantum dot suspension (0.2 mg ml^{-1}) was exposed to the thiolated oligonucleotide secondary DNA probe (probe 2). The mixture was stirred overnight at room temperature (27 °C). The quantum dot-DNA conjugate was collected by centrifugation at 10,000 rpm for 45 min, removal of supernatant, and resuspension in hybridization buffer (750 mM NaCl, 150 mM sodium citrate).

6.3.1.3 Sandwich DNA hybridization assay

The oligonucleotide modified gold substrates were incubated for 1 hour with desired amount of target DNA in 100 μ l of hybridization buffer followed by washing with washing buffer (50 mM Tris-HCl, 0.1% Tween 20; pH 7.4). Then, the gold substrates were incubated with quantum dot-oligonucleotide secondary probe for 60 min at room temperature. The supernatant was then removed, the gold substrates were washed twice with 100 μ l of washing buffer, and transferred to new vials, washed for another 4 times with 100 μ l of washing buffer and 2 times with water.

6.3.1.4 Dissolution and Detection

Hydrogen peroxide was used for dissolution step since it was observed that it can efficiently oxidize the cadmium quantum dots. In the final assay, dissolution of Cd was carried out by the addition of 100 μ l 0.01 M H_2O_2 (in 10^{-4} M CaCl_2) and left for one hour to ensure complete oxidation. Potentiometric detection followed the condition as described in section 5.3.4

6.4 Results and Discussion

As described in section 5.4.1 the developed miniaturized solid-contact Cd-ISE showed a lower limit of detection of 10^{-10} and 10^{-9} M Cd^{2+} in samples of 100 ml and 200 μ l (microwell plates), respectively and it exhibits good selectivity for the relevant ions, with logarithmic selectivity coefficients of -7.04 (Ca^{2+}), -3.88 (H^+), and -4.59 (Na^+)

The new potentiometric nucleic acid measurements rely on a sandwich DNA hybridization for capturing a secondary oligonucleotide bearing CdS-nanocrystal tags. As shown in Figure 6.1, the target DNA (60-mer) is hybridized to the surface-anchored thiolated DNA probe (20-mer) on the gold substrate (Figure 6.1A-B), followed by the capture of the secondary DNA probe (26-mer) conjugated to the CdS label (Figure 6.1C). The nanocrystal is then dissolved in H_2O_2 to yield a dilute electrolyte background solution suitable for the potentiometric detection of the

released Cd^{2+} with a polymer membrane Cd^{2+} -selective microelectrode (Figure 6.1D).

The key parameters of the DNA sandwich hybridization assay were optimized in order to make more efficient the detection of DNA with the ion selective microelectrode, and these parameters were studied as follows.

6.4.1 Concentration of primary DNA probe (Probe1)

The effect of the concentration of primary DNA probe used in the immobilization was studied using 1000 nM secondary DNA probe. The results of binding between 100 nM target DNA with different concentration of primary DNA probe (probe 1) are shown in Figure 6.2. The stable EMF signal was found at 1000 nM of primary DNA probe. Therefore, 1000 nM of primary probe was chosen for the following experiments.

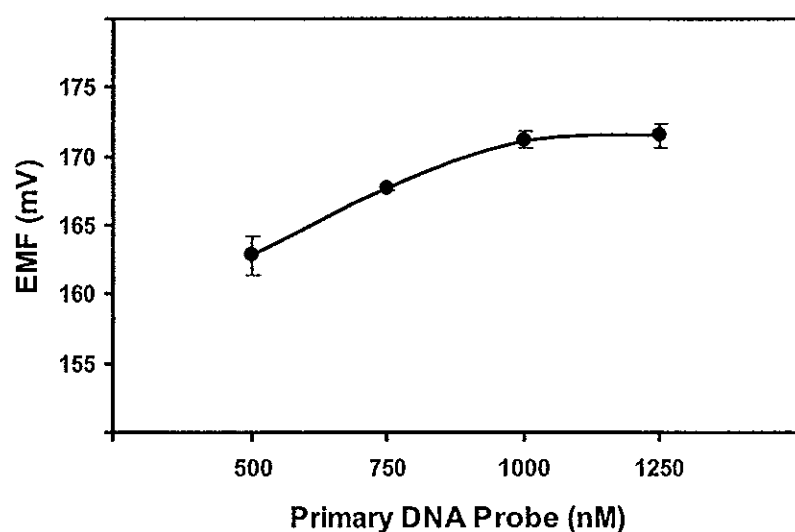


Figure 6.2 Effect of concentration of immobilized primary DNA probe to 100 nM of target DNA using 1000 nM of secondary DNA.

6.4.2 Incubation time between primary DNA probe and target DNA

The effect of the incubation time used in the binding between primary DNA probe and target DNA was then studied. The results from the binding between

1000 nM of immobilized primary probe and 100 nM of target with different incubation times followed by capture of 1000 nM of secondary DNA probe are shown in Figure 6.3. The signal increased as the time with binding time and 60 min gave the stabilized response. Therefore, 60 min of incubation time was chosen for further work.

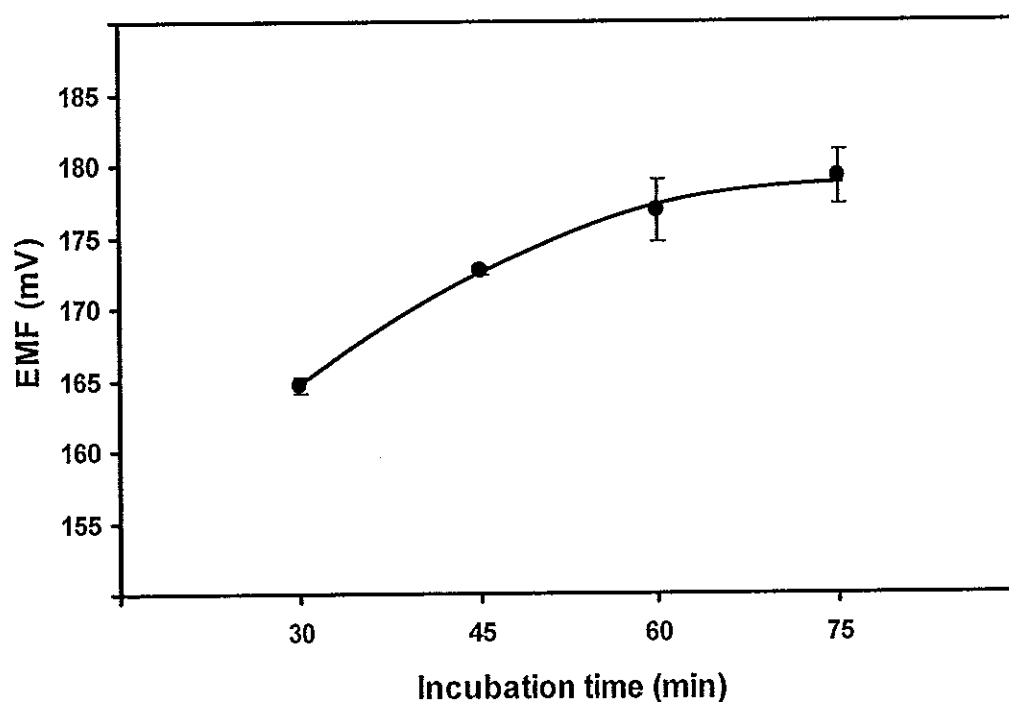


Figure 6.3 Responses of different incubation times between 1000 nM of immobilized primary probe, 100 nM of target DNA and 1000 nM secondary probe.

6.4.3 Concentration of secondary probe (Probe 2).

The effect of the secondary probe was investigated by immobilizing 1000 nM of primary probe on gold substrate and added 100 nM of target DNA. The signal obtained for the different concentration of secondary probe were evaluated. Figure 6.4. shows that the signal increased with secondary DNA probe concentration and stabilized at 1,000nM. Therefore, 1,000 nM of secondary probe was chosen for further experiments.

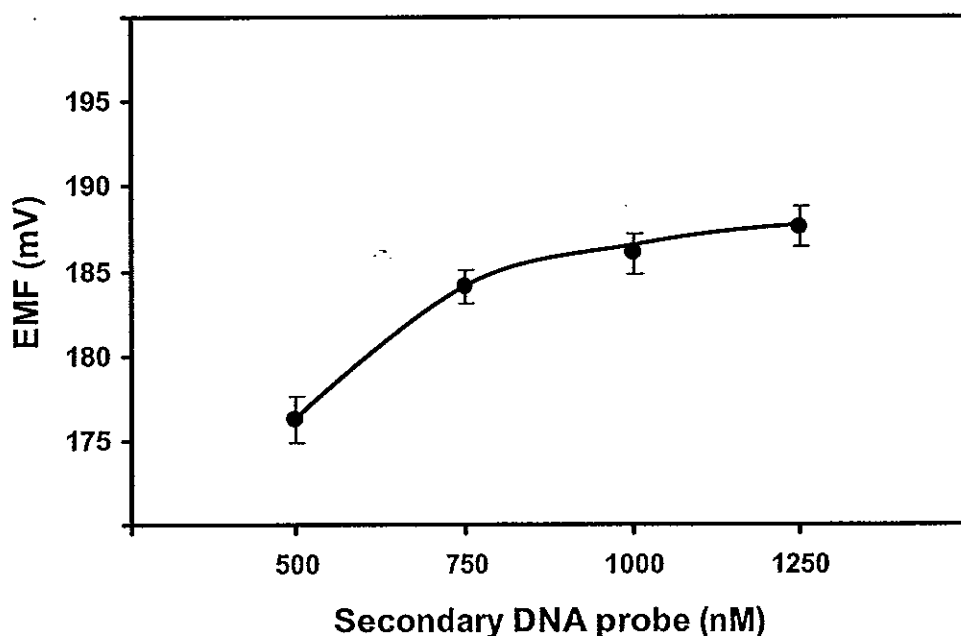


Figure 6.4 Responses of different concentrations of secondary DNA probe with 100 nM target bound to 1000 nM primary probe.

6.4.4 Incubation time between secondary DNA probe and target DNA

The effect of the incubation time used in the binding between secondary DNA probe and target DNA was studied. The results from the binding between 1000 nM of secondary probe and 100 nM target (previously bound to 1,000 nM of primary probe) with different incubation times are shown in Figure 6.5 The signal increased with binding time and 60 min gave the stabilized response. Therefore, 60 min of incubation time was chosen for further work.

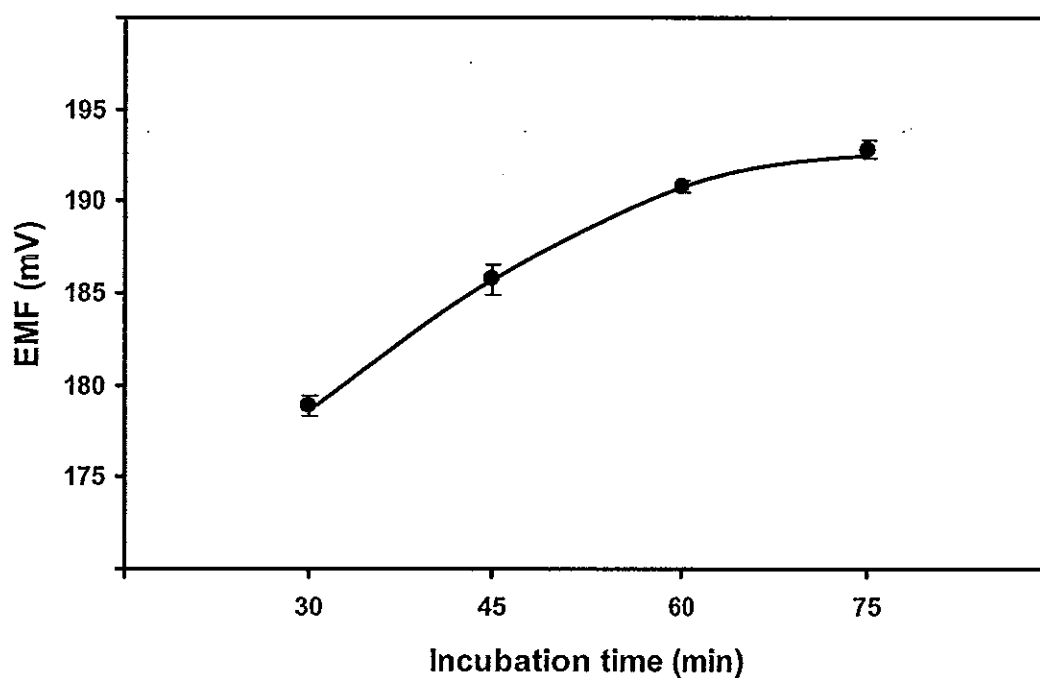


Figure 6.5 Responses of different incubation times between 1000 nM of secondary probe and 100 nM target DNA.

6.4.5 Selectivity

Two different DNA sequences, noncomplementary and 2-base mismatch, were used to test the selectivity, using 500 nM of the respective DNA. Figure 6.6, illustrates the recorded EMF signal of DNA hybridization without the target, with noncomplementary and 2-base mismatch DNA and two different target DNA concentrations. The resulting signal of noncomplementary and 2-base mismatch are similar to those obtained with the control, such behavior indicates the good selectivity of the hybridization assay.

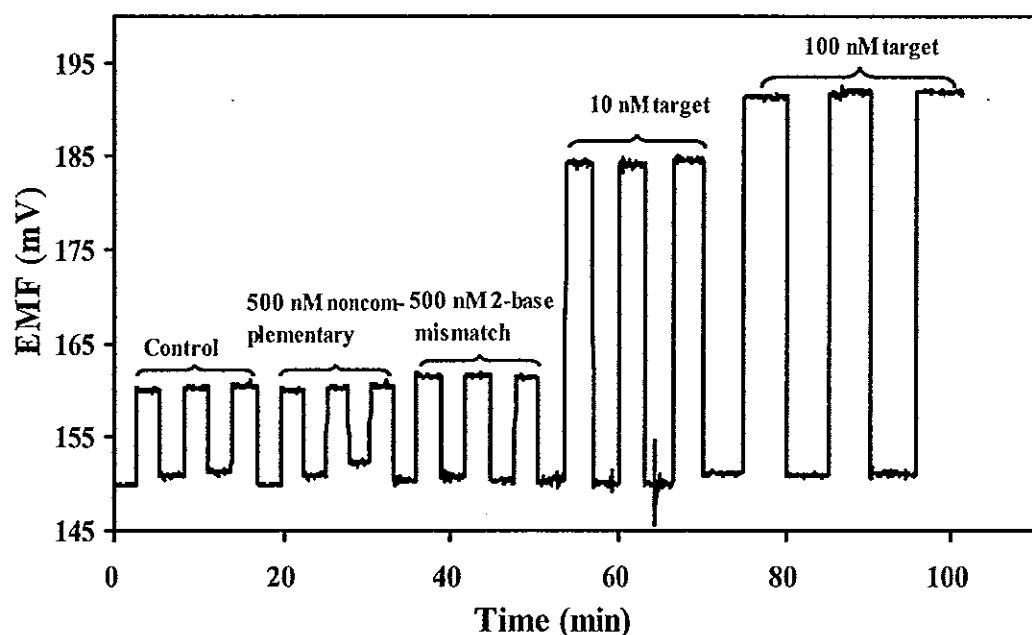


Figure 6.6 Potentiometric responses of the cadmium-selective electrode for the control (zero target), 500 nM noncomplementary, 500 nM 2-base mismatch, 10nM of target and 100 nM of target DNA (as complementary targets) after DNA hybridization.

6.4.6 Calibration curve

The quantitative aspects are documented by a calibration experiment over a concentration range of 0.01-1000 nM target DNA. The resulting calibration plot in Figure 6.7 exhibits a well-defined concentration dependence suitable for DNA analysis, with a wide dynamic range of 0.01-500 nM target DNA. The EMF at the lowest measured concentration of 10 pM was 2.96 mV above that of the control, and the standard deviation of the noise of the control was 0.17 mV ($N = 13$, 1 min). Taking into account the conservative definition of the potentiometric detection limit by which the signal must be three times higher than the standard deviation of noise in background solution (Bakker and Pretsch, 2005). Thus, the lower limit of detection is 10 pM or 37 pg (2 fmol) of the target DNA in the 200 μ l sample. These values compare favorably with those reported for other electrochemical DNA hybridization assays using similar nanoparticle labels (20 pM) (Wang *et al.*, 2002).

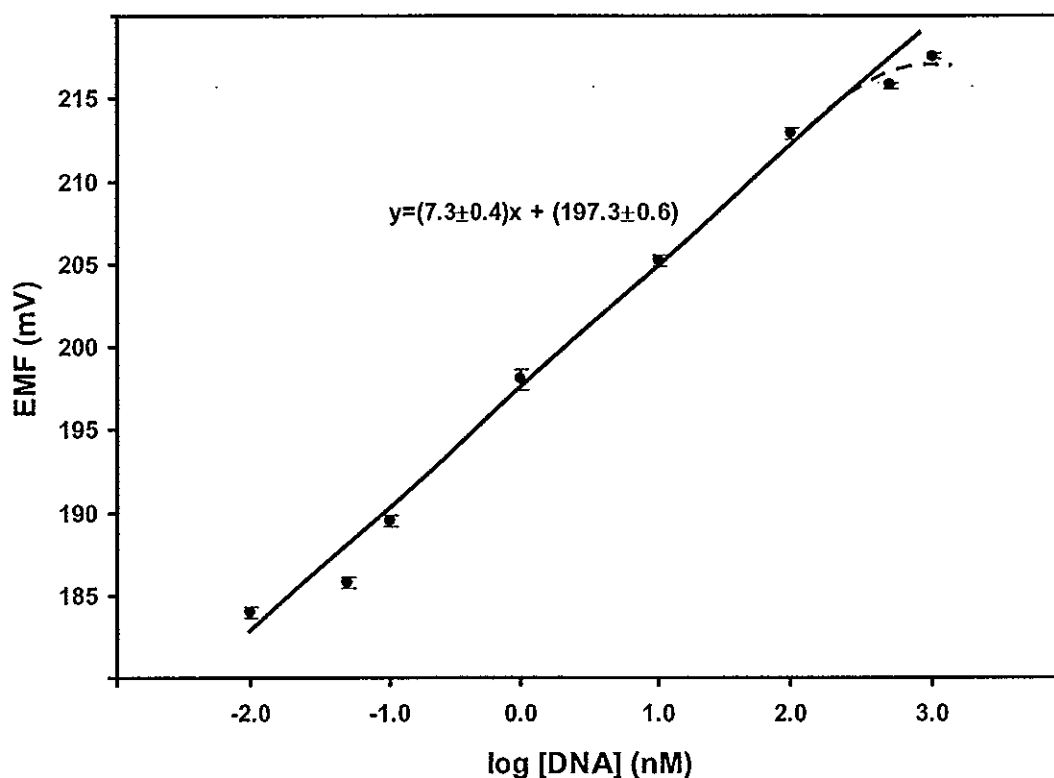


Figure 6.7 Potentiometric monitoring of DNA concentration via CdS quantum dot label in 200 μ L microwells with the DNA hybridization sandwich assay.

6.5 Conclusions

We have demonstrated for the first time the use of potentiometric transducers for detecting DNA hybridization. The use of Cd^{2+} -selective microelectrodes is particularly useful for a microplate operation in connection with CdS nanocrystal tags. The extremely high sensitivity and fmol detection limit of the microelectrode are coupled with a high selectivity of the bioassay, including effective discrimination against 2-base mismatched DNA. The low detection limit was reached without a preconcentration step commonly used in other electrochemical transduction schemes. The new potentiometric detection route can be extended to a wide range of genetic tests in connection with different nanoparticle tags.

Chapter 7

Capacitive Biosensor for Quantification of Trace DNA

7.1 Introduction

DNA quantification is critical for many biological studies since it is often used as a reference for measurements of other biologically active components in biological fluids and genetic diagnosis (Georgiou and Papapostolou *et al.*, 2006; Huang *et al.*, 2002; Prem Kumar *et al.*, 2005). In biological and biopharmaceutical products, such as monoclonal antibodies, lymphokines and vaccines, quantification of residual cellular DNA from the host cell in the purification process is also important since they have to meet specific requirements regarding contaminating cellular DNA. Guidelines of The World Health Organization (WHO) published in 1986 recommend that the residual cellular DNA permitted in purified product contain less than 100 pg per dose (WHO, 1987). In 1997, these increased to 10 ng per dose (WHO, 1998)

The quantification method commonly used for residual DNA determination is real time quantitative polymerase chain reaction (Q-PCR) (Lovatt, 2002). Other biochemical assay methods include spectrophotometry where DNA absorbs maximally around 260 nm (Samuel *et al.*, 2003), densitometric scans of gels from agarose or polyacrylamide electrophoresis (Projan *et al.*, 1983), chemiluminescence (Ma *et al.*, 2004), spectrofluorimetric and resonance light scattering (RLS) methods (Li *et al.*, 2002; Wang *et al.*, 2005). Each method has its strengths and weaknesses in term of sensitivity, specificity, running time, robustness, material safety/toxic waste, reagent stability and cost (Li *et al.*, 2002; Ma *et al.*, 2004). For example, in the case of fluorescence method, many fluorescent reagents have been used to enhance the fluorescence intensity for DNA determination, such as ethidiumbromide, 4,6-diamidino-2-phenyllindole, bis-benzimidazole dye Hoechst 33258. However, the preparation of reagents is inconvenient (Wang *et al.*, 2005) and some reagents, such as ethidiumbromide is a carcinogen (Link and Tempel, 1991). Therefore, development of alternative methods which are more convenient and have

high sensitivity and specificity for the detection of DNA is desirable and use of affinity biosensors is an interesting approach.

Affinity biosensors are based on a binding interaction between the immobilized biomolecule and the analyte of interest (Mattiasson, 1984; Wang, 2000). Affinity biosensors can be categorized as label-free (direct) and labeled. Between the two, label-free affinity biosensor is more attractive since it requires less steps. To detect the affinity binding reaction, capacitive transducers have been applied and found to be very sensitive (Berggren *et al.*, 2001. Berggren *et al.*, 1998; Berggren and Johansson *et al.*, 1997; Botidean *et al.*, 2003; Botidean 1998; Hedström *et al.*, 2005; Hu *et al.*, 2002 Limbut *et al.*, 2006). To detect DNA, it may be possible to apply histones as recognition element since histones are the basic proteins which are complexing with DNA *in vivo* to form the nucleosome (Helliger *et al.*, 1998) as shown in Figure 7.1. The four core histones (H2A, H2B, H3 and H4) form an octamer, which DNA is wrapped around to form the nucleosome particle and the histone H1 acts as the linker between the constituents of the nucleosome particle (Allan *et al.*, 1981; Yoshikawa *et al.*, 2001).

In this work we investigated the application of a flow-injection capacitive biosensor for the rapid determination of DNA based on the affinity binding of DNA to histone by immobilizing whole histone on a gold electrode surface via self-assembled monolayer SAM of thioctic acid. The technique was tested using DNA substrates from various sources, i.e. calf thymus, shrimp and *E.coli*. The signals of the binding reaction of calf thymus and white shrimp histones to DNA were also compared. This system was also validated with real samples by using it to determine genomic DNA contamination in crude shrimp protein preparation.

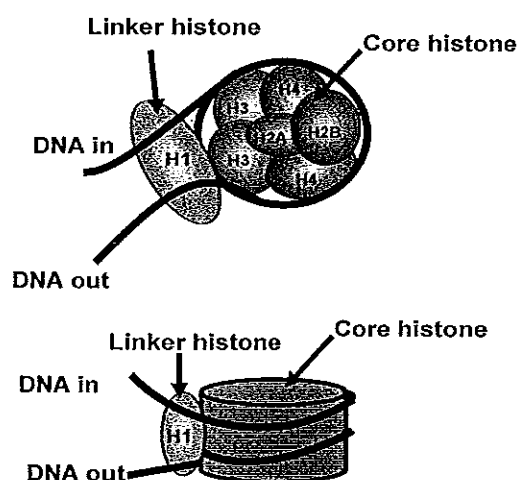


Figure 7.1 Wrapping of DNA around nucleosome core, Nucleosome composed of the pair of histone, H2A, H2B, H3 and H4 to form an octamer core structure and H1 acts as the linker between nucleosome particle. (Adapted from Reece, 2004).

7.2 Materials

Deoxyribonucleic acid (DNA) and histone from calf thymus, *N*-3-(dimethyl-amino-propyl)-*N'*-ethylcarbodiimide hydrochloride (EDC), *N*-hydroxysuccinimide (*N*-Hydroxy-2,5-pyrroindione, NHS) and white saponin were purchased from Sigma-Aldrich (Steinheim, Germany). Thioctic acid and 1-dodecanethiol were obtained from Aldrich (Milwaukee, USA). All other chemicals were of analytical grade. Solutions and buffers used in the capacitive biosensor system were prepared with deionized water. Before use, buffers were filtered through an Albet[®] nylon membrane filter with pore size 0.20 μm with subsequent degassing. DNA from white shrimp (*Penaeus merguensis*) was provided by Center for Genomic and Bioinformatic Research, Faculty of Science, Prince of Songkla University, Songkhla, Thailand. *E.coli* DNA was obtained from Department of Biotechnology, Lund University, Sweden and purified by using Freez'N Squeeze DNA gel extraction spin column (Bio-Rad, USA). Histone from white shrimp (*Penaeus merguensis*) erythrocyte nucleoprotein was prepared by using a slightly modified procedure from that reported by Murray (Murray *et al.*, 1968). In brief, shrimp erythrocytes were

lysed by vigorous stirring with white saponin solution (0.6% (w/v) in 0.14 M NaCl). Nuclei were collected by centrifugation at 500×g for 1 h. Whole histone was then extracted from the nuclei with 0.2 M H₂SO₄ and centrifuged at 18,570×g for 1 h. Ethanol was added to precipitate histones which were collected by centrifugation and washed 3 times with ethanol.

7.3 Methods

7.3.1 Immobilization of histones

Gold electrodes were polished (Grip[®] 2V polishing machine, Melkon Instrument Ltd, Bursa, Turkey) using slurries of alumina oxide powder with particle diameters 5, 1 and 0.3 µm (Melkon Instrument Ltd, Bursa, Turkey) and then cleaned through sonication in deionized water and absolute ethanol, 15 min each. They were then washed with deionized water, followed by electrochemical etching in 0.5 M H₂SO₄ by cyclic potential from 0 to + 1.5 V vs Ag/AgCl reference electrode with a scan rate of 0.1 V s⁻¹. Finally they were dried with pure nitrogen gas. To immobilize histones, electrodes were placed in an ethanolic solution of 250 mM thioctic acid. A self-assembled monolayer, SAM, was formed of thioctic acid and after 12 hours the electrodes were carefully washed with absolute ethanol and then dried in a stream of pure nitrogen. Thioctic acid on the electrode was activated in EDC:NHS solution (EDC 1% (v/v), NHS 2.5 % (v/v)) in 0.05 M sodium phosphate buffer pH 5.00 with 0.05 M KCl for 5 h to introduce reactive groups that can covalently bind to aminogroups of histone molecules. After washing with 50 mM sodium phosphate buffer (pH 7.20), 20 µl of appropriate concentration of histone was placed on each electrode and the reaction took place at 4 °C for 24 h. Finally, the electrodes were washed with phosphate buffer and immersed for 20 minutes in 10 mM of 1-dodecanethiol in ethanol to block any pinhole on the gold electrode surface. During the immobilization steps, the degree of insulation from different layers on the electrode surface is demonstrated by cyclic voltammetry measurements performed in a three electrode electrochemical batch cell containing 5 mM K₃[Fe(CN)₆] and 0.1 M KCl, at a scan rate of 0.1V s⁻¹. The modified gold electrode was used as the working

electrode, Ag/AgCl as a reference electrode and a platinum rod was the auxiliary electrode. The electrodes were coupled to a potentiostat (ML 160, AD Instruments, Australia) connected to a computer.

7.3.2 Capacitance measurements

A flow-injection (FI) technique was applied to determine DNA in the capacitive biosensor system (Figure 7.2). The electrode modified with histone was inserted as the working electrode in a three electrode flow cell with a dead volume of 10 μ l. A stainless steel tube was used as the auxiliary electrode and outlet and a custom built Ag/AgCl was used as reference electrode. They were connected to a potentiostat (ML 160, AD Instruments, and Australia). Capacitance measurements were performed by applying a +50 mV potential pulse, one pulse per minute to the modified gold electrode. The resulting current response from each pulse was sampled with a frequency of 40 kHz. The capacitance of the electrode surface was calculated from the current response.

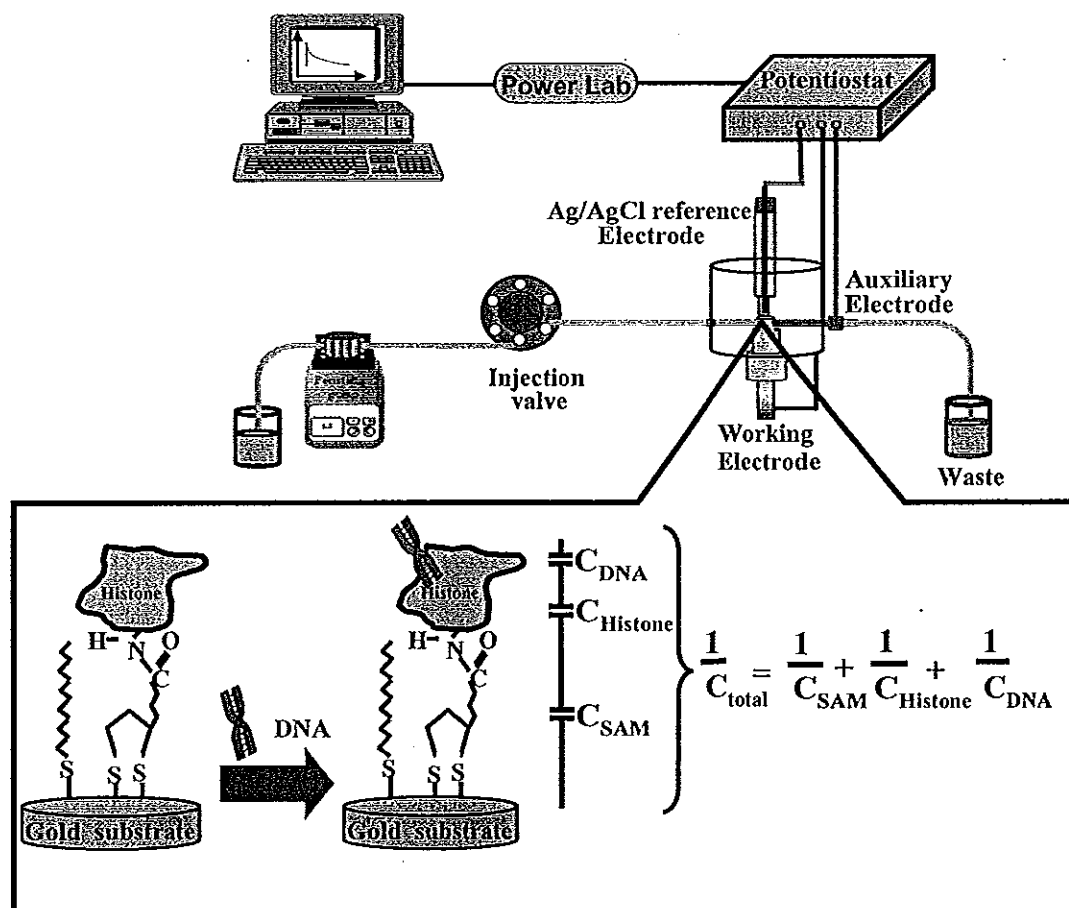


Figure 7.2 Schematic diagram of the flow injection capacitive biosensor system. The total capacitance measured at the working electrode/solution interface (C_{tot}) comes from C_{SAM} ; the capacitance of self-assembled thioctic acid monolayer, C_{Histone} ; the capacitance of histone layer and C_{DNA} ; the capacitance DNA analyte interaction.

7.3.3 Optimization of the capacitive biosensor

Operating conditions of the flow injection capacitive biosensor system were optimized for the affinity binding between DNA and histones from calf thymus. Parameters affecting the capacitive response were studied. These include regeneration solution (type, pH and concentration), sample volume, flow rate, and carrier buffer (type, pH and concentration). The parameters were optimized one by one by comparing responses obtained after injections of standard DNA solution, three replications for each test value. The optimum of each parameter was determined as a compromise between the sensitivity (slope of the calibration curve) or capacitance changes and analysis time. Using the obtained optimum conditions, the performances of the system i.e., linear range, lower detection limit, selectivity were investigated. Effects of histones and DNAs from different sources *i.e.* calf thymus and white shrimp were also tested.

7.3.4 Determination of trace amount DNA in real sample

A crude protein extract from white shrimp was used as a representative of a real sample. This extract is used in the study of protein interaction with white spot syndrome virus in shrimp. In the preparation process, DNA was removed by DNaseI treatment and residual DNA is generally detected by UV spectrometry. To test the capacitive biosensor system, residual DNA in the extract was analyzed under optimum conditions, including the study of matrix effect and recovery.

7.4 Results and discussion

7.4.1 Insulating property of working electrode

Capacitive measurements require a proper insulation of the electrode surface in order to prevent disturbing redox reactions at the applied potential. The degree of insulation obtained at different layers in the electrode preparation was studied with cyclic voltammetry by using the permeable redox couple $K_3 [Fe(CN)_6]$ as

shown in Figure 7.3. The clean gold electrode surface was first studied (Figure 7.3a), the reversible peaks for oxidation and reduction are observed during cycling of potential, with the self-assembled layer of thioctic acid covering the electrode, the redox peaks were significantly reduced (Figure 7.3b). Immobilization of histone protein on the electrode surface further increased the insulating properties of the electrode (Figure 7.3c). After treating with 1-dodecanethiol, the redox peaks disappeared completely (Figure 7.3d) because the electrode became totally insulated.

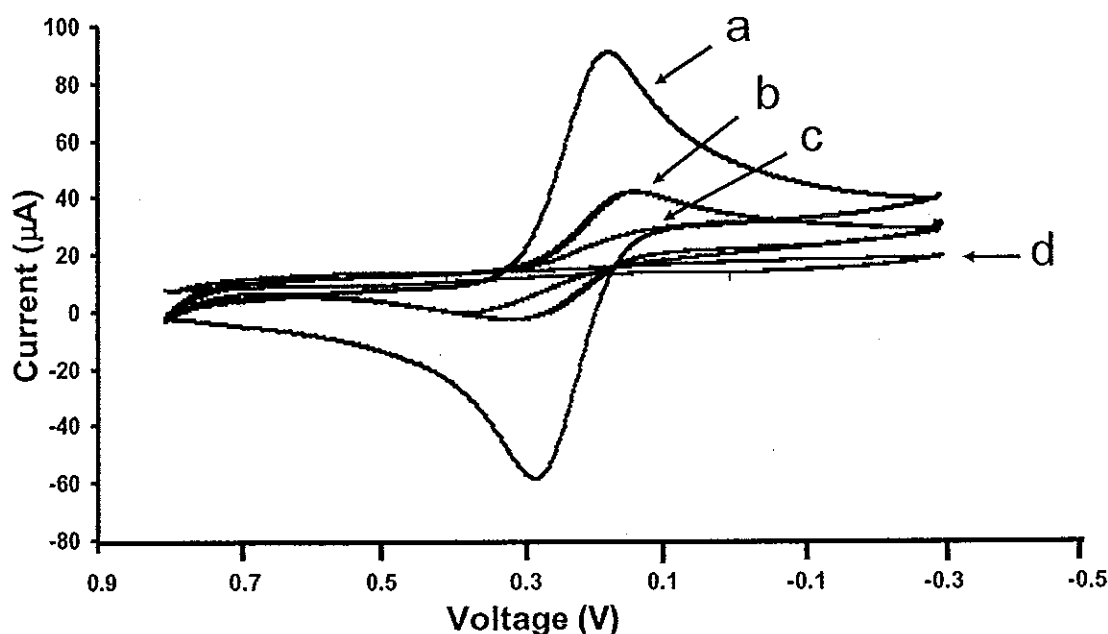


Figure 7.3. Cyclic voltammograms of a gold electrode obtained in 5 mM $K_3[Fe(CN)_6]$ containing 0.1 M KCl solution at scan rate of 0.1 V s^{-1} . All potentials are given vs Ag/AgCl. (A) clean gold, (B) thioctic acid covered gold, (C) histone modified thioctic acid couple gold, and (D) as in (C) but after 1-dodecanethiol treatment.

7.4.2 Capacitance measurement of the binding between immobilized histone and DNA

The capacitance of the binding event between histone and DNA is determined from the current response collected with a frequency of 40 kHz when a

potentiostatic step of 50 mV is applied on the electrode. The first two values were discarded and the next ten current values were used for the evaluation of the capacitance. The transient response for current vs time could be described by

$$i(t) = \frac{u}{R_s} \exp\left(-\frac{t}{R_s C_{tot}}\right) \quad (7.1)$$

where $i(t)$ is the current response as a function of time, u is the applied pulse potential, R_s is the resistance of the capacitive electrode with binder immobilized but without target bound, C_{tot} is the total capacitance over the immobilized layer measured at the working electrode/solution interface and t is the time elapsed after potentiostatic step was applied (Berggren and Johansson, 1997). The capacitance is calculated by taking the logarithm of the current and Eq. (7.1) becomes

$$\ln i(t) = \ln \frac{u}{R_s} - \frac{t}{R_s C_{tot}} \quad (7.2)$$

From the graph of $\ln i(t)$ vs t , R_s and C_{tot} can be calculated from the intercept and the slope, respectively (Berggren and Johansson, 1997). The affinity binding between DNA and the immobilized histone molecules on the working electrode will result in an increase of the thickness of the layer and this would cause C_{tot} to decrease (Figure 7.2). Figure 7.4 shows an example of a plot of the calculated C_{tot} value with respect to time where the capacitance change (ΔC_1 , ΔC_2) due to the binding can be determined. Since the interaction between DNA and histone are via non-covalent bonds, DNA could be dissociated from the histone on electrode surface by using regeneration solution.

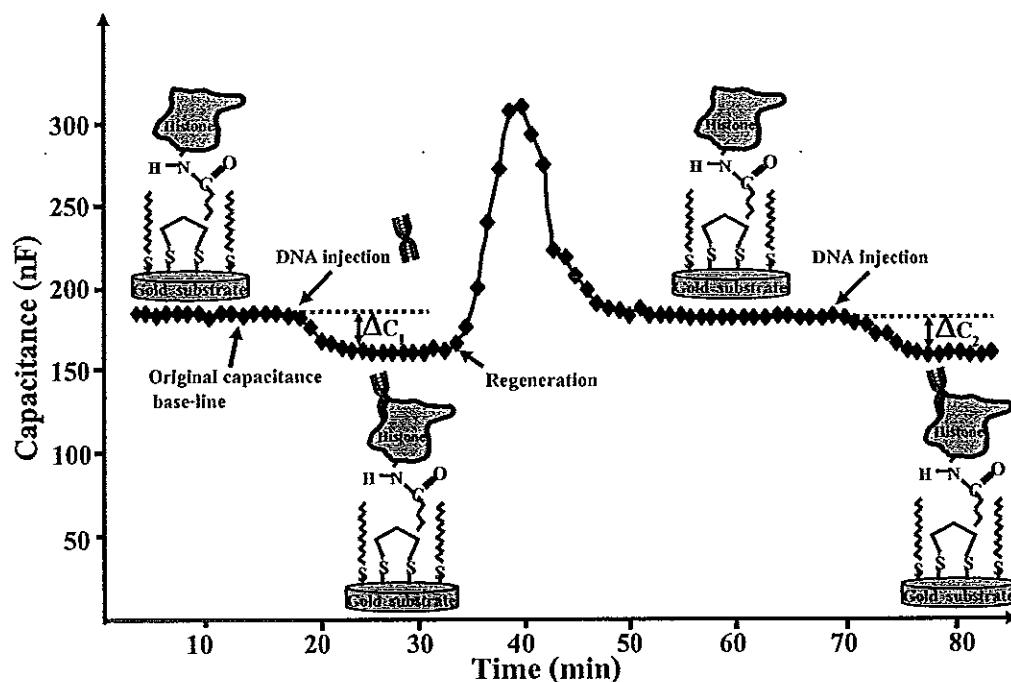


Figure 7.4 An example of the capacitance (C_{tot}) plots as a function of time. The binding between histone and DNA cause the capacitance to decrease (ΔC_1) with subsequent signal increase due to dissociation under regeneration conditions. After regeneration of the system can be reused to detect a new injection of DNA (ΔC_2).

7.4.3 Optimization of the flow injection capacitive biosensor

7.4.3.1 Regeneration solution

The biosensor needs regeneration of the sensor surface before the measurement can be repeated. The goal is to break the non-covalent binding between DNA analyte and histone immobilized on the gold surface, while maintaining the activity of the protein.

To evaluate the performance of the regeneration solution, the percentage of residual activity (% residual activity) of the immobilized histone was calculated from capacitive change given by a consecutive binding between DNA (1

ng l⁻¹ with sample volume 300 µl) and histone before (ΔC_1) and after (ΔC_2) regeneration (Figure 7.4) according to the equation.

$$\% \text{Residual activity} = \frac{\Delta C_2 \times 100}{\Delta C_1} \quad (7.3)$$

Three difference types of regenerating agent were compared, *i.e.*, high ionic strength, low pH and high pH. As can be seen in Table 7.1, high ionic strength (KCl) and high pH (NaOH) were shown to be ineffective with low percentage residual activity and they required a long time for regeneration. However, at low pH. *i.e.* 50 mM glycine-HCl, pH 2.4 gave a better percentage residual activity than HCl pH 2.4, therefore, glycine-HCl was further investigated to see the influence of concentration ranging and. At 25 mM residual activity of 93 % was achieved, whereas almost 97 % residual activity was gained at pH 2.4. Therefore, a concentration of 25 mM glycine-HCl, pH 2.4 was chosen in the continued experiments.

Table 7.1. Assayed and optimized conditions of the type, pH and concentration of regeneration solution. The efficiency of DNA removal from the histone immobilized on the electrode was studied by injecting 1 ng l^{-1} of standard DNA solution.

Parameter of regeneration solution	Investigation condition	Efficiency of DNA removal (%average residual activity)	Regeneration time (min)
Type	50 mM glycine – HCl, pH 2.4	87 ± 2	13-16
	HCl pH 2.4	83 ± 2	12-14
	50 mM NaOH	70 ± 4	17-21
	50 mM KCl	54 ± 4	35-45
Concentration	10 mM Glycine- HCl, pH 2.4	81 ± 2	10-12
	25 mM Glycine- HCl, pH 2.4	93 ± 3	13-16
	50 mM Glycine- HCl, pH 2.4	85 ± 2	14-18
	75 mM Glycine- HCl, pH 2.4	74 ± 1	14-19
	100 mM Glycine- HCl, pH 2.4	58 ± 3	15-21
pH	25 mM Glycine- HCl, pH 2.2	86 ± 3	12-13
	25 mM Glycine- HCl, pH 2.4	97 ± 3	12-15
	25 mM Glycine- HCl, pH 2.6	88 ± 2	12-16
	25 mM Glycine- HCl, pH 2.8	81 ± 1	13-17

7.4.3.2 Buffer solution

7.4.3.2.1 Type

Initially two widely used biochemical buffer types were tested, 10 mM sodium phosphate buffer (SPB) and Tris-HCl buffers, by injected standard DNA between 0.1 and 100 ng l^{-1} . There is no difference between sensitivity (slope of

calibration curve) of sodium phosphate and Tris-HCl buffers (Figure 7.5) However, when comparing the signals at the same concentration of DNA, Tris-HCl gave a higher response and more steady baseline. Therefore, Tris-HCl was chosen to use for further experiment.

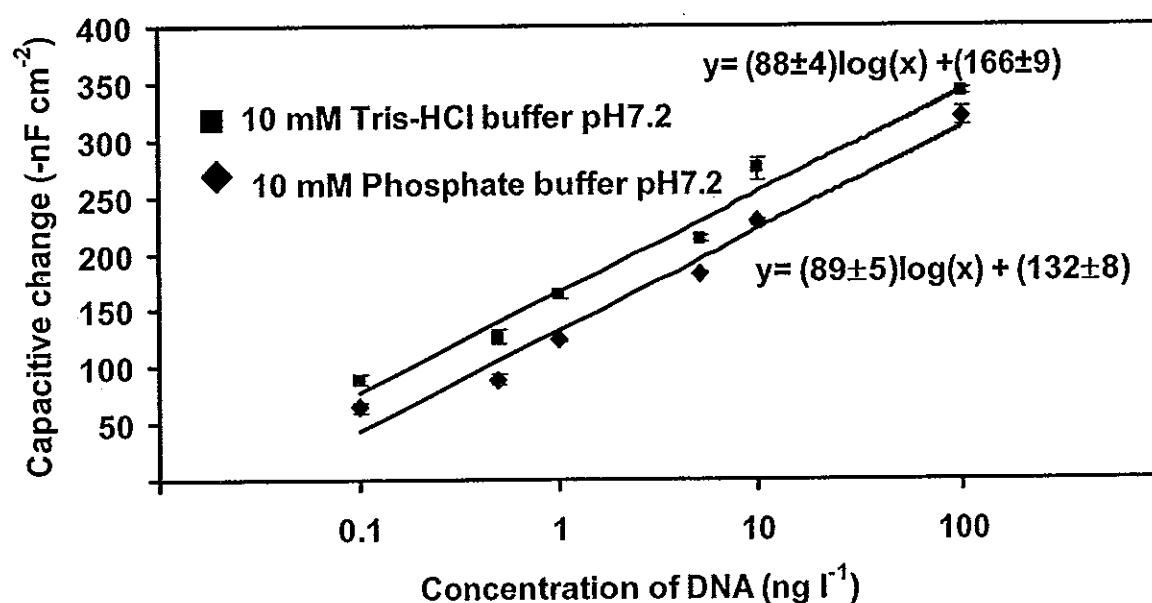


Figure 7.5 Response of the flow injection capacitive biosensor system to DNA using difference buffer solutions.

7.4.3.2.2 Concentration

Different concentrations of the Tris-HCl buffer pH 7.2 were then tested. The highest change in the capacitive signal from injections of 1 ng l⁻¹ DNA was found to be at 5 mM (Figure 7.6) but a more steady baseline was obtained at 10 mM so this concentration was selected for further experiments.

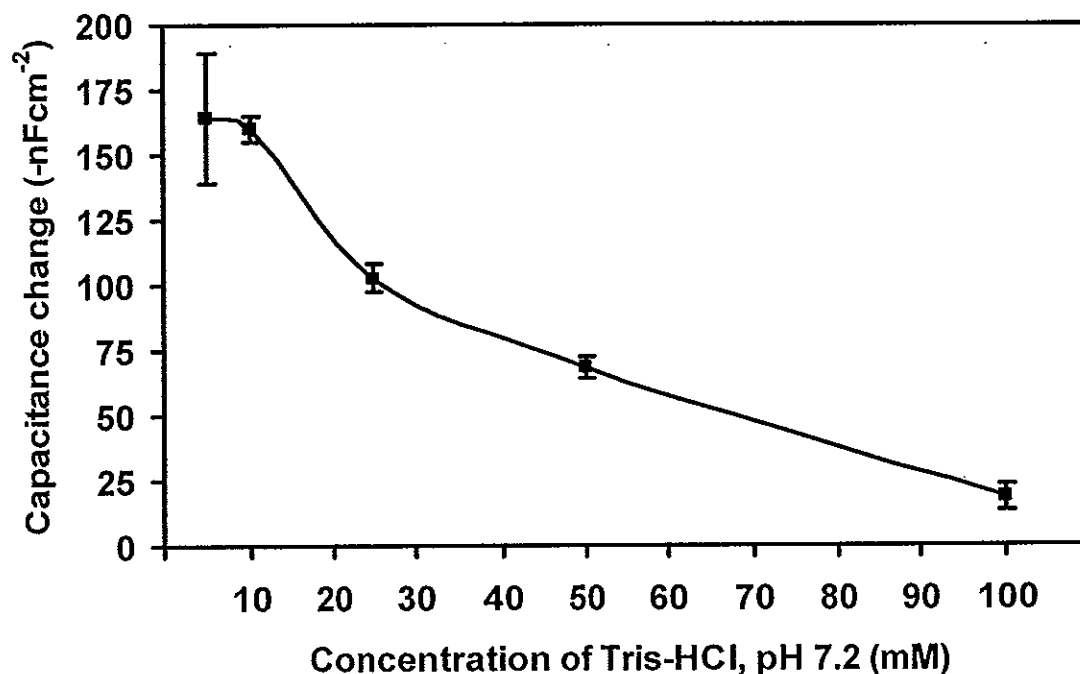


Figure 7.6 Response of the capacitive biosensor system to 1 ng l^{-1} at different concentrations of Tris- HCl buffer at pH 7.2.

7.4.3.2.3 pH

The influence of pH during the binding reaction was studied between 7.00 to 8.00 for the same concentration of DNA at 1 ng l^{-1} in 10 mM Tris-HCl buffer solution. Figure 7.7 shows that the maximal capacitive change in capacitive was found at pH 7.00. Since the binding force of this affinity pair is mainly electrostatic, between the positive of histone and negative of phosphate group of DNA (Reece, 2004) and the isoelectric point of histone is around 10 (Yan *et al.*, 2003), so at pH 7.00 histone has more positive charge to bind with the negative charge of phosphate group in DNA. Therefore, 10 mM Tris-HCl, pH 7.00 was used in the continued experiments.

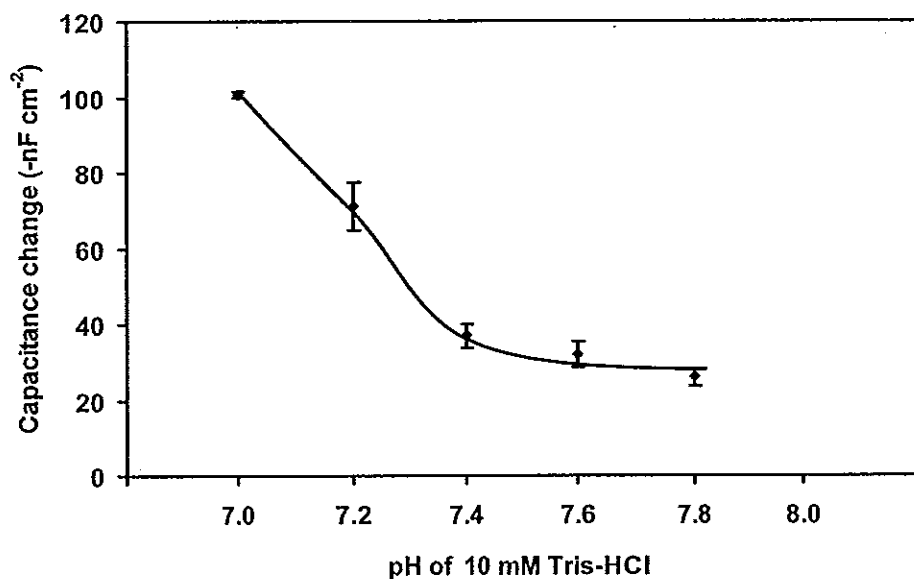


Figure 7.7 Effect of the pH of Tris-HCl buffer solution on response to 1 ng l⁻¹ DNA.

7.4.3.3 Flow rate

The effect of flow rate was investigated by injecting 300 μ l of 1 ng l⁻¹ of DNA solution at different flow-rates (50-500 μ l min⁻¹). The capacitance change decreased as the flow rate increased due to the reduction of binding interaction time. The flow rate of 50 μ l min⁻¹ gave the highest response (Figure 7.8), however, nearly the same response was also obtained at 100 μ l min⁻¹, but the analysis time was much shorter (=14 min compare to 50 μ l min⁻¹= 18 min) so, 100 μ l min⁻¹ was chosen.

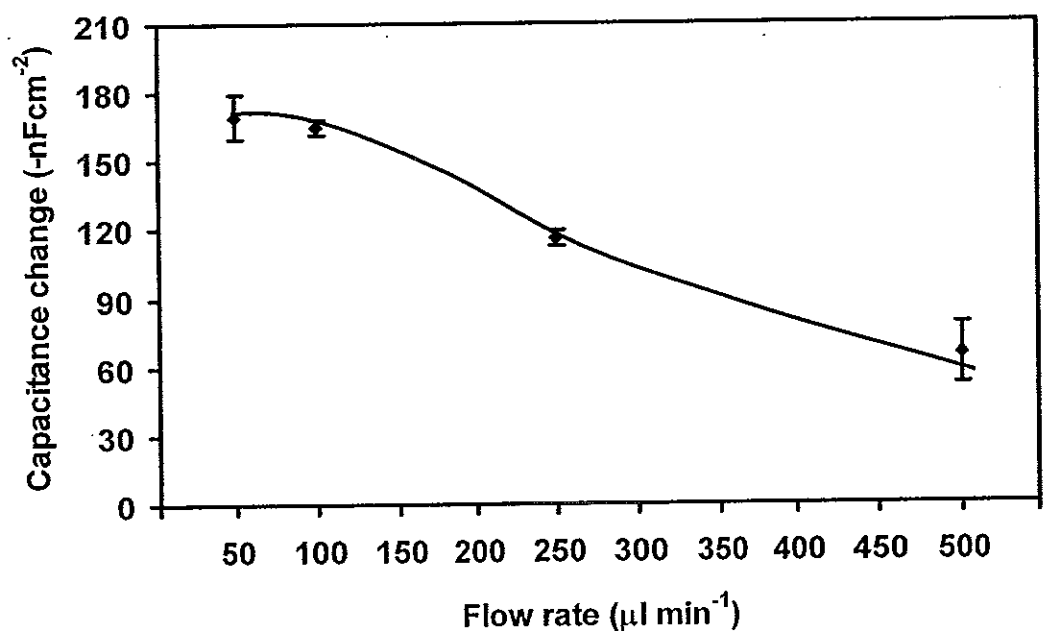


Figure 7.8 Response of the flow injection capacitive biosensor system at different flow rate.

7.4.3.4 Sample volume

Generally, an increase in response can be achieved with an increase in sample volume. Therefore, the effect of sample volume on capacitance change to 1 ng l^{-1} of DNA standard was studied from 50-400 μl . The change in capacitance signal increased with sample volume until 250 μl and become steady (Figure 7.9), therefore, 250 μl was chosen for further study.

Table 7.2 summarizes the optimized parameters, the values tested and the optimum values.

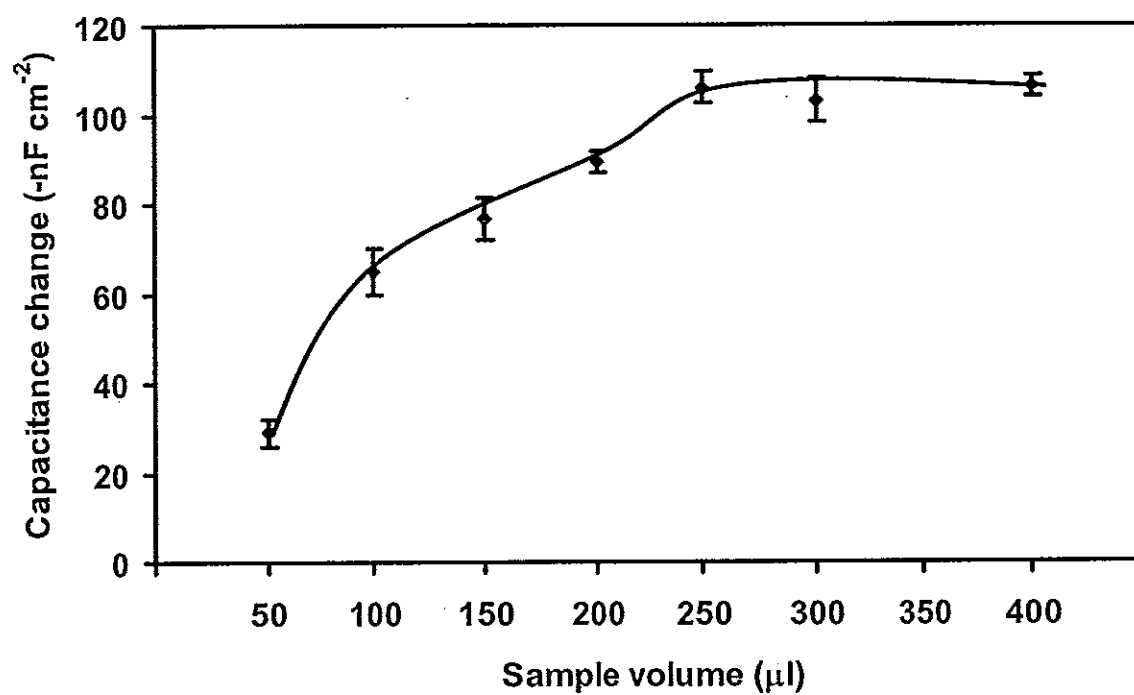


Figure 7.9 Response of capacitive biosensor to 1 ng l⁻¹ DNA at different sample volume.

Table 7.2. Assayed parameters and optimized values of the capacitive system.
Capacitive change is from the injection of 1 ng l^{-1} of calf thymus DNA.

Parameter	Investigated values	Capacitive change (-nF cm^{-2})	Analysis time (minute)	Optimized values
Concentration of buffer Tris-HCl, pH 7.2 (mM)	5 10 25 50 100	164 ± 25 160 ± 5 103 ± 5 68 ± 4 18 ± 5	12 14 15 17 19	10
pH of buffer 10 mM Tris-HCl	7.00 7.20 7.40 7.60 7.80 8.00	101 ± 1 71 ± 6 37 ± 3 32 ± 3 26 ± 2 15 ± 2	14 14 14 14 14 14	7.00
Flow rate ($\mu\text{l min}^{-1}$)	50 100 250 500	169 ± 10 165 ± 3 116 ± 3 65 ± 13	18 14 12 8	100
Sample volume (μl)	50 100 150 200 250 300 400	29 ± 3 65 ± 5 76 ± 5 99 ± 2 106 ± 4 104 ± 5 106 ± 2	10 11 12 12 13 14 17	250

7.4.4 Reproducibility

To test whether the response of the histone modified electrode can be reproduced after the removal of DNA by regeneration solution, the same concentration of 1 ng l^{-1} of DNA was injected into the system with subsequent regeneration. The change of capacitance signal after regeneration was used to calculate the percentage of residual activity of the histone electrode by comparing the response to the initial capacitance change. The histone immobilized on the self assembled monolayer method retained $95.2 \pm 3.1 \%$ of its ability to bind to DNA after 43 times of regeneration and the residual activity after this point dropped below 90 % (Figure 7.10). The results indicate that the immobilized histone electrode can be reused with good reproducibility up to at least 40 times. The reduction in histone binding ability may be caused by the loss of protein from electrode surface, loss of SAM layer or fouling of the sensor surface by proteins deposits. The latter hypothesis was tested by using voltammetry. The voltammogram of the electrode after fifty analysis cycles showed no redox peaks (Figure 7.11). This indicated that the SAM layer on the gold electrode remained intact. Therefore, the decrease of residual activity was likely due to the loss of histone and/or its binding activity.

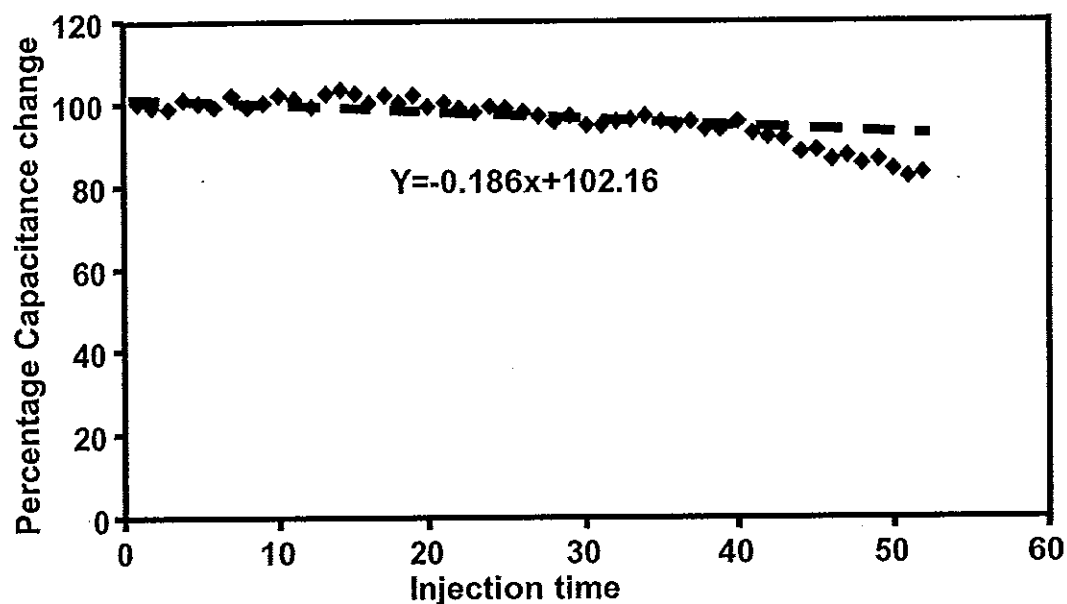


Figure 7.10 Reproducibility of the response from histone modified electrode to injection of 250 μ l standard calf thymus DNA (1 ng l^{-1}) with regeneration steps between each individual assay.

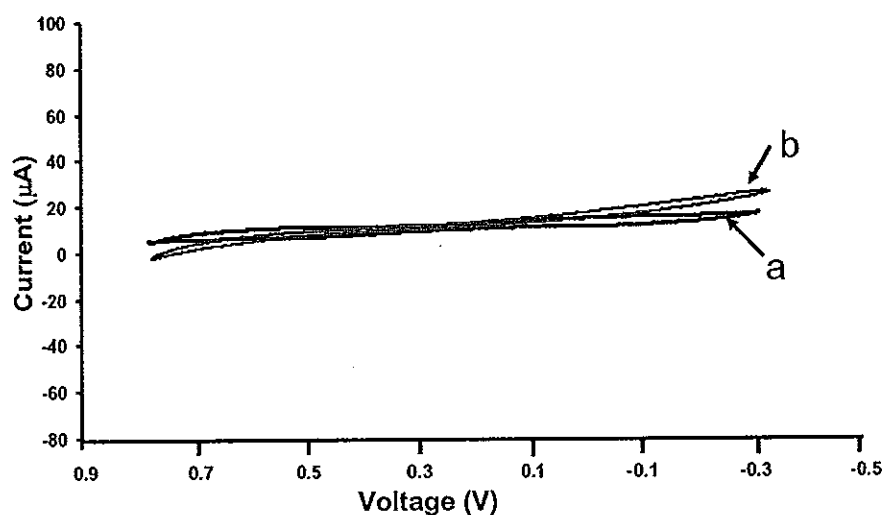


Figure 7.11 Cyclic voltammogram of modified gold electrode obtained in 0.05 M ($\text{K}_3[\text{Fe}(\text{CN})_6]$) solution, (a) is the response when on the electrode surface was blocked by 1-dodecane thiol before used and (b) after used for 50 times

7.4.5 Linear dynamic range and detection limit

Standard calf thymus DNA solutions ranging from 1×10^{-7} ng l⁻¹ to 1×10^3 ng l⁻¹ were injected with intermittent regeneration steps using 25 mM glycine-HCl, pH 2.4. Figure 7.12 shows the calibration curve for DNA under optimal conditions. The plot between capacitance change and logarithm of DNA concentration showed two linear ranges with different sensitivity, *i.e.*, from 10^{-5} ng l⁻¹ to 10^{-2} ng l⁻¹ and 10^{-1} ng l⁻¹ to 10^2 ng l⁻¹. This phenomenon might be explained in two different ways: the effect may be caused by different degrees of affinity for DNA by the different histones. In this work, whole histone of calf thymus which includes histone H1, H2A, H2B, H3 and H4 was immobilized. Since it was reported that DNA has higher affinity binding to histone H1 than the other four histones (Cui *et al.*, 2005), it is possible that at low concentration only histone H1 plays a major role in DNA binding. When concentrations increase, DNA then binds with other histones as well. Therefore, the sensitivity is higher at high DNA concentration. Another interpretation is that DNA at low concentrations can be present in a more extended form and thus possibly be bound tighter to the sensor surface mainly by ionic interactions, while at higher concentrations, DNA may have more of a secondary structure and bind more specifically to the immobilized histones. From the results, the detection limit was found to be 10^{-5} ng l⁻¹ based on IUPAC Recommendation 1994 (Buck and Lindner, 1994).

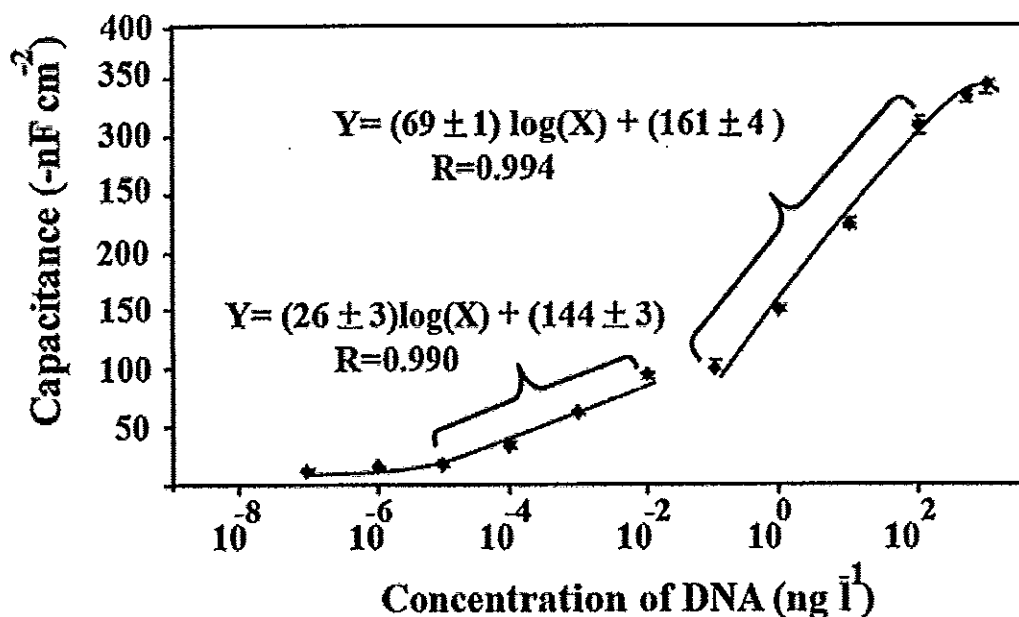


Figure 7.12 Capacitance change vs. the logarithm of calf thymus DNA concentration detected by immobilized calf thymus histone modified electrode under optimum conditions ($100 \mu\text{l min}^{-1}$ flow rate, $250 \mu\text{l}$ sample volume, 10 mM Tris-HCl buffer, pH 7.00).

7.4.6 Selectivity

Since different sources of DNA or histones may affect the binding and, hence, the response of the capacitive system, it is important to investigate this. First, the effect of DNA source was studied by using immobilized calf thymus histone to detect DNA from calf thymus, white shrimp and *E. coli*. The calibration curves were investigated between $10^{-5} \text{ ng l}^{-1}$ and $10^{-2} \text{ ng l}^{-1}$ and these are shown in Figure 7.13a. The sensitivity (slope of calibration curve) obtained with calf thymus DNA was about four folds higher than the one obtained from white shrimp DNA, and the lowest sensitivity was obtained from *E. coli* DNA. This is probably due to the size of DNA, longest DNA is from calf thymus, followed by shrimp and *E. coli* (qualitative comparison of sizes was tested by using agarose gel electrophoresis). The layer on the electrode surface with a longer DNA should be thicker and this would cause C_{tot} to decrease more than when a shorter DNA was bound, so calf thymus DNA would give the highest response. Although the sensitivity of the system to each DNA is different,

the lower limit of detection is the same. That is, when the system was used to detect the DNA of calf thymus, white shrimp, or *E. coli* the lower limit of detection is 10^{-5} ng l⁻¹.

Histones from a different source, i.e. white shrimp, were then immobilized on gold electrodes at the same concentration as that of calf thymus histones ($50 \mu\text{g ml}^{-1}$) and studied by injecting DNA from calf thymus, white shrimp and *E. coli* (Figure 7.13b). The results show that shrimp histone can also bind with DNA from all three sources with the same lower limit of detection of 10^{-5} ng l⁻¹. That is, neither calf nor shrimp histone is selective with its DNA. However, from these results it can be seen that histone can bind better with DNA from the same source and give higher sensitivity than the binding with DNA from different sources.

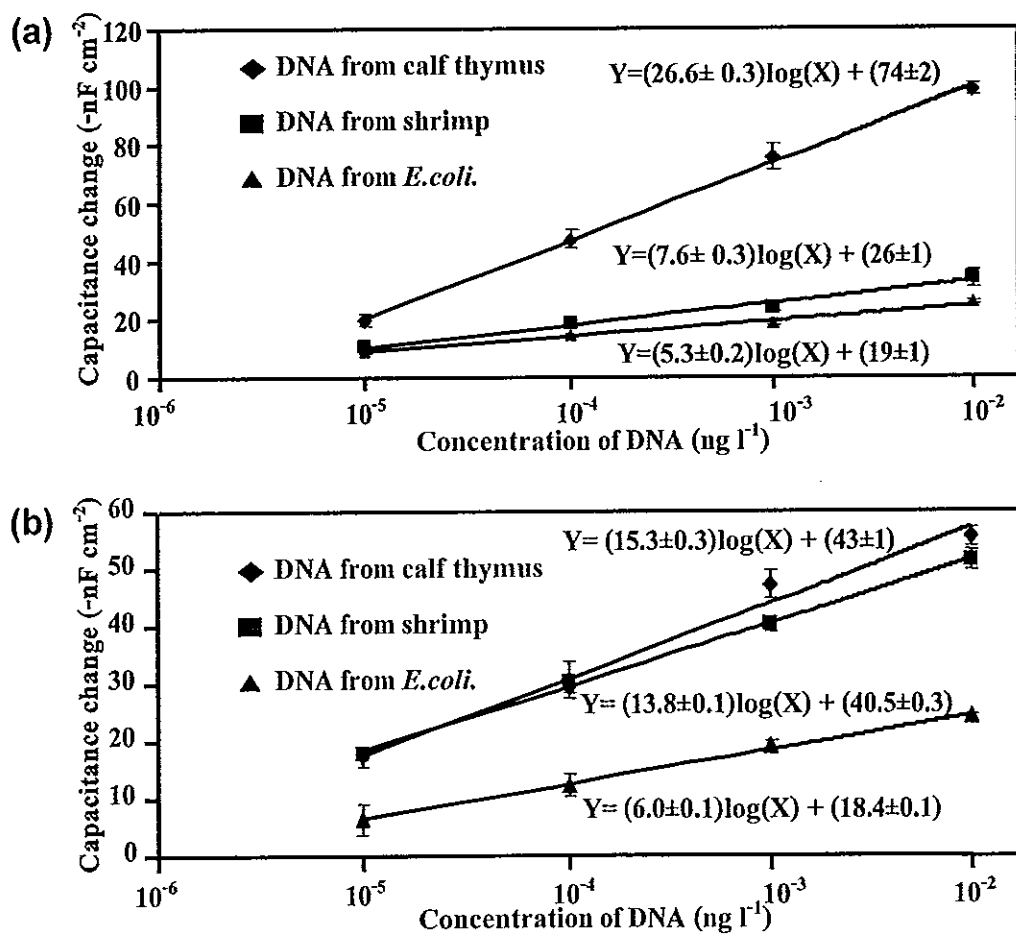


Figure 7.13 Calibration curve for DNA from calf thymus, white shrimp and *E. coli* with (a) immobilized calf thymus histone and (b) white shrimp histone.

7.4.7 Determination of residual shrimp DNA

Determination of residual DNA was carried out using a particle free homogenate of shrimp protein as real sample. This extract is normally used in the study of protein interaction with white spot syndrome virus. Since the protein in the extract may interfere with the detection of residual DNA via non specific binding to the surface of the modified electrode, bovine serum albumin (BSA) was used to test this influence. Using the electrode with immobilized calf thymus histone, the response due to BSA at the concentration range 0.01 to 100 ng l^{-1} were about the same and were much lower than the response from DNA (Figure 7.15). It can be suggested that non specific binding from proteins do not play an important part in the response.

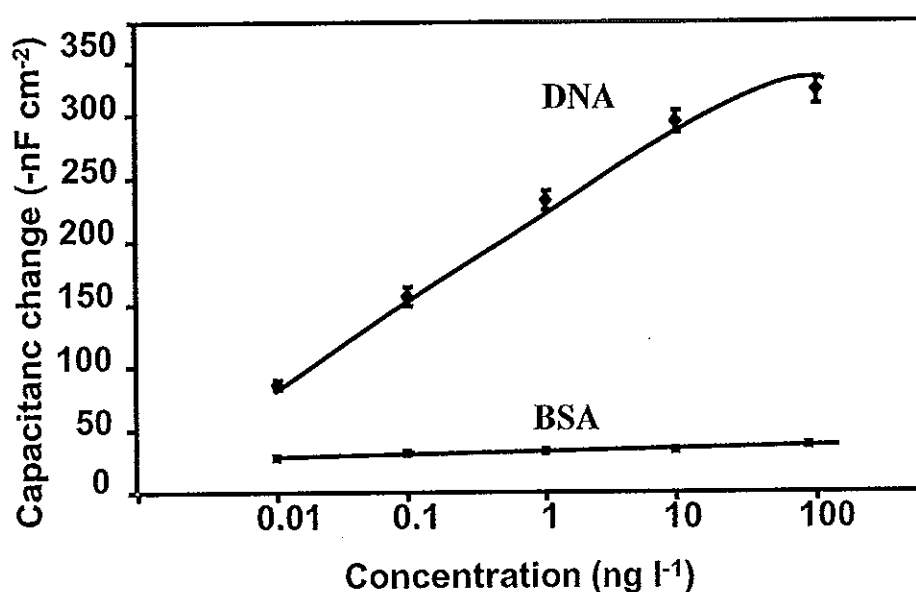


Figure 7.15 Response of the histone to DNA and bovine serum albumin (BSA)

When analyzing real samples, the matrix may also cause some interference to the response. Matrix interference can lead to either a suppression or enhancement of the sample signal compared to the calibrate signal for the same analytes (Eurachem-Guide, 1998). The influence of the matrix in real sample was studied by using immobilized shrimp histone. Crude shrimp protein sample without DNA (prepared by adding excess DNaseI to digest residual DNA) was spiked with known amount of shrimp DNA at 0.1 to 1.5 pg l^{-1} and these were used to performed

the matrix matched calibration curve. Calibration curve was also performed using standard solution in the same concentration ranges (standard calibration curve). The assay for each concentration was carried out in triplicate and the average sensor response and standard deviation were calculated. The slope of standard calibration curve and matrix matched calibration curve were compared if there is no significant difference between slope of the two curves, it indicates that the matrix has no effect on the response of the capacitive system. Figure 7.16, indicating that there was effect of matrix interference on the sensor response (IUPAC Technical Report, 20002). The slope were also compared by two way ANOVA (analysis of variance) calculated by R software (R Development Core Team, 2006). The results showed that the slope of regression lines of standard and matrix matched calibration curves were significantly different ($P < 0.05$).

One way of reducing the matrix effect is by dilution. Since the LOD of this system is very low ($10^{-5} \text{ ng l}^{-1}$), it is possible to dilute the sample several times. This will be appropriate when the concentration of DNA is high, e.g. when DNA is product of process. However, when the detection is for residual DNA only trace amount will exist, in this case matrix matched calibration should be employed.

7.4.7.1 Matrix matched calibration

Matrix matched calibration was used for the detections of the trace amount of DNA. The response when injecting crude shrimp protein sample ($n=3$) were used to calculate the concentration of residual DNA from the matrix matched calibration curve and no DNA was detected.

To further validate the capacitive detection system with real samples, the recovery of spiked DNA ($0.1\text{--}1.5 \text{ pg l}^{-1}$) in crude shrimp protein samples were tested. The analysis was carried out with immobilized shrimp histone. The responses obtained from spiked shrimp protein sample were used to calculate the concentration from the matrix matched calibration curve. Recovery percentage was evaluated by the following equation:

$$\% \text{ Recovery} = \frac{C_1 - C_2}{C_3} \times 100 \quad (7.4)$$

where C_1 is the concentration of analyte measured in the spike sample, C_2 is the concentration of analyte measured in the blank and C_3 is the concentration of analyte spiked into the sample (Taverniers *et al.*, 2004). From the results (Table 7.3), percentage of recovery and relative standard deviation of all spiked DNA (in $\mu\text{g l}^{-1}$ range) in crude shrimp protein are acceptable. Since the acceptable recovery in the $\mu\text{g l}^{-1}$ level is 40-120% and R.S.D. is 30-45.3% (Taverniers *et al.*, 2004).

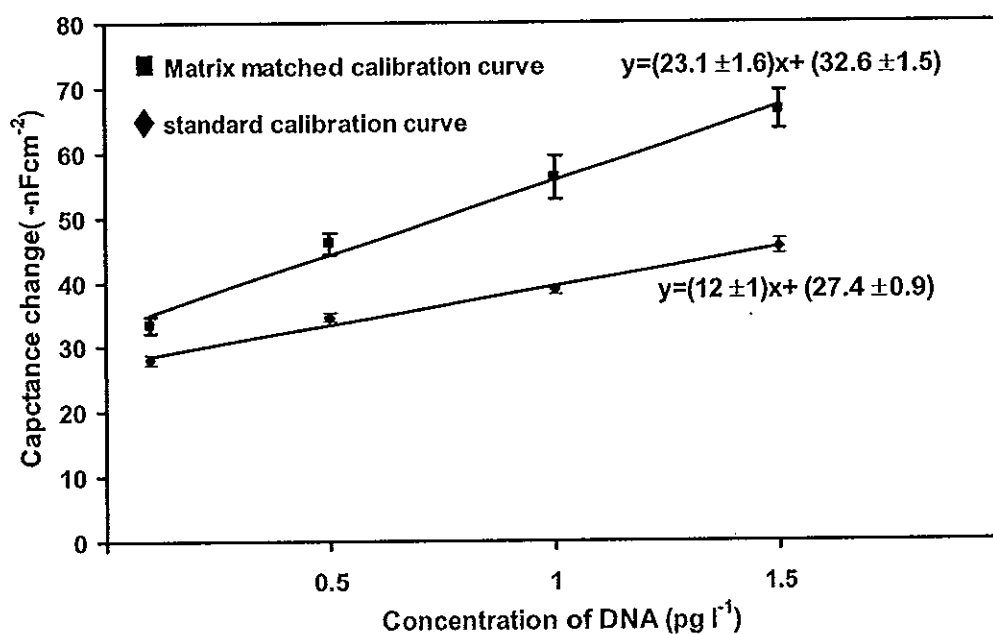


Figure 7.16 Standard and matrix matched calibration curve of crude shrimp protein sample

Table 7.3. Recovery of shrimp DNA from spiked crude shrimp protein (n=3); using Matrix matched calibration (Section 7.3.1) and Dilution methods (section 3.7.2)

Spiked concentration	Immobilized shrimp histone				Immobilized calf thymus histone			
	Sample 1		Sample 2		Sample 1		Sample 2	
	Recovery (%)	R.S.D. (%)	Recovery (%)	R.S.D. (%)	Recovery (%)	R.S.D. (%)	Recovery (%)	R.S.D. (%)
Matrix matched calibration (pg l⁻¹)								
0.10	80 ± 18	22	-	-	-	-	-	-
0.50	116 ± 15	13	-	-	-	-	-	-
1.0	107 ± 7	7	-	-	-	-	-	-
1.5	100 ± 6	6	-	-	-	-	-	-
Dilution (ng l⁻¹)								
10	73 ± 2	3	88 ± 23	26	77 ± 6	8	95 ± 17	18
50	109 ± 5	5	98 ± 17	17	115 ± 15	13	117 ± 22	19
100	103 ± 4	4	113 ± 4	4	101 ± 6	6	116 ± 18	16
150	110 ± 1	1	108 ± 5	5	106 ± 7	7	101 ± 9	9

7.4.7.2 Dilution

Crude shrimp protein samples were spiked with shrimp DNA at 10 ng l⁻¹ to 150 ng l⁻¹ and diluted 10,000 times (followed Thavarungkul *et al.*, 2007) with 10 mM Tris-HCl buffer pH 7.0. These were analyzed (n=3) and the calibration curve was compared to that of the standard solution. The experiment was carried out by two capacitive biosensor systems, one with immobilized shrimp histone and the other with calf thymus histone. The slope of the spiked curve and calibration were also compared by two way ANOVA. The results show no difference between slope of two curves, indicating that there were no matrix effect for the diluted samples for both immobilized calf thymus histone (Figure 7.17 a) and immobilized shrimp histone (Figure 7.17 b), that is, the matrix effect can be reduced by dilution. Therefore, the standard curve could be used to determine the residual DNA contamination in diluted real sample.

The recovery of spiked shrimp DNA at 10 ng l⁻¹ to 150 ng l⁻¹ in crude shrimp protein sample was tested. The spiked samples were then diluted 10,000 times with Tris-HCl buffer pH 7.0 to reduce the matrix effect. The analysis was also carried out by two capacitive biosensor systems, one with immobilized shrimp histone and

the other with calf thymus histone. The capacitance changes obtained from the capacitive systems were used to calculate the concentrations from the calibration curve of standard obtained prior to the test. From the results (Table 7.3) percentage of recovery and relative standard deviation of all spiked DNA (in ng l^{-1} range) in crude shrimp protein are acceptable (Taverniers *et al.*, 2004) (acceptable recovery in the $\mu\text{g l}^{-1}$ level is 40-120% and R.S.D. is 30-45.3%). These results show that the developed capacitive biosensor is suited for quantification of DNA.

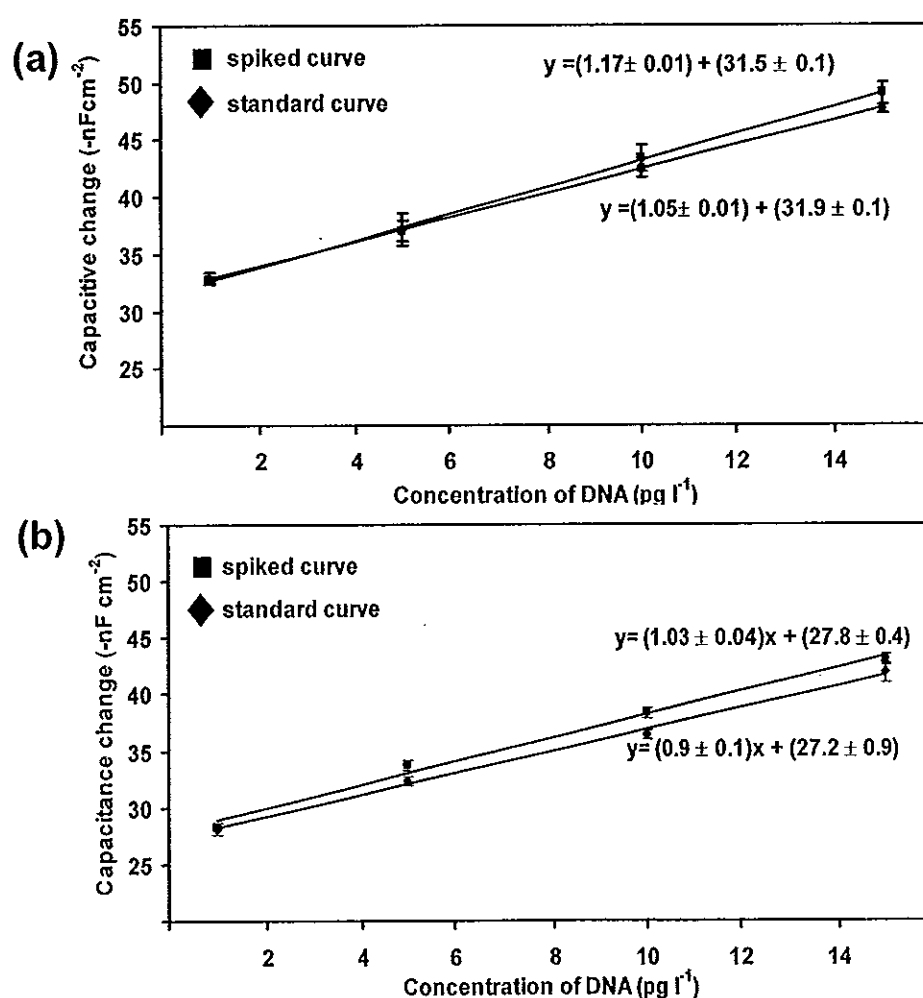


Figure 7.17 The standard curve and spiked curve for the study of matrix interference of crude shrimp sample; (a) for immobilized calf thymus histone and (b) immobilized shrimp histone.

The spiked sample were also measured by UV spectrometry at λ_{260} . However, no response was obtained from any of spiked samples (DNA at 10- 150 ng l⁻¹) since the limitation of this method is 5 $\mu\text{g ml}^{-1}$ (Noites *et al.*, 1999) . That is, the developed capacitive system can detect DNA at a much lower concentration.

7.5 Conclusions

The results demonstrated the possibility of using the capacitive biosensor system for direct assay of affinity binding between DNA and histone protein on self-assembled thioctic acid monolayer modified electrode. For the system using calf thymus histone to detect calf thymus DNA, it provides a low detection limit of 10⁻⁵ ng l⁻¹ and wide linear ranges 10⁻⁵-10⁻² ng l⁻¹ and 10⁻¹ -10² ng l⁻¹. Since histone from one source can also detect DNA from other sources, this system is suitable for screening DNA contaminants independent of their origin. However, if the source of DNA is known a calibration curve can be constructed and this system can be used to quantify the amount of DNA which will be useful for a number of biotechnology processes. This method can be used to investigate DNA in sample with difference matrixes. In case of trace DNA level, matrix matched calibration curve can be applied, for example, residual DNA in biological or biopharmaceutical products. For high level DNA detection such as in lysis cell sample, the matrix interference can be reduced by dilution where the standard curve could be used to determine the DNA in diluted real sample. Major advantage of this system over gel electrophoresis, spectrophotometric or spectrofluorometric technique is the fact that DNA can be determined without using any dye staining such as ethidium bromide (Ebr) or other fluorescence stains that are a powerful carcinogen. In addition, analysis time of this technique (13-15 min) was much shorter than other DNA quantitation methods (30min-5h) (Projan *et al.*, 1983; Schmidt *et al.*, 1996) Using the appropriate regeneration solution, good reproducibility was obtained. The electrode can be reused up to at least 40 times and this helps to reduce the cost of analysis.

Chapter 8

Capacitive Biosensor for Plasmid DNA Detection

8.1 Introduction

DNA vaccination and gene therapy are expected to be a fast growing therapeutic area in the next decade. In DNA vaccination, nucleic acids are administered to the patient with the intent of initiating an immune response to the antigen or protein encoded by the DNA. In gene therapy, nucleic acids are introduced to restore, cancel or enhance an imperfect gene function (Kepka *et al.*, 2004; Kim *et al.*, 1998; Zhang *et al.*, 2002). These result in a need for quantities of gene vectors such as plasmid DNA (Gustavsson *et al.*, 2004; Kepka *et al.*, 2004; Wahlund *et al.*, 2004)

Plasmid DNA are extra-chromosomal closed circular double-stranded DNA molecules found most frequently, but not exclusively, in bacteria. They replicate independently of the cell chromosome, and typically carry genes that code for antibiotic resistance, toxin production and breakdown of natural products (Clemson and Kelly., 2003). Plasmids for gene therapy are usually produced in *Escherichia coli* host by fermentation (Prazeres *et al.*, 1998). For the purification of plasmid DNA, various chromatographic techniques are normally used (Ferreira *et al.*, 1998; Gustavsson *et al.*, 2004; Kepka *et al.*, 2004; Noites *et al.*, 1999). Plasmid content in a preparation is typically accessed using gel electrophoresis with subsequent gel staining, photography and densitometric scanning. Typically, when producing plasmid DNA small amounts of the substance are retrieved. Hence, sensitive analytical methods are required.

The most common methods for determining plasmid DNA concentration are based on gel electrophoresis or spectrophotometric methods where the molecule absorbs maximally around 260 nm. This latter method is accurate and reproducible when applied to purified samples. However, it is relatively insensitive, measuring DNA concentrations above 5 µg/ml (Noites *et al.*, 1999). DNA concentration can also be determined from densitometric scans of agarose or polyacrylamide gel electrophoresis (Projan *et al.*, 1983). However, analysis can take

between 3 and 5 h. Capillary electrophoresis and certain chromatographic techniques can also be used for this purpose (Middaugh *et al.*, 1998; Schmidt *et al.*, 1999). Most of these methods are time consuming and labour intensive and typically require relatively large amounts of sample (Levy *et al.*, 2000), which may hamper their use for rapid monitoring of plasmid DNA. Therefore, development of new methods with high sensitivity and specificity for the detection of plasmid DNA is desirable and affinity biosensors are an interesting approach.

As described in chapter 7, electrochemical based capacitive transducers are attractive for label-free affinity biosensors since these device give high sensitivity, specificity, are label-free and have been developed to detect compounds at low concentration. (Berggren and Johansson, 1997; Berggren *et al.*, 1998; Bontidean *et al.*, 1998; 2000; Hedström *et al.*, 2005; Hu *et al.*, 2002; 2005; Jiang *et al.*, 2003; Limbut *et al.*, 2006a; 2006b; 2007).

To detect plasmid DNA of a prokaryote such as *E. coli*, a capacitive measurement was applied to construct a biosensor based on immobilized lactose repressor (*lac* repressor) recognition element. *Lac* repressor is one member of a large family of related proteins, found both in *E. coli* and other prokaryotes. The *lac* repressor derived from *E. coli* is a tetrameric protein (Suckow *et al.*, 1996) with binding sites for inducer molecules and lactose operator (*lac* operator), which is a group of genes located on the DNA material (Butler *et al.*, 1977; Bell and Lewis, 2001; Record *et al.*, 1977). Both electrostatic and hydrophobic forces are involved in the specific binding of *lac* repressor with *lac* operator (deHaseth *et al.*, 1977; Record *et al.*, 1977).

In this work we describe a flow-injection capacitive biosensor for the rapid determination of plasmid DNA concentration by immobilizing *lac repressor* on gold electrode surface via SAM of thioctic acid. The technique was tested using different isoforms of plasmid DNA that contain a *lac* operator, such as supercoiled DNA (sc pDNA) and open circular plasmid DNA (oc pDNA).

8.2 Materials

Lac repressor protein and *E. coli* cells BMH8117 (genotype: F⁻, $\Delta(lac-proAB)$ thi, *gyrA* (Nal^R), *SupE*, λ), Ap^R harbouring a p310 plasmid (2455 bp)

containing the *lac* ideal operator and ampicillin resistance gene (Hanora *et al*, 2006) were provided by Dr. Ashok Kumar from Indian Institute of Technology, Kanpur, India. Thiocetic acid, 1-dodecanethiol and *N*-3-(dimethylamino-propyl-*N'*-ethylcarbodiimide hydrochloride (EDC) were from Sigma-Aldrich (st Louis, USA). All other chemicals used were of analytical grade. Solutions and buffers were prepared using Milli-Q gradient ultra pure water (Millipore, Bedford, MA, USA). Before use, buffers were filtered through a millipore filter with pore size 0.22 μm with subsequent degassing. Monolith columns produced from macroporous polyacrylamide gel (2.5 cm \times 1 cm i.d., bed volume of 2 ml), with a pore size of 1–100 μm (Plieva *et al.*, 2004; 2005), were provided by Protista Biotechnology AB (Lund, Sweden). The monolith column was grafted with (2-(methacryloyloxy)ethyl)-trimethyl ammonium chloride to introduce ion exchange groups on the surface and produce poly META-grafted cryogel column (Hanora *et al*, 2006).

8.3 Methods

8.3.1 Preparation of plasmid DNA from *E. coli*.

8.3.1.1 Bacterial culture and isolation of plasmid DNA

E. coli cells (200 μl in glycerol) were grown in Luria-Bertani (LB) medium (Kumar *et al*, 2003) supplemented with 100 mg ml⁻¹ of ampicillin, at 200 rpm, 37 °C. The overnight cell cultures were harvested by centrifugation at 16,300 $\times g$ in a Sorvall GSA rotor (WIFUG AB, LAB CENTRIFUGES, Stockholm, Sweden) for 10 min at 4 °C and the supernatants were removed. The pellet was suspended by gentle stirring in 2.16 ml of suspension buffer (61mM glucose, 50mM EDTA, 10mM Tris-HCl, pH 8). Then 4.68 ml of lysis buffer (0.2MNaOH, 1% (w/v) sodiumdodecylsulfate (SDS)) was added while stirring until a complete mix was achieved. An ice-cold neutralising solution was then added (3.54 ml of 3M potassium acetate, pH 5.5) to the lysate. The solution was kept on ice for 20 min. A white precipitate was formed containing SDS, genomic DNA, protein and cell debris. The non-clarified cell lysate was kept at -20 °C until further processing.

8.3.1.2 Plasmid DNA purification

For plasmid purification, two chromatographic methods were used, ion exchange and size-exclusion chromatography. For the removal of protein and organelles a PolyMETA cryogel was utilized. The cryogel column (12 x 32 mm²) was connected to a Biologic Duo-Flow fast protein liquid chromatography (FPLC) system (BIO-RAD, USA) and equilibrated with 0.5 M NaCl in Tris-HCl, pH 8.00. One milliliter of sample was injected and eluted with 4.0 ml min⁻¹ of a salt gradient from 0.0 to 2.0 M NaCl in the same buffer, pH 8.00. The eluted peaks were spectrophotometrically detected at the wavelengths 260 and 280 nm. Thereafter, size-exclusion chromatography (SEC) was performed to separate and remove RNA from the product. The SEC purification was carried out by using sephadex G-15 packed in a column with dimensions 10 x 400 mm connected to FPLC. The column was equilibrated with 25 mM Tris-HCl, pH 8.00. Two milliliters of elutant sample from ion-exchange chromatography run was injected and runned at a flow rate of 0.5 ml min⁻¹ and the eluted peaks were detected at 260 and 280 nm.

The interchange between supercoiled plasmid DNA (sc pDNA) to open circular plasmid DNA (oc pDNA) was performed using a thermal transition method described by Uedaira and coworkers (Uedaira *et al.*, 1994). To force the plasmid to become open circular form, purified supercoiled plasmid DNA was heated at 95 °C for 15 min and incubated for 5 min on ice. The solution was injected into a size-exclusion chromatography to separate the open circular form from supercoiled plasmid DNA which was carried out by using Sepharyl S-1000 packed in a glass column with diameter 10 x 92 mm connected to FPLC.

The purity of supercoiled and open circular plasmid DNA were analysed by 1.0 % agarose gel electrophoresis in TBE buffer (0.089 M tris-borate, pH8.0, 2 mM EDTA) at 80 V for 2 h. The pDNA concentration was determined by UV absorbance at 260 nm.

8.3.2 Preparation of *lac* repressor modified electrodes

Lac repressor was covalently immobilized onto the capacitive biosensor transducer constructed of a gold rod (Ø 3 mm, 99.99% purity) connected to

a stainless steel holder. Prior to immobilization, the gold electrodes were cleaned by thoroughly polishing with alumina slurries down to 0.1 μm in particle size (Struers, Denmark). After washing with distilled water, the electrodes were mounted in teflon holders and plasma cleaned (Mod. PDC-3XG, Harrich, New York) for 10 minutes. Immediately thereafter the electrodes were placed in an ethanolic solution of 2 % (w/v) thiocetic acid. The thiocetic acid self-assembled electrodes were then carefully washed with absolute ethanol and dried in a stream of ultra pure nitrogen. The thiocetic acid on the electrode was activated in 1% (w/v) solution of EDC in dried acetonitrile for 5 h to transform the carboxyl group to an activated ester intermediate. After washing with 100 mM potassium phosphate buffer (pH 8.00), the electrode was incubated in 0.1 mg/ml of *lac* repressor solution in phosphate buffer at 4 °C for 24 h. Finally, the electrode was washed with phosphate buffer and immersed for 20 minutes in 10 mM of 1-dodecanethiol in ethanol to block any pinhole on the gold electrode surface.

8.3.3 Capacitive measurement

The electrode modified with *lac* repressor was inserted as the working electrode in a three electrode flow cell with a volume of 10 μl . As reference and auxiliary electrodes, a platinum wire and a platinum foil were used, respectively. An extra Ag/AgCl reference was placed in the outlet flow, as can be seen from Figure 8.1. The electrode was coupled to a fast potentiostat via a data acquisition and control unit (Keithley Instruments, Inc. Tuanton. MA, USA). Capacitance measurements were performed by applying a +50 mV potential pulse to the modified gold electrode.

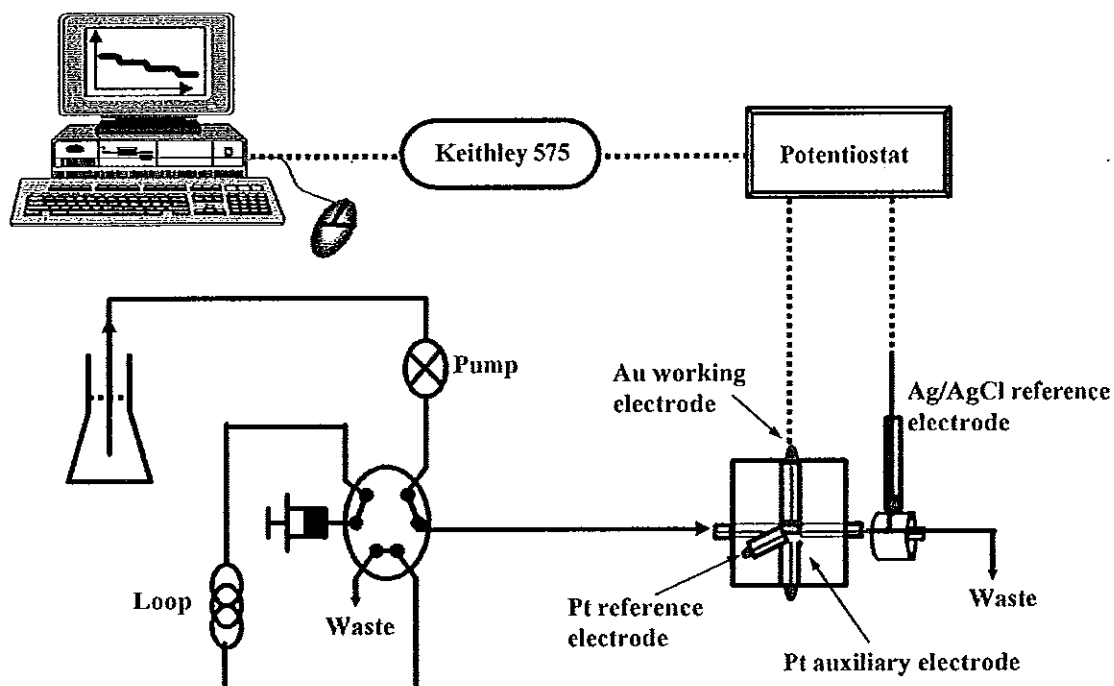


Figure 8.1 Schematic diagram showing the flow injection capacitive biosensor system. The electrode modified with *lac* repressor was inserted as the working electrode in a three electrode flow cell with a volume of 10 μl . As reference and auxiliary electrodes, a platinum wire and a platinum foil were used, respectively. An extra Ag/AgCl reference was placed in the outlet flow.

8.3.4 Cyclic voltammetry measurements

Cyclic voltammograms were recorded in a three electrode electrochemical batch cell containing 5 mM $\text{K}_3[\text{Fe}(\text{CN})_6]$ and 0.01 M KCl, at a scan rate of 10 mV s^{-1} . Gold electrodes, unmodified or from different stages in the preparation procedure, were used as working electrode. A saturated calomel electrode (SCE) was used as a reference and a platinum wire constituted the auxiliary electrode. The electrodes were coupled to a potentiostat (Bioanalytical system. Inc., West Lafayette, IN, USA) connected to a computer.

8.3.5 Optimization of the capacitive biosensor

The operating conditions for the capacitive biosensor and the flow injection analysis (FIA) system were optimized with regard to the affinity binding between plasmid DNA and the *lac* repressor protein. Parameters affecting the capacitive response were studied, i. e., pH and the concentration of regeneration solution, flow rate of carrier buffer solution and type, pH and concentration of carrier buffer solution. The parameters were optimized one by one through injections of supercoiled plasmid DNA.

8.4 Results and Discussion

8.4.1 Plasmid DNA quality

The quality of plasmid isolated in the eluting fraction of the column was tested by performing FPLC analysis. Gel electrophoresis was used to indicate the isolation of supercoiled form from other plasmid variants (Figure 8.2a). Agarose gel electrophoresis showed that the purified plasmid was the supercoiled form with a size of 2455 bp, the same size found by Hanora *et al.* (Hanora *et al.*, 2006). Gel electrophoresis was also used to indicate the band of the open circular plasmid DNA which changed from its supercoiled form by heating (Figure 8.2b, lane 3-6) and Figure 2c shows gel electrophoresis of the only band of the open circular (lane 2 and 4) which was separated from supercoiled plasmid DNA by using size-exclusion chromatography.

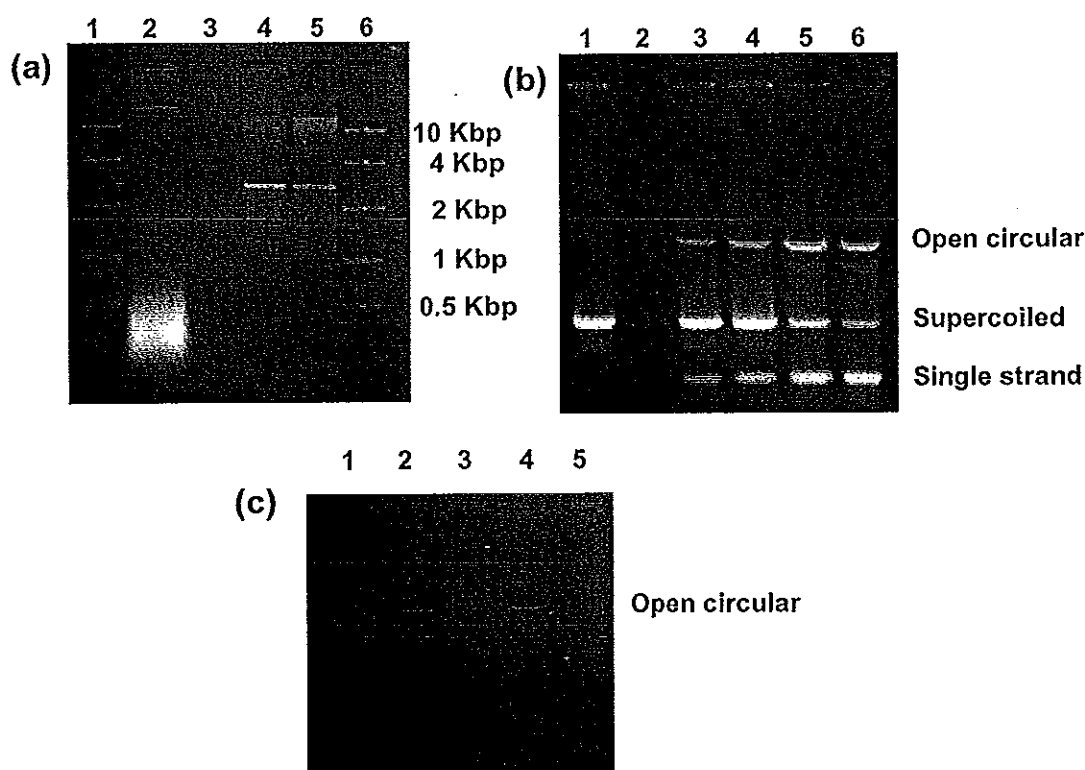


Figure 8.2 (a) Agarose gel electrophoresis of plasmid DNA from clarified lysate. Lane 1 and 6, supercoiled DNA ladder; lane 2, clarified lysate; lane 3, after size-exclusion chromatography; lane 4 and 5, after pre-concentration with isopropanol. (b) Agarose gel electrophoresis when the interchange between supercoiled plasmid DNA (sc pDNA) to open circular plasmid DNA (oc pDNA) was performed using a thermal transition. Lane 1, purified supercoiled plasmid DNA (before heating); lane 2, empty; lane 3-6, after heat 95 °C for 15 min and (c) showing the band of open circular form (lane 2 and 4) after purification by using size-exclusion chromatography.

8.4.2 Insulating property of working electrode

Capacitive measurements require a proper insulation of the electrode surface in order to prevent disturbing redox reactions at the applied potential. The degree of insulation obtained at different layers in the electrode preparation was studied with cyclic voltammetry by using the permeable redox couple $K_3[Fe(CN)_6]$ as

shown in Figure 8.3. The polished but otherwise unmodified electrode surface was first studied (Figure 8.3A), with the self-assembled layer of thioctic acid covering the electrode, the redox peaks were significantly reduced (Figure 8.3B). Immobilization of *lac* repressor protein on the electrode surface further increased the insulating property of the electrode (Figure 8.3C) whereas after blocking with 1-dodecanethiol, the redox peaks disappeared completely (Figure 8.3D).

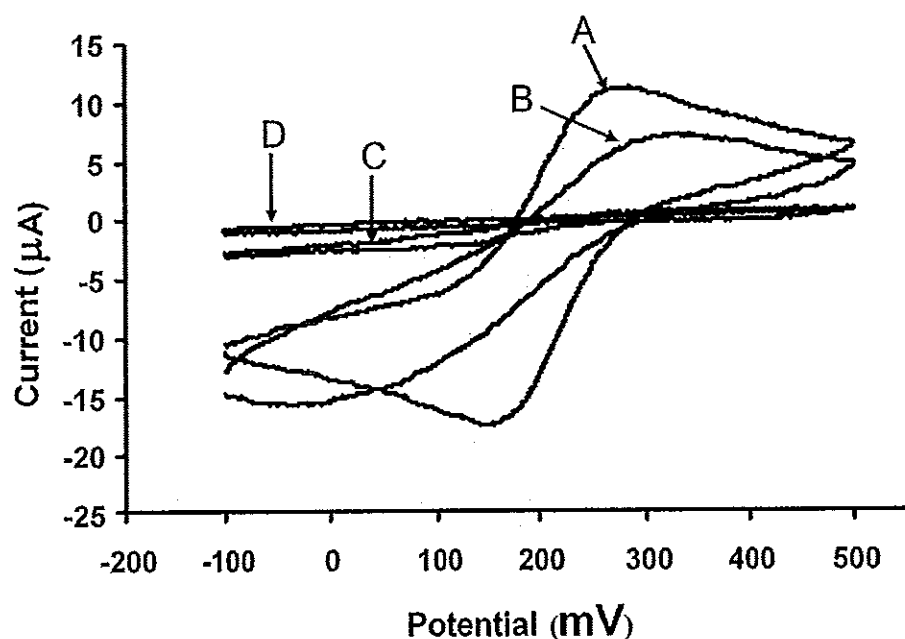


Figure 8.3. Cyclic voltammograms of a gold electrode obtained in 5 mM $K_3[Fe(CN)_6]$ containing 10 mM KCl solution at a scan rate of 10 mV s^{-1} . All potentials are given vs SCE. (A) clean gold, (B) thioctic acid covered gold, (C) *lac* repressor modified thioctic acid couple gold, and (D) as in (C) but after 1-dodecanethiol treatment.

8.4.3 Capacitance measurement

The measurement of capacitance of the binding event between immobilized *lac* repressor protein and plasmid DNA was done as described previously in chapter 7 section 7.4.2. However, in this system the capacitance values are evaluated directly in the program, plotted as a function of time (real time and shown on the monitor and stored in computer (Berggren *et al.*, 1999). Figure 8.4

shows the change in capacitance due to affinity binding between plasmid and *lac* repressor protein on the working electrode. When plasmid DNA was injected into the flow cell inbound to *lac* repressor immobilized on the electrode causing the thickness to increase and this would decrease the total capacitance (C_{tot}) as shown in Figure 8.4.

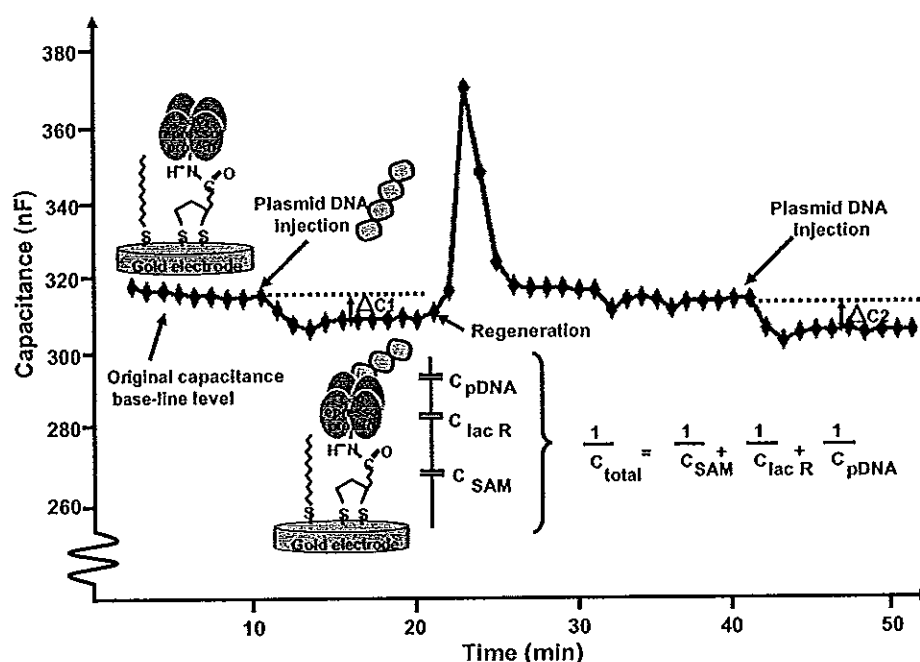


Figure 8.4 Schematic view of the capacitance (C) as a function of time resulting from the binding between *lac* repressor and pDNA with subsequent signal increase due to dissociation under regeneration conditions where C_{SAM} is the capacitance of the self-assembled thiol monolayer, $C_{lac R}$; the capacitance of *lac* repressor protein layer, C_{pDNA} ; the capacitance of plasmid DNA analyte interaction and C_{total} ; the total capacitance change measured at the working electrode/solution interface.

8.4.4 Optimization of the capacitive biosensor system

8.4.4.1 Regeneration solution

The vast majority of biosensor methods need regeneration of the sensor surface before the measurement can be repeated. The optimization of regeneration conditions is of general interest. The goal is to break the non-covalent binding

between plasmid DNA analyte and *lac* repressor immobilized on the gold surface, while maintaining the activity of the protein.

The performance of the regeneration solution was evaluated by the percentage of residual activity (% residual activity) as described in section 7.4.3.1. Two types of regeneration solutions were compared, glycine-HCl and citric-NaOH by injecting 250 μl of these regeneration solutions with a flow rate of 100 $\mu\text{l min}^{-1}$. As can be seen in Table 8.1 glycine-HCl gave a better percentage residual activity of more than 90 %. The pH (2.30 to 2.60) and concentration (10-100 mM) of glycine-HCl regeneration buffer were then optimized. At pH 2.40 residual activity of 98 % was achieved, whereas almost 97 % residual activity was gained at 50 mM glycine-HCl concentration. However, when comparing this result with that of 25 mM (94 % of residual activity) other effects needed to be taken in to consideration. At the lower concentration a much higher residual base line stability could be achieved. It can also help to avoid the deterioration of the insulating SAM layer which can be a result of high concentration effects (Jiang *et al.*, 2003). Therefore, in this work a concentration of 25 mM glycine-HCl was chosen in the continued experiments.

Table 8.1. Assayed and optimized values of the type, pH and concentration of regeneration solution with sample volume of 250 μl and 100 $\mu\text{l min}^{-1}$ of flow rate. The efficiency of plasmid DNA removal from the *lac* repressor immobilized on the electrode was studied by injecting 10 ng ml^{-1} of plasmid DNA standard.

Regeneration solution	Values	Percentage of average residual activity (n=3)
Type	50 mM Glycine buffer pH 2.40	92 \pm 3
	50 mM Citric-NaOH buffer pH 2.40	59 \pm 6
pH	50 mM Glycine buffer pH 2.30	77 \pm 5
	50 mM Glycine buffer pH 2.40	98 \pm 5
	50 mM Glycine buffer pH 2.50	95 \pm 4
	50 mM Glycine buffer pH 2.60	81 \pm 6
Concentration	10 mM Glycine buffer pH 2.40	84 \pm 5
	25 mM Glycine buffer pH 2.40	94 \pm 3
	50 mM Glycine buffer pH 2.40	97 \pm 6
	75 mM Glycine buffer pH 2.40	84 \pm 7
	100 mM Glycine buffer pH 2.40	55 \pm 9

8.4.4.2 Buffer solution

8.4.4.2.1 Type

It is necessary to minimize the ionic strength in the carrier and sample buffers to prevent a high background which will suppress the analyte signal. Initially, three widely used biochemical buffers were tested as carrier and sample buffers in the capacitive biosensor system, 10 mM of sodium phosphate buffer (SPB), potassium phosphate buffer (PPB) and Tris-HCl buffers pH 7.2. The experiment was performed by injecting standard of plasmid DNA from 1 to 1000 ng ml^{-1} . The results show that the highest sensitivity (slope of calibration) was obtained from Tris-HCl buffer (Figure 8.5) and gave the steadiest baseline, therefore, Tris-HCl was chosen for further study.

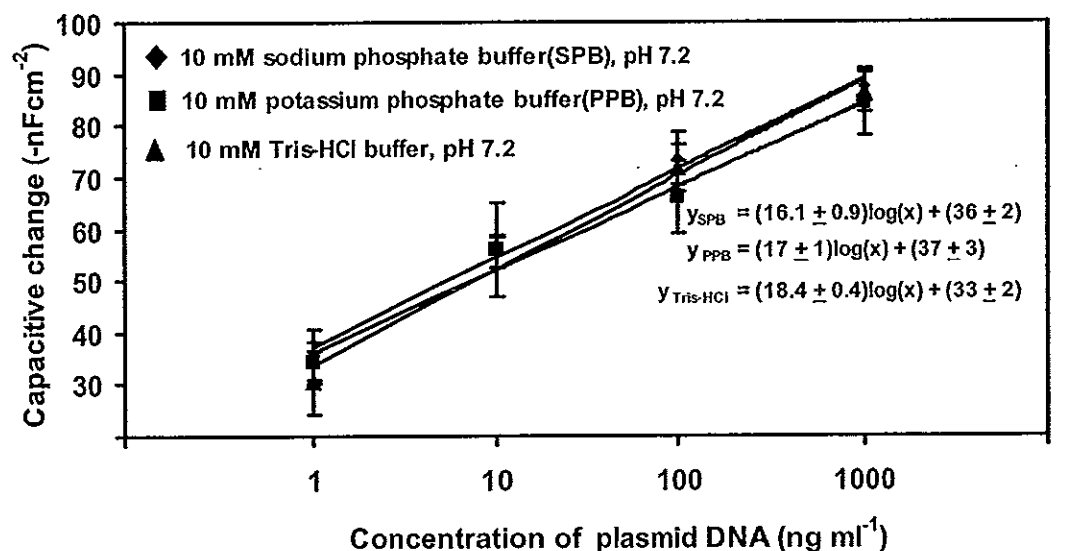


Figure 8.5 Response of the flow injection capacitive biosensor system from different buffer solution.

8.4.4.2.2 pH

The influence of pH of 10 mM Tris-HCl during the binding between *lac* repressor protein and plasmid DNA was further studied between 7.00 and 8.20 for the same concentration of plasmid DNA (10 ng ml⁻¹). Figure 8.6 shows that the maximal capaciance change was found at pH 7.40. The isoelectric point of *lac* repressor is 9.2-9.9 (Alexeyev and Winkler, 2002), this suggests that for the pH range investigated *lac* repressor has a net positive charge that can bind with the negatively charged DNA phosphate backbone (Bulter *et al.*, 1977) and at pH 7.4 the binding is maximal. Therefore, this pH was used in the continued experiments.

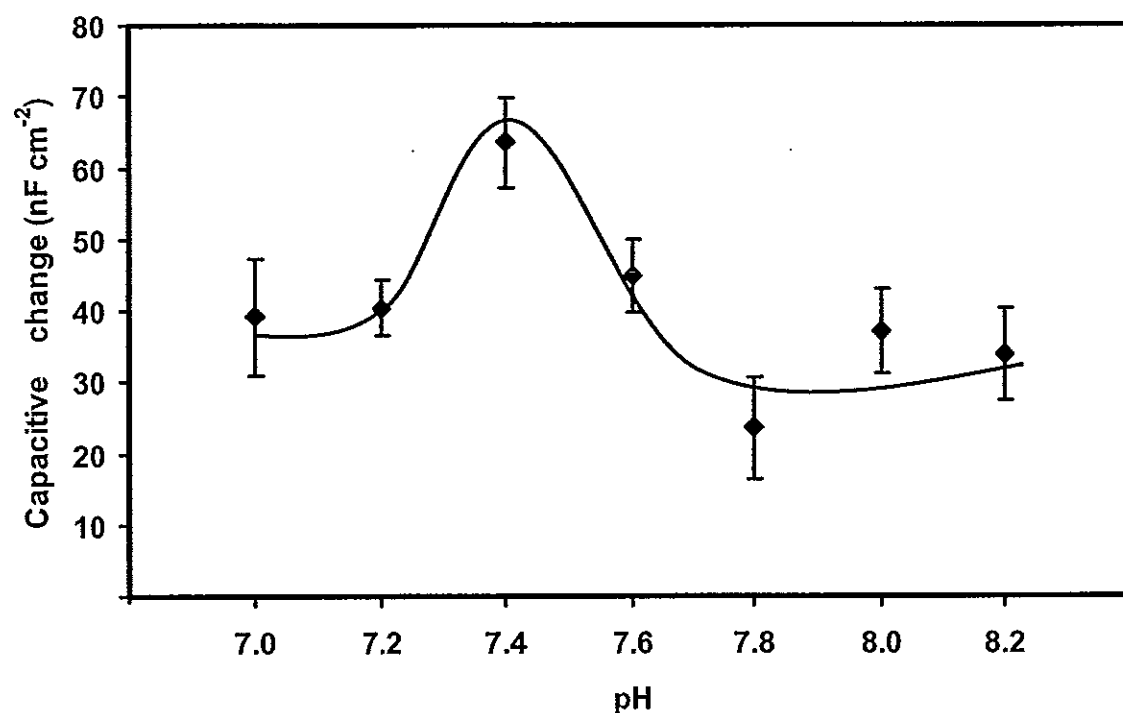


Figure 8.6 Effect of the pH of Tris-HCl buffer solution.

8.4.4.2.3 Concentration

The responses of injected 10 ng ml^{-1} of plasmid DNA to the *lac* repressor modified electrode were also tested with different concentrations of the tris-buffer between 10 and 100 mM. The result of the optimization of the concentration for Tris-HCl buffer pH 7.4 found that highest change in the capacitive signal was found to be at concentration 10 mM (Figure 8.7). At 100 mM base line is not stable and signal after injection of plasmid DNA can not be detected. This result might be explained that at the high concentration of Tris-HCl the ion in solution can penetrate into the insulating layer of the electrode, the layers on the electrode should be destroyed. Therefore, 10 mM of Tris-HCl buffer was chosen to use as the carrier and sample buffers.

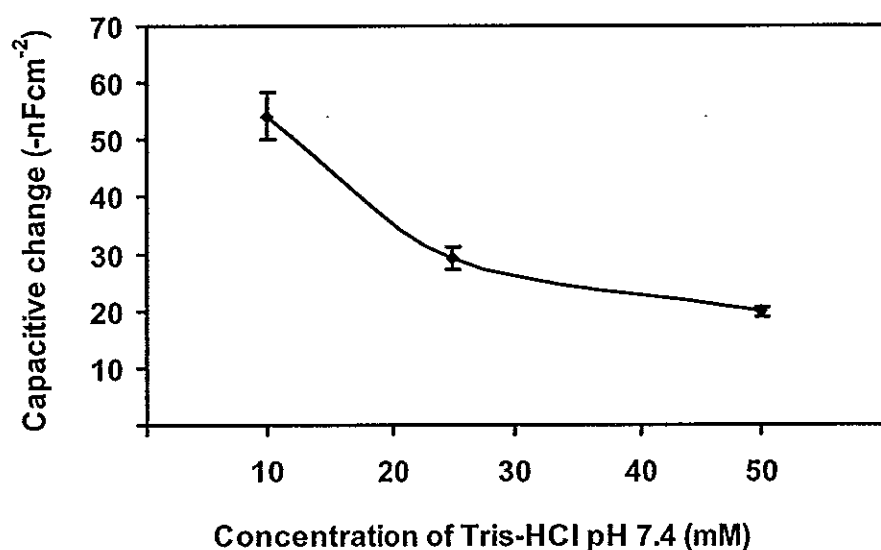


Figure 8.7 Response of the capacitive biosensor system to different concentration of Tris- HCl buffer at pH 7.4.

8.4.4.3 Flow rate

The flow rate of the solution through the capacitance flow cell is the main factor affecting the yield of interaction between analyte and immobilized biorecognition element on the transducer and hence the response of the system. The effect of the flow rate was investigated by injecting 250 μl of different concentrations of plasmid DNA solution increasing from 1 ng ml^{-1} up to 1000 ng ml^{-1} . The calibration curves obtained for the different flow rates, ranging from 100 to 500 $\mu\text{l min}^{-1}$ were evaluated. The capacitance changes and the sensitivities increased as the flow rate decreased due to the increasing time for the binding interaction. However, the analysis times also increased in a proportional fashion. Hence, a flow rate of 100 $\mu\text{l min}^{-1}$ (Figure 8.8) was chosen for further study, although its analysis time (9 min) was longer than at 250 $\mu\text{l min}^{-1}$ (6 min), its sensitivity was 44% higher.

The optimized condition for flow injection capacitive system of the binding between immobilized *lac* repressor protein and plasmid DNA are also summarized in Table 8.2

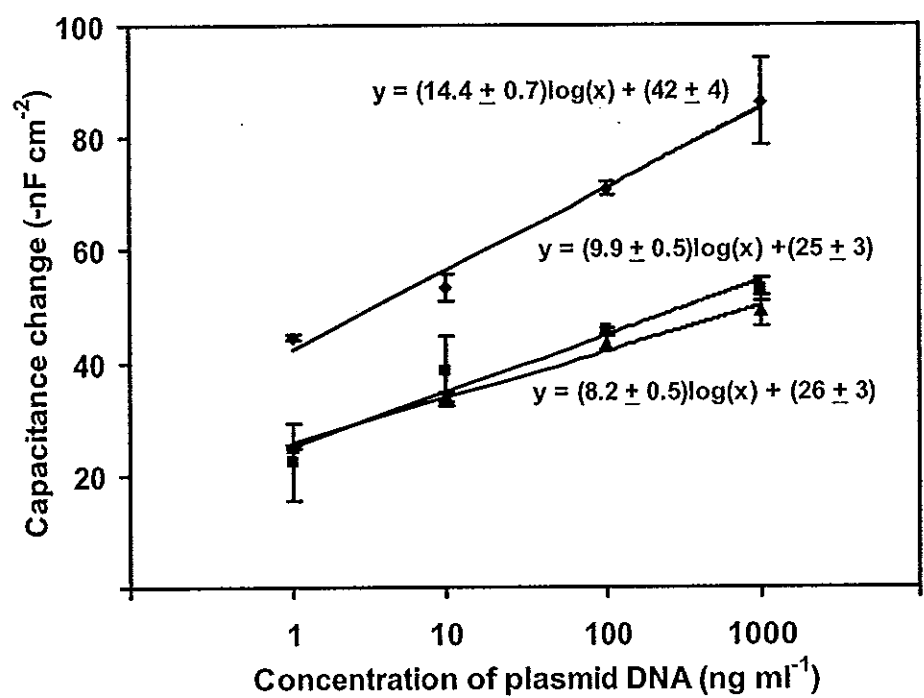


Figure 8.8 Response of the flow injection capacitive biosensor system at different flow rates.

Table 8. 2. Assayed and optimized values of parameters for plasmid DNA analysis by a capacitive biosensor system

Parameter	Investigated values	Sensitivity (-nF ml ng ⁻¹ cm ⁻²)	Capacitive change values (-nF cm ⁻²)	Analysis time (minute)	Optimum
Buffer type 10 mM, pH 7.2	PPB	7.5	-	9	Tris-HCl
	SPB	7.0	-	9	
	Tris-HCl	8.0	-	9	
pH of buffer 10 mM Tris HCl	pH 7.00	-	39 ± 8	9	7.4
	pH 7.20	-	40 ± 4	8	
	pH 7.40	-	64 ± 6	9	
	pH 7.60	-	44 ± 5	10	
	pH 7.80	-	23 ± 7	9	
	pH 8.00	-	37 ± 6	9	
	pH 8.20	-	34 ± 6	9	
Concentration of buffer Tris-HCl pH 7.4	10 mM	-	54 ± 4	9	10 mM
	25 mM	-	29 ± 2	11	
	50 mM	-	20 ± 1	12	
	100 mM	-	n.d	-	
Flow rate (μl min ⁻¹)	100	6.2	-	9	100
	250	4.3	-	6	
	500	3.5	-	4	

8.4.5 Reproducibility of the *lac* repressor electrode

After regeneration, to remove plasmid DNA analyte from the *lac* repressor immobilized on the electrode, plasmid DNA was detected repeatedly by the regenerated electrode. The reproducibility of the *lac* repressor modified electrode was evaluated by injecting the same concentration of plasmid DNA (10 ng ml^{-1}) for 40 times and measuring the capacitance change (ΔC). The average response was $45.9 \pm 1.8 \text{ nF cm}^{-2}$ (relative standard deviation, RSD=3.9%) (Figure 8.9). The results indicated that the *lac* repressor electrode can be reused with good reproducibility for at least up to 40 times.

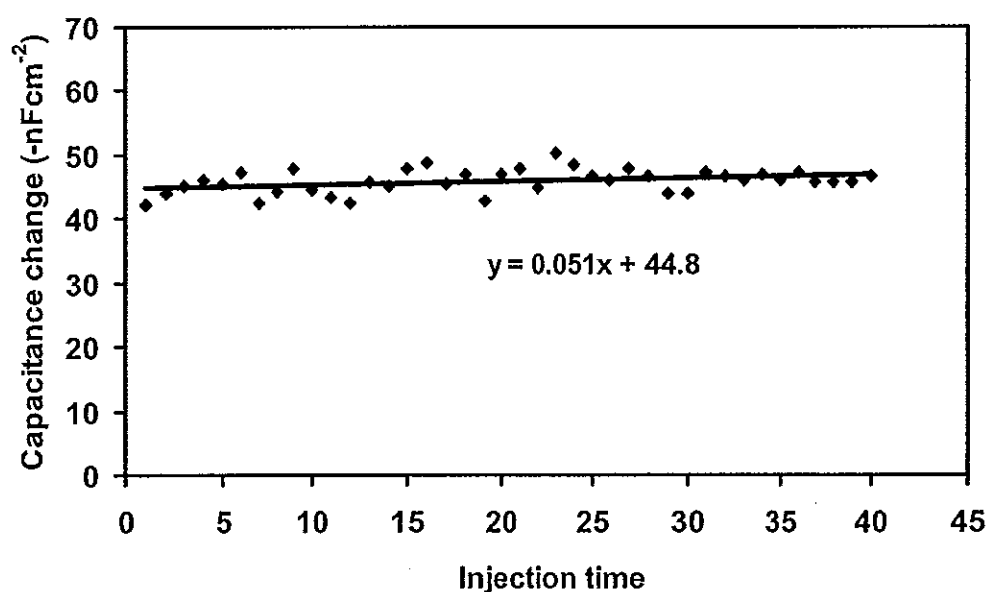


Figure 8.9 Reproducibility of the response from *lac* repressor modified electrode to injection of $250 \mu\text{l}$ standard plasmid DNA (10 ng ml^{-1}) with regeneration steps between each individual assay.

8.5 Response for plasmid DNA with different molecular forms

Under optimum conditions (Tables 8.1 and 8.2) the flow injection capacitive system of the influence of the isoforms of the plasmid DNA, supercoiled and open circular (relaxed form) plasmid DNA was studied. Two linear ranges with

different sensitivity were obtained for both forms, $0.0001\text{--}0.1\text{ ng ml}^{-1}$ and $1\text{--}1000\text{ ng ml}^{-1}$ (Figure 8.10). The detection limit (signal to noise ratio of 3:1, 3σ) (Miller and Miller, 2000) for open circular plasmid DNA was 0.002 pg ml^{-1} compared to 0.03 pg ml^{-1} of supercoiled plasmid DNA. From the results, the response or sensitivity obtained from both sc pDNA and oc pDNA are not so different which indicated that *lac* repressor capacitive biosensor can be applied to detect either supercoiled, open circular or the mixture of both forms in purified plasmid DNA with the same result. It is well - suited for DNA quantification, which gave detection limit lower than other techniques such as gel electrophoresis, spectrophotometry and capillary electrophoresis (Middaugh *et al.*, 1998; Noites *et al.*, 1999).

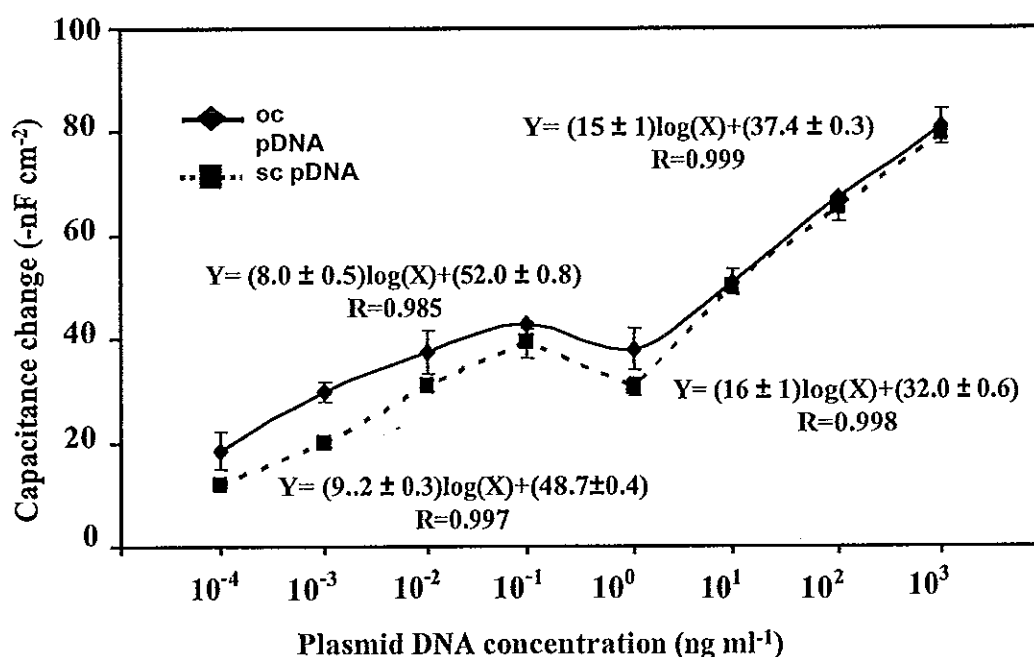


Figure 8.10 Calibration curve of supercoiled and open circular plasmid DNA at optimum conditions, showing two linear ranges with difference sensitivity from 0.0001 to 0.1 ng ml^{-1} and 1 to 1000 ng ml^{-1} .

8.6 Conclusions

This work, demonstrated the possibility of using the capacitive biosensor system to directly assay the interaction between plasmid DNA, containing *lac* operator and *lac* repressor protein on self-assembled thioctic acid monolayer modified electrode. It provides a lower detection limit of 0.03 pg. ml^{-1} for supercoiled plasmid and 0.002 pg ml^{-1} for open circular form. The system can be used for direct determination of purified plasmid DNA with contains only supercoiled, open circular form or both. A major advantage of this system over gel electrophoresis or spectrophotometric technique is the fact that plasmid DNA can be determined without using any dye staining such as ethidium bromide (Ebr) or other fluorescence stains that are a powerful carcinogen. In addition, analysis time of this technique was 9-11 min was much shorter than other DNA quantitation methods (30min-5h) (Projan *et al.*, 1983; Schmidt *et al.*, 1996). Using the appropriate regeneration solution, good reproducibility was obtained. The electrode can be reused up to more than 40 times and this helps to reduce the cost of analysis.

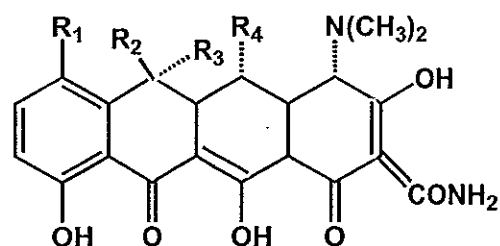
Chapter 9

Capacitive DNA Biosensor for Tetracyclines Detection

9.1 Introduction

The presence of pharmaceutical compounds (e. g. anti-inflammatories, lipid regulators, antibiotics etc.) in environmental samples including surface, ground and drinking water, that may have possible adverse effects on humans and ecological systems, has considerably increased (Santiago Valverdi *et al.*, 2006). After they have been administered, a considerable amount of some of these pharmaceuticals are excreted unmetabolized and can persist in the environment. Because these compounds are only partially eliminated in waste water treatment plants, they can be found in their effluents (Golet *et al.*, 2001; Stumpf *et al.*, 1999; Ternes *et al.*, 2001) and can, therefore, reach the water (Hirsch *et al.*, 1998; Stumpf *et al.*, 1999; Winkler *et al.*, 2001).

Tetracyclines (TCs) constitute a group of antibiotics, their basic structure consists of a tetracyclic backbone containing four fused rings (Figure 9.1) (Yang *et al.*, 2005; Zhu *et al.*, 2001). They are extensively used in human and veterinary medicine to treat and prevent bacterial infection (Kim *et al.*, 2005; Santiago Valverdi *et al.*, 2007; 2006; Yang *et al.*, 2005). These compounds have been widely used for both prevention and treatment of disease and as feed additives to promote growth in animals (Lindsey *et al.*, 2001; Nozal *et al.*, 2004; Reverté *et al.*, 2003; Zhu *et al.*, 2001). They have also found application in preserving harvested fruit and vegetables, exterminating insect pest (Hernández *et al.*, 2003). Their widespread use has raised the suspicion that it might be excreted or leak into ground and surface water.



Compound	R ₁	R ₂	R ₃	R ₄
Tetracycline	H	OH	CH ₃	H
Chlortetracycline	Cl	OH	CH ₃	H
Oxytetracycline	H	OH	CH ₃	OH
Doxycycline	H	H	CH ₃	OH
Demeclocycline	Cl	OH	H	H

Figure 9.1 Structure of tetracycline and its derivatives (Modified from Santiago Valverde *et al.*, 2007).

Recently, concerns have been raised regarding public health issues over the occurrence of antibiotics in the environment (Halling-Sørensen *et al.*, 1998), as well as by indications of increased bacterial resistance in waste influence from hospitals and pharmaceutical plants (Goni-Urriza *et al.*, 2000; Guardabasi *et al.*, 1998). The occurrence and fate of tetracycline antibiotic in wastewater and the possible contamination of ground water is largely unknown (Guardabasi *et al.*, 1998; Halling-Sørensen *et al.*, 1998). There is thus a need for a sensitive and rapid analytical method for quantifying tetracyclines in waste, ground and surface water.

Liquid chromatography (LC) with different detectors such as fluorescence (Croubels *et al.*, 1997; Santiago Valverde *et al.*, 2006; Wan *et al.*, 2005), UV (Anderson *et al.*, 2005; Cooper *et al.*, 1998), diode array (Ding and Mou, 2000) and mass spectrometry (Carson *et al.*, 1998; Cherlet *et al.*, 2003; Yang *et al.*, 2005, Zhu *et al.*, 2001) is the most widely use technique for determination of tetracyclines (TCs) residuals. However, the large amount of volatile organic solvents used in LC

mobile phase are still undesirable for most analyses. Column contamination is an additional disadvantage of LC system (Nazal *et al.*, 2004). In recent years, capillary electrophoresis (CE) has gained increasing interest as a powerful tool by virtue of its high efficiency and resolution, short analysis time and its low sample and solvent consumption relative to LC. However, CE are not applied to determine TCs residues, mainly due to the lack of sufficient sensitivity for practical applications and the interference suffered from complex matrices (Oka *et al.*, 2000). In addition, as pharmaceuticals appear at low concentrations in environmental, enrichment steps are needed before applying LC or CE technique. The techniques have been commonly used for preconcentration including liquid-liquid extraction (LLE) (Haller *et al.*, 2002), solid-phase extraction (SPE) (Golet *et al.*, 2001; Kamel *et al.*, 1999; Ternes *et al.*, 2001) and solid-phase microextraction (SPME) (Moeder *et al.*, 2000). All of these techniques are usually accomplished by time consuming extraction steps. Cleaning procedures often use toxic organic solvent, which are not environmentally friendly. Therefore, an alternative method with fewer steps and lesser impact to the environment is required and affinity biosensors have shown great promise for the task of environmental monitoring and control (Wang *et al.*, 1997).

In recent decades nucleic acid have been increasingly used as a tool in the recognition and monitoring of many compounds of interest. Nucleic acid layers combined with transducers produce a new kind of affinity biosensor for rapid screening of small molecular weight molecules including target toxic pollutants such as polychlorinated biphenyls (PCBs), polycyclic aromatic hydrocarbon, aflatoxin, and aromatic amines, herbicides (Chiti *et al.*, 2001; Marazza *et al.*, 1999; Oliveira-Brett *et al.*, 2002) or drug, i.e. antibiotic (Erdem, 2002; Nawaz *et al.*, 2006; Oliveira-Brett *et al.*, 2002; Ozsoz and Piedae *et al.*, 2002). As described in chapter 2 (section 2.3.3.2) these molecules can interact with the DNA double helical structure in many ways, including electrostatic interaction with the negatively charged nucleic sugar-phosphate structure, intercalation between adjacent base pairs and minor and major DNA grooves binding of the side groups of the molecules via hydrogen bonds, electrostatic interactions, or van der Waals contacts, with edges of base pairs or sugar-phosphate backbone (Erdem and Ozsoz, 2002; Gherghi, *et al.*, 2004; Rauf *et al.*, 2005). Consequences of these binding interaction involve the conformation

changes to both the DNA and analyte molecules to accommodate formation (Erdem and Ozsoz, 2002).

It has been reported that tetracycline and its derivatives can act both as surface binder and intercalator with DNA, involving the electrostatic and hydrophobic binding force (Khan and Musarrat, 2000). To detect tetracycline, it may be possible to apply this principle of interaction by using double strand DNA as recognition element. It should be noted that these affinity biosensors for tetracycline detection is not specific. However its high level of sensitivity together with a rapid analysis time (Chitti *et al.*, 2001) would be an advantageous if it is used to precede the currently used chromatographic methods. When tetracyclines are detected by a biosensor technique the result should then be confirmed with standard method, and to our knowledge no one has applied this principle of affinity binding to detect tetracyclines (TCs).

In this work we describe a flow-injection capacitive biosensor to be used as a rapid screening step for the determination of tetracyclines (TCs) in water by immobilizing double-stranded DNA on gold electrode surface via SAM of thioctic acid. The technique was tested using tetracycline (TC, parent molecule) and its derivative *i.e.*, chlortetracycline (CTC) and oxytetracycline (OTC). This system was also validated with real samples by using it to determine residue tetracyclines in wastewater treatment ponds of a hospital and compared to the results obtained from HPLC-UV.

9.2 Materials

Double-stranded calf thymus DNA (dsDNA), *N*-3-(dimethylaminopropyl)-*N'*-ethylcarbodiimide hydrochloride (EDC), *N*-hydroxysuccinimide (*N*-Hydroxy-2,5-pyrroindione, NHS) were purchased from Sigma-Aldrich (Steinheim, Germany). Oxytetracycline hydrochloride, tetracycline hydrochloride and chlortetracycline hydrochloride were purchased from Sigma (USA). Thioctic acid and 1-dodecanethiol were obtained from Aldrich (Milwaukee, USA). All other chemicals were of analytical grade. Solutions and buffers used in the capacitive biosensor system were prepared with deionized water. Before use, buffers were filtered through an Albet[®] nylon membrane filter with pore size 0.20 μm with subsequent degassing.

9.3 Methods

9.3.1 Immobilization of double-stranded DNA (dsDNA)

The condition used for immobilization of dsDNA to gold surface modified with self-assembled monolayer of thioctic followed the process as described in chapter 7. The thioctic acid on the electrode was activated in EDC:NHS solution (EDC 1% (v/v), NHS 2.5 % (v/v) in 0.05 M phosphate buffer pH 5.00 with 0.05 M KCl for 5 h. After washing with 50 mM phosphate buffer (pH 7.20), 20 μ l of 50 μ g ml^{-1} ds DNA was placed on the electrode and the reaction took place at 4 °C for 24 h. Finally, the electrode was washed with phosphate buffer and immersed for 20 minutes in 10 mM of 1-dodecanethiol in ethanol to block any pinhole on the gold electrode surface. As described by Huang *et al.* (Huang *et al.*, 2000), DNA molecules are attached on the carboxylate-terminated alkanethiol self-assembled monolayers (SAMs) on the gold surface via the N-hydroxysuccinimide (NHS)/ N-3-(dimethylaminopropyl)-N'-ethylcarbodiimide hydrochloride (EDC) cross-linking reaction. The DNA attachment is attributed to the formation of amide bond between the carboxylate groups and the amino groups on DNA bases. The reaction mechanism for DNA immobilized on self-assembled thioctic monolayer is shown in Figure 9.2.

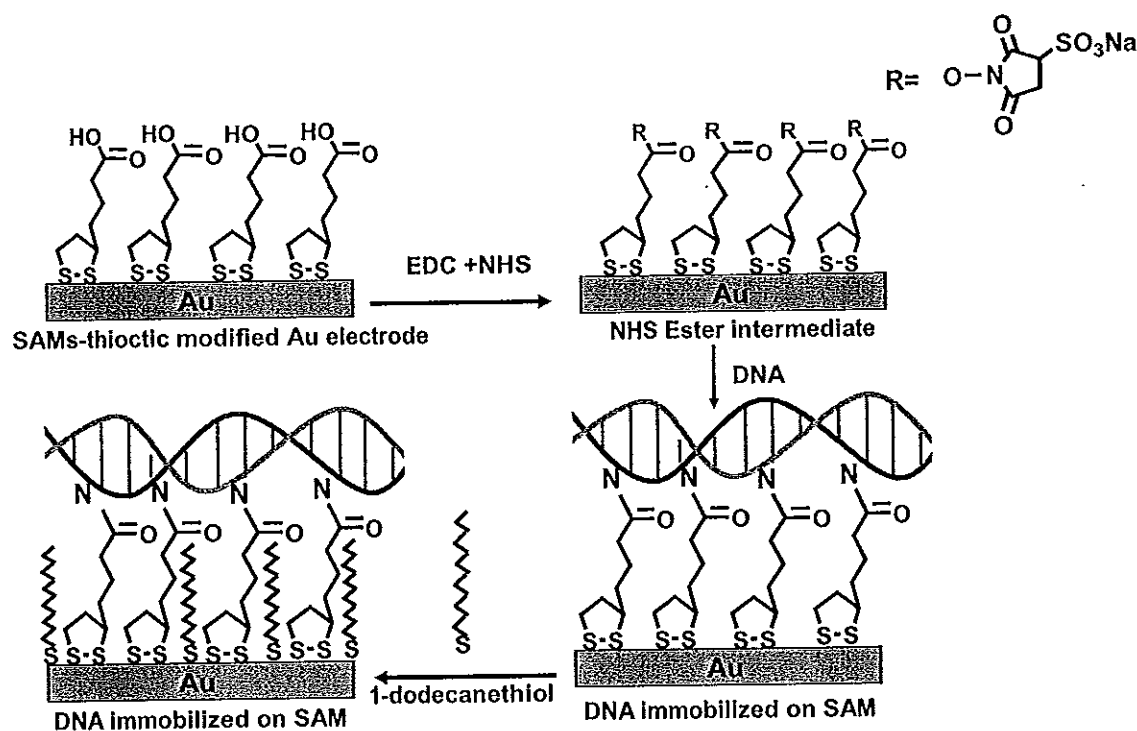


Figure 9.2 Schematic reaction mechanism for dsDNA immobilized on a self-assembled thioctic monolayer (Modified from Huang *et al.*, 2000; Limbut *et al.*, 2006a).

During the immobilization steps, the degree of insulation at different layers on the electrode surface is demonstrated by cyclic voltammetry measurements performed in a three electrode electrochemical batch cell containing 5 mM $\text{K}_3[\text{Fe}(\text{CN})_6]$ and 0.1 M KCl, at a scan rate of 0.1 V s^{-1} . Gold electrodes, from the preparation procedure, were used as working electrodes. Ag/AgCl was used as a reference electrode and a platinum rod was the auxiliary electrode. The electrodes were coupled to a potentiostat (ML 160, AD Instruments, Australia) connected to a computer.

9.3.2 Capacitance measurements

The experiment set-up of the flow-injection based capacitive affinity biosensor system is as described in section 7.3.2 (Figure 7.2). When the tetracyclines was injected into the flow cell it bound to DNA causing the total capacitance (C_{tot}) at the working electrode/solution interface to change. The affinity binding between

tetracycline and the immobilized dsDNA on the working electrode will result in an increase of the thickness of the layer and this would cause C_{tot} to decrease (Figure 9.3). The measurement of C_{tot} was done every minute and the results were later plotted as a function of time. Figure 9.4 shows an example of the capacitance changes (ΔC_1 , ΔC_2) due to the binding of tetracycline and dsDNA.

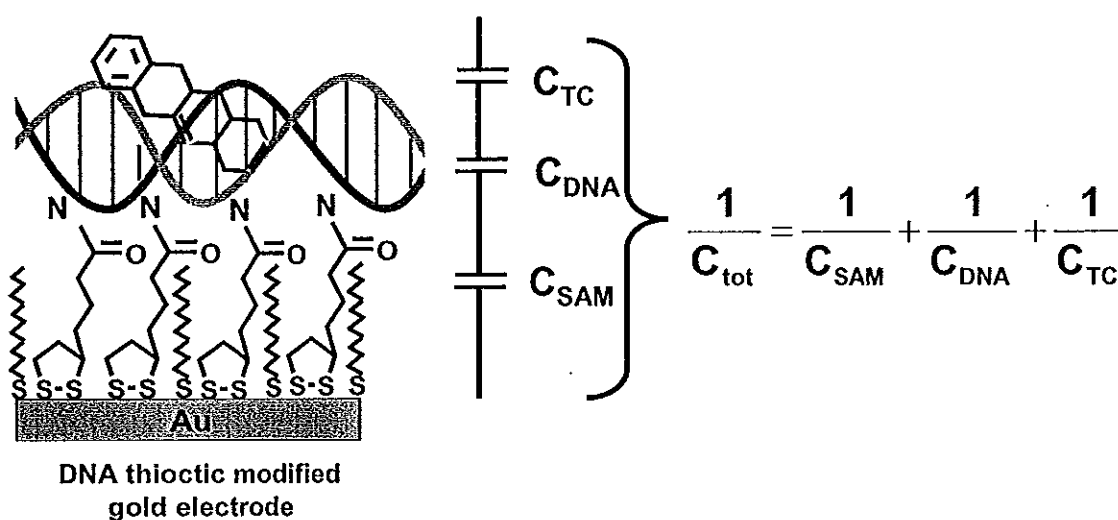


Figure 9.3 Schematic representation of the different layers on the electrode surface. The total capacitance measured at the working electrode/solution interface (C_{tot}) comes from C_{SAM} ; the capacitance of self-assembled thioctic acid monolayer, C_{DNA} ; the capacitance of DNA layer and C_{TC} ; the capacitance of tetracyclines analyte interaction.

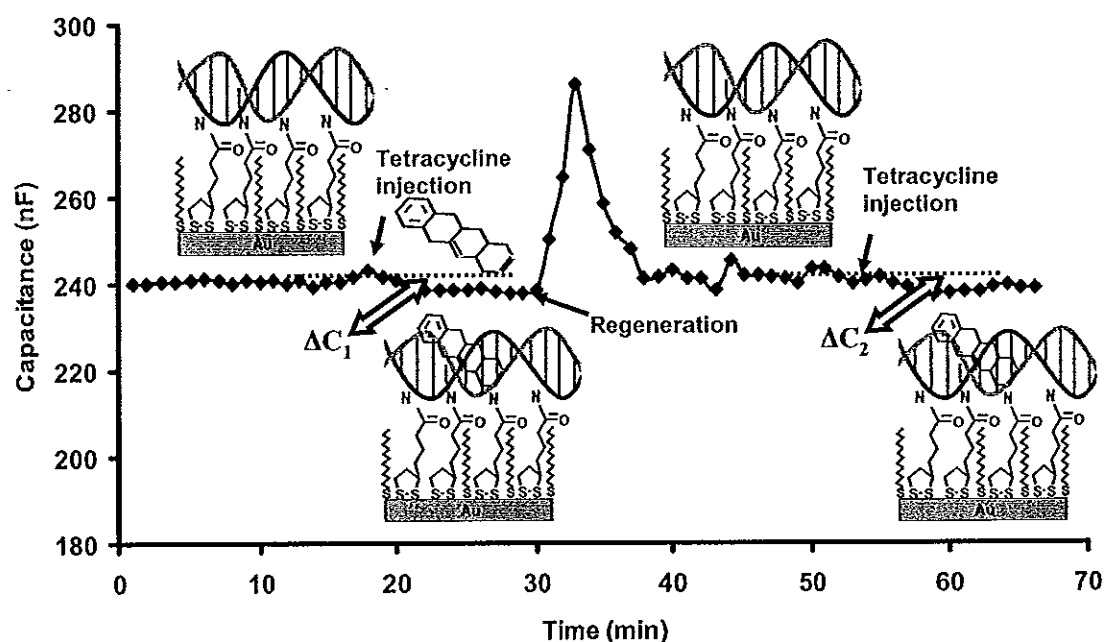


Figure 9.4 An example of the capacitance (C_{Tot}) plots as a function of time. The binding between tetracycline and DNA cause the capacitance to decrease (ΔC_1) with subsequent signal increase due to dissociation under regeneration conditions. After regeneration of the system can be reused to detect a new injection of tetracycline (ΔC_2).

9.3.3 Optimization of the flow injection capacitive biosensor

The operating conditions for the capacitive biosensor and the flow injection analysis (FIA) system were optimized. Parameters affecting the capacitive response were studied including type, pH, concentration of regeneration solution, type, pH, concentration of carrier buffer solution, flow rate of carrier buffer solution and sample volume. The parameters were optimized one by one through injections of parent compound of tetracycline (TC).

9.3.4 Determination of the amount of tetracyclines in real sample

Wastewater samples were collected from wastewater treatment pond of Songklanakrind Hospital, Prince of Songkla University. The samples were collected twice times from two sampling sites, *i.e.*, prior to the treatment ponds and after the treatment ponds. Before testing, wastewater samples were filtered through a 0.22 μm nylon membrane to eliminate suspended matter. To test the capacitance biosensor, matrix effect, recovery and tetracyclines in wastewater were analyzed under optimum conditions.

For comparison, the samples were also tested by an HPLC with UV detector (Water, USA) at the wavelength 385 nm with ultra C18 5 μm 250 mm.x 4.6mm I.D. (REstek, USA) column. The HPLC conditions were 0.8 ml min⁻¹ of mobile phase (0.1 M oxalic acid-methanol-acetonitrile (65:15:20 v/v/v) and 20 μl sample volume (Vongsavatsot, 2008)

9.4 Results and Discussion

9.4.1 Electrochemical performance of the immobilization process

The degree of insulating was examined using cyclic voltammetry with a permeable redox couple of as shown in Figure 9.5. The redox peaks decreased steadily after each step of immobilization and after the last step, because the electrode became totally insulated.

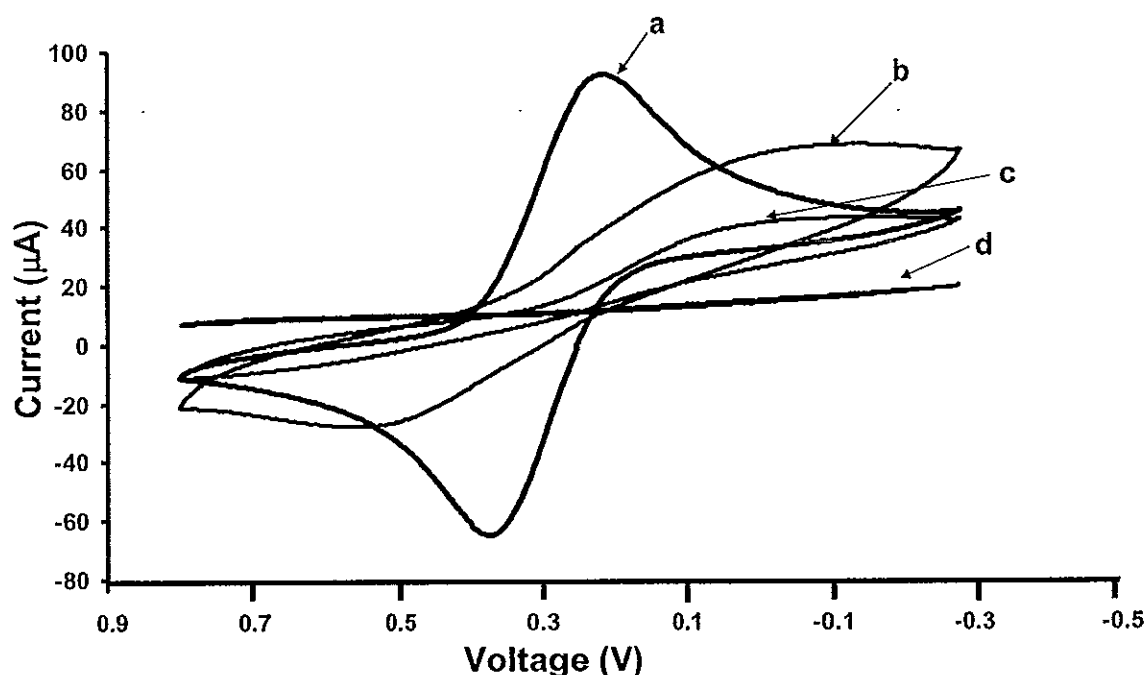


Figure 9.5 Cyclic voltammograms of a gold electrode obtained in 5 mM $K_3[Fe(CN)_6]$ containing 0.1 M KCl solution at scan rate of 0.1 V s^{-1} . All potentials are given vs Ag/AgCl. (A) clean gold, (B) thiocetic acid covered gold, (C) dsDNA modified thiocetic acid couple gold, and (D) as in (C) but after 1-dodecanethiol treatment.

9.4.2 Optimization of flow injection capacitive biosensor

9.4.2.1 Regeneration solution

Since the interaction between tetracycline and the immobilized dsDNA via electrostatic and hydrophobic binding force (Khan et al., 2003), tetracycline can be removed from DNA by using regeneration solution. Four different types of regenerating agent were compared, *i.e.*, glycine-HCl, HCl, NaOH and KCl. The performance of these regeneration solution was evaluated by the percentage of residual activity (% residual activity), as described in chapter 7 (section 7.4.3.1), from capacitive change given by consecutive binding between 100 ng l^{-1} tetracycline (with sample volume $250 \text{ } \mu\text{l}$) and dsDNA before (ΔC_1) and after regeneration (ΔC_2) (Figure 9.4) by injecting $250 \text{ } \mu\text{l}$ of these regeneration solutions with a flow rate $100 \text{ } \mu\text{l min}^{-1}$. As can be seen in Table 9.1, 25 NaOH gave the better percentage residual activity of more than 90%, therefore, NaOH was further optimized to see the influence of the

concentration. The best of residual activity (91%) was achieved at 25 mM. Therefore, 25 mM NaOH was chosen in the continued experiments.

Table 9.1. Assayed and optimized conditions of the type, and concentration of regeneration solution. The efficiency of tetracycline removal from the dsDNA immobilized on the electrode was studied by injecting 100 ng l⁻¹ of standard tetracycline solution.

Parameter of regeneration solution	Investigation condition	Efficiency of DNA removal (%average residual activity)	Regeneration time (min)
Type	25 mM glycine-HCl, pH 2.5	78 ± 2	13-16
	HCl pH 2.5	79 ± 4	12-14
	25 mM NaOH	92 ± 1	14-17
	25 mM KCl	58 ± 2	35-40
Concentration of NaOH	10 mM	71 ± 8	12-14
	20 mM	86 ± 6	13-14
	25 mM	91 ± 3	14-17
	30 mM	85 ± 2	14-18
	40 mM	74 ± 1	15-19
	50 mM	58 ± 3	15-21

9.4.2.2 Buffer solution

9.4.2.2.1 Type

The influence of the type of buffer used in the flow injection capacitive biosensor system was investigated. Initially, three widely used biochemistry buffer were tested as carrier and sample buffers 10 mM of Tris-HCl buffer, sodium phosphate buffer (SPB) and potassium phosphate buffer (PPB) pH 7.2. The experiment was performed by injecting standard tetracycline (TC) between 1 ng l^{-1} to 1000 ng l^{-1} . There is no difference in sensitivity (slope of calibration curve) between Tris-HCl, sodium phosphate and potassium phosphate (Figure 9.6). However, when comparing the signals at the same concentration of tetracycline, Tris-HCl gave the higher response and more steady baseline. Therefore, Tris-HCl was chosen to use for further experiment.

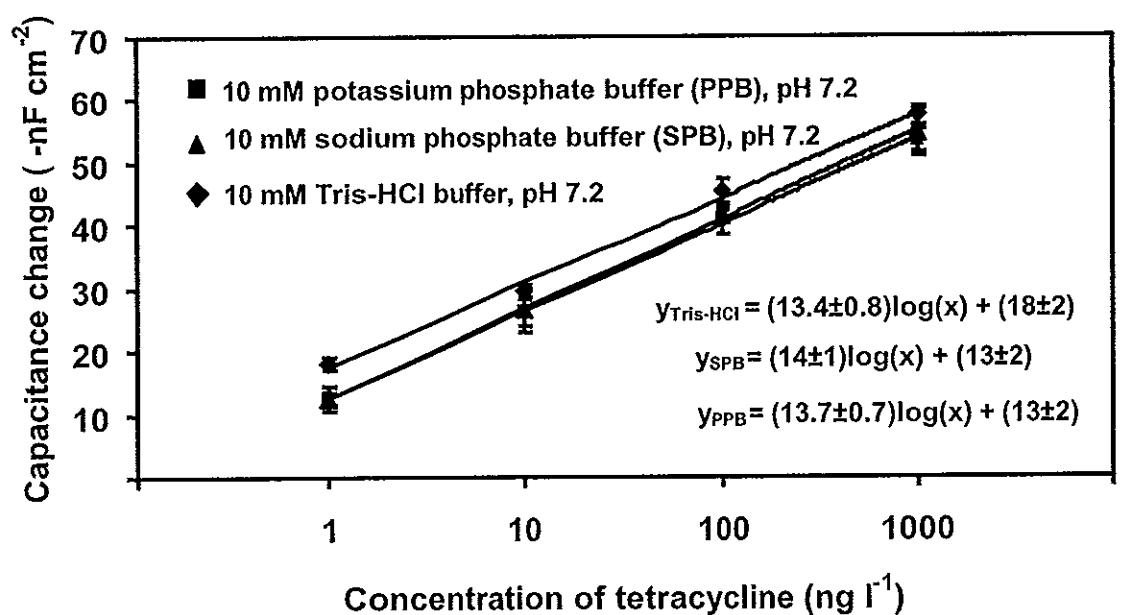


Figure 9.6 Response of the flow injection capacitive biosensor system from different buffer solutions.

9.4.2.2.2 pH

The influence of pH between 7.00-7.80 of 10 mM Tris-HCl during the binding reaction between tetracycline and DNA was studied for the same concentration of tetracycline (100 ng l^{-1}). Figure 9.7 shows that the maximal capacitance change was found at pH 7.2. Since the binding involves the intercalation of tetracyclines between two adjacent bases of DNA (Khan and Musarrat, 2000) and normally the DNA intercalation, which is hydrophobic, prefers the intercalating between molecules with zero charge and it is found that at pH below 7.6, tetracycline shows no net charge (Andersen *et al.*, 2005). Therefore, it is easier for tetracycline to intercalate into the DNA double helix at pH below 7.6, and 7.2 is found to be maximal.

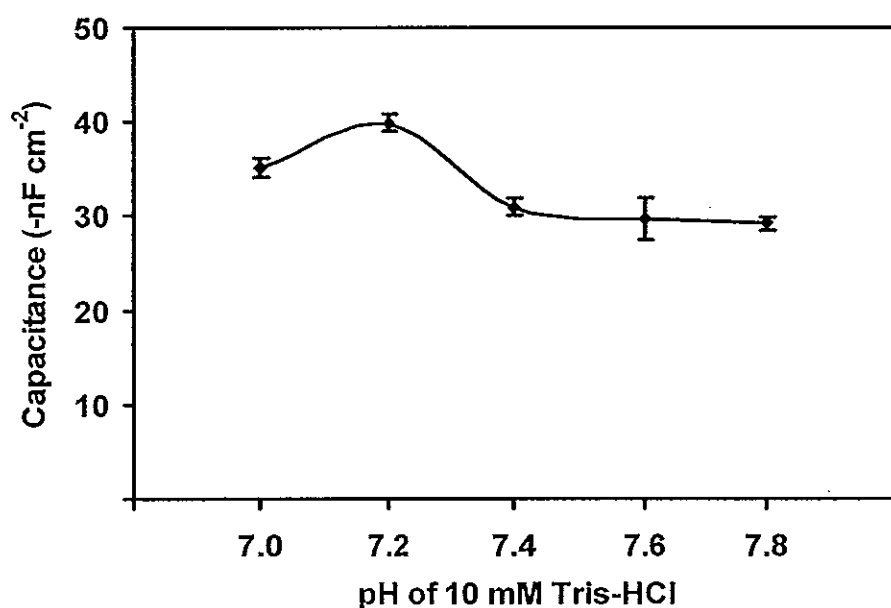


Figure 9.7 Effect of the pH of Tris-HCl buffer solution on response to 100 ng l^{-1} tetracycline

9.4.2.2.3 Concentration

The responses of dsDNA modified electrode to 100 ng l^{-1} of tetracycline were then tested with different concentrations of Tris-HCl buffer pH 7.2 between 5 and 40 mM. The highest change in the capacitive signal was found to be at 10 mM so this concentration was selected for further experiments.

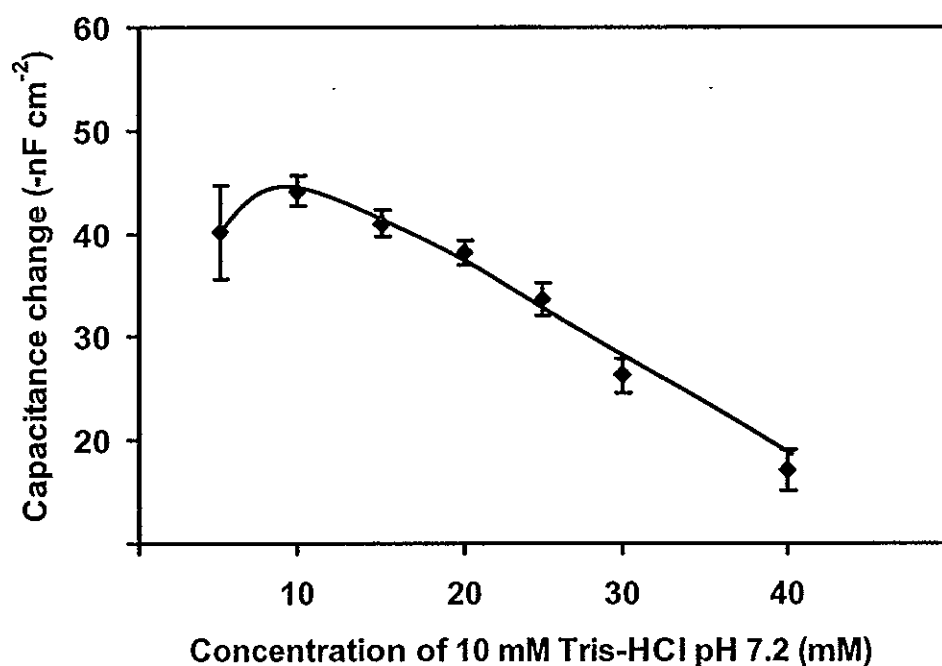


Figure 9.8 Response of the capacitive biosensor system to 100 ng l^{-1} at different concentrations of Tris-HCl buffer pH 7.2

9.4.2.3 Flow rate

In a flow injection capacitive biosensor system, the flow rate of buffer passing through the capacitive flow cell is the main factor affecting the yield of interaction between tetracycline and immobilized dsDNA on the electrode surface. So optimization of the flow rate is necessary. The experiment was investigated by injecting $250 \mu\text{l}$ of 100 ng l^{-1} of tetracycline solution at different flow rates ($25\text{--}200 \mu\text{l min}^{-1}$). The capacitance change decreased as the flow rate increased due to the reduction of binding interaction time. However, the analysis time also increased in a proportional fashion. The flow rate of $25 \mu\text{l min}^{-1}$ gave the highest response (Figure 9.9), however, nearly the same response was also obtained at $50 \mu\text{l min}^{-1}$ but the analysis time was shorter so, $50 \mu\text{l min}^{-1}$ was chosen.

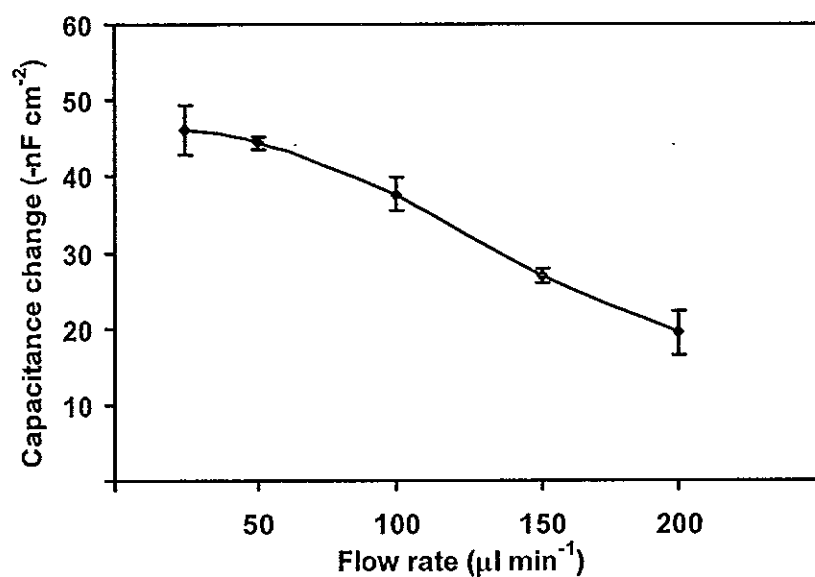


Figure 9.9 Response of the flow injection capacitive biosensor at different flow rate

9.4.2.4 Sample volume

The effect of sample volume was investigated by injecting 50-400 μl of 100 ng l^{-1} . The change in capacitance signal increased with volume until 250 μl (Figure 9.10) after which the capacitance change reached a maximum plateau. So 250 μl was chosen because it has the lower analysis time than 300 and 400 μl .

The optimum conditions of the flow injection system are summarized in Table 9.2

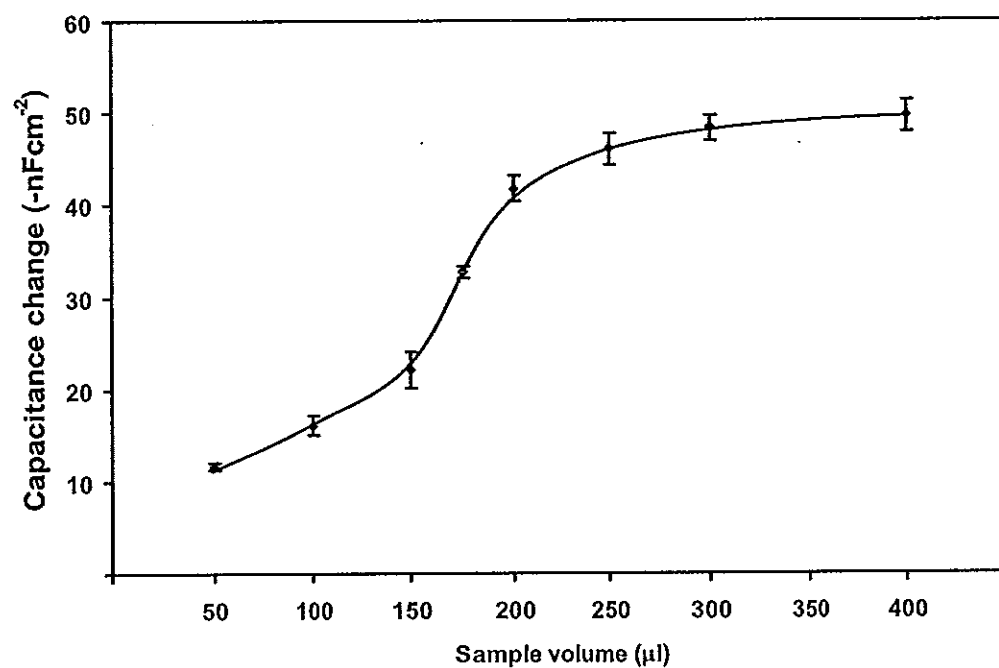


Figure 9.10 Response of the flow injection capacitive biosensor at different sample volume

Table 9.2. Assayed parameters and optimized values of the capacitive system.
Capacitive change is from the injection of 100 ng l⁻¹ of tetracycline.

Parameter	Investigated values	Capacitive change (-nF cm ⁻²)	Analysis time (minute)	Optimum
pH of 10 mM Tris-HCl	7.00	35 ± 1	15	7.2
	7.20	40 ± 1	15	
	7.40	31 ± 2	15	
	7.60	30 ± 2	15	
	7.80	29 ± 1	15	
Concentration of Tris- HCl buffer pH 7.2 (mM)	5	40 ± 1	11	10
	10	44 ± 2	12	
	15	41 ± 1	12	
	20	38 ± 1	14	
	25	34 ± 2	15	
	30	26 ± 2	16	
	40	17 ± 2	16	
Flow rate (μl min ⁻¹)	25	44 ± 3	18	50
	50	44 ± 1	16	
	100	38 ± 2	15	
	150	27 ± 1	13	
	200	19 ± 3	11	
Sample volume (μl)	50	12 ± 1	10	250
	100	16 ± 1	12	
	150	22 ± 2	12	
	175	33 ± 1	13	
	200	42 ± 2	14	
	250	46 ± 2	15	
	300	48 ± 1	17	
	400	50 ± 1	18	

9.4.3 Reproducibility

The reproducibility of dsDNA modified electrode was evaluated by monitoring the capacitance change ($-nF\text{ cm}^{-2}$) at the same concentration of standard tetracycline (100 ng l^{-1}). After each analysis, $250\text{ }\mu\text{l}$ of 25 mM NaOH was injected to break the binding between tetracycline and dsDNA. The percentage of residual activity of dsDNA modified electrode versus the number of injections is shown in Figure 9.11. The result showed that dsDNA immobilized electrode provided $96 \pm 4\%$ of its original response during 54 injections. The residual activity decreased rapidly after this point. The reduction of the activity may be caused either by the loss of DNA activity or loss SAM layer after prolonged use. The latter hypothesis was tested by using voltammetry. The voltammogram electrode after 63 analysis cycles showed no redox peaks (Figure 9.12). These indicated that the SAM layer was still intact on the electrode. Therefore, the decrease of residual activity was likely due to the loss of DNA and/or its binding activity.

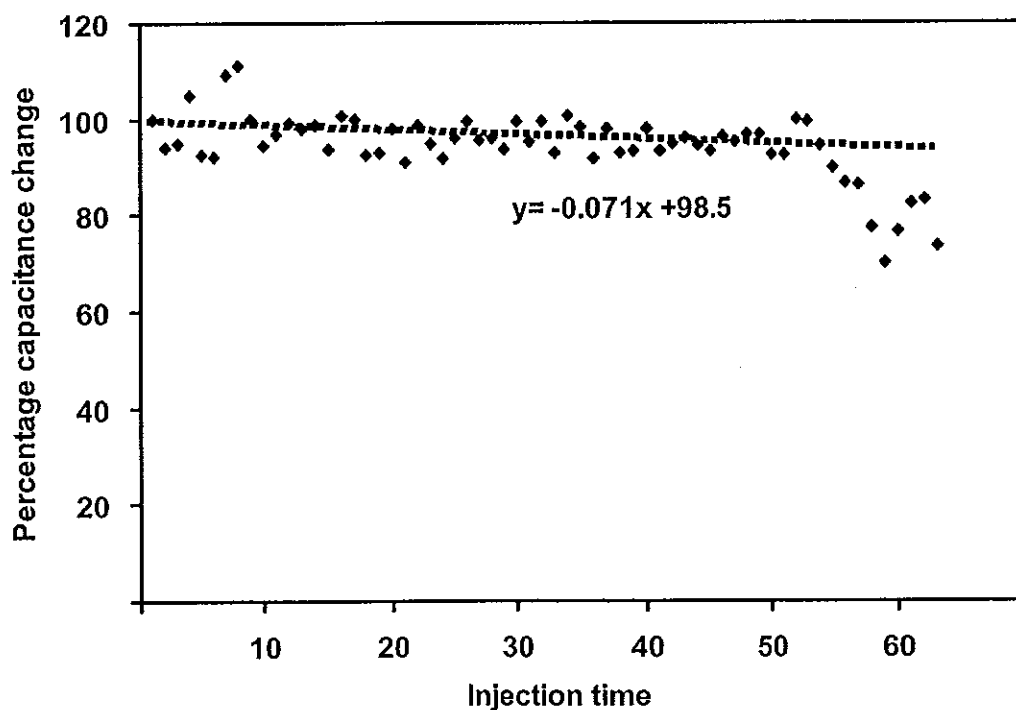


Figure 9.11 Reproducibility of the response from dsDNA modified electrode to injection of $250\text{ }\mu\text{l}$ standard tetracycline (100 ng l^{-1}) with regeneration steps between each individual assay

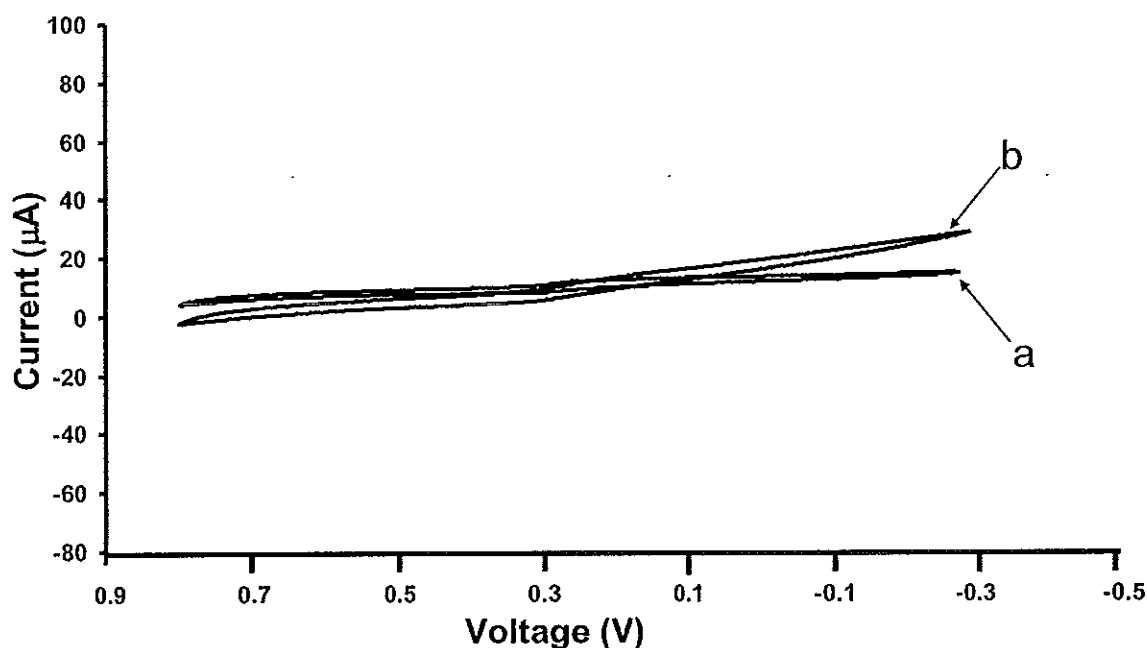


Figure 9.12 Cyclic voltammogram of modified gold electrode obtained in 0.05 M ($K_3[Fe(CN)_6]$) solution, (a) is the response when on the electrode surface was blocked by 1-dodecane thiol before used and (b) after used for 63 times

9.4.4 Response for dsDNA with Tetracycline(TCs)

The response of the immobilized dsDNA to three different compounds of the most commonly used tetracycline(s) were studied, *i.e.*, the parent compound (Tetracycline, TC), chlortetracycline (CTC) and oxytetracycline (OTC). Figure 9.13 shows their structure when compared with tetracycline (TC), the carbon atom of chlortetracycline (CTC) and oxytetracycline were substituted with Cl and OH at carbon atom at position 7 and 5, respectively.

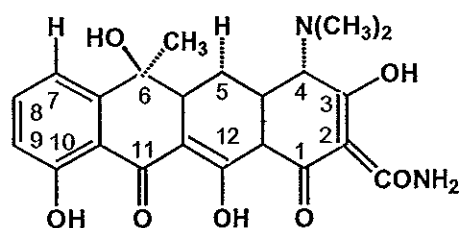
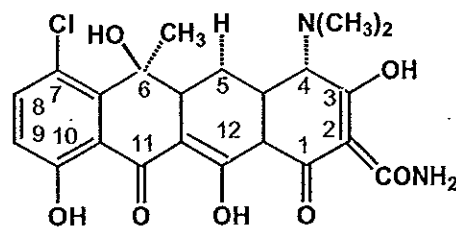
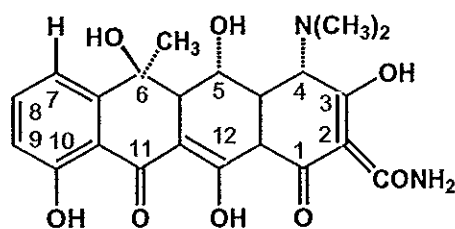
**Tetracycline (TC)****Chlortetracycline (CTC)****Oxytetracycline (OTC)**

Figure 9.13 Structure of Tetracycline , Chlortetracycline and Oxytetracycline

Calibration curves of the three compounds under optimum conditions (Table 9.1 and 9.2) are shown in Figure 9.14. The plot between the capacitance change and the concentration of tetracycline show the linear dynamic range from 10^{-4} to $10^2 \mu\text{g l}^{-1}$ for tetracycline and chlortetracycline and 10^{-3} - $10^3 \mu\text{g l}^{-1}$ for oxytetracycline. From the results, the detection limit for tetracycline, chlortetracycline were found to be $10^{-5} \mu\text{g l}^{-1}$ and 0.5×10^{-4} for oxytetracycline.

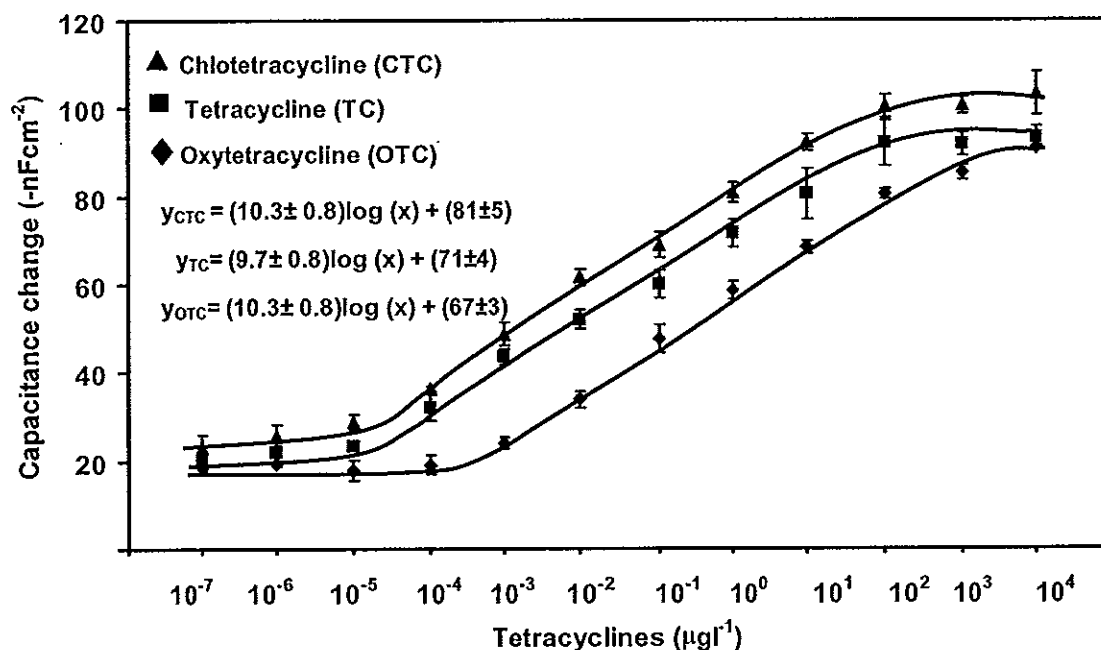


Figure 9.14 Calibration curves of tetracycline, chlortetracycline and oxytetracycline at optimum conditions.

From the result, the response from oxytetracycline was lower than tetracycline and chlortetracycline. This can be explained by the effect of their structure on the intercalative binding into the DNA double helix. Since oxytetracycline has a hydroxyl group (-OH) at C5 in place of H in the tetracycline molecule (Figure 9.13). This can cause a steric effect between DNA and oxytetracycline molecule making it more difficult to intercalate into DNA than chlortetracycline that has Cl substitution at C7 (Figure 9.13). When comparing the response between chlortetracycline and tetracycline, chlortetracycline gave slightly higher response. It is possible that the substitute Cl of chlortetracycline may participate in the binding on the surface of DNA (Khan and Musarrat, 2000).

9.4.5 Mixture of different tetracyclines

In real sample there would be a mixture of different compounds of tetracycline and these were tested. The measurement of each compound was first determined, then combination of two compounds at different concentration and finally the combination of three. Figure 9.15 shows that responses obtained from the

mixture were not equal to the sum of individual of each compound. This is because the interaction between the three compounds of tetracycline might be competitively binding with DNA.

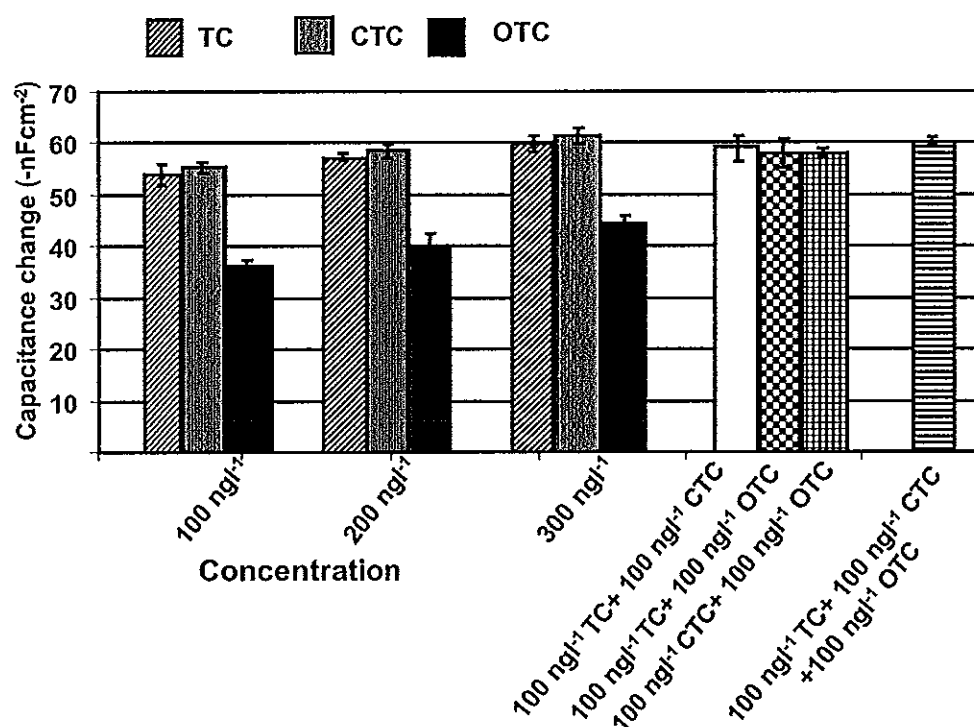


Figure 9.15 Effect of tetracycline (TC), chlortetracycline (CTC), oxytetracycline (OTC) and their mixture on binding with dsDNA

From these results if the type of tetracycline is not known, this biosensor systems can be used for screening. Since tetracycline has many compound and bind to DNA with different degree, parent compound of tetracycline (TC) was suitable to use as representative for tetracycline screening.

9.4.6 Determination of tetracyclines in wastewater

To test the capacitive biosensor system tetracyclines residues in wastewater were determined. Tetracycline was chosen because it is the parent compound and also gave the highest response (Figure 9.14). Wastewater samples were collected from water treatment pond of Prince of Songklanakarind Hospital, Prince of Songkla University. The samples were collected from two sampling sites

i.e., treatment and after treatment. To study the influence of matrix effect on the capacitive biosensor response, wastewater from two sampling sites were spiked with standard tetracycline from $0.2 \mu\text{g l}^{-1}$ to $0.8 \mu\text{g l}^{-1}$, these were used to perform a “spiked curve”. A calibration curve was also performed using “standard curve” at the same concentrations. The assay for each concentration was carried out in triplicate and the average sensor response and standard deviation were calculated.

The slope of standard curve and the spike sample curve were compared by two-way ANOVA test (analysis of variance) calculated by R software (R Development Core Team, 2006) to test whether they differ significantly. If no difference was found, it indicated that the matrix has no effect on the response of the sensor (IUPAC Technical Report, 2002). Figure 9.16 indicated that there was the matrix effect in both wastewaters (untreated and treated waste water).

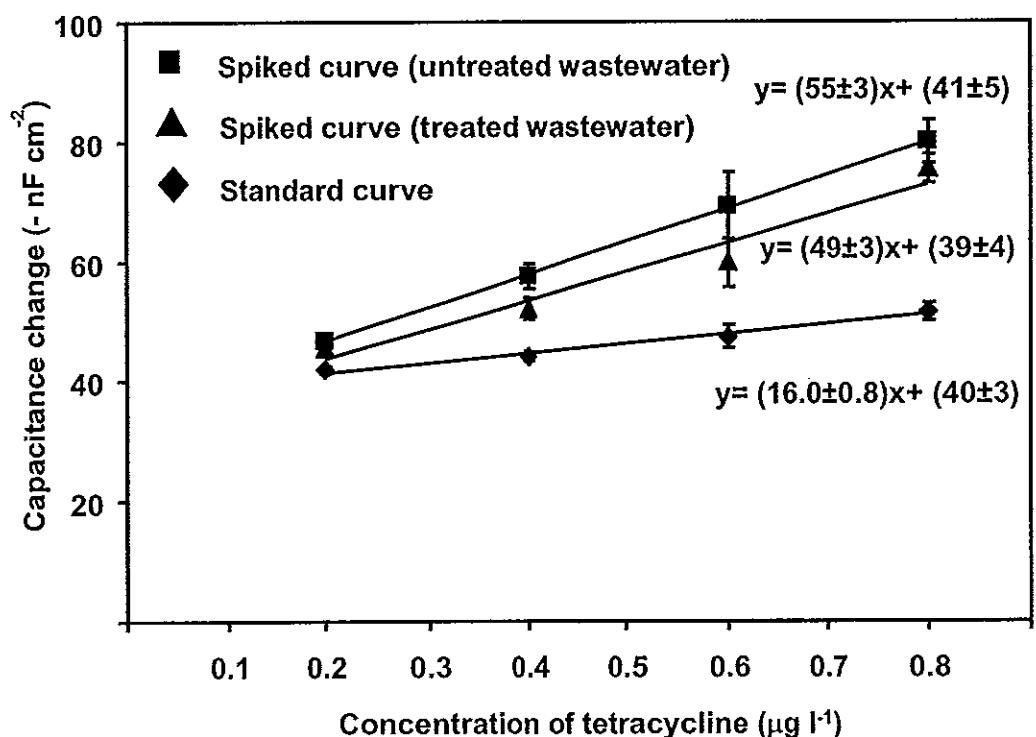


Figure 9.16 Standard calibration curve and spiked curve of untreated and treated wastewater

One way of reducing the matrix effect is by dilution. Wastewater samples were diluted 100 and 1,000 times dilution were tested and found that there was no significantly difference between the slopes of the spiked diluted sample and standard curve when the wastewaters were diluted 1,000 times as shown in Figure 9.17. That is the matrix effect can be eliminated by dilution.

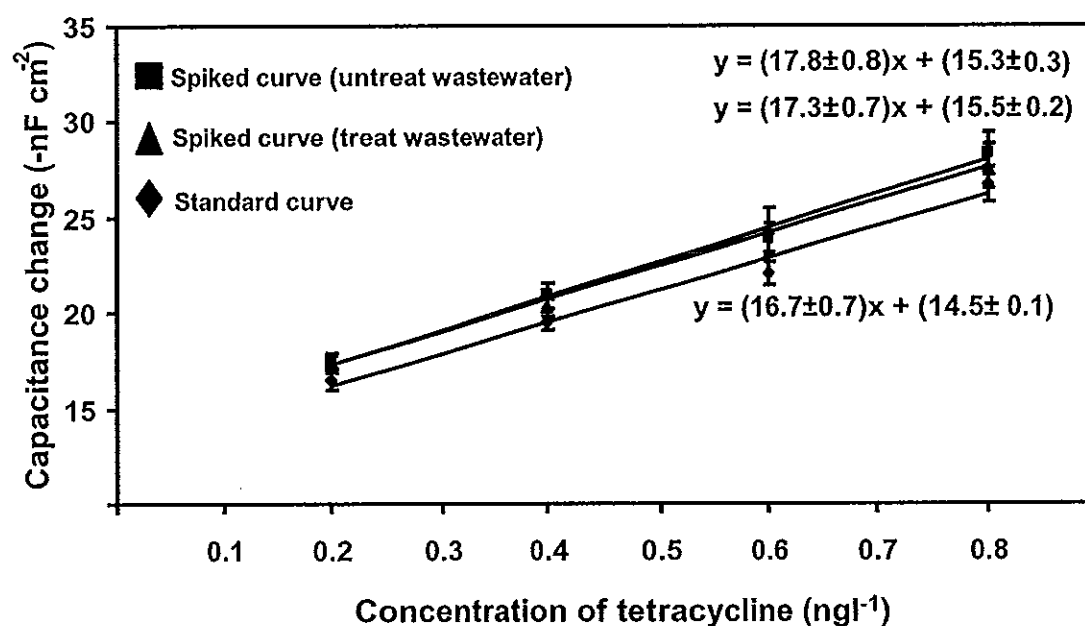


Figure 9.17 Standard calibration curve and spiked curve of untreated and treated wastewater after 1,000 times dilution

The recovery of tetracycline was tested by spiking all wastewater sample with tetracycline at 0.2 μgl^{-1} to 0.8 μgl^{-1} . The spiked samples were then diluted 1,000 times with Tris-HCl buffer pH 7.20 to reduce the matrix effect. The response obtained from spiked wastewater were used to calculate the concentration from the calibration curve. Recovery percentage was evaluated as described in chapter 7 (section 7.4.7.1) and the obtained recoveries are summarized in Table 9.3.

Table 9.3 Recovery tetracycline from spiked wastewater (n=3)

Spiked concentration ($\mu\text{g l}^{-1}$)	1 st sampling				2 nd sampling			
	Untreat wastewater		Treated wastewater		Untreat wastewater		Treated wastewater	
	Recovery (%)	R.S.D. (%)	Recovery (%)	R.S.D. (%)	Recovery (%)	R.S.D. (%)	Recovery (%)	R.S.D. (%)
0.2	95 \pm 10	11	84 \pm 8	10	72 \pm 5	7	102 \pm 6	6
0.4	76 \pm 5	6	94 \pm 7	7	71 \pm 10	9	95 \pm 3	3
0.6	90 \pm 4	4	99 \pm 3	3	93 \pm 1	1	90 \pm 3	3
0.8	97 \pm 1	1	90 \pm 3	3	97 \pm 3	3	94 \pm 2	2

The percentage of recovery and relative standard deviation of tetracycline spiked in all wastewater samples are acceptable for this concentration range (Taverniers *et al.*, 2004) (in the $\mu\text{g l}^{-1}$ level is 40-120 % and R.S.D. is 30-45.3%).

The concentrations of tetracycline in wastewater samples were detected as shown in table 9.4

Table 9.4 Concentration Tetracycline obtained by capacitive biosensor

Sampling time	Detected concentration of tetracycline ($\mu\text{g l}^{-1}$)	
	Untreated wastewater	Treated wastewater
	pond	pond
1 st	96 \pm 3	63 \pm 2
2 nd	102 \pm 5	68 \pm 3

9.4.7 Comparison between capacitive and HPLC

Tetracycline in the same wastewater samples was analyzed using HPLC with UV detector at 365 nm. Since in HPLC techniques the mixture of three compounds can be separated and showed the chromatogram peak of OTC, TC and CTC at different retention times (Figure 9.18). So the measurement of tetracyclines with HPLC was done by mixing the OTC, TC and CTC and injected into the system.

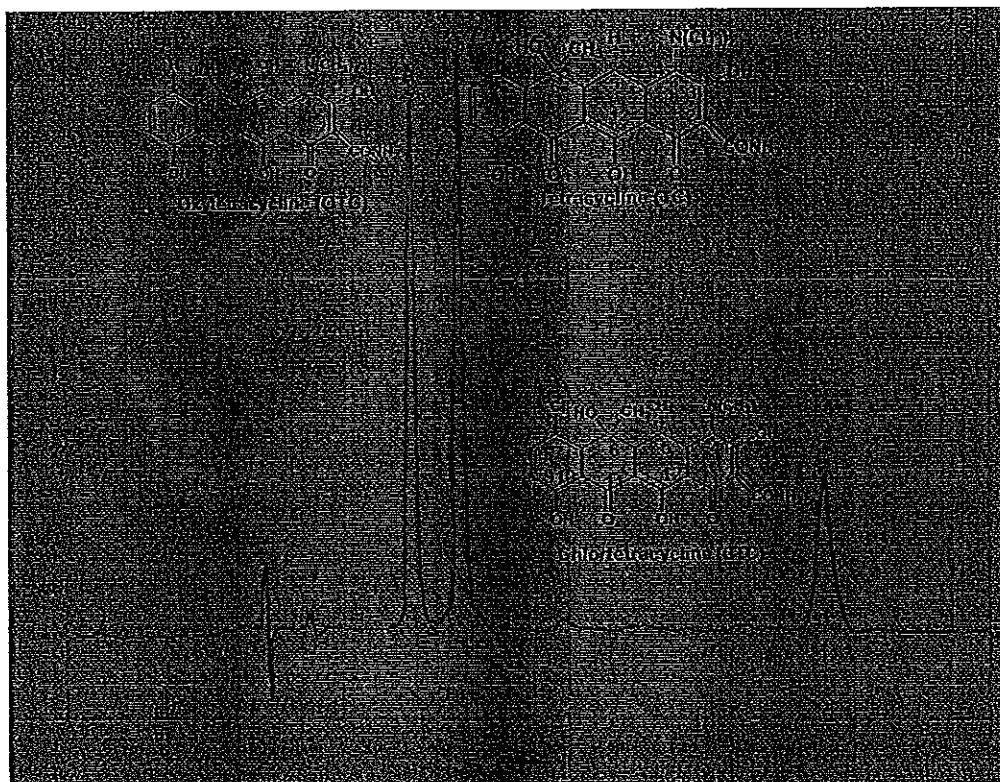


Figure 9.18 Chromatogram of OTC, TC and CTC

Preliminary study with HPLC indicated that it could determine OTC, TC and CTC in the range of 0.2 to 0.8 mg l^{-1} . The measurement of tetracycline with HPLC was carried out by standard addition method. Wastewaters spiked with the mixed standard solution of OTC, TC and CTC at 0.2 , 0.4 , 0.6 and 0.8 mg l^{-1} were injected into the HPLC. Standard addition calibration was prepared by plotting the peak area of OTC, TC and CTC *versus* corresponding spiked concentration. Its regression line was calculated in the normal way, but space was provided to extrapolated to the point on the x-axis at which $y=0$. The negative intercept on the x-axis corresponded to the concentration of analyte in sample.

Figure 9.19 shows an example of the standard addition calibration curve of tetracycline (TC) from in untreated wastewater of 1st sampling.

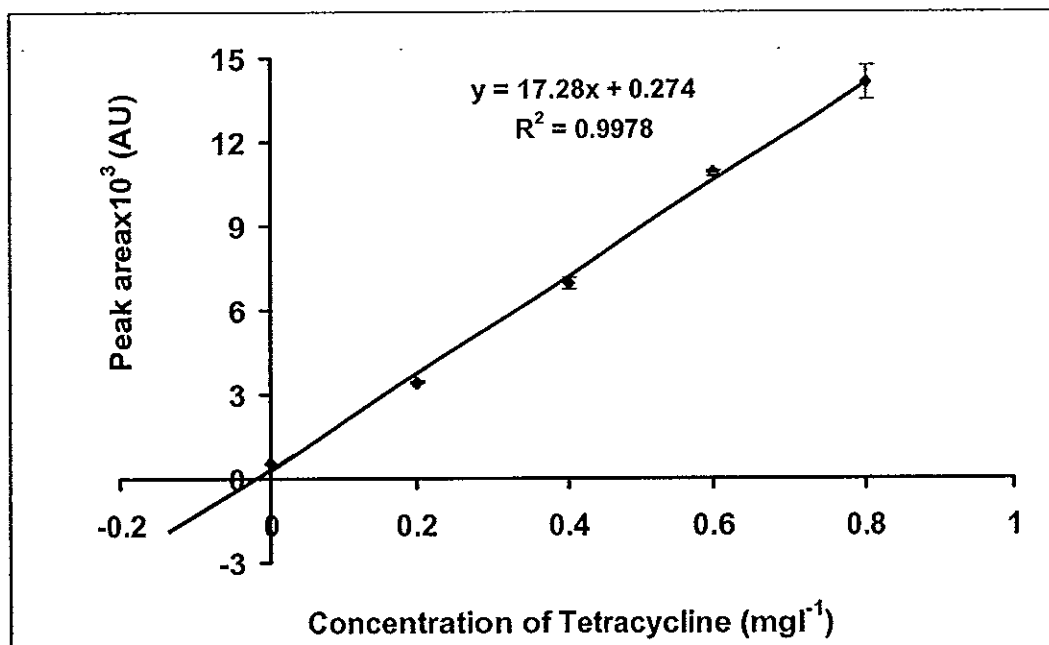


Figure 9.19 Standard addition calibration of tetracycline in untreated wastewater sample.

Table 9.5 shows concentration of OTC, TC and CTC in wastewater analyzed by standard addition method

Sampling time	Detected concentration of tetracyclines ($\mu\text{g l}^{-1}$) \pm SD							
	Untreated wastewater pond				Treated waste water pond			
	OTC	TC	CTC	Total	OTC	TC	CTC	Total
1 st	13.6 \pm 0.5	15.9 \pm 0.4	ND	29.5 \pm 0.6	ND	11.4 \pm 0.2	ND	11.4 \pm 0.2
2 nd	14.5 \pm 0.4	16.5 \pm 0.6	ND	31.0 \pm 0.7	ND	10.3 \pm 0.4	ND	10.3 \pm 0.4

ND= Not detectable.

Total= OTC+TC+CTC

The results from biosensor (Table 9.4) and HPLC (Table 9.5) for analyzing residue tetracycline before and after treatment show the same trend *i.e.*,

residue tetracyclines were found in the untreated wastewater pond more than the treated one. When comparing the results from the biosensor and HPLC, the total amount of residues tetracycline determined by HPLC method are lower than to those obtain from the biosensor system. It is lokely that the immobilized DNA in the biosensor not only bind with tetracyclines but also other DNA binding compounds. These maybe other compounds of tetracycline family, e.g. doxycycline, demeclocycline, or other drug contaminant in wastewater sample such as mitomycin, mitoxantrone, antamycin, or toxic compound in wastewater such as polychlorinated biphenyls (PCBs), polycyclic aromatic hydrocarbon, aflatoxin, and aromatic amines, herbicides.

Although this biosensor system is not able to distinguish specific compounds in wastewater but it could be convenient to use as monitoring or screening tool for tetracycline compounds. The major advantage of biosensor screening that it allows the analysis of a large number of samples and only the positive ones need to be further tested by conventional methods such as chromatography method.

9.5 Conclusions

The developed capacitive DNA biosensor can be used to detect tetracycline in wastewater sample with good sensitivity and low detection limit. In addition, using the appropriate regeneration solution, good reproducibility was obtained. The electrode can be reused up to at least 54 times and this helps to reduce the cost of analysis. The result obtained by these capacitive biosensor provide a good recoveries. The presence of tetracyclines (TCs) in wastewater sample could be detected by both biosensor and HPLC. The advantages of these system are easy to operation, and that sample can be tested without any preconcentration. Otherwise it can be readily applied for screening tetracycline or other drugs residual prior to the currently used chromatographic method.

Chapter 10

Conclusions

In this thesis, development and evaluation of the performance of electrochemical affinity biosensors has been investigated. The binding of target analyte with immobilized bioaffinity molecules are based on indirect (labeled) or direct (label-free) assay and detected with electrochemical transducers.

The investigation of indirect electrochemical detection of bioaffinity reaction is based on potentiometry with ion-selective microelectrode. The detection relies on sandwich assay where target analyte was bound to immobilized bioaffinity molecules on the gold substrate and secondary bioaffinity molecule conjugated with CdS quantum dot label was further added. CdS was later dissolved with H_2O_2 yielding a diluted electrolyte background suitable for potentiometric detection of released Cd^{2+} with polymeric membrane Cd^{2+} -selective microelectrode. This was performed in a 200 μl of solution with 10^{-4} M CaCl_2 as background using a Ca-ion selective microelectrode as reference electrode. Two affinity binding pairs, thrombin aptamer-thrombin and DNA-DNA (DNA hybridization), were investigated as described in chapters 5 and 6, respectively. This is the first time for both of these affinity pairs that they are detected with potentiometric ion selective electrode.

For thrombin aptamer-thrombin binding, ion selective microelectrode is clearly suitable for the measurement. It gave the linearity range in the range of 10-250 ppb with a limit of detection at 5 ppb, this corresponding to 28 fmol in 200 μl or 0.14 nM. Table 10.1 shows the comparison between analytical assay of potentiometry with ion selective electrode and other biosensors for aptamer-thrombin binding detection. The performances of this system are much better than most study. The only exception being the lower detection limit obtained by Hansen *et al.* (2006). Since the detection was performed by anodic stripping voltammetry (ASV), i.e., it has a step where the analyte was preconcentrated onto the electrode prior to measurement that allows the technique to achieve ultra-low detection limit. However, the detection required more steps than direct potentiometry with ion-selective electrode.

For of DNA hybridization detection, this ion selective can detect the target DNA with high selectivity. It can effectively discriminate against a 2-base mismatched DNA. This technique also showed a very wide linear dynamic range of 0.01-500 nM with the limit of detection at 10 pM or 37 pg or 2 fmol in 200 μ l. Table 10.2 compares the performance of potentiometry with ion selective electrode developed in this work and other biosensors for DNA hybridization detection. It can be seen that this system can provide comparable or better performance than the existing systems.

The results form Table 10.1 and 10.2 indicate that potentiometer ion selective electrode can be applied for indirect detection of target DNA and protein. This technique shows extremely high sensitivity, low detection limit when compared to other biosensors for DNA and protein detection. It is expected that various biomolecular interaction can be monitored with similar assay based different nanoparticles and corresponding ISEs.

Table 10.1 Comparison of Analytical features of aptamer-thrombin biosensors.

Analytical feature	Labeled (molecule)	Detection limit	Linear dynamic range
Potentiometric ion selective electrode (This work)	Yes (CdS)	5 ppb or 0.14 nM	10-250 ppb
Piezoelectric			
Bini <i>et al.</i> , 2007	No	50 nM	50-200 nM
Hianik <i>et al.</i> , 2005	No	1 nM	N/A
Amperometric			
Polsky <i>et al.</i> , 2006	Yes (Pt-nanoparticle)	1 nM	N/A
Centi <i>et al.</i> , 2007	Yes (alkaline phosphatase)	0.5 mM	N/A
Baldrich <i>et al.</i> , 2005	Yes (horseradish peroxidase)	1 nM	N/A
Stripping voltammetry			
Hansen <i>et al.</i> , 2006	Yes (CdS)	0.5 pM	N/A
Impedimetric			
Radi <i>et al.</i> , 2005	No	2 nM	5-35 nM

N/A: Not applicable

Table 10.2 Comparison of Analytical features of DNA hybridization biosensors

Analytical Feature	Labeled (molecule)	Detection limit	Linear dynamic range
Potentiometric ion selective electrode (This work)	Yes (CdS)	10 pM or 0.18 ng ml ⁻¹	0.01-500 nM
Piezoelectric			
Zhou <i>et al.</i> , 2002	No	0.02 mg ml ⁻¹	0.02-0.15 mg ml ⁻¹
He and Liu, 2004	No	0.1 mg ml ⁻¹	1-100 mg ml ⁻¹
Surface plasmon Resonance			
Piliarik <i>et al.</i> , 2007	No	100 pM	N/A
Amperometric			
Djellouli <i>et al.</i> , 2007	Yes (Horseradish peroxidase)	200 pM	N/A
Ikebukuro <i>et al.</i> , 2005	Yes (Glucose dehydrogenase)	1 nm	0.05-10 mM
Stripping voltammetry			
Wang <i>et al.</i> , 2002	Yes (Ag nanoparticle)	0.15 pg ml ⁻¹	20-250 ng ml ⁻¹
Wang <i>et al.</i> , 2002	Yes (CdS)	20 pM	-
Impedimetric			
Li <i>et al.</i> , 2007	No	3.8 pM	0.01-10 nM

N/A: Not applicable

For label-free affinity biosensor, the detection was performed by capacitive transducer. This affinity biosensor is based on the immobilization of bioaffinity molecule via a self-assembled monolayer (SAM) of thioctic acid on working gold electrode (WE). Binding of target analyte with immobilized bioaffinity molecule on the electrode cause the capacitance to decrease. The capacitance due to the direct affinity reaction could then be determined using a potential step method coupled to flow injection system. Three affinity binding pairs, histone-DNA, *lac* repressor protein-plasmid DNA and DNA-tetracyclines (TCs) were investigated as described in chapters 7, 8 and 9, respectively.

For the first capacitive direct affinity biosensor, DNA was detected by the immobilized histone on the electrode surface. Histones from calf thymus and shrimp were immobilized on gold electrodes covered with self-assembled monolayer (SAM) of thioctic acid. Each of these histones were used to detect DNA from calf thymus, shrimp and *E. coli*. The studies indicated that histones can bind better with DNA from the same source and give higher sensitivity than the binding with DNA from different sources. Under optimum conditions, both histones from calf thymus and shrimp provided the same lower detection limit of $10^{-5} \text{ ng l}^{-1}$ for DNA from different sources i.e., calf thymus, shrimp and *E.coli*. For the affinity reaction between calf thymus histone and DNA two linear ranges, 10^{-5} to $10^{-2} \text{ ng l}^{-1}$ and 10^{-1} to 10^2 ng l^{-1} , were obtained (Table 10.3). The immobilized histones were stable and after regeneration good reproducibility of the signal could be obtained up to 43 times with a %RSD of 3.1. When applied to analyze residual DNA in crude protein extracted from white shrimp good recoveries were obtained between 80-116 %.

Further application of capacitive transducer is plasmid DNA detection with immobilized *lac* repressor protein. Under optimum conditions, a study of the influence of different isoforms of plasmid DNA was detected by injecting supercoiled plasmid DNA (sc pDNA) and open circular (relaxed form) plasmid DNA (oc pDNA) into the capacitive biosensor system. The observed capacitance signal from open circular or

relaxed form was similar to that of supercoiled plasmid DNA. The linear ranges were the same for both isoforms, from 0.0001 to 0.1 ng ml^{-1} and 1 to $1,000 \text{ ng ml}^{-1}$, with lower detection limits of 0.002 pg ml^{-1} and 0.03 pg ml^{-1} for open circular and supercoiled plasmid DNA, respectively (Table 10.3). The immobilized *lac* repressor protein on self-assembled monolayer (SAM) gold electrode was stable and could be reused up to more than 40 times with RSD lower than 4.0 %.

A major advantage of capacitive for detection of DNA and/or plasmid DNA over conventional method *i.e.*, gel electrophoresis or spectrophotometric technique, is that it can determine DNA without using any dye staining such as ethidium bromide (Ebr) or other fluorescence stains that are a powerful carcinogen. In addition, analysis time of capacitive biosensor system was much shorter than other DNA quantitation methods (30min-5h) (Projan *et al.*, 1983; Schmidt *et al.*, 1996).

In addition, this technique was also applied for screening detection of tetracycline by immobilized double-stranded DNA on gold electrode surface. Under optimum conditions, influence of three different compounds of tetracycline(s), *i.e.*, tetracycline (TC), chlortetracycline (CTC) and oxytetracycline (OTC), to immobilized dsDNA was studied. It showed a linear dynamic range of 10^{-4} - $10^2 \text{ } \mu\text{g l}^{-1}$ for tetracycline and chlortetracycline, and 10^{-3} - $10^3 \text{ } \mu\text{g l}^{-1}$ for oxytetracycline. The detection limit was $10^{-5} \text{ } \mu\text{g l}^{-1}$ for tetracycline and chlortetracycline, and 0.5×10^{-4} for oxytetracycline (Table 10.3). The immobilized DNA was stable and after regeneration good reproducibility of signal could be obtained up to 54 times with % RSD < 4. When applied to analyze residual tetracycline in wastewater from hospital recoveries were obtained between 71-102%. The presence of tetracyclines (TCs) in wastewater sample could be detected by both biosensor and HPLC. The advantages of these system are easy to operate, sample can be tested without any preconcentration. It can be readily applied for screening tetracycline or other drugs residual prior to the currently used chromatographic method.

Table 10.3 summarized the performance of all flow injection capacitive biosensor. The results show that the flow injection capacitive affinity biosensor system can be applied for direct detection of several target analytes. This technique is highly sensitive and required short analysis time. The detection limit of the system is very low, making this techniques a good alternative approach to detect trace amount of affinity binding analytes. It is expected that this technique can definitely be applied to other affinity binding pairs.

Table10.3 Performance of flow injection capacitive biosensor systems for different analytes studied in this work

immobilized bioaffinity molecule	Analyte	Linear range	Linear regression equation	Limit of detection	Regeneration solution	Reusable time	Analysis time
Histone	DNA	10^{-5} - 10^{-2} ng l ⁻¹	$y=(26\pm3)\log(x) + (144\pm3)$	0.01 pg l ⁻¹	25 mM glycine -HCl pH 2.4	43 times	14-16 min
		and 10^{-1} - 10^2 ng l ⁻¹	$y=(69\pm1)\log(x) + (161\pm4)$				
lac repressor protein	sc pDNA	10^{-4} - 10^{-1} ng l ⁻¹	$y=(8.0\pm0.5)x + (52.0\pm0.8)$	0.03 pg ml ⁻¹	25 mM glycine HCl pH 2.4	at least 40 time	13-15 min
		and $1-10^3$ ng l ⁻¹	and $y=(15\pm1)x + (37.4\pm0.3)$				13-15 min
	oc pDNA	10^{-4} - 10^{-1} ng l ⁻¹	$y=(9.2\pm0.3)x + (48.7\pm0.4)$	0.002 pg ml ⁻¹			
		and $1-10^3$ ng l ⁻¹	and $y=(16\pm1)x + (32.0\pm0.6)$				
DNA	tetracycline	10^{-4} - 10^{-2} µg l ⁻¹	$y=(9.7\pm0.8)x + (71\pm4)$	0.01 ng l ⁻¹	25 mM NaOH	54 times	15-18
	chlortetracycline	10^{-4} - 10^{-2} µg l ⁻¹	$y=(10.3\pm0.8)x + (81\pm5)$	0.01 ng l ⁻¹			
	oxytetracycline	10^{-3} - 10^{-3} µg l ⁻¹	$y=(10.3\pm0.8)x + (67\pm3)$	0.5 ng l ⁻¹			

sc pDNA: supercoiled plasmid DNA

oc pDNA: open circular plasmid DNA

In this thesis the results indicate that both indirect detection with potentiometric ion selective electrode and direct detection with capacitive transducer can provide good performances, *i.e.*, high sensitivity, selectivity, accuracy and precision and short time analysis.

For potentiometric ion selective electrode, although it needs label molecules which requires additional steps in the detection process, the sensitivity and limit of detection for aptamer-thrombin and DNA hybridization demonstrated in our work were much improved (Tables 10.1 and 10.2). That is, for the detection of trace amount of affinity binding analyte, indirect potentiometric with ion selective electrode can be employed.

In case of capacitive transducer the binding of analyte with immobilized bioaffinity molecules is detected directly and can provide very low detection limit in the range of ng l^{-1} to pg l^{-1} . The advantages of capacitive transducer is that the analysis step is simple (does not require label molecules), fast, uncomplicated and possible for real-time measurement. It can be an alternative approach for direct detection of trace amount of analyte which can be applied for many areas including diagnosis, food processing and environmental monitoring.

References

- Abrahamsson, D., Kriz, K., Lu, M. and Kriz, D. 2004. A preliminary study on DNA detection based on relative magnetic permeability measurements and histone H1 conjugated superparamagnetic nanoparticles as magnetic tracers. *Biosensors and Bioelectronics*. **19**: 1549-1557.
- Alexeyev, M. F. and Winkler, H. H. 2002. Complete replacement of basic amino acid residues with cysteines in *Rickettsia prowazekii* ATP/ADP translocase. *Biochimica et Biophysica Acta (BBA) - Biomembranes*. **1565**: 136-142.
- Alfonta, L., Singh, A. K. and Willner, I. 2001. Liposomes Labeled with Biotin and Horseradish Peroxidase: A Probe for the Enhanced Amplification of Antigen-Antibody or Oligonucleotide-DNA Sensing Processes by the Precipitation of an Insoluble Product on Electrodes. *Analytical Chemistry*. **73**: 91-102.
- Allan, J., Cowling, G. J., Harborne, N., Cattini, P., Craigie, R. and Gould, H. 1981. Regulation of the higher-order structure of chromatin by histones H1 and H5. *Journal of Cell Biology*. **90**: 279-288.
- Ambrosi, A., Merkoçi, A. and de la Escosura-Muñiz, A. 2008. Electrochemical analysis with nanoparticle-based biosystems. *TrAC Trends in Analytical Chemistry*. **27**: 568-584.
- Andersen, W. C., Roybal, J. E., Gonzales, S. A., Turnipseed, S. B., Pfenning, A. P. and Kuck, L. R. 2005. Determination of tetracycline residues in shrimp and whole milk using liquid chromatography with ultraviolet detection and residue confirmation by mass spectrometry. *Analytica Chimica Acta*. **529**: 145-150.
- Authier, L., Grossiord, C., Brossier, P. and Limoges, B. 2001. Gold Nanoparticle-Based Quantitative Electrochemical Detection of Amplified Human Cytomegalovirus DNA Using Disposable Microband Electrodes. *Analytical Chemistry*. **73**: 4450-4456.

- Baeumner, A. J. 2003. Biosensors for environmental pollutants and food contaminants. *analytical and Bioanalytical Chemistry*. **377**: 434-445.
- Bakaltcheva, I. B., Ligler, F. S., Patterson, C. H. and Shriver-Lake, L. C. 1999. Multi-analyte explosive detection using a fiber optic biosensor. *Analytica Chimica Acta*. **399**: 13-20.
- Bakaltcheva, I. B., Shriver-Lake, L. C. and Ligler, F. S., 1998. A fiber optic biosensor for multianalyte detection: importance of preventing fluorophore aggregation. *Sensors and Actuators B: Chemical*. **51**: 46-51.
- Baker, B. R., Lai, R. Y., Wood, M. S., Doctor, E. H., Heeger, A. J. and Plaxco, K. W. 2006. An Electronic, Aptamer-Based Small-Molecule Sensor for the Rapid, Label-Free Detection of Cocaine in Adulterated Samples and Biological Fluids. *Journal of the American Chemical Society*. **128**: 3138-3139.
- Bakker, E. 1997. Determination of Unbiased Selectivity Coefficients of Neutral Carrier-Based Cation-Selective Electrodes. *Analytical Chemistry*. **69**: 1061-1069.
- Bakker, E. and Pretsch, E. 2002. The new wave of ion-selective electrodes. *Analytical Chemistry*. **74**: 420A-426A.
- Bakker, E. and Pretsch, E. 2005. Potentiometric sensors for trace-level analysis. *TrAC Trends in Analytical Chemistry*. **24**: 199-207.
- Bakker, E., Pretsch, E. and Buhlmann, P. 2000. Selectivity of Potentiometric Ion Sensors. *Analytical Chemistry*. **72**: 1127-1133.
- Baldrich, E., Acero, J. L., Reekmans, G., Laureyn, W. and O'Sullivan, C. K. 2005. Displacement Enzyme Linked Aptamer Assay. *Analytical Chemistry*. **77**: 4774-4784.

- Bang, G. S., Cho, S. and Kim, B.-G. 2005. A novel electrochemical detection method for aptamer biosensors. *Biosensors and Bioelectronics*. **21**: 863-870.
- Bard, A. J. and Faulkner, L. R. 2001. *Electrochemical methods; fundamentals and applications*. New York, John Wiley & Sons, INC.
- Barker, S. L. R., Clark, H. A., Swallen, S. F., Kopelman, R., Tsang, A. W. and Swanson, J. A. 1999a. Ratiometric and Fluorescence-Lifetime-Based Biosensors Incorporating Cytochrome c ' and the Detection of Extra- and Intracellular Macrophage Nitric Oxide. *Analytical Chemistry*. **71**: 1767-1772.
- Barker, S. L. R., Zhao, Y., Marletta, M. A. and Kopelman, R. 1999b. Cellular Applications of a Sensitive and Selective Fiber-Optic Nitric Oxide Biosensor Based on a Dye-Labeled Heme Domain of Soluble Guanylate Cyclase. *Analytical Chemistry*. **71**: 2071-2075.
- Bart, M., Stigter, E. C. A., Stapert, H. R., de Jong, G. J. and van Bennekom, W. P. 2005. On the response of a label-free interferon-[gamma] immunosensor utilizing electrochemical impedance spectroscopy. *Biosensors and Bioelectronics*. **21**: 49-59.
- Baskerville, S., Zapp, M. and Ellington, A. D. 1999. Anti-Rex Aptamers as Mimics of the Rex-Binding Element. *Journal of Virology*. **73**: 4962-4971.
- Bell, C. E., Lewis, M. 2001. Crystallographic Analysis of Lac Repressor Bound to Natural Operator O1. *Journal of Molecular Biology* **312**, 921-926.

- Benilova, I. V., Arkhypova, V. N., Dzyadevych, S. V., Jaffrezic-Renault, N., Martelet, C. and Soldatkin, A. P. 2006. Kinetics of human and horse sera cholinesterases inhibition with solanaceous glycoalkaloids: Study by potentiometric biosensor. *Pesticide Biochemistry and Physiology*. **86**: 203-210.
- Berdat, D., Marin, A., Herrera, F. and Gijs, M. A. M. 2006. DNA biosensor using fluorescence microscopy and impedance spectroscopy. *Sensors and Actuators B: Chemical*. **118**: 53-59.
- Berggren, C., Bjarnason, B., Johansson, G. 1999. Instrumentation for Direct Capacitive Biosensors. *Instrumentation Science and Technology*. **27**: 131-140.
- Berggren, C., Bjarnason, B. and Johansson, G. 1998. An immunological Interleukine-6 capacitive biosensor using perturbation with a potentiostatic step. *Biosensors and Bioelectronics*. **13**: 1061-1068.
- Berggren, C., Bjarnason, B. and Johansson, G. 1998. An immunological Interleukine-6 capacitive biosensor using perturbation with a potentiostatic step. *Biosensors and Bioelectronics*. **13**: 1061-1068.
- Berggren, C., Bjarnason, B. and Johansson, G. 2001. Capacitive Biosensors. *Electroanalysis*. **13**: 173-180.
- Berggren, C. and Johansson, G. 1997. Capacitance Measurements of Antibody-Antigen Interactions in a Flow System. *Analytical Chemistry*. **69**: 3651-3657.
- Berggren, C. and Johansson, G. 1997. Capacitance Measurements of Antibody-Antigen Interactions in a Flow System. *Analytical Chemistry*. **69**: 3651-3657.

- Bertucci, C., Cimitan, S. and Menotti, L. 2003. Optical biosensor analysis in studying herpes simplex virus glycoprotein D binding to target nectin1 receptor. *Journal of Pharmaceutical and Biomedical Analysis*. **32**: 697-706.
- Betty, C. A., Lal, R., Yakhmi, J. V. and Kulshreshtha, S. K. 2007. Time response and stability of porous silicon capacitive immunosensors. *Biosensors and Bioelectronics*. **22**: 1027-1033.
- Bichler, J., Heit, J. A. and Owen, W. G. 1996. DETECTION OF THROMBIN IN HUMAN BLOOD BY EX-VIVO HIRUDIN. *Thrombosis Research*. **84**: 289-294.
- Bilitewski, U. 2006. Protein-sensing assay formats and devices. *Analytica Chimica Acta*. **568**: 232-247.
- Bini, A., Minunni, M., Tombelli, S., Centi, S. and Mascini, M. 2007. Analytical Performances of Aptamer-Based Sensing for Thrombin Detection. *Analytical Chemistry*. **79**: 3016-3019.
- Bjorn, A. C., Cocklin, S., Madani, N., Si, Z., Ivanovic, T., Samanen, J., VanRyk, D. I., Pantophlet, R., Burton, D. R., Freire, E., Sodroski, J. and Chaiken, I. 2004. Mode of Action for Linear Peptide Inhibitors of HIV-1 gp120 Interactions. *Biochemistry*. **43**: 1928-1938.
- Bock, L. C., Griffin, L. C., Latham, J. A., Vermaas, E. H. and Toole, J. J. 1992. Selection of single-stranded DNA molecules that bind and inhibit human thrombin. *Nature*. **355**: 564-566.
- Boitieux, J. L., Lemay, C., Desmet, G. and Thomas, D. 1981. Use of solid phase biochemistry for potentiometric enzyme immunoassay of oestradiol-17 [beta]-preliminary report. *Clinica Chimica Acta*. **113**: 175-181.

- Bonanni, A., Esplandiu, M., Pividori, M., Alegret, S. and del Valle, M. 2006. Impedimetric genosensors for the detection of DNA hybridization. *analytical and Bioanalytical Chemistry*. **385**: 1195-1201.
- Bontidean, I., Kumar, A., Csoregi, E., Yu Galaev, I., Mattiasson, S. 2001. Highly sensitive novel biosensor based on an immobilized *lac* repressor. *Angewandte Chemie International Edition*. **40**: 2676-2678.
- Bontidean, I., Ahlqvist, J., Mulchandani, A., Chen, W., Bae, W., Mehra, R. K., Mortari, A. and Csöregi, E. 2003. Novel synthetic phytochelatin-based capacitive biosensor for heavy metal ion detection. *Biosensors and Bioelectronics*. **18**: 547-553.
- Bontidean, I., Berggren, C., Johansson, G., Csoregi, E., Mattiasson, B., Lloyd, J. R., Jakeman, K. J. and Brown, N. L. 1998. Detection of Heavy Metal Ions at Femtomolar Levels Using Protein-Based Biosensors. *Analytical Chemistry*. **70**: 4162-4169.
- Bordi, F., Cametti, C. and Gliozzi, A. 2002. Impedance measurements of self-assembled lipid bilayer membranes on the tip of an electrode. *Bioelectrochemistry*. **57**: 39-46.
- Buck, R. P. and Lindner, E. 1994. Recommendations for nomenclature of ion-selective electrode (IUPAC Recommendation 1994). *Pure and Applied Chemistry*. **66**: 2527-2536.
- Bunde, R. L., Jarvi, E. J. and Rosentreter, J. J. 1998. Piezoelectric quartz crystal biosensors. *Talanta*. **46**: 1223-1236.

- Burke, M., O'Sullivan, P. J., Soini, A. E., Berney, H. and Papkovsky, D. B. 2003. Evaluation of the phosphorescent palladium(II)-coproporphyrin labels in separation-free hybridization assays. *Analytical Biochemistry*. **320**: 273-280.
- Butler, A. P., Revzin, A., von Hippel, P.H. 1977. Molecular parameters characterizing the interaction of *Escherichia coli lac* repressor with non operator DNA and Inducer. *Biochemistry* **16**, 4757-4768.
- Byfield, M. P. and Abuknesha, R. A. 1994. Biochemical aspects of biosensors. *Biosensors and Bioelectronics*. **9**: 373-399.
- Cai, H., Lee, T. M.-H. and Hsing, I. M. 2006. Label-free protein recognition using an aptamer-based impedance measurement assay. *Sensors and Actuators B: Chemical*. **114**: 433-437.
- Campanella, L., Attioli, R., Colapicchioni, C. and Tomassetti, M. 1999. New amperometric and potentiometric immunosensors for anti-human immunoglobulin G determinations. *Sensors and Actuators B: Chemical*. **55**: 23-32.
- Carmon, K. S., Baltus, R. E. and Luck, L. A. 2005. A biosensor for estrogenic substances using the quartz crystal microbalance. *Analytical Biochemistry*. **345**: 277-283.
- Carpini, G., Lucarelli, F., Marrazza, G. and Mascini, M. 2004. Oligonucleotide-modified screen-printed gold electrodes for enzyme-amplified sensing of nucleic acids. *Biosensors and Bioelectronics*. **20**: 167-175.
- Carson, M. C., Ngoh, M. A. and Hadley, S. W. 1998. Confirmation of multiple tetracycline residues in milk and oxytetracycline in shrimp by liquid chromatography-particle beam mass spectrometry. *Journal of Chromatography B: Biomedical Sciences and Applications*. **712**: 113-128.

- Castillo, J., Guspur, S., Leth, S., Niculescu, M., Mortari, A., Bontidean, I., Soukharev, V., Dorneanu, S. A., Ryabov, A. D. and Csöregi, E. 2004. Biosensors for life quality: Design, development and applications. *Sensors and Actuators B: Chemical*. **102**: 179-194.
- Ceresa, A., Radu, A., Peper, S., Bakker, E. and Pretsch, E. 2002. Rational Design of Potentiometric Trace Level Ion Sensors. A Ag⁺-Selective Electrode with a 100 ppt Detection Limit. *Analytical Chemistry*. **74**: 4027-4036.
- Chee, M., Yang, R., Hubbell, E., Berno, A., Huang, X. C., Stern, D., Winkler, J., Lockhart, D. J., Morris, M. S. and Fodor, S. P. A. 1996. Accessing Genetic Information with High-Density DNA Arrays. *Science*. **274**: 610-614.
- Chen, Y. M., Yu, C. J., Cheng, T. L. and Tseng, W. L. 2008. Colorimetric Detection of Lysozyme Based on Electrostatic Interaction with Human Serum Albumin-Modified Gold Nanoparticles. *Langmuir*. **24**: 3654-3660.
- Cheng, A. K. H., Ge, B. and Yu, H. Z., 2007. Aptamer-Based Biosensors for Label-Free Voltammetric Detection of Lysozyme. *Analytical Chemistry*. **79**: 5158-5164.
- Cherlet, M., Schelkens, M., Croubels, S. and De Backer, P. 2003. Quantitative multi-residue analysis of tetracyclines and their 4-epimers in pig tissues by high-performance liquid chromatography combined with positive-ion electrospray ionization mass spectrometry. *Analytica Chimica Acta*. **492**: 199-213.
- Chiti, G., Marrazza, G. and Mascini, M. 2001. Electrochemical DNA biosensor for environmental monitoring. *Analytica Chimica Acta*. **427**: 155-164.

- Choi, J. H., Chen, K. H. and Strano, M. S. 2006. Aptamer-Capped Nanocrystal Quantum Dots: A New Method for Label-Free Protein Detection. *Journal of the American Chemical Society*. **128**: 15584-15585.
- Chu, J., Lin, Z. H., Shen, G. L. and Yu, R. Q. 1995. Piezoelectric immunosensor for the detection of immunoglobulin M. *Analyst*. **120**: 2829-2832.
- Chumbimuni-Torres, K. Y., Dai, Z., Rubinova, N., Xiang, Y., Pretsch, E., Wang, J. and Bakker, E. 2006. Potentiometric Biosensing of Proteins with Ultrasensitive Ion-Selective Microelectrodes and Nanoparticle Labels. *Journal of the American Chemical Society*. **128**: 13676-13677.
- Chumbimuni-Torres, K. Y., Rubinova, N., Radu, A., Kubota, L. T. and Bakker, E. 2006. Solid Contact Potentiometric Sensors for Trace Level Measurements. *Analytical Chemistry*. **78**: 1318-1322.
- Claire, L. M., David J. Newman and Price, C. P. 1996. Immunosensors: technology and opportunities in laboratory medicine. *Chemical Chemistry*. **42**: 193-209.
- Clemson, M., Kelly, W.J. 2003. Optimizing alkaline lysis for DNA plasmid recovery. *Biotechnology and Applied Biochemistry* **37**,235-244.
- Collings, A. F., Caruso, F. 1997. Biosensor: recent advances. *Report on Progress in Physics*. **60**
- Cooper, A. D., Stubbings, G. W. F., Kelly, M., Tarbin, J. A., Farrington, W. H. H. and Shearer, G. 1998. Improved method for the on-line metal chelate affinity chromatography-high-performance liquid chromatographic determination of tetracycline antibiotics in animal products. *Journal of Chromatography A*. **812**: 321-326.

- Cooreman, P., Thoelen, R., Manca, J., vandeVen, M., Vermeeren, V., Michiels, L., Ameloot, M. and Wagner, P. 2005. Impedimetric immunosensors based on the conjugated polymer PPV. *Biosensors and Bioelectronics*. **20**: 2151-2156.
- Croubels, S. M., Vanoosthuyze, K. E. I. and Van Peteghem, C. H. 1997. Use of metal chelate affinity chromatography and membrane-based ion-exchange as clean-up procedure for trace residue analysis of tetracyclines in animal tissues and egg. *Journal of Chromatography B: Biomedical Sciences and Applications*. **690**: 173-179.
- Cui, R., Pan, H. C., Zhu, J. J. and Chen, H. Y. 2007. Versatile Immunosensor Using CdTe Quantum Dots as Electrochemical and Fluorescent Labels. *Analytical Chemistry*. **79**: 8494-8501.
- Cui, X., Yang, F., Li, A. and Yang, X. 2005. Chip surface charge switch for studying histone-DNA interaction by surface plasmon resonance biosensor. *Analytical Biochemistry*. **342**: 173-175.
- Cui, X., Yang, F., Sha, Y. and Yang, X. 2003. Real-time immunoassay of ferritin using surface plasmon resonance biosensor. *Talanta*. **60**: 53-61.
- Cummins, C. M., Koivunen, M. E., Stephanian, A., Gee, S. J., Hammock, B. D. and Kennedy, I. M. 2006. Application of europium(III) chelate-dyed nanoparticle labels in a competitive atrazine fluoroimmunoassay on an ITO waveguide. *Biosensors and Bioelectronics*. **21**: 1077-1085.
- Currell, G. 2000. *Analytical in Instrument; Performance Characteristics and Quality*. John Wiley & Sons Ltd, New York, West Sussex, English.
- Dai, Z., Kawde, A. N., Xiang, Y., LaBelle, J. T., Gerlach, J., Bhavanandan, V. P., Joshi, L. and Wang, J. 2006. Nanoparticle-Based Sensing of Glycan-Lectin Interactions. *Journal of the American Chemical Society*. **128**: 10018-10019.

- Das, J., Aziz, M. A. and Yang, H. 2006. A Nanocatalyst-Based Assay for Proteins: DNA-Free Ultrasensitive Electrochemical Detection Using Catalytic Reduction of p-Nitrophenol by Gold-Nanoparticle Labels. *Journal of the American Chemical Society*. **128**: 16022-16023.
- Davis, J., Huw Vaughan, D. and Cardosi, M. F. 1995. Elements of biosensor construction. *Enzyme and Microbial Technology*. **17**: 1030-1035.
- Deinum, J., Gustavsson, L., Gyzander, E., Kullman-Magnusson, M., Edström, a. and Karlsson, R. 2002. A Thermodynamic Characterization of the Binding of Thrombin Inhibitors to Human Thrombin, Combining Biosensor Technology, Stopped-Flow Spectrophotometry, and Microcalorimetry. *Analytical Biochemistry*. **300**: 152-162.
- Deng, Z., Zhang, Y., Yue, J., Tang, F. and Wei, Q. 2007. Green and Orange CdTe Quantum Dots as Effective pH-Sensitive Fluorescent Probes for Dual Simultaneous and Independent Detection of Viruses. *Journal of the Physical Society*. **111**: 12024-12031.
- Dequaire, M., Degrand, C. and Limoges, B. 2000. An Electrochemical Metalloimmunoassay Based on a Colloidal Gold Label. *Analytical Chemistry*. **72**: 5521-5528.
- Ding, X. and Mou, S. 2000. Ion chromatographic analysis of tetracyclines using polymeric column and acidic eluent. *Journal of Chromatography A*. **897**: 205-214.

- Djellouli, N. m., Rochelet-Dequaire, M., Limoges, B., Druet, M. and Brossier, P. 2007. Evaluation of the analytical performances of avidin-modified carbon sensors based on a mediated horseradish peroxidase enzyme label and their application to the amperometric detection of nucleic acids. *Biosensors and Bioelectronics*. **22**: 2906-2913.
- Dong, S. and Chen, X., 2002. Aome new aspects in biosensors. *Reviews in Molecular Biotechnology*. **82**: 303-323.
- Dortant, P. M., Claassen, I. J. T. M., van Kreyl, C. F., van Steenis, G. and Wester, P. W. 1997. Risk Assessment on the Carcinogenic Potential of Hybridoma Cell DNA: Implications for Residual Contaminating Cellular DNA in Biological Products. *Biologicals*. **25**: 381-390.
- Drummond, T. G., Hill, M. G. and Barton, J. K. 2003. Electrochemical DNA sensors. *Nature Biotechnology*. **21**: 1192-1199.
- Eggins, B. R. 1996. *Biosensor: an introduction*. Chichester: John Wiley&Son Ltd.
- Ellington, A. D. and Szostak, J. W. 1990. In vitro selection of RNA molecules that bind specific ligands. *Nature*. **346**: 818-822.
- Erdem, A. and Ozsoz, M. 2002. Electrochemical DNA Biosensors Based on DNA-Drug Interactions. *Electroanalysis*. **14**: 965-974.
- Eremenko, A. V., G. Bauer, C., Makower, A., Kanne, B., Baumgarten, H. and Scheller, F. W. 1998. The development of a non-competitive immunoenzymometric assay of cocaine. *Analytica Chimica Acta*. **358**: 5-13.

- Eugenii, K. and Itamar, W. 2003. Probing Biomolecular Interactions at Conductive and Semiconductive Surfaces by Impedance Spectroscopy: Routes to Impedimetric Immunosensors, DNA-Sensors, and Enzyme Biosensors. *Electroanalysis*. **15**: 913-947.
- Fang, X., Cao, Z., Beck, T. and Tan, W. 2001. Molecular Aptamer for Real-Time Oncoprotein Platelet-Derived Growth Factor Monitoring by Fluorescence Anisotropy. *Analytical Chemistry* **73**: 5752-5757.
- Ferreira, G.N. M., Cabral, J.M.S., Prazeres, D. M.F. 1998. Purification of supercoiled plasmid DNA using chromatographic processes. *Journal of Molecular Recognition* **11**, 250-251.
- Fonong, T., Rechnitz, G. A. 1984. Homogeneous potentiometric enzyme immunoassay for human immunoglobulin G. *Analytical Chemistry*. **56**: 2586-2590.
- Fu-Chun, G., De-Si, H., Zhong, C., Shu-Zhen, T. and Ya-Fei, T. 2007. An Amperometric Enzyme-linked Immunosensor Using Resveratrol as the Substrates for Horseradish Peroxidase for Brucella Melitensis Antibody Assay. *Chinese Journal of Analytical Chemistry*. **35**: 1783-1786.
- Gau, J., Jr., Lan, E. H., Dunn, B., Ho, C.-M. and Woo, J. C. S. 2001. A MEMS based amperometric detector for E. Coli bacteria using self-assembled monolayers. *Biosensors and Bioelectronics*. **16**: 745-755.
- Gautier, C., Cougnon, C., Pilard, J.-F., Casse, N., Chnais, B. and Laulier, M. 2007. Detection and modelling of DNA hybridization by EIS measurements: Mention of a polythiophene matrix suitable for electrochemically controlled gene delivery. *Biosensors and Bioelectronics*. **22**: 2025-2031.

- Gebauer, C. R. and Rechnitz, G. A. 1982. Deaminating enzyme labels for potentiometric enzyme immunoassay. *Analytical Biochemistry*. **124**: 338-348.
- Gebbert, A., Alvarez-Icaza, M., Stoecklein, W. and Schmid, R. D. 1992. Real-time monitoring of immunochemical interactions with a tantalum capacitance flow-through cell. *Analytical Chemistry*. **64**: 997-1003.
- Georgiou, C. D. and Papapostolou, I. 2006. Assay for the quantification of intact/fragmented genomic DNA. *Analytical Biochemistry*. **358**: 247-256.
- Gherghi, I. C., Girousi, S. Th., Vougaropoulos, A. N., Tzimou-Tsitouridou, R. 2004. Differentiations in the Electrochemical Behavior of the Interactions Between DNA and Compounds with affinity for DNA. *Analytical Letter*. **37**: 957-966.
- Ghindilis, A. L., Atanasov, P., Wilkins, M. and Wilkins, E. 1998. Immunosensors: electrochemical sensing and other engineering approaches. *Biosensors and Bioelectronics*. **13**: 113-131.
- Ghindilis, A. L., Skorobogat'ko, O. V., Gavrilova, V. P. and Yaropolov, A. I. 1992. A new approach to the construction of potentiometric immunosensors. *Biosensors and Bioelectronics*. **7**: 301-304.
- Giezeli, E. and Lowe, C. R. 1996. Immunosensor. *Current opinion in Biotechnology*. **7**: 66-71.
- Golet, E. M., Alder, A. C., Hartmann, A., Ternes, T. A. and Giger, W. 2001. Trace Determination of Fluoroquinolone Antibacterial Agents in Urban Wastewater by Solid-Phase Extraction and Liquid Chromatography with Fluorescence Detection. *Analytical Chemistry*. **73**: 3632-3638.

- Goni-Urriza, M., Capdepuy, M., Arpin, C., Raymond, N., Caumette, P. and Quentin, C. 2000. Impact of an Urban Effluent on Antibiotic Resistance of Riverine Enterobacteriaceae and Aeromonas spp. *Applied and Environmental Microbiology*. **66**: 125-132.
- Gonzalez Garça, M. B. and Costa Garça, A. 1995. Adsorptive stripping voltammetric behaviour of colloidal gold and immunogold on carbon paste electrode. *Bioelectrochemistry and Bioenergetics*. **38**: 389-395.
- Gooding, J. J., Erokhin, P., Losic, D., Yang, W., Policarpio, V., Liu, J., Ho, F. M., Situmorang, M., Hibbert, D. B. and Shapter, J. G. 2001. Parameters Important in Fabricating Enzyme Electrodes Using Self-Assembled Monolayers of Alkanethiols. *Analytical Sciences*. **17**
- Granek, V. and Rishpon, J. 2002. Detecting Endocrine-Disrupting Compounds by Fast Impedance Measurements. *Environmental Science and Technology*. **36**: 1574-1578.
- Grant, S., Davis, F., Law, K. A., Barton, A. C., Collyer, S. D., Higson, S. P. J. and Gibson, T. D. 2005. Label-free and reversible immunosensor based upon an ac impedance interrogation protocol. *Analytica Chimica Acta*. **537**: 163-168.
- Green, M. J. 1987. Electrochemical Immunoassays. *Philosophical Transactions of the Royal Society of London. Series B, Biological Sciences*. **316**: 135-142.
- Gregory, C. A., Rigg, G. P., Illidge, C. M. and Matthews, R. C. 2001. Quantification of Escherichia coli Genomic DNA Contamination in Recombinant Protein Preparations by Polymerase Chain Reaction and Affinity-Based Collection. *Analytical Biochemistry*. **296**: 114-121.

- Guan, J.-G., Miao, Y.-Q. and Zhang, Q.-J. 2004. Impedimetric Biosensors. *The Society for Biotechnology, Japan*. **97**: 219-226.
- Guardabassi, L., Petersen, A., Olsen, J.E., Dalsgaard, A. 1998. Antibiotic Resistance in *Acinetobacter* spp. Isolated from Sewers Receiving Waste Effluent from a Hospital and a Pharmaceutical Plant. *Applied and Environmental Microbiology*. **64**: 3499-3505.
- Guiducci, C., Stagni, C., Zuccheri, G., Bogliolo, A., Benini, L., Samor, B. and Ricco, B. 2004. DNA detection by integrable electronics. *Biosensors and Bioelectronics*. **19**: 781-787.
- Gustavsson, P.E., Lemmens, R., Nyhammar, T., Busson, P., Larsson, P. O. 2004. Purification of plasmid DNA with a new type of anion-exchange beads having a non-charged surface. *Journal of Chromatography A* **1038**, 131-140.
- Haga, T. 1995. *Molecular Biology and Biotechnology, A Comprehensive Desk Reference*, VCH, New York.
- Haller, M. Y., Müller, S. R., McArdell, C. S., Alder, A. C. and Suter, M. J. F. 2002. Quantification of veterinary antibiotics (sulfonamides and trimethoprim) in animal manure by liquid chromatography-mass spectrometry. *Journal of Chromatography A*. **952**: 111-120.
- Halling-Sorensen, B., Nors Nielsen, S., Lanzky, P. F., Ingerslev, F., Holten Lützhøft, H. C. and Jorgensen, S. E. 1998. Occurrence, fate and effects of pharmaceutical substances in the environment- A review. *Chemosphere*. **36**: 357-393.

- Hanaee, H., Ghourchian, H. and Ziaee, A. A. 2007. Nanoparticle-based electrochemical detection of hepatitis B virus using stripping chronopotentiometry. *Analytical Biochemistry*. **370**: 195-200.
- Hanora, A., Savina, I., Plieva, F. M., Izumrudov, V.A., Mattiasson, B. Galaev, I.Yu. 2006. Direct capture of plasmid DNA from non-clarified bacterial lysate using polycation grafted monoliths, *Journal of Biotechnology*, **123**, 343-355.
- Hansen, J. A., Wang, J., Kawde, A. N., Xiang, Y., Gothelf, K. V. and Collins, G. 2006. Quantum-Dot/Aptamer-Based Ultrasensitive Multi-Analyte Electrochemical Biosensor. *Journal of American Chemical Society*. **128**: 2228-2229.
- He, F. and Liu, S. 2004. Detection of *P. aeruginosa* using nano-structured electrode-separated piezoelectric DNA biosensor. *Talanta*. **62**: 271-277.
- Hedström, M., Galaev, I. Y. and Mattiasson, B. 2005. Continuous measurements of a binding reaction using a capacitive biosensor. *Biosensors and Bioelectronics*. **21**: 41-48.
- Helliger, W., Lindner, H., Hauptlorenz, S., Puschendorf, B. 1988. A new h.p.l.c. isolation procedure for chicken and goose erythrocyte histones. *The Biochemical Journal* **225**: 23-27.
- Hermanson, G. T., Mallia, A. K. and Smith, P. K. 1992. *Immobilized affinity ligand Technique*. San Diego: Academic Press Inc.
- Hernández, M., Borrull, F. and Calull, M. 2003. Analysis of antibiotics in biological samples by capillary electrophoresis. *TrAC Trends in Analytical Chemistry*. **22**: 416-427.

- Hesselberth, J., Robertson, M. P., Jhaveri, S. and Ellington, A. D. 2000. In vitro selection of nucleic acids for diagnostic applications. *Reviews in Molecular Biotechnology*. **74**: 15-25.
- Heyduk, E. and Heyduk, T. 2005. Nucleic Acid-Based Fluorescence Sensors for Detecting Proteins. *Analytical Chemistry*. **77**: 1147-1156.
- Hianik, T., Ostatný, V., Zajíčková, Z., Stoikova, E. and Evtugyn, G. 2005. Detection of aptamer-protein interactions using QCM and electrochemical indicator methods. *Bioorganic & Medicinal Chemistry Letters*. **15**: 291-295.
- Hibbert, D. B., Gooding, J.J. 2006. *Data Analysis for Chemistry: An Introductory Guide for Students and Laboratory Scientists*. Oxford, New York Oxford University Press .USA
- Hirsch, R., Ternes, T., Haberer, K. and Kratz, K.-L. 1999. Occurrence of antibiotics in the aquatic environment. *The Science of The Total Environment*. **225**: 109-118.
- Hirsch, R., Ternes, T. A., Haberer, K., Mehlich, A., Ballwanz, F. and Kratz, K.-L. 1998. Determination of antibiotics in different water compartments via liquid chromatography-electrospray tandem mass spectrometry. *Journal of Chromatography A*. **815**: 213-223.
- Hleli, S., Martelet, C., Abdelghani, A., Bessueille, F., Errachid, A., Samitier, J., Hays, H. C. W., Millner, P. A., Burais, N. and Jaffrezic-Renault, N., 2006a. An immuno- sensor for haemoglobin based on impedimetric properties of a new mixed self-assembled monolayer. *Materials Science and Engineering: C*. **26**: 322-327.

- Hleli, S., Martelet, C., Abdelghani, A., Burais, N. and Jaffrezic-Renault, N. 2006b. Atrazine analysis using an impedimetric immunosensor based on mixed biotinylated self-assembled monolayer. *Sensors and Actuators B: Chemical*. **113**: 711-717.
- Hock, B. 1997. Antibodies for immunosensors a review. *Analytica Chimica Acta*. **347**: 177-186.
- Hoffman, T. L., Canziani, G., Jia, L., Rucker, J. and Doms, R. W. 2000. A biosensor assay for studying ligand-membrane receptor interactions: Binding of antibodies and HIV-1 Env to chemokine receptors. *Proceedings of the National Academy of Sciences*. **97**: 11215-11220.
- Holden, M. J., Blasic, J. R., Bussjaeger, L., Kao, C., Shokere, L. A., Kendall, D. C., Freese, L. and Jenkins, G. R. 2003. Evaluation of Extraction Methodologies for Corn Kernel (*Zea mays*) DNA for Detection of Trace Amounts of Biotechnology-Derived DNA. *Journal of Agricultural and Food Chemistry*. **51**: 2468-2474.
- Homola, J. 2003. Present and future of surface plasmon resonance biosensors. *Analytical and Bioanalytical Chemistry*. **377**: 528-539.
- Homola, J. 2008. Surface Plasmon Resonance Sensors for Detection of Chemical and Biological Species. *Chemical Review*. **108**: 462-493.
- Homola, J., Yee, S. S. and Gauglitz, G. n. 1999. Surface plasmon resonance sensors: review. *Sensors and Actuators B: Chemical*. **54**: 3-15.
- Hu, S.-Q., Wu, Z.-Y., Zhou, Y.-M., Cao, Z.-X., Shen, G.-L. and Yu, R.-Q. 2002. Capacitive immunosensor for transferrin based on an o-aminobenzenethiol oligomer layer. *Analytica Chimica Acta*. **458**: 297-304.

- Hu, S.-Q., Xie, Z.-M., Lei, C.-X., Shen, G.-L. and Yu, R.-Q. 2005. The integration of gold nanoparticles with semi-conductive oligomer layer for development of capacitive immunosensor. *Sensors and Actuators B: Chemical*. **106**: 641-647.
- Huang, C. C., Huang, Y. F., Cao, Z., Tan, W. and Chang, H. T. 2005. Aptamer-Modified Gold Nanoparticles for Colorimetric Determination of Platelet-Derived Growth Factors and Their Receptors. *Analytical Chemistry* **77**: 5735-5741.
- Huang, C. Z., Fan, M. K. and Li, Y. F. 2002. Fluorescence microscopic quantification of DNA with $[\alpha], [\beta], [\gamma], [\delta]$ -tetrakis[4-(trimethylammonium)phenyl] porphine by a ring-like deposition technique. *Analytica Chimica Acta*. **466**: 193-200.
- Huang, E., Zhou, F. and Deng, L. 2000. Studies of Surface Coverage and Orientation of DNA Molecules Immobilized onto Preformed Alkanethiol Self-Assembled Monolayers. *Langmuir*. **16**: 3272-3280.
- Hur, Y., Han, J., Seon, J., Pak, Y. E. and Roh, Y. 2005. Development of an SH-SAW sensor for the detection of DNA hybridization. *Sensors and Actuators A: Physical*. **120**: 462-467.
- Ikebukuro, K., Kiyohara, C. and Sode, K. 2005. Novel electrochemical sensor system for protein using the aptamers in sandwich manner. *Biosensors and Bioelectronics*. **20**: 2168-2172.
- Ion, A. C., Bakker, E. and Pretsch, E. 2001. Potentiometric Cd^{2+} -selective electrode with a detection limit in the low ppt range. *Analytica Chimica Acta*. **440**: 71-79.

- Itamar Willner, F. P. J. W. 2001. Photoelectrochemistry with Controlled DNA-Cross-Linked CdS Nanoparticle Arrays¹³. *Angewandte Chemie International Edition*. **40**: 1861-1864.
- Ito, T. 2001. Ion-channel-mimetic sensor for trivalent cations based on self-assembled monolayers of thiol-derivatized 4-acyl-5-pyrazolones on gold. *Journal of Electroanalytical Chemistry*. **495**: 87-97.
- Jayasena, S. D. 1999. Aptamers: An Emerging Class of Molecules That Rival Antibodies in Diagnostics. *Clinical Chemistry*. **45**: 1628-1650.
- Jenison, R. D., Gill, S. C., Pardi, A. and Polisky, B. 1994. High-Resolution Molecular Discrimination by RNA. *Science*. **263**: 1425-1429.
- Jhaveri, S., Rajendran, M. and Ellington, A. D. 2000. In vitro selection of signaling aptamers. *Nature Biotechnology*. **18**: 1293-1297.
- Jhaveri, S. D., Kirby, R., Conrad, R., Maglott, E. J., Bowser, M., Kennedy, R. T., Glick, G. and Ellington, A. D. 2000. Designed Signaling Aptamers that Transduce Molecular Recognition to Changes in Fluorescence Intensity. *Journal of the American Chemical Society*. **122**: 2469-2473.
- Jhaveri, S. D., Kirby, R., Conrad, R., Maglott, E. J., Bowser, M., Kennedy, R. T., Glick, G. and Ellington, A. D. 2000. Designed Signaling Aptamers that Transduce Molecular Recognition to Changes in Fluorescence Intensity. *Journal of the American Chemical Society*. **122**: 2469-2473.
- Jiang, X., Li, D., Xu, X., Ying, Y., Li, Y., Ye, Z. and Wang, J. 2008. Immunosensors for detection of pesticide residues. *Biosensors and Bioelectronics*. **23**: 1577-1587.

- Jie, M., Ming, C. Y., Jing, D., Cheng, L. S., Huai na, L., Jun, F. and Xiang, C. Y. 1999. An electrochemical impedance immunoanalytical method for detecting immunological interaction of human mammary tumor associated glycoprotein and its monoclonal antibody. *Electrochemistry Communications*. 1: 425-428.
- Jonathan S. Daniels, N. P. 2007. Label-Free Impedance Biosensors: Opportunities and Challenges. *Electroanalysis*. 19: 1239-1257.
- Junhui, Z., Hong, C. and Y, F. 1997. DNA Based Biosensors. *Biotechnology Advances*. 15: 43-58.
- Järvinen, H., Lahtinen, L., Näsman, J., Hormi, O. and Tammi, A. L. 1995. A new method to prepare 3-octylthiophene and poly-(3-octylthiophene). *Synthetic Metals*. 69: 299-300.
- Kaku, S., Nakanishi, S., Horiguchi, K. and Sato, M. 1993. Amperometric enzyme immunoassay for urinary human serum albumin using plasma-treated membrane. *Analytica Chimica Acta*. 272: 213-220.
- Kamel, A. M., Brown, P. R. and Munson, B. 1999. Electrospray Ionization Mass Spectrometry of Tetracycline, Oxytetracycline, Chlorotetracycline, Minocycline, and Methacycline. *Analytical Chemistry*. 71: 968-977.
- Kaneki, N., Xu, Y., Kumari, A., Halsall, H. B., Heineman, W. R. and Kissinger, P. T. 1994. Electrochemical enzyme immunoassay using sequential saturation technique in a 20- μ l capillary: digoxin as a model analyte. *Analytica Chimica Acta*. 287: 253-258.
- Kanungo, M., Srivastava, D. N., Kumar, A. and Contractor, A. Q. 2002. Conductimetric immunosensor based on poly(3,4-ethylenedioxythiophene). *Chemical Communications*. 680-681.

- Karin Björnhall, T. M. P. D. 2005. Comparison of different depletion strategies for improved resolution in proteomic analysis of human serum samples. *PROTEOMICS*. **5**: 307-317.
- Karlström, A. and Nygren, P. 2001. Dual Labeling of a Binding Protein Allows for Specific Fluorescence Detection of Native Protein. *Analytical Biochemistry*. **295**: 22-30.
- Katz, E., Alfonta, L. and Willner, I. 2001. Chronopotentiometry and Faradaic impedance spectroscopy as methods for signal transduction in immunosensors. *Sensors and Actuators B: Chemical*. **76**: 134-141.
- Katz, E. and Willner, I. 2003. Probing Biomolecular Interactions at Conductive and Semiconductive Surfaces by Impedance Spectroscopy: Routes to Impedimetric Immunosensors, DNA-Sensors, and Enzyme Biosensors. *Electroanalysis*. **15**: 913-947.
- Kenney, R. T., Frech, S. A., Muenz, L. R., Villar, C. P. and Glenn, G. M. 2004. Dose Sparing with Intradermal Injection of Influenza Vaccine. *New England Journal of Medicine*. **351**: 2295-2301.
- Kepka, C., Rhodin, J., Lemmens, R., Tjerneld, F., Gustavsson, P. E. 2004. Extraction of plasmid DNA from *Escherichia coli* cell lysate in a thermoseparating aqueous two- phase system. *Journal of Chromatography A* **1024**, 95-104.
- Kerman, K., Endo, T., Tsukamoto, M., Chikae, M., Takamura, Y. and Tamiya, E. 2007. Quantum dot-based immunosensor for the detection of prostate-specific antigen using fluorescence microscopy. *Talanta*. **71**: 1494-1499.

- Khan, M. A. and Musarrat, J. 2003. Interactions of tetracycline and its derivatives with DNA in vitro in presence of metal ions. *International Journal of Biological Macromolecules*. **33**: 49-56.
- Kharitonov, A. B., Alfonta, L., Katz, E. and Willner, I. 2000. Probing of bioaffinity interactions at interfaces using impedance spectroscopy and chronopotentiometry. *Journal of Electroanalytical Chemistry*. **487**: 133-141.
- Killard, A. J., Deasy, B., O'Kennedy, R. and Smyth, M. R. 1995. Antibodies: production, functions and applications in biosensors. *TrAC Trends in Analytical Chemistry*. **14**: 257-266.
- Kim, E., Kim, K., Yang, H., Kim, Y. T. and Kwak, J. 2003. Enzyme-Amplified Electrochemical Detection of DNA Using Electrocatalysis of Ferrocenyl-Tethered Dendrimer. *Analytical Chemistry*. **75**: 5665-5672.
- Kim, J. J., Nottingham, L. K., Wilson, D. M., Bagarazzi, M. L., Tsai, A., Morrison, L. D., Javadian, A., Chalian, A. A., Agadjanyan, M. G., Weiner, D. B. 1998. Engineering DNA vaccines via co-delivery of co-stimulatory molecule genes. *Vaccine* **16**, 1828-1835.
- Klammt, C., Srivastava, A., Eifler, N., Junge, F., Beyermann, M., Schwarz, D., Michel, H., Doetsch, V. and Bernhard, F. 2007. Functional analysis of cell-free-produced human endothelin B receptor reveals transmembrane segment 1 as an essential area for ET-1 binding and homodimer formation. *FEBS Journal*. **274**: 3257-3269.
- Koenig, B. and Graetzel, M. 1994. A novel immunosensor for herpes viruses. *Analytical Chemistry*. **66**: 341-344.

- Koncki, R., Owczarek, A., Dzwolak, W. and Glb, S. 1998. Immunoenzymatic sensitisation of membrane ion-selective electrodes. *Sensors and Actuators B: Chemical*. **47**: 246-250.
- Kunert, R., Gach, J. S., Vorauer-Uhl, K., Engel, E. and Katinger, H. 2006. Validated Method for Quantification of Genetically Modified Organisms in Samples of Maize Flour. *Journal of Agricultural and Food Chemistry*. **54**: 678-681.
- Kurosawa, S., Park, J.-W., Aizawa, H., Wakida, S.-I., Tao, H. and Ishihara, K. 2006. Quartz crystal microbalance immunosensors for environmental monitoring. *Biosensors and Bioelectronics*. **22**: 473-481.
- LaGier, M. J., Scholin, C. A., Fell, J. W., Wang, J. and Goodwin, K. D. 2005. An electrochemical RNA hybridization assay for detection of the fecal indicator bacterium *Escherichia coli*. *Marine Pollution Bulletin*. **50**: 1251-1261.
- Lazerges, M., Perrot, H., Antoine, E., Defontaine, A. and Compere, C. 2006. Oligonucleotide quartz crystal microbalance sensor for the microalgae *Alexandrium minutum* (Dinophyceae). *Biosensors and Bioelectronics*. **21**: 1355-1358.
- Lee, L. Y., Ong, S. L., Hu, J. Y., Ng, W. J., Feng, Y., Tan, X. and Wong, S. W. 2004. Use of Semiconductor Quantum Dots for Photostable Immunofluorescence Labeling of *Cryptosporidium parvum*. *Applied and Environmental Microbiology*. **70**: 5732-5736.
- Lei, Y., Chen, W. and Mulchandani, A. 2006. Microbial biosensors. *Analytica Chimica Acta*. **568**: 200-210.

- Lenigk, R., Liu, R. H., Athavale, M., Chen, Z., Ganser, D., Yang, J., Rauch, C., Liu, Y., Chan, B., Yu, H., Ray, M., Marrero, R. and Grodzinski, P. 2002. Plastic biochannel hybridization devices: a new concept for microfluidic DNA arrays. *Analytical Biochemistry*. **311**: 40-49.
- Li, A., Yang, F., Ma, Y. and Yang, X. 2007. Electrochemical impedance detection of DNA hybridization based on dendrimer modified electrode. *Biosensors and Bioelectronics*. **22**: 1716-1722.
- Li, Y. F., Huang, C. Z. and Li, M. 2002. Study of the interaction of Azur B with DNA and the determination of DNA based on resonance light scattering measurements. *Analytica Chimica Acta*. **452**: 285-294.
- Ligler, F., Taitt, C., Shriver-Lake, L., Sapsford, K., Shubin, Y. and Golden, J. 2003. Array biosensor for detection of toxins. *analytical and Bioanalytical Chemistry*. **377**: 469-477.
- Limbut, W., Hedström, M., Thavarungkul, P., Kanatharana, P. and Mattiasson, B. 2007. Capacitive Biosensor for Detection of Endotoxin. . *Analytical and Bioanalytical Chemistry*. **389**: 517-525.
- Limbut, W., Kanatharana, P., Mattiasson, B., Asawatreratanakul, P. and Thavarungkul, P. 2006a. A comparative study of capacitive immunosensors based on self-assembled monolayers formed from thiourea, thioctic acid, and 3-mercaptopropionic acid. *Biosensors and Bioelectronics*. **22**: 233-240.
- Limbut, W., Kanatharana, P., Mattiasson, B., Asawatreratanakul, P. and Thavarungkul, P. 2006b. A reusable capacitive immunosensor for carcinoembryonic antigen (CEA) detection using thiourea modified gold electrode. *Analytica Chimica Acta*. **561**: 55-61.

- Lin, X.-H., Wu, P., Chen, W., Zhang, Y.-F. and Xia, X.-H. 2007. Electrochemical DNA biosensor for the detection of short DNA species of Chronic Myelogenous Leukemia by using methylene blue. *Talanta*. **72**: 468-471.
- Lindsey, M. E., Meyer, M. and Thurman, E. M. 2001. Analysis of Trace Levels of Sulfonamide and Tetracycline Antimicrobials in Groundwater and Surface Water Using Solid-Phase Extraction and Liquid Chromatography/Mass Spectrometry. *Analytical Chemistry*. **73**: 4640-4646.
- Link, A. and Tempel, K. 1991. Inhibition of O6-alkylguanine-DNA alkyltransferase and DNase I activities in vitro by some alkylating substances and antineoplastic agents. *Journal of Cancer Research and Clinical Oncology*. **117**: 549-555.
- Liu, G., Wang, J., Kim, J., Jan, M. R. and Collins, G. E. 2004. Electrochemical Coding for Multiplexed Immunoassays of Proteins. *Analytical Chemistry*. **76**: 7126-7130.
- Liu, J., Lee, J. H. and Lu, Y. 2007. Quantum Dot Encoding of Aptamer-Linked Nanostructures for One-Pot Simultaneous Detection of Multiple Analytes. *Analytical Chemistry*. **79**: 4120-4125.
- Liu, J. and Lu, Y. 2004. Adenosine-Dependent Assembly of Aptazyme-Functionalized Gold Nanoparticles and Its Application as a Colorimetric Biosensor. *Analytical Chemistry*. **76**: 1627-1632.
- Lovatt, A. 2002. Applications of quantitative PCR in the biosafety and genetic stability assessment of biotechnology products. *Reviews in Molecular Biotechnology*. **82**: 279-300.
- Lu, H. C., Chen, H. M., Lin, Y. S. and Lin, J. W. 2000. A reusable and specific protein A-coated piezoelectric biosensor for flow injection immunoassay. *Biotechnology Process*. **16**: 1116-1124.

- Lundström, I. and Svensson, S. 1998. Biosensing with G-protein coupled receptor systems. *Biosensors and Bioelectronics*. **13**: 689-695.
- Luppa, P. B., Sokoll, L. J. and Chan, D. W. 2001. Immunosensors--principles and applications to clinical chemistry. *Clinica Chimica Acta*. **314**: 1-26.
- Luzi, E., Minunni, M., Tombelli, S. and Mascini, M. 2003. New trends in affinity sensing: aptamers for ligand binding. *TrAC Trends in Analytical Chemistry*. **22**: 810-818.
- Ma, Y., Zhou, M., Jin, X., Zhang, Z., Teng, X. and Chen, H. 2004. Flow-injection chemiluminescence assay for ultra-trace determination of DNA using rhodamine B-Ce(IV)-DNA ternary system in sulfuric acid media. *Analytica Chimica Acta*. **501**: 25-30.
- Ma, Z., Li, J., Liu, M., Cao, J., Zou, Z., Tu, J. and Jiang, L. 1998. Colorimetric Detection of Escherichia coli by Polydiacetylene Vesicles Functionalized with Glycolipid. *Journal of the American Chemical Society*. **120**: 12678-12679.
- Mallat, E., Barcel, D., Barzen, C., Gauglitz, G. and Abuknesha, R. 2001. Immunosensors for pesticide determination in natural waters. *TrAC Trends in Analytical Chemistry*. **20**: 124-132.
- Malon, A., Vigassy, T., Bakker, E. and Pretsch, E., 2006. Potentiometry at Trace Levels in Confined Samples: Ion-Selective Electrodes with Subfemtomole Detection Limits. *Journal of the American Chemical Society*. **128**: 8154-8155.
- Mandong, G., Yanqing, L., Hongxia, G., Xiaoqin, W. and Lifang, F. 2007. Electrochemical detection of short sequences related to the hepatitis B virus using MB on chitosan-modified CPE. *Bioelectrochemistry*. **70**: 245-249.

- Mansfeld, F., Han, L. T., Lee, C.C., Zhang, G. 1998. Evaluation of corrosion protection by polymer coatings using electrochemical impedance spectroscopy and noise analysis. *Electrochimica Acta*. **43**: 2933-2495.
- Marco, M. P. and Barcel, D. 1996. Environmental applications of analytical biosensors. *Measurement Science and Technology*. **7**: 1547-1562.
- Marrazza, G., Chianella, I. and Mascini, M. 1999. Disposable DNA electrochemical biosensors for environmental monitoring. *Analytica Chimica Acta*. **387**: 297-307.
- Mattiasson, B. 1984. Immunochemical assays for process control: potentials and limitations. *Trends in Analytical Chemistry*. **2**: 245-250.
- McCauley, T. G., Hamaguchi, N. and Stanton, M., 2003. Aptamer-based biosensor arrays for detection and quantification of biological macromolecules. *Analytical Biochemistry*. **319**: 244-250.
- McDonnell, J. M. 2001. Surface plasmon resonance: towards an understanding of the mechanisms of biological molecular recognition. *Current Opinion in Chemical Biology*. **5**: 572-577.
- McKnight, R. E., Zhang, J. and Dixon, D. W. 2004. Binding of a homologous series of anthraquinones to DNA. *Bioorganic & Medicinal Chemistry Letters*. **14**: 401-404.
- Medyantseva, E. P., Khaldeeva, E. V. and Budnikov, G. K. 2001. Immunosensors in Biology and Medicine: Analytical Capabilities, Problems, and Prospects. *Journal of Analytical Chemistry*. **56**: 886-900.

- Mello, L. D. and Kubota, L. T. 2002. Review of the use of biosensors as analytical tools in the food and drink industries. *Food Chemistry*. **77**: 237-256.
- Meric, B., Kerman, K., Ozkan, D., Kara, P., Erensoy, S., Akarca, U. S., Mascini, M. and Ozsoz, M. 2002. Electrochemical DNA biosensor for the detection of TT and Hepatitis B virus from PCR amplified real samples by using methylene blue. *Talanta*. **56**: 837-846.
- Miao, Y., Cui, T., Leng, F. and Wilson, W. D. 2008. Inhibition of high-mobility-group A2 protein binding to DNA by netropsin: A biosensor-surface plasmon resonance assay. *Analytical Biochemistry*. **374**: 7-15.
- Michalzik, M., Wendler, J., Rabe, J., Böttgenbach, S. and Bilitewski, U. 2005. Development and application of a miniaturised quartz crystal microbalance (QCM) as immunosensor for bone morphogenetic protein-2. *Sensors and Actuators B: Chemical*. **105**: 508-515.
- Middaugh, C. R., Evans, R. K., Montgomery, D.L. Casimiro, D. R. 1998. Analysis of plasmid DNA from a pharmaceutical perspective. *Journal of Pharmaceutical Sciences* **87**, 130-146.
- Millan, K. M. and Susan, R. M. 1993. Sequence-selective biosensor for DNA based on electroactive hybridization indicators. *Analytical Chemistry*. **2317-2313**
- Miller, J. C. and Miller, J. N. 1993. *Statistics for Analytical Chemistry*, third edition. Simon&Schuster International Group. West Sussex.
- Minunni, M., Tombelli, S., Gullotto, A., Luzzi, E. and Mascini, M. 2004. Development of biosensors with aptamers as bio-recognition element: the case of HIV-1 Tat protein. *Biosensors and Bioelectronics*. **20**: 1149-1156.
- Mir, M., Vreeke, M. and Katakis, I. 2006. Different strategies to develop an electrochemical thrombin aptasensor. *Electrochemistry Communications*. **8**: 505-511.

- Mir, M. n. and Katakis, I. 2008. Target label-free, reagentless electrochemical DNA biosensor based on sub-optimum displacement. *Talanta*. **75**: 432-441.
- Moeder, M., Schrader, S., Winkler, M. and Popp, P. 2000. Solid-phase microextraction-gas chromatography-mass spectrometry of biologically active substances in water samples. *Journal of Chromatography A*. **873**: 95-106.
- Morgan, C. L., Newman, D. J. and Price, C. P. 1996. Immunosensors: technology and opportunities in laboratory medicine. *Clinical Chemistry*. **42**: 193-209.
- Mu, Y., Zhang, H., Zhao, X., Song, D., Wang, Z., Sun, J., Li, M. and Jin, Q. 2001. An optical biosensor for monitoring antigen recognition based on surface plasmon resonance using avidin-biotin system. *Sensors*. **1**: 91-101.
- Muhammad-Tahir, Z. and Alocilja, E. C. 2003. A conductometric biosensor for biosecurity. *Biosensors and Bioelectronics*. **18**: 813-819.
- Murry, K. Vidali, G., Neelin, J.M. 1968. The stepwise removal of histone from chicken erythrocyte nucleoprotein. *The Biochemical Journal* **107**. 207-215.
- Navrátilove, I. and Skládal, P. 2004. The immunosensors for measurement of 2,4-dichlorophenoxyacetic acid based on electrochemical impedance spectroscopy. *Bioelectrochemistry*. **62**: 11-18.
- Nawaz, H., Rauf, S., Akhtar, K. and Khalid, A. M. 2006. Electrochemical DNA biosensor for the study of ciprofloxacin-DNA interaction. *Analytical Biochemistry*. **354**: 28-34.

- Ngundi, M. M., Taitt, C. R., McMurry, S. A., Kahne, D. and Ligler, F. S. 2006. Detection of bacterial toxins with monosaccharide arrays. *Biosensors and Bioelectronics*. **21**: 1195-1201.
- Nguyen, B., Tanious, F. A. and Wilson, W. D. 2007. Biosensor-surface plasmon resonance: Quantitative analysis of small molecule-nucleic acid interactions. *Methods*. **42**: 150-161.
- Niu, S., Singh, G. and Saraf, R. F. 2007. Label-less fluorescence-based method to detect hybridization with applications to DNA micro-array. *Biosensors and Bioelectronics*. **23**: 714-720.
- Noites, I.S., O'Kennedy, R.D., Levy, M.S., Abidi, N., Keshvarz-Moore, E. 1999. Rapid quantitation and monitoring of plasmid DNA using an ultrasensitive DNA-binding dye. *Biotechnology and Bioengineering* **66**, 195-201.
- Nozal, L., Arce, L., Simonet, B. M., Ros, A. and Valcarcel, M. 2004. Rapid determination of trace levels of tetracyclines in surface water using a continuous flow manifold coupled to a capillary electrophoresis system. *Analytica Chimica Acta*. **517**: 89-94.
- Nuzzo, R. G. and Allara, D. L. 1983. Adsorption of bifunctional organic disulfides on gold surfaces. *Journal of the American Chemical Society*. **105**: 4481-4483.
- Ohmichi, T., Kawamoto, Y., Wu, P., Miyoshi, D., Karimata, H. and Sugimoto, N. 2005. DNA-Based Biosensor for Monitoring pH in Vitro and in Living Cells. *Biochemistry*. **44**: 7125-7130.
- Oillic, C., Mur, P., Blanquet, E., Delapierre, G., Vinet, F. and Billon, T. 2007. DNA microarrays on silicon nanostructures: Optimization of the multilayer stack for fluorescence detection. *Biosensors and Bioelectronics*. **22**: 2086-2092.

- Oka, H., Ito, Y. and Matsumoto, H. 2000. Chromatographic analysis of tetracycline antibiotics in foods. *Journal of Chromatography A*. **882**: 109-133.
- Oliveira-Brett, A. and da Silva, L. 2002. A DNA-electrochemical biosensor for screening environmental damage caused by s-triazine derivatives. *analytical and Bioanalytical Chemistry*. **373**: 717-723.
- Orazio, P. D. 2003. Review Biosensors in clinical chemistry. *Clinica Chimica Acta*. **334**: 41-69.
- Osborne, S. E., Matsumura, I. and Ellington, A. D. 1997. Aptamers as therapeutic and diagnostic reagents: problems and prospects. *Current Opinion in Chemical Biology*. **1**: 5-9.
- O'Sullivan, C. 2002. Aptasensors - the future of biosensing? *analytical and Bioanalytical Chemistry*. **372**: 44-48.
- Packirisamy, S. and Kolb, D. M. 1996. Reconstruction phenomena at metal-electrolyte interfaces. *Progress in Surface Science*. **51**: 109-173.
- Palecek, E. and Fojta, M. 1994. Differential Pulsed Voltammetric Determination of RNA at the Picomole Level in the Presence of DNA and Nucleic Acid Components. *Analytical Chemistry* **6**: 1566-1571.
- Pandolfi, P. P. 2001. Transcription therapy for cancer. *Oncogene*. **20**: 3116-3127.
- Pang, D.-W., Zhang, M., Wang, Z.-L., Qi, Y.-P., Cheng, J.-K. and Liu, Z.-Y. 1996. Modification of glassy carbon and gold electrodes with DNA. *Journal of Electroanalytical Chemistry*. **403**: 183-188.
- Park, S.-M. and Yoo, J., -S. 2003. Electrochemical impedance spectroscopy for better electrochemical measurements. *Analytical Chemistry*. **1**: 455A-461A.

- Patel, D. J. and Suri, A. K. 2000. Structure, recognition and discrimination in RNA aptamer complexes with cofactors, amino acids, drugs and aminoglycoside antibiotics. *Reviews in Molecular Biotechnology*. **74**: 39-60.
- Pattnaik, P. 2005. Surface Plasmon Resonance. *Applied Biochemistry and Biotechnology* **126**: 79-92.
- Peano, C., Samson, M. C., Palmieri, L., Gulli, M. and Marmiroli, N. 2004. Qualitative and Quantitative Evaluation of the Genomic DNA Extracted from GMO and Non-GMO Foodstuffs with Four Different Extraction Methods. *Journal of American Chemical Society*. **52**: 6962-6968.
- Peng, H., Soeller, C., Vigar, N. A., Caprio, V. and Travas-Sejdic, J. 2007. Label-free detection of DNA hybridization based on a novel functionalized conducting polymer. *Biosensors and Bioelectronics*. **22**: 1868-1873.
- Pestourie, C., Tavitian, B. and Duconge, F. 2005. Aptamers against extracellular targets for in vivo applications. *Biochimie*. **87**: 921-930.
- Piedade, J. A. P., Fernandes, I. R. and Oliveira-Brett, A. M. 2002. Electrochemical sensing of DNA-adriamycin interactions. *Bioelectrochemistry*. **56**: 81-83.
- Pinar, K., Burcu, M., Aysin, Z. and Mehmet O. 2004. Electrochemical DNA biosensor for the detection and discrimination of herpes simplex Type I and Type II viruses from PCR amplified real samples *Analytica Chimica Acta*. **518**: 69-76.
- Plieva, F.M., Karlsson, M., Aguilar, M.-R., Gomez, D., Mikhalovsky, S., Galaev, I. Yu. 2005. Pore structure in supermacroporous polyacrylamide based cryogels *Soft Matter* **1**, 303-309.

- Plieva, F.M., Savina, I.N., Deraz, S., Andersson, J., Galaev, I.Yu, Mattiasson, B. 2004. Characterization of supermacroporous monolithic polyacrylamide based matrices designed for chromatography of bioparticles. *Journal of Chromatography B* 807 1, 129–137.
- Polsky, R., Gill, R., Kaganovsky, L. and Willner, I. 2006. Nucleic Acid-Functionalized Pt Nanoparticles: Catalytic Labels for the Amplified Electrochemical Detection of Biomolecules. *Analytical Chemistry*. **78**: 2268-2271.
- Porter, M. D., Bright, T. B., Allara, D. L. and Chidsey, C. E. D. 1987. Spontaneously organized molecular assemblies. 4. Structural characterization of n-alkyl thiol monolayers on gold by optical ellipsometry, infrared spectroscopy, and electrochemistry. *Journal of the American Chemical Society*. **109**: 3559-3581.
- Prazeres, D. M.F., Moteiro, G. A., Ferreira, G.N. M., Diogo, M. M., Ribeiro, S.C., Cabral, J.M.S. 2001. Purification of plasmids for gene therapy and DNA vaccination. *Biotechnology Annual Review* **7**, 1-30.
- Prem Kumar, A. A., Mani, K. R., Palaniappan, C., Bhau, L. N. R. and Swaminathan, K. 2005. Purification, potency and immunogenicity analysis of Vero cell culture-derived rabies vaccine: a comparative study of single-step column chromatography and zonal centrifuge purification. *Microbes and Infection*. **7**: 1110-1116.
- Projan, S. J., Carleton, S. and Novick, R. P. 1983. Determination of plasmid copy number by fluorescence densitometry. *Plasmid*. **9**: 182-190.
- Pumera, M., Castaneda, M. T., Pividori, M. I., Eritja, R., Merkoci, A. and Alegret, S. 2005. Magnetically Triggered Direct Electrochemical Detection of DNA Hybridization Using Au67 Quantum Dot as Electrical Tracer. *Langmuir*. **21**: 9625-9629.

- Rabbany, R. Y., Donner, B. L. and Ligler, F. S., 1994. Optical Immunosensors. *Critical Review in Biomedical Engineering*. **22**: 307-346.
- Radi, A. E., AceroSanchez, J. L., Baldrich, E. and O'Sullivan, C. K. 2005. Reusable Impedimetric Aptasensor. *Analytical Chemistry*. **77**: 6320-6323.
- Radi, A. E., AceroSanchez, J. L., Baldrich, E. and O'Sullivan, C. K. 2006b. Reagentless, Reusable, Ultrasensitive Electrochemical Molecular Beacon Aptasensor. *Journal of the American Chemical Society*. **128**: 117-124.
- Radi, M. C., Osalivan, C.K. 2006a. Aptamer conformational switch as sensitive electrochemical biosensor for potassium ion recognition. *Chemical Communications*. 3432-3434.
- Rahman, M. A., Shiddiky, M. J. A., Park, J.-S. and Shim, Y.-B. 2007. An impedimetric immunosensor for the label-free detection of bisphenol A. *Biosensors and Bioelectronics*. **22**: 2464-2470.
- Ramanaviciene, A. and Ramanavicius, A. 2004. Pulsed amperometric detection of DNA with an ssDNA/polypyrrole-modified electrode. *Analytical and Bioanalytical Chemistry*. **379**: 287-293.
- Ramanavicius, A., Kurilcik, N., Jursenas, S., Finkelsteinas, A. and Ramanaviciene, A., 2007. Conducting polymer based fluorescence quenching as a new approach to increase the selectivity of immunosensors. *Biosensors and Bioelectronics*. **23**: 499-505.
- Rauf, S., Nawaz, H., Akhtar, K., Ghauri, M. A. and Khalid, A. M. 2007. Studies on sildenafil citrate (Viagra) interaction with DNA using electrochemical DNA biosensor. *Biosensors and Bioelectronics*. **22**: 2471-2477.

- Record, M. T., deHaseth, P. L., Lohman, T.M. 1977. Interpretation of monovalent and divalent cation effect on the *lac* repressor-operator interaction. *Biochemistry* **16**; 4791- 4796.
- Reece, R. J. 2004. *Analysis of Genes and Genomes*. John Wiley & Sons Ltd. West Sussex, England
- Reverté, S., Borrull, F., Pocurull, E. and Marcé, o. M. 2003. Determination of antibiotic compounds in water by solid-phase extraction-high-performance liquid chromatography-(electrospray) mass spectrometry. *Journal of Chromatography A*. **1010**: 225-232.
- Ricci, F., Volpe, G., Micheli, L. and Palleschi, G. 2007. A review on novel developments and applications of immunosensors in food analysis. *Analytica Chimica Acta*. **605**: 111-129.
- Riepl, M., Mirsky, V. M., Novotny, I., Tvarozek, V., Rehacek, V. and Wolfbeis, O. S. 1999. Optimization of capacitive affinity sensors: drift suppression and signal amplification. *Analytica Chimica Acta*. **392**: 77-84.
- Rodriguez, M. C., Kawde, A-N., Wang, J. 2005. Aptamer biosensor for label-free impedimetric detection of proteins based on recognition-induced switching of the surface charge. *Chemical Communication*. 4267-4269.
- Rogers, K. 2000. Principles of affinity-based biosensors. *Molecular Biotechnology*. **14**: 109-129.
- Rogers, K. R., Fernando, J. C., Thompson, R. G., Valdes, J. J. and Eldefrawi, M. E. 1992. Detection of nicotinic receptor ligands with a light addressable potentiometric sensor. *Analytical Biochemistry*. **202**: 111-116.

- Rubanova, N., Chumbimuni-Torres, K. and Bakker, E. 2007. Solid-contact potentiometric polymer membrane microelectrodes for the detection of silver ions at the femtomole level. *Sensors and Actuators B: Chemical*. **121**: 135-141.
- Ryan Preston, R. and McFadden, P. N. 2001. A two-cell biosensor that couples neuronal cells to optically monitored fish chromatophores. *Biosensors and Bioelectronics*. **16**: 447-455.
- Samuel, M., Lu, M., Pachuk, C. J. and Satishchandran, C. 2003. A spectrophotometric method to quantify linear DNA. *Analytical Biochemistry*. **313**: 301-306.
- Santiago Valverde, R., Sanchez Prez, I., Franceschelli, F., Martínez Galera, M. and Gil Garça, M. D. 2007. Determination of photoirradiated tetracyclines in water by high-performance liquid chromatography with chemiluminescence detection based reaction of rhodamine B with cerium (IV). *Journal of Chromatography A*. **1167**: 85-94.
- Schmickler, W., 1996. Electronic Effects in the Electric Double Layer. *Chemical Review*. **96**: 3177-3200.
- Schmidt, P. M., Lehmann, C., Matthes, E. and Bier, F. F. 2002. Detection of activity of telomerase in tumor cells using fiber optical biosensors. *Biosensors and Bioelectronics*. **17**: 1081-1087.
- Schmidt T, Friehs K, Flaschel E. 1996. Rapid determination of plasmid copy number. *Journal of Biotechnology* **49**:219-229.
- Schürer, H., Stembera, K., Knoll, D., Mayer, G. n., Blind, M., Forster, H.-H., Famulok, M., Welzel, P. and Hahn, U. 2001. Aptamers that bind to the antibiotic moenomycin A. *Bioorganic & Medicinal Chemistry*. **9**: 2557-2563.

- Sergeyeva, T. A., Lavrik, N. V., Rachkov, A. E., Kazantseva, Z. I. and El'skaya, A. V. 1998. An approach to conductometric immunosensor based on phthalocyanine thin film. *Biosensors and Bioelectronics*. **13**: 359-369.
- Shankaran, D. R., Gobi, K. V. and Miura, N. 2007. Recent advancements in surface plasmon resonance immunosensors for detection of small molecules of biomedical, food and environmental interest. *Sensors and Actuators B: Chemical*. **121**: 158-177.
- Shen, G., Wang, H., Tan, S., Li, J., Shen, G. and Yu, R. 2005. Detection of antisperma antibody in human serum using a piezoelectric immunosensor based on mixed self-assembled monolayers. *Analytica Chimica Acta*. **540**: 279-284.
- Shin, J., Wood, D., Robertson, J., Minor, P. and Peden, K. 2007. WHO informal consultation on the application of molecular methods to assure the quality, safety and efficacy of vaccines, Geneva, Switzerland, 7-8 April 2005. *Biologicals*. **35**: 63-71.
- Skládal, P., Riccardi, C. d. S., Yamanaka, H. and da Costa, P. I. 2004. Piezoelectric biosensors for real-time monitoring of hybridization and detection of hepatitis C virus. *Journal of Virological Methods*. **117**: 145-151.
- Samuel, M., Lu, M., Pachuk, C. J., Satishchandran, C. 2003. A spectrophotometric method to quantify linear DNA. *Analytical Biochemistry* **312**, 301-306.
- Song, X. and Swanson, B. I. 1999. Direct, Ultrasensitive, and Selective Optical Detection of Protein Toxins Using Multivalent Interactions. *Analytical Chemistry* **71**: 2097-2107.
- Stadtherr, K., Wolf, H. and Lindner, P. 2005. An Aptamer-Based Protein Biochip. *Analytical Chemistry*. **77**: 3437-3443.

- Stojanovic, M. N., de Prada, P. and Landry, D. W. 2001. Aptamer-Based Folding Fluorescent Sensor for Cocaine. *Journal of the American Chemical Society*. **123**: 4928-4931.
- Stojanovic, M. N. and Landry, D. W. 2002. Aptamer-Based Colorimetric Probe for Cocaine. *Journal of the American Chemical Society*. **124**: 9678-9679.
- Storhoff, J. J., Marla, S. S., Bao, P., Hagenow, S., Mehta, H., Lucas, A., Garimella, V., Patno, T., Buckingham, W., Cork, W. and Müller, U. R. 2004. Gold nanoparticle-based detection of genomic DNA targets on microarrays using a novel optical detection system. *Biosensors and Bioelectronics*. **19**: 875-883.
- Stumpf, M., Ternes, T. A., Wilken, R.-D., Silvana Vianna, R. and Baumann, W. 1999. Polar drug residues in sewage and natural waters in the state of Rio de Janeiro, Brazil. *The Science of The Total Environment*. **225**: 135-141.
- Su, X., Chew, F. T. and Li, S. F. Y. 1999. Self-Assembled Monolayer-Based Piezoelectric Crystal Immunosensor for the Quantification of Total Human Immunoglobulin E. *Analytical Biochemistry*. **273**: 66-72.
- Subrahmanyam, S., Piletsky, S. A. and Turner, A. P. F. 2002. Application of Natural Receptors in Sensors and Assays. *Analytical Chemistry*. **74**: 3942-3951.
- Suckow, J., Markiewicz, P., Kleina, L.G., Miller, J. Kisters-Woike, B., Muller-Hill, B. 1996. Genetic studies of the lac repressor XV: 4000 single amino acid substitutions and analysis of the resulting phenotypes on the basis of the protein structure. *Journal of Molecular Biology* **261**, 509-523.
- Sung, J. H., Ko, H. J. and Park, T. H. 2006. Piezoelectric biosensor using olfactory receptor protein expressed in Escherichia coli. *Biosensors and Bioelectronics*. **21**: 1981-1986.

- Sung, J. H., Ko, H. J. and Park, T. H. 2006. Piezoelectric biosensor using olfactory receptor protein expressed in *Escherichia coli*. *Biosensors and Bioelectronics*. **21**: 1981-1986.
- Suri, C. R., Jain, P. K. and Mishra, G. C. 1995. Development of piezoelectric crystal based microgravimetric immunoassay for determination of insulin concentration. *Journal of Biotechnology*. **39**: 27-34.
- Swartz, M. E. and Krull, I.S. 1997. *Analytical Method development and validation*. New York. Marcel Dekker, INC
- Tajima, I., Asami, O. and Sugiura, E. 1998. Monitor of antibodies in human saliva using a piezoelectric quartz crystal biosensor. *Analytica Chimica Acta*. **365**: 147-149.
- Tang, D., Yuan, R., Chai, Y., Dai, J., Zhong, X. and Liu, Y. 2004. A novel immunosensor based on immobilization of hepatitis B surface antibody on platinum electrode modified colloidal gold and polyvinyl butyral as matrices via electrochemical impedance spectroscopy. *Bioelectrochemistry*. **65**: 15-22.
- Taverniers, I., De Loose, M. and Van Bockstaele, E. 2004. Trends in quality in the analytical laboratory. II. Analytical method validation and quality assurance. *TrAC Trends in Analytical Chemistry*. **23**: 535-552.
- Tereshko, V., Skripkin, E. and Patel, D. J. 2003. Encapsulating Streptomycin within a Small 40-mer RNA. *Chemistry and Biology*. **10**: 175-187.
- Ternes, T., Bonerz, M. and Schmidt, T. 2001. Determination of neutral pharmaceuticals in wastewater and rivers by liquid chromatography-electrospray tandem mass spectrometry. *Journal of Chromatography A*. **938**: 175-185.

- Ternes, T. A., Hirsch, R., Mueller, J. and Haberer, K. 1998. Methods for the determination of neutral drugs as well as betablockers and β_2 -sympathomimetics in aqueous matrices using GC/MS and LC/MS/MS. *Fresenius' Journal of Analytical Chemistry*. **362**: 329-340.
- Thavarungkul, P., Dawan, S., Kanatharana, P. and Asawatreratanakul, P. 2007. Detecting penicillin G in milk with impedimetric label-free immunosensor. *Biosensors and Bioelectronics*. **23**: 688-694.
- Thurer, R., Vigassy, T., Hirayama, M., Wang, J., Bakker, E. and Pretsch, E. 2007. Potentiometric Immunoassay with Quantum Dot Labels. *Analytical Chemistry*. **79**: 5107-5110.
- Thévenot, D. R., Toth, K., Durst, R. A. and Wilson, G. S. 1999. Electrochemical biosensors: recommended definitions and classification. *Pure and Applied Chemistry*. **77**: 2333-2348.
- Thévenot, D. R., Toth, K., Durst, R. A. and Wilson, G. S. 2001. Electrochemical biosensors: recommended definitions and classification. *Biosensors and Bioelectronics*. **16**: 121-131.
- Tombelli, S., Minunni, M. and Mascini, M. 2005a. Analytical applications of aptamers. *Biosensors and Bioelectronics*. **20**: 2424-2434.
- Tombelli, S., Minunni, M., Luzi, E. and Mascini, M. 2005b. Aptamer-based biosensors for the detection of HIV-1 Tat protein. *Bioelectrochemistry*. **67**: 135-141.
- Tombelli, S., Minunni, M. and Mascini, M. 2005c. Piezoelectric biosensors: Strategies for coupling nucleic acids to piezoelectric devices. *Methods*. **37**: 48-56.

- Tuerk, C. and Gold, L. 1990. Systematic Evolution of Ligands by Exponential Enrichment: RNA Ligands to Bacteriophage T4 DNA Polymerase. *Science*. **249**: 505-510.
- Turner, A. P. F., Isao, K. and George, S. W. 1987. *Biosensors fundamentals and application* : Oxford Oxford University Press
- Uedaira, H., Kidokoro, S., Ohgiya, S., Ishizaki, K., Shinriki N. 1994. Thermal transition of plasmid pBR332 closed circular, open circular and linear DNAs, *Thermochimica Acta* **232**, 7-18.
- Uto, M., Michaelis, E.K., Hu, I.E., Umezawa, Y., Kuwana, T. 1990. Biosensor Development with a Glutamate Receptor Ion-Channel Reconstituted in a Lipid Bilayer. *Analytical Science*. **2**: 221-225.
- Vagin, M. Y., Karyakin, A. A. and Hianik, T. 2002. Surfactant bilayers for the direct electrochemical detection of affinity interactions. *Bioelectrochemistry*. **56**: 91-93.
- Vaisocherovii, H., Mrkvovii, K., Piliarik, M., Jinoch, P., Steinbachovii, M. and Homola, J. 2007. Surface plasmon resonance biosensor for direct detection of antibody against Epstein-Barr virus. *Biosensors and Bioelectronics*. **22**: 1020-1026.
- Vestergard, M., Kerman, K., Tamiya, E. 2007. An overview of Label-free Electrochemical Protein Sensor. *Sensors*. **7**: 3442-3458.
- Vongsavatsot, N. 2008. *Analysis of Tetracycline Antibiotics in Animal Tissues by High Performance Liquid Chromatography*. Master of Science Thesis, Prince of Songkla University.

- Vollenhofer, S., Burg, K., Schmidt, J. and Kroath, H. 1999. Genetically Modified Organisms in Food-Screening and Specific Detection by Polymerase Chain Reaction. *Journal of Agricultural and Food Chemistry*. **47**: 5038-5043.
- Wadu-Mesthrige, K., Amro, N. A. and Liu, G. Y. 2000. Immobilization of proteins on self-assembled monolayers. *Scanning*. **22**: 380-388.
- Wahlund, P. -O., Gustavsson, P. E., Izumrudov, V.A., Larsson, P. O., Galaev, I. Y. 2004. Polyelectrolyte complexes as tool for purification of plasmid DNA background and development. *Journal of Chromatography B* **807**,121-127.
- Wan, G.-H., Cui, H., Zheng, H.-S., Zhou, J., Liu, L.-J. and Yu, X.-F. 2005. Determination of tetracyclines residues in honey using high-performance liquid chromatography with potassium permanganate-sodium sulfite-[beta]-cyclodextrin chemiluminescence detection. *Journal of Chromatography B*. **824**: 57-64.
- Wang, J. 1985. *Stripping Analysis*.; VCH: New York.
- Wang, J. 1999. Electroanalysis and Biosensors. *Analytical Chemistry*. **71**: 328-332.
- Wang, J. 2000. Analytical Electrochemistry. New York: John, Wiley & Sons
- Wang, J. 2000. SURVEY AND SUMMARY: From DNA biosensors to gene chips. *Nucleic Acids Research*. **28**: 3011-3016.
- Wang, J., 2003. Nanoparticle-based electrochemical DNA detection. *Analytica Chimica Acta*. **500**: 247-257.
- Wang, J., Chicharro, M., Rivas, G., Cai, X., Dontha, N., Farias, P. A. M. and Shiraishi, H. 1996. DNA Biosensor for the Detection of Hydrazines. *Analytical Chemistry* **68**: 2251-2254.

- Wang, J., Kawde, A.-N. and Jan, M. R. 2004. Carbon-nanotube-modified electrodes for amplified enzyme-based electrical detection of DNA hybridization. *Biosensors and Bioelectronics*. **20**: 995-1000.
- Wang, J., Liu, G., Polsky, R. and Merkoi, A. 2002. Electrochemical stripping detection of DNA hybridization based on cadmium sulfide nanoparticle tags. *Electrochemistry Communications*. **4**: 722-726.
- Wang, J., Polsky, R. and Xu, D. 2001. Silver-Enhanced Colloidal Gold Electrochemical Stripping Detection of DNA Hybridization. *Langmuir*. **17**: 5739-5741.
- Wang, J., Rivas, G., Cai, X., Palecek, E., Nielsen, P., Shiraishi, H., Dontha, N., Luo, D., Parrado, C., Chicharro, M., Farias, P. A. M., Valera, F. S., Grant, D. H., Ozsoz, M. and Flair, M. N. 1997. DNA electrochemical biosensors for environmental monitoring. A review. *Analytica Chimica Acta*. **347**: 1-8.
- Wang, J. K., Li, J. L., Li, M. L., Hua, D. and Chen, H. M. 2006. Assay of DNA-binding proteins with a dsDNA-coupled plate. *Clinical Biochemistry*. **39**: 167-175.
- Wang, R.-Y., Gao, X. and Lu, Y.-T. 2005. A surfactant enhanced stopped-flow kinetic fluorimetric method for the determination of trace DNA. *Analytica Chimica Acta*. **538**: 151-158.
- Wang, X., Zhou, J., Yun, W., Xiao, S., Chang, Z., He, P. and Fang, Y. 2007. Detection of thrombin using electrogenerated chemiluminescence based on Ru(bpy)₃²⁺-doped silica nanoparticle aptasensor via target protein-induced strand displacement. *Analytica Chimica Acta*. **598**: 242-248.

- Wen, J. D., Gray, C. W. and Gray, D. M. 2001. SELEX Selection of High-Affinity Oligonucleotides for Bacteriophage Ff Gene 5 Protein. *Biochemistry*. **40**: 9300-9310.
- Wendler, J., Hoffmann, A., Gross, G., Weich, H. A. and Bilitewski, U. 2005. Development of an enzyme-linked immunoreceptor assay (ELIRA) for quantification of the biological activity of recombinant human bone morphogenetic protein-2. *Journal of Biotechnology*. **119**: 425-435.
- WHO, 1987. Acceptability of cell substrate for production of biological. 747, 1-29.
- WHO, 1998. WHO Requirements for the Use of Animal Cells asin vitroSubstrates for the Production of Biologicals (Requirements for Biological Substances No. 50). *Biologicals*. **26**: 175-193.
- Wilson, C., Nix, J. and Szostak, J. 1998. Functional Requirements for Specific Ligand Recognition by a Biotin-Binding RNA Pseudoknot. *Biochemistry*. **37**: 14410-14419.
- Winkler, M., Lawrence, J. R. and Neu, T. R. 2001. Selective degradation of ibuprofen and clofibric acid in two model river biofilm systems. *Water Research*. **35**: 3197-3205.
- Wrobel, N. 2001. Optimization of Interfaces for Genosensor Base on Thiol Layers on Gold Films. Diploma Thesis of Chemie and Phamazie der Universitat Regensburge, Rengensburge Universiity, Regensburge.
- Wu, S., Zhao, H., Ju, H., Shi, C. and Zhao, J. 2006. Electrodeposition of silver-DNA hybrid nanoparticles for electrochemical sensing of hydrogen peroxide and glucose. *Electrochemistry Communications*. **8**: 1197-1203.

- Wu, Z. S., Guo, M. M., Zhang, S. B., Chen, C. R., Jiang, J. H., Shen, G. L. and Yu, R. Q. 2007. Reusable Electrochemical Sensing Platform for Highly Sensitive Detection of Small Molecules Based on Structure-Switching Signaling Aptamers. *Analytical Chemistry*. **79**: 2933-2939.
- Wu, Z.-S., Li, J.-S., Deng, T., Luo, M.-H., Shen, G.-L. and Yu, R.-Q. 2005. A sensitive immunoassay based on electropolymerized films by capacitance measurements for direct detection of immunospecies. *Analytical Biochemistry*. **337**: 308-315.
- Xiao, Y., Piorek, B. D., Plaxco, K. W. and Heeger, A. J. 2005. A Reagentless Signal-On Architecture for Electronic, Aptamer-Based Sensors via Target-Induced Strand Displacement. *Journal of the American Chemical Society*. **127**: 17990-17991.
- Xu, D., Xu, D., Yu, X., Liu, Z., He, W. and Ma, Z. 2005. Label-Free Electrochemical Detection for Aptamer-Based Array Electrodes. *Analytical Chemistry*. **77**: 5107-5113.
- Yagiuda, K., Hemmi, A., Ito, S., Asano, Y., Fushinuki, Y., Chen, C.-Y. and Karube, I. 1996. Development of a conductivity-based immunosensor for sensitive detection of methamphetamine (stimulant drug) in human urine. *Biosensors and Bioelectronics*. **11**: 703-707.
- Yang, S., Cha, J. and Carlson, K. 2005. Simultaneous extraction and analysis of 11 tetracycline and sulfonamide antibiotics in influent and effluent domestic wastewater by solid-phase extraction and liquid chromatography-electrospray ionization tandem mass spectrometry. *Journal of Chromatography A*. **1097**: 40-53.

- Yang, V. C. and Ngo, T. T. 2000. *Biosensor and their applications*. New York, Kluwer academic/plenum publisher.
- Yeh, H.-C., Ho, Y.-P. and Wang, T.-H. 2005. Quantum dot-mediated biosensing assays for specific nucleic acid detection. *Nanomedicine: Nanotechnology, Biology and Medicine*. 1: 115-121.
- Yoshikawa, Y., Velichko, Y.S., Ichoba, Y., Yoshikawa, K. 2001. Self-assemble pearling structure of long duplex DNA with histone H1. *European Journal of Biochemistry* 268, 2593-2599.
- Xiao, Y., Arica, A., Lubin, A. J., Heeger, K. and Plaxco, W. 2005. Label-Free Electronic Detection of Thrombin in Blood Serum by Using an Aptamer-Based Sensor13. *Angewandte Chemie International Edition*. 44: 5456-5459.
- Xu, Y., Yang, L., Ye, X., He, P and Fang, Y. 2006. An Aptamer-Based Protein Biosensor by Detecting the Amplified Impedance Signal. *Electroanalysis*. 18: 1449-1456.
- Yu Qin, S. P. E. B., 2002. Plasticizer-Free Polymer Membrane Ion-Selective Electrodes Containing a Methacrylic Copolymer Matrix. *Electroanalysis*. 14: 1375-1381.
- Zayats, M., Huang, Y., Gill, R., Ma, C. a. and Willner, I. 2006. Label-Free and Reagentless Aptamer-Based Sensors for Small Molecules. *Journal of the American Chemical Society*. 128: 13666-13667.
- Zezza, F., Pascale, M., Mul, G. and Visconti, A. 2006. Detection of *Fusarium culmorum* in wheat by a surface plasmon resonance-based DNA sensor. *Journal of Microbiological Methods*. 66: 529-537.

- Zhang, L., Nolan, E., Kreitschitz, S., Rabussay, D. P. 2002. Enhanced delivery of naked DNA to the skin by non-invasive in vivo electroporation. *Biochimica et Biophysica Acta* **1572**, 1-9.
- Zhai, J., Cui, H. and Yang, R. 1997. DNA based biosensors. *Biotechnology Advances*. **15**: 43-58.
- Zhou, X., Liu, L., Hu, M., Wang, L. and Hu, J. 2002. Detection of hepatitis B virus by piezoelectric biosensor. *Journal of Pharmaceutical and Biomedical Analysis*. **27**: 341-345.
- Zhu, J., Snow, D. D., Cassada, D. A., Monson, S. J. and Spalding, R. F. 2001. Analysis of oxytetracycline, tetracycline, and chlortetracycline in water using solid-phase extraction and liquid chromatography-tandem mass spectrometry. *Journal of Chromatography A*. **928**: 177-186.
- Zhu, L., Ang, S. and Liu, W.-T. 2004. Quantum Dots as a Novel Immunofluorescent Detection System for *Cryptosporidium parvum* and *Giardia lamblia*. *Applied and Environmental Microbiology*. **70**: 597-598.
- Zimmermann, A., Lüthy, J. and Pauli, U. 1998. Quantitative and qualitative evaluation of nine different extraction methods for nucleic acids on soya bean food samples. *Zeitschrift für Lebensmitteluntersuchung und -Forschung A*. **207**: 81-90.
- Zou, Z., Kai, J., Rust, M. J., Han, J. and Ahn, C. H. 2007. Functionalized nano interdigitated electrodes arrays on polymer with integrated microfluidics for direct bio-affinity sensing using impedimetric measurement. *Sensors and Actuators A: Physical*. **136**: 518-526.

Appendices

Appendix A

Aptamer-Based Potentiometric Measurements of Proteins Using Ion-Selective Microelectrodes

Apon Nunnunam,^{†,‡,§} Karin Y. Chumbimuni-Torres,[†] Yun Xiang,[†] Ralph Bash,[†] Panote Thavarungkul,[§] Proespichaya Kanatharana,[§] Ernst Pretsch,^{*,†} Joseph Wang,^{*,†} and Eric Bakker^{*,†,‡}

Department of Chemistry, Purdue University, West Lafayette, Indiana 47907, The Biodesign Institute and Fulton School of Engineering, Arizona State University, Tempe, Arizona 85287, Faculty of Science, Prince of Songkla University, Hat Yai, Songkhla, 90112, Thailand, Laboratorium für Organische Chemie, ETH Zürich, CH-8093 Zürich, Switzerland, and Nanochemistry Research Institute, Department of Applied Chemistry, Curtin University of Technology, Perth, WA 6845, Australia

We here report on the first example of an aptamer-based potentiometric sandwich assay of proteins. The measurements are based on CdS quantum dot labels of the secondary aptamer, which were determined with a novel solid-contact Cd²⁺-selective polymer membrane electrode after dissolution with hydrogen peroxide. The electrode exhibited cadmium ion detection limits of 100 pM in 100 mL samples and of 1 nM in 200 μ L microwells, using a calcium-selective electrode as a pseudoreference electrode. As a prototype example, thrombin was measured in 200 μ L samples with a lower detection limit of 0.14 nM corresponding to 28 fmol of analyte. The results show great promise for the potentiometric determination of proteins at very low concentrations in microliter samples.

Aptamers are nucleic acid ligands that have been designed through an in vitro selection process called SELEX (systematic evolution of ligands by exponential enrichment).¹ Such aptamers hold great promise as affinity ligands for the biosensing of disease-related proteins and for developing protein-sensing arrays.^{2–7} Owing to their relative ease of isolation and modification, good stability, and wide applicability, they appear to be excellent alternatives to antibodies.^{8,9} The attractive biosensing properties of aptamer recognition elements have been illustrated in connec-

tion with a colorimetric method, but the lower detection limit was only in the micromolar range.^{10,11} Another detection scheme has been based on changes in fluorescence properties upon binding the fluorophore-labeled aptamer to the target.^{12–16} However, this fluorescence response is usually weak, and owing to the difficult design of signaling aptamers, the method is not easy to generalize. Lower detection limits in the 10 nM range have been obtained with piezoelectric analyzers.¹⁷

In recent years, different electrochemical strategies have been developed for monitoring the interaction between aptamer and target analytes. The electrochemical methods are, in general, superior to the optical ones because of rapid response, simple handling, and low cost.^{18–20} Electrochemical aptamer biosensors are based, among others, on a binding-induced label-free detection,^{21–25} on enzymes,^{26,27} or on nanoparticle labels.²⁸ Excellent values in the femtomolar range have been achieved with impedance spectroscopy and amplification by chemical means to denature the protein captured by an aptamer on the electrode

* To whom correspondence should be addressed. E-mail: bakker@purdue.edu (E.B.); Joseph.Wang@asu.edu (J.W.); pretsch@ethz.ch (E.P.).

[†] Purdue University.

[‡] Arizona State University.

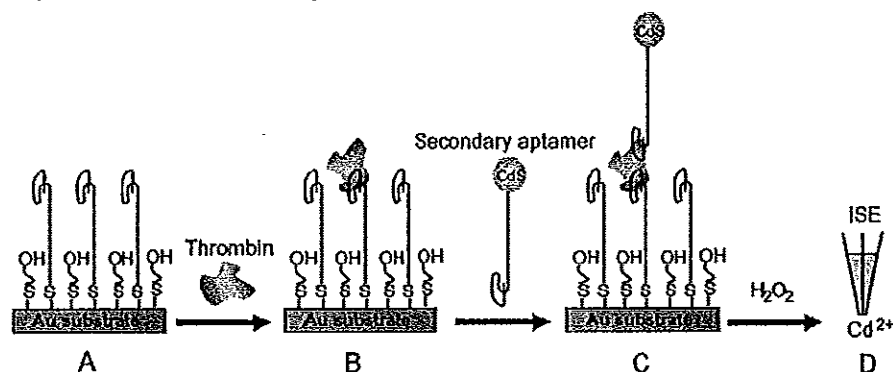
[§] Prince of Songkla University.

^{||} ETH Zürich.

[¶] Curtin University of Technology.

- (1) Ellington, A. D.; Szostak, J. W. *Nature* 1990, 346, 818–822.
- (2) Hesselbert, J.; Robertson, M. P.; Jhaveri, S.; Ellington, A. D. *Rev. Mol. Biotechnol.* 2000, 74, 15–25.
- (3) Osbourne, S. E.; Matsumura, E.; Ellington, A. D. *Curr. Opin. Chem. Biol.* 1997, 1, 5–9.
- (4) O'Sullivan, C. K. *Anal. Bioanal. Chem.* 2002, 372, 44–48.
- (5) Xu, D.; Xu, D.; Yu, X.; Liu, Z.; He, W.; Ma, Z. *Anal. Chem.* 2005, 77, 5107–5113.
- (6) Stadtherr, K.; Wolf, H.; Lindner, P. *Anal. Chem.* 2005, 77, 3437–3443.
- (7) McCauley, T. G.; Hamaguchi, N.; Stanton, M. *Anal. Biochem.* 2003, 319, 244–250.
- (8) Jayasena, S. D. *Clin. Chem.* 1999, 45, 1628–1650.
- (9) Luzzi, E.; Minunni, M.; Tombelli, S.; Mascini, M. *Trends Anal. Chem.* 2003, 22, 810–818.

- (10) Stojanovic, M. N.; Landry, D. W. *J. Am. Chem. Soc.* 2002, 124, 9678–9679.
- (11) Liu, J.; Lu, Y. *Anal. Chem.* 2004, 76, 1627–1632.
- (12) Stojanovic, M. N.; de Prada, P.; Landry, D. W. *J. Am. Chem. Soc.* 2001, 123, 4928–4931.
- (13) Heyduk, E.; Heyduk, T. *Anal. Chem.* 2005, 77, 1147–1156.
- (14) Fang, X.; Cao, Z.; Beck, T.; Tan, W. *Anal. Chem.* 2001, 73, 5752–5757.
- (15) Jhaveri, S.; Kirby, R.; Conrad, R.; Maglott, E.; Bowser, M.; Kennedy, R. T.; Glick, G.; Ellington, A. D. *J. Am. Chem. Soc.* 2000, 122, 1566–1571.
- (16) Jhaveri, S.; Rajendra, M.; Ellington, A. D. *Nat. Biotechnol.* 2000, 18, 1293–1297.
- (17) Bini, A.; Minunni, M.; Tombelli, S.; Centi, S.; Mascini, A. *Anal. Chem.* 2007, 79, 3016–3019.
- (18) Palecek, E.; Fojta, M. *Anal. Chem.* 1994, 66, 1566–1571.
- (19) Wang, J. *Anal. Chem.* 1999, 71, 328–332.
- (20) Wang, J. *Nucleic Acids Res.* 2000, 28, 3011–3016.
- (21) Xiao, Y.; Lubin, A. A.; Heger, A. J.; Plaxco, K. W. *Angew. Chem., Int. Ed.* 2005, 44, 5456–5459.
- (22) Rodriguez, M. C.; Kawde, A.-N.; Wang, J. *Chem. Commun.* 2005, 4267–4269.
- (23) Cai, H.; Lee, T. M.-H.; Hsing, I.-M. *Sens. Actuators, B* 2006, 114, 433–437.
- (24) Cheng, A. K. H.; Ge, B.; Yu, H. Z. *Anal. Chem.* 2007, 79, 5158–5164.
- (25) Xu, Y.; Yang, L.; Ye, X.; He, P.; Fang, Y. *Electroanalysis* 2006, 18, 1449–1456.
- (26) Ikebukuro, K.; Kiyohara, C.; Sode, K. *Biosens. Bioelectron.* 2005, 20, 2168–2172.
- (27) Baldrich, E.; Accero, J. L.; Reekmans, G.; Laureyn, W.; O'Sullivan, C. K. *Anal. Chem.* 2004, 77, 4774–4784.
- (28) Hansen, J. A.; Wang, J.; Kawde, A.-N.; Xiang, Y.; Gohelf, K. V.; Collins, G. J. *Am. Chem. Soc.* 2006, 128, 2228–2229.

Scheme 1. Representation of the Analytical Protocol^a

^a (A) Formation of a mixed monolayer of thiolated aptamer on gold substrate; (B) thrombin addition and binding with aptamer; (C) secondary binding with CdS-labeled aptamer; (D) dissolution of CdS label followed by detection using a solid-contact Cd²⁺-selective microelectrode.

surface (10 fM)²⁵ and, very recently, by electrogenerated chemiluminescence via target protein-induced strand displacement (1 fM).²⁶ Recently, the nanomaterial-based electrochemical detection of proteins has received considerable attention. The methods include the use of gold nanoparticles^{20,21} or semiconductor nanocrystal tracers.^{22,23} Usually, detection is made by anodic stripping voltammetry (ASV), which due to its intrinsic preconcentration step allows one to achieve ultralow detection limits.²⁴

Potentiometry with ion-selective electrodes (ISEs) represents an attractive tool for trace metal analysis in confined samples. Since, with this method, the direct relationship between analyte activity and observed potential is independent of the sample volume, no deterioration of the signal or lower detection limit is expected upon reducing the volume. This is rather unique and establishes potentiometry as a preferred method when dealing with miniaturized analytical microsystems.^{25,26}

Recent improvements in the detection limits of ISEs based on polymeric membranes containing selective receptors (ionophores) have yielded sensors for the direct measurement in the subnanomolar concentration range.²⁷ It is now possible to use miniaturized ISEs for detecting subfemtomole amounts of ions in micro-volume samples.^{25,26}

Recently, we have demonstrated that such potentiometric microsensors are very attractive for ultrasensitive immunoassays in connection with nanoparticle amplification labels.²⁸ By reducing the sample volume and using quantum dot tags, the lower

detection limit has been improved to <10 ppb.²⁸ Here, for the first time, we demonstrate the use of a potentiometric microsensor for monitoring biomolecular interactions of an aptamer coupled to nanocrystal tags. As illustrated in Scheme 1, the target protein is captured by the thiolated aptamer anchored on the surface of a gold substrate. Then, a secondary aptamer with CdS nanoparticle labels is added, upon which CdS is dissolved with H₂O₂, yielding a dilute electrolyte background suitable for the potentiometric detection of the released Cd²⁺ with a polymer membrane Cd²⁺-selective microelectrode.

In this work, we use an aptamer known to bind the blood-clotting protein thrombin as a model system.⁴⁰ Thrombin, the last enzyme protease involved in the coagulation cascade, converts fibrinogen to insoluble fibrin, which forms the fibrin gel either in physiological conditions or a pathological thrombus. The concentration of thrombin in blood can vary considerably. However, since a trace level of thrombin (high picomolar range) in blood has been found to be associated with coagulation abnormalities,⁴¹ it is important to assess this protein with high sensitivity.

EXPERIMENTAL SECTION

Reagents. Thrombin from human plasma, TRIS-HCl, 6-mercapto-1-hexanol, tris(carboxethyl) phosphine (TCEP), potassium dihydrogenphosphate, and dipotassium hydrogen phosphate were purchased from Sigma (St. Louis, MO). The nucleic acid aptamers were obtained from Integrated DNA Technologies Inc. (Coralville, IA). The following oligonucleotide sequences were used: aptamer 1 (primary aptamer), 5'-HS-TTT TTT TTT TGG TTG GTG TGG TTG G-3'; aptamer 2 (secondary aptamer), 5'-HS-TTT TTT AGT CCG TGG TAG GGC AGG TTG GGG TGA CT-3'.

Chemicals for the synthesis of CdS quantum dots, sodium bis-(2-ethylhexyl) sulfosuccinate (AOT), Cd(NO₃)₂, Na₂S, cystamine, sodium 2-mercaptoethane sulfonate, and the solvents were obtained from Sigma. The ionophores, *N,N,N',N'*-tetradodecyl-3,6-dioxaoctanedithioamide (ETH 5435), *N,N*-dicyclohexyl-*N',N'*-

(29) Wang, X.; Zhou, J.; Yun, W.; Xiao, S.; Chang, Z.; He, P.; Fang, Y. *Anal. Chem.* 2007, 79, 242–248.

(30) Deguire, M.; Degrand, C.; Linoges, B. *Anal. Chem.* 2000, 72, 5521–5528.

(31) Das, J.; Aziz, M. A.; Yang, H. *J. Am. Chem. Soc.* 2006, 128, 16022–16023.

(32) Liu, G.; Wang, J.; Kim, J.; Jan, M. R. *Anal. Chem.* 2004, 76, 7126–7130.

(33) Choi, J. H.; Chen, K. H.; Strano, M. S. *J. Am. Chem. Soc.* 2006, 128, 15581–15585.

(34) Wang, J. *Stripping Analysis*; VCH: New York, 1985.

(35) Rubinova, N.; Chumbimuni-Torres, K.; Bakker, E. *Sens. Actuators, B* 2007, 121, 135–141.

(36) Malon, A.; Vigassy, T.; Bakker, E.; Pretsch, E. *J. Am. Chem. Soc.* 2006, 128, 8154–8155.

(37) Ceresa, A.; Radu, A.; Bakker, A.; Pretsch, E. *Anal. Chem.* 2002, 74, 4027–4036.

(38) Chumbimuni-Torres, K. Y.; Dai, Z.; Rubinova, N.; Xiang, Y.; Pretsch, E.; Wang, J.; Bakker, E. *J. Am. Chem. Soc.* 2006, 128, 13675–13677.

(39) Thüner, R.; Vigassy, T.; Hirayama, M.; Wang, J.; Bakker, E.; Pretsch, E. *Anal. Chem.* 2007, 79, 5107–5110.

(40) Bock, L. C.; Griffin, L. C.; Latham, J. A.; Vermaas, E. H.; Toole, J. J. *Nature* 1992, 355, 561–563.

(41) Bichler, J.; Heit, J.; Owen, W. G. *Thromb. Res.* 1996, 84, 289–294.

dioctadecyl-3-oxapentanediamide (ETH 5234), the lipophilic cation exchanger, sodium tetrakis[3,5-bis(trifluoromethyl)phenyl]borate (NaTFPB), the lipophilic salt, tetradodecylammonium tetrakis(4-chlorophenyl)borate (ETH 500), 2-nitrophenyl octyl ether (*o*-NPOE), poly(vinyl chloride) (PVC), and tetrahydrofuran (THF) were purchased in Selectophore or puriss. p. a. grade from Fluka (Buchs, Switzerland). The solvent CH_2Cl_2 and H_2O_2 were obtained from Fisher (Pittsburgh, PA). Poly(3-octylthiophene) (POT) was synthesized as reported⁴² and purified according to the patent application.⁴³ The methyl methacrylate-decyl methacrylate (MMA-DMA) copolymer matrix was obtained as described previously.⁴⁴ All stock and buffer solutions were prepared using doubly deionized water (18.2 M Ω cm).

Preparation of Oligonucleotide Aptamer on Gold Surface. The immobilization of oligonucleotides was based on a previously reported protocol.²⁸ Thiolated aptamers were received with disulfide protecting groups.

Cleavage of Dithiol Protecting Group. The disulfide-protected nucleotides (100 μM , 10 μL) were diluted with autoclave water to 100 μL and treated with TCEP (1 mg) for 30 min, followed by purification using a MicroSpin G-25 column obtained from Amersham Biosciences (Buckinghamshire, U.K.).

Gold Substrates. The gold substrates were obtained from Denton Vacuum LLC (Moorestown, NJ), machine cut (Advotech Company Inc., Tempe, AZ) to identical pieces (6 \times 3 \times 0.2 mm³), assuming a uniform thickness.

Preparation of Mixed Monolayers. Gold substrates were cleaned in Piranha solution and rinsed with water prior to use. (*Safety note:* the Piranha solution should be handled with extreme caution.) The oligonucleotide monolayer was generated by treating the gold substrates with a 1 μM thiolated oligonucleotide aptamer solution (100 μL) in a potassium phosphate buffer (1 M, pH 8.0) overnight, followed by removal of the solution. The surface of the gold substrates was then blocked by a 10 min treatment with 6-mercapto-1-hexanol (0.1 M, 100 μL), followed by washing with water.

Preparation of CdS Quantum Dot Nanocrystals. The quantum dot nanoparticles were prepared using a slightly modified procedure reported previously.⁴⁵ First, AOT (14.0 g) was dissolved in a mixture of *n*-hexane (200 mL) and water (4 mL). The resulting solution was separated into two subvolumes of 120 and 80 mL. A 0.48 mL aliquot of a 1 M $\text{Cd}(\text{NO}_3)_2$ solution was added to the 120 mL subvolume, whereas 0.32 mL of a 1 M Na_2S solution was added to the 80 mL subvolume. The two solutions were stirred for 1 h, then mixed and stirred for an additional hour under N_2 . The quantum dots were capped by adding cystamine (0.34 mL, 0.32 M) and sodium 2-mercaptoethane sulfonate (0.66 mL, 0.32 M) and mixing under N_2 for 24 h. Evaporation of hexane in vacuo yielded the CdS quantum dot nanocrystals, which were washed with pyridine, hexane, and methanol.

Preparation of CdS Quantum Dot-Oligonucleotide Aptamer Conjugates. The CdS-oligonucleotide conjugate was prepared

by using a modified protocol published earlier.^{28,46} First, CdS quantum dot suspension (0.2 mg mL⁻¹, 500 μL) was exposed to 750 nM of the thiolated oligonucleotide secondary aptamer (aptamer 2). The mixture was stirred overnight at room temperature. The quantum dot-aptamer conjugate was collected by centrifugation at 10 000 rpm for 45 min, removal of supernatant, and resuspension in binding buffer (50 mM TRIS-HCl, 100 mM NaCl, 5 mM KCl, and 1 mM MgCl_2 ; pH 7.4).

Sandwich Aptamer-Protein Assay. The aptamer-modified gold substrates were incubated for 1 h with the desired amount of thrombin in binding buffer (100 μL) followed by washing with washing buffer (50 mM TRIS-HCl, 0.1% Tween 20; pH 7.4). Then, the gold substrates were incubated with quantum dot-oligonucleotide secondary aptamer for 1 h at room temperature. The supernatant was removed, the gold substrates were washed twice with washing buffer (each 100 μL), and transferred to new microwells, where they were washed four times again with the washing buffer (each 100 μL) and twice with water.

Dissolution and Detection. Hydrogen peroxide was used for the dissolution step since it was observed that it can efficiently oxidize the CdS quantum dots after carefully optimizing concentration and reaction time.³⁹ Preliminary experiments of dissolving CdS quantum dots with 0.01 M H_2O_2 and potentiometric detection of the released Cd^{2+} showed that it was fully oxidized after 15 min. In the final assay, dissolution of CdS was carried out by the addition of 0.01 M H_2O_2 in 10^{-4} M CaCl_2 (100 μL) for 1 h to ensure complete oxidation. The detection was performed in polystyrene microtiter plates (Corning Inc., NY). Prior to the measurements, each microwell was pretreated with 10% HNO_3 overnight and then washed at least five times with deionized water and left to dry.

Ion-Selective Electrode Membranes. The Cd ISE membrane was prepared by dissolving 60 mg of the following components in CH_2Cl_2 (0.8 mL): ETH 5435 (1.27 wt %, 15 mmol kg⁻¹), NaTFPB (0.46 wt %, 5 mmol kg⁻¹), ETH 500 (1.15 wt %, 10 mmol kg⁻¹), and copolymer MMA-DMA (97.12 wt %). The membrane solution was deaerated by purging it with N_2 before coating the microelectrodes. The membrane for the Ca ISE used as a reference electrode was prepared by dissolving 140 mg of the following components in THF (1 mL): ETH 5234 (0.87 wt %, 10.9 mmol kg⁻¹), NaTFPB (0.47 wt %, 5.12 mmol kg⁻¹), PVC (32.2 wt %), and *o*-NPOE (66.3 wt %). The solution was left to evaporate for 1 h, after which it was filled into a 100 μL pipet tip and left to dry for at least 24 h. Then, the membrane was conditioned in 10^{-3} M CaCl_2 for 1 day.

Microelectrodes. The solid-contact Cd^{2+} -selective microelectrode was prepared by using a 2 cm long Au wire (200 μm diameter) as solid substrate soldered to a Ag wire for electric contact. Before use, the Au wires were thoroughly cleaned with 10% sulfuric acid and rinsed with water, then acetone, and left in CHCl_3 for 5 min. The solution of POT (25 mM with respect to the monomer in CHCl_3) was applied along the length of Au wire at least three times or until the color of the wire became black. After the Au wires were fully covered with POT they were left to dry. The wires were then inserted into a polypropylene tip so that they were level with the end of the micropipette tip. Finally, the membrane cocktail was applied to the top of the wire covered

(42) Järvinen, H.; Lahlunen, L.; Niskanen, J.; Horni, O.; Tammi, A.-L. *Synth. Met.* 1995, 69, 299–300.

(43) Xiao, S.; Qiu, C.; Qiu, C. X. U.S. Patent Application 20040254336, 2004.

(44) Qin, Y.; Peper, S.; Bakker, E. *Electroanalysis* 2002, 14, 1375–1384.

(45) Willner, I.; Patolsky, F.; Wasserman, J. *Angew. Chem. Int. Ed.* 2001, 40, 1861–1864.

(46) Wang, J.; Liu, G.; Polsky, R.; Merkoci, A. *Electrochim. Commun.* 2002, 4, 722–726.

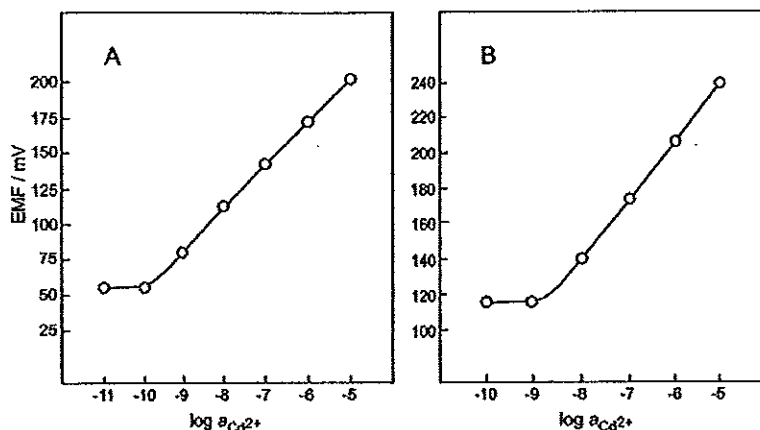


Figure 1. Calibration curves of a solid-contact Cd^{2+} -selective electrode in (A) 100 mL and (B) 200 μL samples with 10^{-4} M CaCl_2 as background using ELISA microplates.

with POT for three times at 15 min intervals and allowed to dry for 2–3 h until full evaporation of CH_2Cl_2 . The microelectrodes were conditioned first in 10^{-3} M CdCl_2 and subsequently in 10^{-9} M CdCl_2 with 10^{-4} M CaCl_2 (1 day each). Measurements were performed in ELISA microwells containing 180 μL of 10^{-4} M CaCl_2 and adding 20 μL of sample, using a Ca ISE as reference and a small magnetic stirring bar. All stock solutions used for measurements were freshly prepared daily.

For selectivity measurements, the Cd ISE membranes were conditioned in 10^{-3} M CaCl_2 for 2 days in order to avoid primary ions leaching from the membrane.⁴⁷ For each ion, a calibration curve was recorded and the selectivity coefficients were calculated using the separate solutions method.⁴⁸ For measurements in 100 mL samples with a customary reference electrode, the electromotive force (emf) values were corrected for liquid-junction potentials according to the Henderson equation. Activity coefficients were calculated by the Debye–Hückel approximation.

Electromotive Force Measurements. Potentiometric measurements were performed in stirred solutions at room temperature (22 °C) with a PCI MIO16XE data acquisition board (National Instruments, Austin, TX) connected to a four-channel high Z interface (WPI, Sarasota, FL).

RESULTS AND DISCUSSION

Solid-contact ISEs with nanomolar detection limits can now be routinely prepared for different ions.⁹ Such electrodes are easily miniaturized to operate in samples of very small volume.^{35,39} In this work, a novel solid-contact Cd^{2+} -selective microelectrode has been developed, which is based on the copolymer matrix MMA–DMA and the ionophore ETH 5435.⁵⁰

The novel Cd ISE was first characterized in large samples of 100 mL. As shown in Figure 1A, with a background of 10^{-4} M CaCl_2 , it displays a very good lower detection limit of 100 pM. In microwell plates of 200 μL sample volume, the detection limit is less good by 1 order of magnitude (Figure 1B). Yet, it is still in

the nanomolar range (1 nM) with the same background. Although we do not expect deterioration of the detection limit upon reducing the sample volume, the changes observed here are likely attributed to impurities due to the unfavorable surface-to-volume ratio of the small sample. The reproducibility of the solid-contact microelectrodes in 200 μL samples was also evaluated by recording three different calibration curves over the concentration range of 10^{-10} to 10^{-5} M. After each measurement, the electrode was washed for 5 min to eliminate possible memory effects. The standard deviation of the emf for each concentration was <1 mV. Another important performance parameter is the long-term stability of the ISE. During continuous experiments, it was observed that the electrodes are capable of measuring more than 45 samples with good response times and a standard deviation of <1.5 mV. After recalibration, they can be used for more analyses. After 1 month, the Cd ISEs showed a loss of detection limit by half an order of magnitude.

The membranes exhibit good selectivities for the relevant interfering ions, Ca^{2+} , Na^+ , and H^+ with the corresponding logarithmic selectivity coefficients, $\log K_{\text{Ca}^{2+}}^{\text{Pot}}$, of -7.04 , -3.88 , and -4.59 , respectively. Note that the selectivity over sodium ions is inferior relative to a recently reported liquid inner contact cadmium ISE based on the same ionophore.³⁹ This might be explained by intermixing of POT and the membrane during casting, resulting in some selectivity deterioration. Owing to its high level of discrimination, Ca^{2+} was selected as the background electrolyte together with a Ca^{2+} -selective electrode as the reference electrode. For this purpose, the selectivity of the Ca ISE for Cd^{2+} , $\log K_{\text{Ca}^{2+}}^{\text{Pot}} = -3.15$, is sufficiently high.

For aptamer-based protein detection, the CdS quantum dot labels were oxidized with H_2O_2 since HNO_3 , the standard oxidizing agent for ASV,²⁸ would deteriorate the lower detection limit due to proton interference. The influence of H_2O_2 on the response of the solid-contact microelectrodes was examined by taking calibration curves in the range of 10^{-3} to 10^{-1} M Cd^{2+} at different background concentrations of H_2O_2 (10^{-3} to 10^{-1} M). Although an increase in its concentration accelerates the dissolution,³⁹ no influence on the potentiometric response was observed at $\leq 10^{-2}$ M H_2O_2 . A concentration of 10^{-2} M H_2O_2 was selected for further

(47) Bakker, E. *Anal. Chem.* 1997, 69, 1061–1069.

(48) Bakker, E.; Pretsch, E.; Bühlmann, P. *Anal. Chem.* 2000, 72, 1127–1133.

(49) Chumbimuni-Torres, K. Y.; Rubinova, N.; Radu, A.; Kubota, I. T.; Bakker, E. *Anal. Chem.* 2006, 78, 1318–1322.

(50) Ion, A.; Bakker, E.; Pretsch, E. *Anal. Chim. Acta* 2001, 440, 71–79.

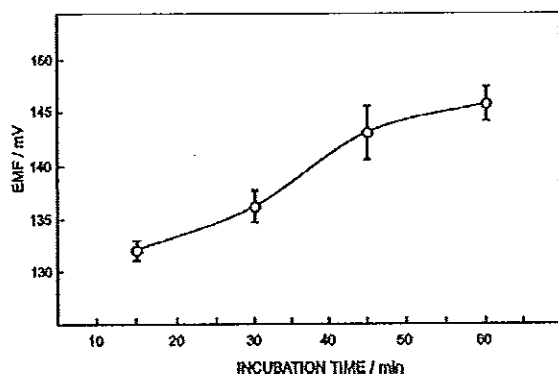


Figure 2. Response of different incubation times between immobilized 1000 nM primary aptamer and 100 ppb of thrombin in 15, 30, 45, and 60 min (error bars: SD, $N = 3$). Potentiometric measurements were performed in 200 μ L samples with 10^{-4} M CaCl₂ as background electrolyte and a Ca ISE as reference electrode.

experiments since some signal drifts were observed with 10^{-1} M H₂O₂, which was probably due to the interaction of H₂O₂ with the conducting polymer.

Next, the possible interference by the other components of the assay was investigated. When performing the measurement according to Scheme 1 but without labeling the secondary aptamer, as expected, no change of the emf was observed upon addition of H₂O₂ after binding the secondary aptamer. On the other hand, when using the CdS quantum dot-labeled secondary aptamer, the control samples, i.e., zero target, lysozyme, and IgG, initially showed emf changes that were similar to those obtained with the target (data not shown). Hence, to reduce such nonspecific adsorption effects, the washing steps were improved including a transfer into new microwells (see the Experimental Section).

The effect of the incubation time of the aptamer–thrombin binding was examined over the range of 15–60 min (Figure 2) using a 100 ppb thrombin solution, which gives about half the maximum signal in this assay (see below). For this case, the emf increased with increasing binding time, but at times longer than 45 min, the increase was no longer significant. On the basis of these results, an incubation time of 60 min was chosen for all further experiments.

The concentration of the CdS-labeled secondary aptamer was varied between 250 and 1000 nM using 1000 nM primary aptamer and 100 ppb thrombin (Figure 3). The signal increased with increasing concentration, but this trend declined at >500 nM. Since the nonspecific absorption slightly increased at 1000 nM concentration, 750 nM was chosen for subsequent experiments.

The selectivity of the thrombin aptamer was tested with the assay parameters as selected above. As shown in Figure 4, 500 ppb of lysozyme or IgG showed emf responses that were not significantly higher than for the control, corresponding to about 0.25 ppb of cadmium ions. This residual cadmium ion level may partly originate from impurities in the water and reagents that were used. In contrast, the response to a 10 times smaller concentration of thrombin was found to be about 6 times higher in cadmium ion concentration (1.6 ppb, note the logarithmic response characteristics of the ISE).

The results of a typical series of measurements with thrombin concentrations from 5 to 1000 ppb are shown in Figure 5. The

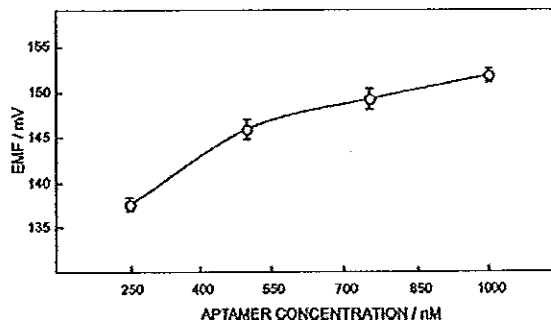


Figure 3. Response to 250, 500, 750, and 1000 nM secondary aptamer with 100 ppb of target thrombin previously bound to 1000 nM primary aptamer (error bars: SD, $N = 3$). Other conditions are as in Figure 2.

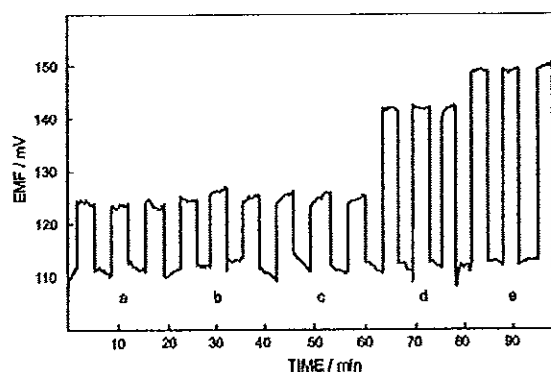


Figure 4. Potentiometric responses of the Cd²⁺-selective electrode for (a) the control (zero target), (b) lysozyme, 500 ppb, and (c) 500 ppb IgG (as noncomplementary targets), (d) thrombin, 50 ppb, and (e) thrombin, 100 ppb (as complementary target) after aptamer–thrombin interaction. Other conditions are as in Figure 2.

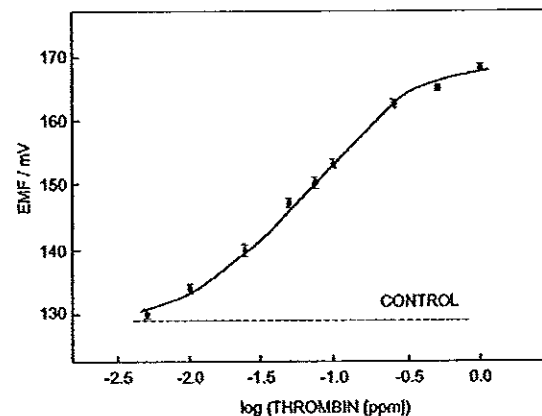


Figure 5. Potentiometric monitoring of thrombin concentration via CdS quantum dot label in 200 μ L microwells with the aptamer–thrombin sandwich assay (error bars: SD, $N = 3$). Other conditions are as in Figure 2.

emf response of the Cd ISE versus log[thrombin] is close to linear and offers a sufficient concentration dependence suitable for thrombin measurements over a dynamic range of 10–250 ppb and with a lower detection limit of ca. 5 ppb. This corresponds to 28 fmol of thrombin in 200 μ L samples or 0.14 nM and compares

well to results obtained with other reported sensors such as piezoelectric transducers (ca. 10 nM¹⁷ and 1 nM⁵¹) or electrochemical sensors (of the order of 10 nM).^{21,51,52} Significantly lower detection limits were obtained with impedance spectroscopy and amplification by chemical means to denature the protein captured by an aptamer on the electrode surface (10 fM)²⁵ and, very recently, by electrogenerated chemiluminescence via target protein-induced strand displacement (1 fM).²⁹

CONCLUSIONS

For the first time, we demonstrate that ion-selective microelectrodes can be used for monitoring protein–aptamer interactions with semiconductor nanocrystal labels in an ELISA microplate format. It is important to emphasize that a low detection limit of 5 ppb or 28 fmol of thrombin was reached without a

preconcentration step typically used in other electrochemical techniques. This was possible in conjunction with a reduction of the sample volume and the excellent lower detection limit of the Cd ISE used. It is expected that various biomolecular interactions can be monitored with similar assays based on different nanoparticle tracers and corresponding ISEs.

ACKNOWLEDGMENT

This work was supported by Grants from the National Institutes of Health (R01 EB002189 and R01 1056047). Apon Nunnunam acknowledges The Royal Golden Jubilee Ph.D. Program (Thailand Research Fund). We thank Dr. D. Wegmann for careful reading of the manuscript.

Received for review September 12, 2007. Accepted October 27, 2007.

AC701910R

(51) Hianik, T.; Ostáňá, V.; Zajíčková, Z.; Stolková, E.; Evtugyn, G. *Bioorg. Med. Chem. Lett.* 2005, 15, 291–295.

(52) Mir, M.; Vreeke, M.; Katakis, I. *Electrochim. Commun.* 2006, 8, 505–511.

Appendix B

Potentiometric Detection of DNA Hybridization

Apon Numnuam,^{†,‡,§} Karin Y. Chumbimuni-Torres,[†] Yun Xiang,[‡] Ralph Bash,[‡] Panote Thavarungkul,[§] Proespichaya Kanatharana,[§] Ernő Pretsch,^{*,†} Joseph Wang,^{*,‡} and Eric Bakker^{*,†,‡}

Department of Chemistry, Purdue University, West Lafayette, Indiana 47907, The Biodesign Institute and Fulton School of Engineering, Arizona State University, Tempe, Arizona 85287, Faculty of Science, Prince of Songkla University, Hat Yai, Songkhla, 90112 Thailand, Institute of Biogeochemistry & Pollutant Dynamics ETH Zürich, CH-8092 Zürich, Switzerland, and Nanochemistry Research Institute, Department of Applied Chemistry, Curtin University of Technology, Perth, Western Australia 6845, Australia

Received October 1, 2007; E-mail: bakker@purdue.edu; joseph.wang@asu.edu; pretsch@ethz.ch

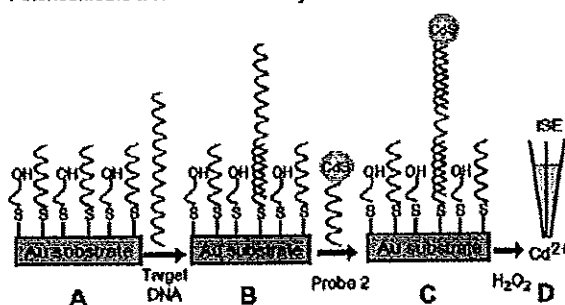
Tremendous fundamental advances over the past decade have led to dramatic improvements in the performance of ion-selective electrodes (ISEs).¹ In particular, new insights into the principles dictating the limits of detection (LODs) of such potentiometric sensors have led to ISEs capable of convenient measurements down to the subnanomolar (parts per trillion) level.² Recent efforts have also demonstrated that potentiometric sensors with low LODs can be miniaturized to allow trace (subfemtomole) measurements in very small (microliter) sample volumes.³ Such major improvements in the performance of ISEs have facilitated new applications for which potentiometric sensors have not been used traditionally. For example, recent progress in our laboratories has led to highly sensitive immunoassays of proteins based on different ISE transducers.⁴

Here, we demonstrate for the first time the use of potentiometric microsenors for monitoring DNA hybridization. The detection of sequence-specific DNA is of central importance in the diagnosis and treatment of genetic diseases, detection of infectious agents, drug screening, and in forensic science.⁵ Various approaches have been successfully used to detect sequence-selective DNA hybridization, including optical,⁶ electrochemical,⁷ and piezoelectric methods.⁸ Electrochemical methods for detecting DNA hybridization have received considerable attention because of their high sensitivity, portability, low cost, minimal power requirement, and/or independence of sample turbidity or optical pathway.⁹ Various amperometric and voltammetric detection strategies¹⁰ have been used for transducing electronically DNA hybridization events based on oligonucleotide-bearing enzyme tags,¹¹ redox tracers,¹² or nanoparticle labels (i.e., gold nanoparticles, silver tags, and semiconductor nanocrystals).¹³

The new potentiometric nucleic acid measurements rely on a sandwich DNA hybridization for capturing a secondary oligonucleotide bearing CdS-nanocrystal tags. As illustrated in Scheme 1, the target DNA (60-mer) is hybridized (B) to the surface-anchored thiolated DNA probe (20-mer) on the gold substrate (A), followed by the capture of the secondary DNA probe (26-mer) conjugated to the CdS label (C). The nanocrystal is then dissolved in H₂O₂ to yield a dilute electrolyte background solution suitable for the potentiometric detection of the released Cd²⁺ with a polymer membrane Cd²⁺-selective microelectrode (D).

The assay was based on a recently developed miniaturized solid-contact Cd-ISE showing a lower LOD of 10⁻¹⁰ and 10⁻⁹ M Cd²⁺ in samples of 100 nL and 200 μ L (microwell plates), respectively.¹⁴

Scheme 1. Steps Involved in the Nanoparticle-Based Potentiometric Detection of DNA Hybridization*



* (A) Formation of a mixed monolayer of DNA probe on gold substrate; (B) hybridization with target DNA; (C) second hybridization with CdS-labeled probe; (D) dissolution of the CdS tag, followed by detection using a Cd²⁺-selective electrode.

It exhibits excellent selectivity for the relevant ions, with logarithmic selectivity coefficients of -7.04 (Ca²⁺), -3.88 (H⁺), and -4.59 (Na⁺). A miniaturized liquid-contact Ca-ISE was used as a pseudoreference electrode.¹⁴

The key parameters of the DNA sandwich hybridization assay were optimized as follows (cf. Supporting Information): The optimal concentration of the primary and secondary (CdS-nanocrystal-labeled) DNA probe was each 1 μ M, and the optimal time for both hybridization steps (cf. Scheme 1) was 60 min.

The high selectivity of the new DNA detection is illustrated in Figure 1 displaying the potentiometric responses of the Cd²⁺-selective microelectrode to (a) control solution (zero target), (b) 500 nM of a noncomplementary DNA, (c) 500 μ M of 2-base mismatch DNA, and to two significantly lower levels of the target DNA of (d) 10 nM and (e) 100 nM. The responses to the noncomplementary and the 2-base mismatch DNA are similar to those obtained with the control solution. Larger signals are observed for significantly lower (nanomolar) concentrations of the target DNA. Notice in particular the effective discrimination against the large excess (500 nM) of mismatch DNA (c) vs 10 nM target DNA (d). Such behavior confirms the good selectivity of the hybridization assay. Considering the logarithmic response of the Cd-ISE, the potential differences correspond to 2.8 nM for the 500 nM 2-base mismatch DNA (c) and 21 nM Cd²⁺ for the 10 nM target DNA (d), that is, to a ~ 8 -fold lower amount of captured tags for a 50-fold excess of the 2-base mismatch DNA.

The quantitative aspects are documented by a calibration experiment over a concentration range of 0.01–1000 nM target DNA. The resulting calibration plot in Figure 2 exhibits a well-defined concentration dependence suitable for DNA analysis, with

[†] Purdue University.

[‡] Arizona State University.

[§] Prince of Songkla University.

^{*} ETH Zürich.

[‡] Curtin University of Technology.

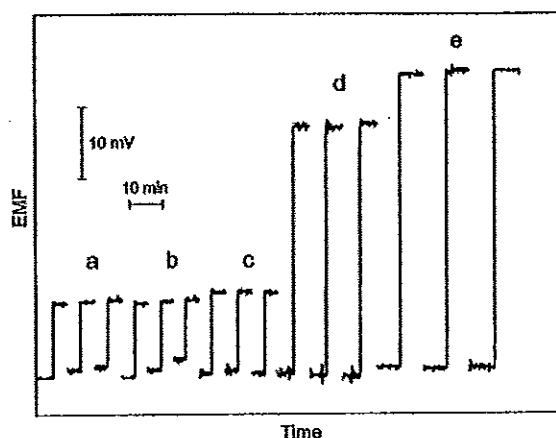


Figure 1. Potentiometric responses of the Cd^{2+} -selective electrode to: (a) control solution (10^{-4} M CaCl_2 , zero target), (b) 500 nM noncomplementary DNA, (c) 500 nM 2-base mismatch DNA, (d) 10 nM target DNA, and (e) 100 nM target DNA (as complementary targets) after DNA hybridization. Potentiometric measurements were performed in 200 μL of solutions with 10^{-4} M CaCl_2 as background (shown as baseline traces) with a Ca-ISE as pseudoreference electrode.

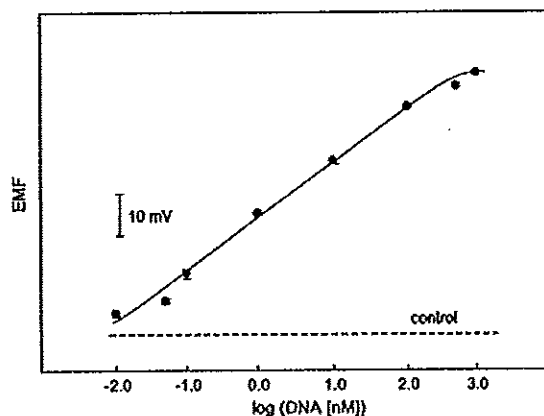


Figure 2. Calibration plot for the potentiometric monitoring of DNA with a sandwich array based on CdS quantum dot tags in 200- μL microwells (error bars: SD, $N=3$). The dashed line corresponds to control signal (no target). Other conditions as in Figure 1.

a wide dynamic range of 0.01–300 nM target DNA. The EMF at the lowest measured concentration of 10 pM was 2.96 mV above that of the control, and the standard deviation of the noise of the control was 0.17 mV ($N=13$, 1 min). Thus, the lower LOD is 10 pM or 37 pg (2 fmol) of the target DNA in the 200 μL sample. These values compare favorably with those reported for other electrochemical DNA hybridization assays using similar nanoparticle labels.^{13a,b}

In conclusion, we have demonstrated for the first time the use of potentiometric transducers for detecting DNA hybridization. The use of Cd^{2+} -selective microelectrodes is particularly useful for a microplate operation in connection with CdS nanocrystal tags. The extremely high sensitivity and fmol detection limit of the microelectrode are coupled with a high selectivity of the bioassay, including effective discrimination against 2-base mismatched DNA. Note that the low detection limit was reached without a preconcentration step commonly used in other electrochemical transduction schemes. The new potentiometric detection route can be extended to a wide range of genetic tests in connection with different nanoparticle tags.

Acknowledgment. This work was supported by the grants from the National Institutes of Health (Grants R01 EB002189 and R01 1056047). A.N. acknowledges The Royal Golden Jubilee PhD Program (Thailand Research Fund). We thank Dr. D. Wegmann for careful reading of the manuscript.

Supporting Information Available: Optimization of the DNA sandwich hybridization assay, experimental details, instrumentation, and reagents. This material is available free of charge via the Internet at <http://pubs.acs.org>.

References

- (1) Pretsch, E. *Trends Anal. Chem.* 2007, 26, 46–51.
- (2) Ceresa, A.; Rada, A.; Bakker, E.; Pretsch, E. *Anal. Chem.* 2002, 74, 4027–4036.
- (3) (a) Robinova, N.; Chumbimuni-Torres, K.; Bakker, E. *Sens. Actuators B* 2007, 121, 135–141. (b) Malon, A.; Vigassy, T.; Bakker, E.; Pretsch, E. *J. Am. Chem. Soc.* 2006, 128, 8154–8155.
- (4) (a) Chumbimuni-Torres, K. Y.; Dai, Z.; Robinova, N.; Xiang, Y.; Pretsch, E.; Wang, J.; Bakker, E. *J. Am. Chem. Soc.* 2006, 128, 13676–13677. (b) Thüner, R.; Vigassy, T.; Hirayama, M.; Wang, J.; Bakker, E.; Pretsch, E. *Anal. Chem.* 2007, 79, 5107–5110.
- (5) (a) Millan, K. M.; Mikkelsen, S. R. *Anal. Chem.* 1993, 65, 2317–2323. (b) Pinar, K.; Burcu, M.; Aysin, Z.; Mehmet, O. *Anal. Chim. Acta* 2004, 518, 69–76. (c) Ohmichi, T.; Kawamoto, Y.; Wu, P.; Miyoshi, D.; Karimata, H.; Sugimoto, N. *Biochemistry* 2005, 44, 7125–7130.
- (6) Talon, T. A.; Mirkin, C. A.; Litsinger, R. I. *Science* 2000, 289, 1757–1760.
- (7) Wang, J. *Anal. Chim. Acta* 2003, 500, 247–257.
- (8) Wu, V. C. H.; Chen, S.-H.; Lin, C.-S. *Biosens. Bioelectron.* 2007, 22, 2967–2975.
- (9) (a) Wang, J. *Anal. Chim. Acta* 2002, 496, 63–71. (b) Wang, J.; Liu, G.; Mercoçi, A. *J. Am. Chem. Soc.* 2003, 125, 3214–3215. (c) Hansen, J. A.; Mukhopadhyay, R.; Hansen, J. O.; Gothelf, K. V. *J. Am. Chem. Soc.* 2006, 128, 3860–3861.
- (10) Wang, J. *Stripping Analysis*; VCH: New York, 1985.
- (11) (a) Kim, E.; Kim, K.; Yang, H.; Kim, Y. T.; Kwak, J. *Anal. Chem.* 2003, 75, 5665–5672. (b) Alfonsi, L.; Singh, A. K.; Willner, I. *Anal. Chem.* 2001, 73, 91–102.
- (12) Ibara, T.; Nakayama, M.; Murata, M.; Nakano, K.; Marda, M. *Chem. Commun.* 1997, 1609–1610.
- (13) (a) Wang, J.; Liu, G.; Polsky, R.; Mercoçi, A. *Electrochem. Commun.* 2001, 4, 722–726. (b) Kawde, A.-N.; Wang, J. *Electroanalysis* 2004, 16, 101–107. (c) Wang, J.; Rincón, O.; Polsky, R.; Domínguez, E. *Electrochem. Commun.* 2003, 5, 83–86.
- (14) Nunnham, A.; Chumbimuni-Torres, K. Y.; Xiang, Y.; Bash, R.; Thavarungkul, P.; Kanatharana, P.; Pretsch, E.; Wang, J.; Bakker, E. *Anal. Chem.*, in press.

JA0775467

Vitae

Name Mr. Apon Numnuam

Student ID 4623009

Education Attainment

Degree	Name of Institute	Year of Graduation
Bachelor of Science (Chemistry), First Class Honor	Prince of Songkla University	2002

Scholarship Awards during Enrolment

1. The Development and Promotion of Science and Technology Talent Project (DPST)
2. The Royal Golden Jubilee Ph.D. Program (RGJ) of the Thailand Research Fund (TRF)
3. The Center of Excellence for Innovation in Chemistry (PERCH-CIC), Commission on Higher Education, Ministry of Education and Graduate School

List of Publications and Proceeding

Publications

1. Numnuam, A., Chumbimuni-Torres, K.Y., Xiang, Y., Bash, R., Thavarungkul, P., Kanatharana, P., Pretsch, E. Wang, J., Bakker, E. 2008. Aptamer-Based Potentiometric Measurement of Proteins Using Ion-Selective Microelectrode. *Analytical Chemistry*. **80**: 707-712.
2. Numnuam, A., Chumbimuni-Torres, K.Y., Xiang, Y., Bash, R., Thavarungkul, P., Kanatharana, P., Pretsch, E. Wang, J., Bakker, E. 2008. Potentiometric Detection of DNA Hybridization *Journal of the American Chemical Society*. **130**: 410-411.

3. Numnuam, A. Kanatharana, P., Mattiasson, B., Asawatreratanakul, P., Wongkittisuksa, B., Limsakul, C., Thavarungkul, P. 2008. Capacitive Biosensor for Quantification of Trace Amounts of DNA. *Biosensors and Bioelectronic*. Submitted.

Presentations

Oral presentations

1. Apon Numnuam, Karin Y. Chumbimuni-Torres, Yun Xiang, Ralph Bash, Panote Thavarungkul, Proespichaya Kanatharana, Ernö Pretsch, Joseph Wang, and Eric Bakker 2008. "Ion-Selective Microelectrode for Trace Bioaffinity Detection Based on CdS Quantum Dot Labels". RGJ-Ph.D Congress IX. Jomtein Palm Beach Pattaya, Chonburi. 4th-6th April 2008.

Poster Presentations

1. Apon Numnuam, Proespichaya Kanatharana, Panote Thavarungkul, Punnee Asawatreratanakul, Bo Mattiasson. 2009. "Capacitive Biosensor for Trace DNA Detection". Capacitive Biosensor for Trace DNA. Pittcon 2009; 60th Annual Pittsburgh Conference on Analytical Chemistry and Applied Spectroscopy. Chicago, Illinois, USA. 8th-12th March, 2009.
2. Apon Numnuam, Proespichaya Kanatharana, Panote Thavarungkul, Yun Xiang, Ralph Bash, Joseph Wang. 2008. Detection of DNA Hybridization by Anodic Stripping of CdS Quantum Dot. 1st Regional Electrochemistry Meeting of South-East Asia REMSEA. National University of Singapore 5th-7th August 2008.

3. Apon Numnuam, Yun Xiang, Ralph Bash, Panote Thavarungkul, Proespichaya Kanatharana, Joseph Wang. 2007. "Aptamer –based Stripping Measurment for Detection of Thrombin". The Sixth Princess Chulabhorn International Science Congress ; THE INTERFACE OF CHEMISTRY AND BIOLOGY IN THE "OMICS" ERA: ENVIRON MENTAL & HEALTH AND DRUG DISCOVERY. Bangkok, Thailand. 25th -27th November 2007.